

Laboratory Medicine

November 2023 Vol 54 No 6 Pgs 551-659

labmedicine.com



BOARD OF EDITORS

Editor in Chief

Roger L. Bertholf, PhD
Houston Methodist Hospital
Weill Cornell Medicine

Reviews

ASSOCIATE EDITOR
Madhu Menon, MD
ARUP Laboratories
ASSISTANT EDITOR
Rahul Matnani, MD, PhD
Rutgers Robert Wood Johnson Medical School

Biostatistics

ASSOCIATE EDITOR
Michal Ordak, PhD
Medical University of Warsaw

Clinical Chemistry

ASSOCIATE EDITOR
Uttam Garg, PhD
University of Missouri Kansas City School of Medicine
ASSISTANT EDITORS
David Alter, MD
Emory University School of Medicine
Hong Kee Lee, PhD
NorthShore University HealthSystem
Veronica Luzzi, PhD
Providence Regional Core Laboratory
Alejandro R. Molinelli, PhD
St Jude Children's Research Hospital

Cytology

ASSOCIATE EDITOR
Antonio Cajigas, MD
Montefiore Medical Center

Hematology

ASSOCIATE EDITOR
Shiyong Li, MD, PhD
Emory University School of Medicine
ASSISTANT EDITORS
Elizabeth Courville, MD
University of Virginia School of Medicine
Alexandra E. Kovach, MD
Children's Hospital Los Angeles
Lisa Senzel, MD, PhD
Stony Brook Medicine

Histology

ASSOCIATE EDITOR
Carol A. Gomes, MS
Stony Brook University Hospital

STAFF

EXECUTIVE EDITOR FOR JOURNALS
Kelly Swails, MT(ASCP)
DIRECTOR OF SCIENTIFIC PUBLICATIONS
Joshua Weikersheimer, PhD
SENIOR EDITOR, JOURNALS
Philip Rogers

Immunohematology

ASSOCIATE EDITOR
Richard Gammon, MD
OneBlood
ASSISTANT EDITORS
Phillip J. DeChristopher, MD, PhD
Loyola University Health System
Gregory Denomme, PhD
Grifols Laboratory Solutions
Amy E. Schmidt, MD, PhD
CSL Plasma

Immunology

ASSOCIATE EDITOR
Ruifeng Yang, MD, PhD
Nova Scotia Health

Laboratory Management and Administration

ASSOCIATE EDITOR
Lauren Pearson, DO, MPH
University of Utah Health
ASSISTANT EDITORS
Kayode Balogun, MD
Montefiore Medical Center
Vrajesh Pandya, MD
ARUP Laboratories

Microbiology

ASSOCIATE EDITOR
Yvette S. McCarter, PhD
University of Florida College of Medicine
ASSISTANT EDITORS
Alexander J. Fenwick, MD
University of Kentucky College of Medicine
Allison R. McMullen, PhD
Augusta University—Medical College of Georgia
Elitza S. Theel, PhD
Mayo Clinic

Molecular Pathology

ASSOCIATE EDITOR
Jude M. Abadie, PhD
Texas Tech University Health Science Center
ASSISTANT EDITORS
Holli M. Drendel, PhD
Atrium Health Molecular Pathology Laboratory
Rongjun Guo, MD, PhD
ProMedica Health System
Shuko Harada, MD
University of Alabama at Birmingham
Hongda Liu, MD, PhD
The First Affiliated Hospital of Nanjing Medical University

Pathologists' Assistant

ASSOCIATE EDITOR
Anne Walsh-Feeks, MS, PA(ASCP)
Stony Brook Medicine

Laboratory Medicine (ISSN 0007-5027), is published 6 times per year (bimonthly). Periodicals Postage paid at Chicago, IL and additional mailing offices. POSTMASTER: Send address changes to *Laboratory Medicine*, Journals Customer Service Department, Oxford University Press, 2001 Evans Road, Cary, NC 27513-2009.

SUBSCRIPTION INFORMATION: Annually for North America, \$182 (electronic) or \$241 (electronic and print); single issues for individuals are \$32 and for institutions \$71. Annually for Rest of World, £118/€167 (electronic) or £154/€220 (electronic and print); single issues for individuals are £21/€30 and for institutions £44/€63. All inquiries about subscriptions should be sent to Journals Customer Service Department, Oxford Journals, Great Clarendon Street, Oxford OX2 6DP, UK, Tel: +44 (0) 1865-35-3907, e-mail: jnl.cust.serv@oup.com. In the Americas, please contact Journals Customer Service Department, Oxford Journals, 4000 CentreGreen Way, Suite 310, Cary, NC 27513, USA. Tel: 800-852-7323 (toll-free in USA/Canada) or 919-677-0977, e-mail: jnlorders@oup.com.

MEMBERSHIP INFORMATION: The ASCP membership fees for pathologists are as follows: fellow membership is \$349; fellow membership plus 1-year unlimited online CE is \$519; 2-year fellow membership is \$675; and 2-year fellow membership plus 2-year unlimited online CE is \$1,015. The ASCP membership fees for laboratory professionals are as follows: newly certified membership is \$49; annual membership is \$99; annual membership plus 1-year unlimited online CE is \$129; 3-year membership is \$349. All inquiries about membership should be sent to American Society for Clinical Pathology, 33 West Monroe Street, Suite 1600, Chicago, IL 60603, Tel: 312-541-4999, e-mail: ascp@ascp.org.

CLAIMS: Publisher must be notified of claims within four months of dispatch/ order date (whichever is later). Subscriptions in the EEC may be subject to European VAT. Claims should be made to Laboratory Medicine, Journals Customer Service Department, Oxford University Press, 4000 CentreGreen Way, Suite 310, Cary, NC 27513, USA, Tel: 800-852-7323 (toll-free in USA/Canada) or 919-677-0977, e-mail: jnlorders@oup.com.

Laboratory Medicine is published bimonthly by Oxford University Press (OUP), on behalf of the ASCP, a not-for-profit corporation organized exclusively for educational, scientific, and charitable purposes. Devoted to the continuing education of laboratory professionals, *Laboratory Medicine* features articles on the scientific, technical, managerial, and educational aspects of the clinical laboratory. Publication of an article, column, or other item does not constitute an endorsement by the ASCP of the thoughts expressed or the techniques, organizations, or products described therein. *Laboratory Medicine* is indexed in the following: MEDLINE/PubMed, Science Citation Index, Current Contents—Clinical Medicine, and the Cumulative Index to Nursing and Allied Health Literature.

Laboratory Medicine is a registered trademark. Authorization to photocopy items for internal and personal use, or the internal and personal use of specific clients, is granted by ASCP Press for libraries and other users registered with the Copyright Clearance Center (CCC) Transactional Reporting Service, provided that the base fee of USD 15.00 per copy is paid directly to the CCC, 222 Rosewood Drive, Danvers, MA 01923, 978.750.8400. In the United States prior to photocopying items for educational classroom use, please also contact the CCC at the address above.

Printed in the USA

© 2023 American Society for Clinical Pathology (ASCP)

Advertising Sales Office Classified and Display Advertising

CORPORATE ADVERTISING
Jane Liss
732-890-9812
jliss@americanmedicalcomm.com

RECRUITMENT ADVERTISING
Lauren Morgan
267-980-6087
lmorgan@americanmedicalcomm.com

ASCP

Laboratory Medicine
33 West Monroe Street, Suite 1600
Chicago, IL 60603

T: 312-541-4999
F: 312-541-4750

EDITORIAL

- 553 **Designer Drugs**
Amadeo J. Pesce, Kevin Krock

SPECIAL REPORT

- 555 **Interprofessional Education in NAACLS MLT and MLS Programs: Results of a National Survey**
Shafisha Bamfield-Cummings, Kendra Bufkin, Stephanie Jones, Giti Bayhaghi, Hari Kashyap, Gianluca De Leo

SCIENCE

- 562 **Identification of Differential Metabolites Between Type 2 Diabetes and Postchronic Pancreatitis Diabetes (Type 3c) Based on an Untargeted Metabolomics Approach**
Liang Qi, Zheng Ye, Hao Lin
- 574 **Application of the FMEA Method in Improving the Quality Management of Emergency Complete Blood Count Testing**
Shuangshuang Lv, Yingqian Sun, Jian Zhang, Tingting Jin, Xiaxuan Hu
- 582 **Evaluation of Serum Creatinine Levels With Reference Change Value in Patients Receiving Colistin Treatment**
Havva Yasemin Cincolat, Sevil Alkan, Hatice Betül Altinisik, Dilek Ulker Cakir, Hamdi Oguzman
- 587 **Oxidative Stress Levels and Dynamic Thiol-Disulfide Balance in Preterm Newborns With Bronchopulmonary Dysplasia**
Mehmet Semih Demirtas, Fatih Kilicbay, Huseyin Erdal, Gaffari Tunc
- 593 **Diagnostic Performance of 10 Mathematical Formulae for Identifying Blood Donors With Thalassemia Trait**
Egarit Noulisri, Surada Lerdwana, Duangdao Palasuwan, Attakorn Palasuwan
- 598 **Evaluation of Methods to Eliminate Analytical Interference in Multiple Myeloma Patients With Spurious Hyperphosphatemia**
Xin Tian, Li Zhao, Jin Ma, Jie Lu, Tian-yi Zhu, Yan Liu, Hong-xun Sun
- 603 **The Importance of the Trisomy 21 Local Cutoff Value Evaluation for Prenatal Screening in the Second Trimester of Pregnancy**
Yiming Chen, Yijie Chen, Long Sun, Liyao Li, Wenwen Ning
- 608 **Serum Aspartate Aminotransferase Is an Adverse Prognostic Indicator for Patients With Resectable Pancreatic Ductal Adenocarcinoma**
Meifang He, Yin Liu, Hefei Huang, Jiali Wu, Juehui Wu, Ruizhi Wang, Dong Wang
- 613 **Serum Expression of Tumor Marker CA242 in Patients With Different Gynecological Diseases**
Jing Zhu, Huidan Li
- 618 **A Population-Based Characterization Study of Anti-Mitochondrial M2 Antibodies and Its Consistency With Anti-Mitochondrial Antibodies**
En-yu Liang, Miao Liu, Pei-feng Ke, Guang Han, Cheng Zhang, Li Deng, Yun-xiu Wang, Hui Huang, Wu-jiao Huang, Rui-ping Liu, Guo-hua Li, Ze-min Wan, Yi-ting He, Min He, Xian-zhang Huang
- 626 **Serum Ribonucleotide Reductase Subunit M2 in Patients With Chronic Liver Diseases and Hepatocellular Carcinoma**
Xuehang Jin, Wei Yu, Ange Wang, Yunqing Qiu
- 633 **Associations Between Apolipoprotein B/A1 Ratio, Lipoprotein(a), and the Risk of Metabolic-Associated Fatty Liver Diseases in a Korean Population**
Kyoung-Jin Park

- 638 **Clinical Role of Serum Tumor Markers SCC, NSE, CA 125, CA 19-9, and CYFRA 21-1 in Patients With Lung Cancer**
Aiwen Sun
- 646 **Semaphorin 3A Levels in Vascular and Nonvascular Phenotypes in Systemic Sclerosis**
Mehmet Kayaalp, Abdulsamet Erden, Hakan Apaydin, Serdar Can Güven, Berkan Armağan, Merve Çağlayan Kayaalp, Esma Andac Uzdogan, Şeymanur Ala Enli, Ahmet Omma, Orhan Kucuksahin
- 652 **Comparison of the Optimized Direct Spectrophotometric Serum Prolidase Enzyme Activity Assay Method With the Currently Used Spectrophotometric Assay Methods and Liver Fibrosis Indexes to Distinguish the Early Stages of Liver Fibrosis in Patients With Chronic Hepatitis B Infection**
Huseyin Kayadibi, Ibrahim Hakki Köker, Zuhal Guzin, Hakan Şentürk, Sakine Candan Merzifonlu, Ali Tüzün İnce

CORRECTION

- 659 **Correction to: A Meta-Analysis of the Accuracy of Xpert MTB/RIF in Diagnosing Intestinal Tuberculosis**

The following are online-only papers that are available as part of Issue 54(6) online.

- e170 **Is Very High Platelet Count Always Associated With Essential Thrombocythemia? An Unusual Presentation in a Child**
Elif Habibe Aktekin, Nalan Yazici, İlknur Kozanoğlu, Ayşe Erbay
- e177 **Plasmablastic Transformation of Chronic Lymphocytic Leukemia: A Review of Literature and Report on 2 Cases**
Anurag Khanna, Bradley R. Drumheller, George Deeb, Ethan Wade Tolbert, Saja Asakrah
- e186 **A Novel Internal Training Program Using Kern's 6-Step Approach to Curriculum Development for Medical Laboratory Scientists Training to be International Quality Assurance/Quality Control Coordinators**
Anne Leach, Josephine Shim, Kristin Murphy, Mandana Godard, Felix Ortiz, Mark Swartz, Lori J. Sokoll
- e197 **The Exclusion of Anti-D Alloantibody in a Suspected Anti-G Antibody in a Pregnant 28-Year-Old Odiya Indian Woman**
Kella Nivedita, Somnath Mukherjee, Satya Prakash, Ansuman Sahu, Debashish Mishra
- e201 **Evusheld, a SARS-CoV-2 Spike Protein-Directed Attachment Inhibitor, Appears in Serum Protein Electrophoresis and Immunofixation: A Case Study**
Sumit K. Shah, Hoda A. Hagrass
- e204 **Utilization of an Immunochromatographic Lateral Flow Assay for Rapid Detection of Carbapenemase Production in Gram Negative Bacilli**
Emily Sullivan, Maria D. Macias Jimenez, Nicholas M. Moore
- e207 **Impact of COVID-19 Pandemic on Accredited Programs and Graduates Who Sat for the American Society for Clinical Pathology-Board of Certification Examination: Program Directors' Perspective**
Dana Duzan, Karen Fong, Vicki S. Freeman, Nancy Goodyear, Teresa S. Nadder, Amy Spiczka, Teresa Taff, Patricia Tanabe



ON THE COVER: Statistics compiled by the Centers for Disease Control and Prevention reveal that overdoses with synthetic opioids caused nearly 71,000 deaths in the United States in 2021, a total that is almost 23 times the number in 2013 and representing a 22% increase over 2020. This staggering increase in overdose deaths is being driven by the widespread availability of fentanyl and its derivatives that are up to 100 times more potent than morphine and often contaminate common street drugs such as heroin, producing a concoction with unknown and unpredictable lethality. Detection and quantitation of these fentanyl analogs in blood and urine is challenging because of their low concentration and structural diversity. In this issue of *Laboratory Medicine*, Drs Amadeo Pesce and Kevin Krock of the Precision Diagnostics laboratory in San Diego argue for a more rational reimbursement structure for drug testing that will sustain the capability of laboratories to detect and measure these drugs.

Designer drugs

Amadeo J. Pesce, PhD, Kevin Krock, PhD

Precision Diagnostics, San Diego, US. Corresponding author: Amadeo J. Pesce; pesceaj@ucmail.uc.edu

Abbreviations: LC-MS/MS, liquid chromatography–tandem mass spectrometry; TOF, time of flight

Laboratory Medicine 2023;54:553–554; <https://doi.org/10.1093/labmed/Imad087>



Amadeo J. Pesce, PhD

Designer drugs are synthetic compounds developed to mimic the physiologic effects of other abused drugs. Many designer drugs are chemically similar to other abused drugs but are modified to avoid being classified as illegal. Moreover, they are often altered in ways that render them undetectable by conventional drug screening tests.

Most designer drugs try to imitate opiates or cocaine, ecstasy, and other stimulants.

Unfortunately, it is also possible to overdose on designer drugs.¹ The unpredictable pharmacology of these synthetic drugs puts users at risk of dangerous side effects, including overdose and death.² One of the greatest challenges associated with detecting designer drugs is the fact that they are developed in secret. Therefore, the ingredients, chemical structure, and potency of the drugs are largely unknown. The US Drug Enforcement Administration recognizes 7 different types of designer drugs: cannabinoids, phenethylamines, phencyclidines (or arylcyclohexamines), tryptamines, piperazines, pipradrols, and N-ring systems. Most laboratories using liquid chromatography–tandem mass spectrometry (LC-MS/MS) for definitive drug testing are targeting well-known drugs and are not configured to detect or quantify these synthetically modified drugs.

These designer drugs can be detected in urine using newer analytical methods such as time of flight (TOF) or Orbitrap mass spectrometry. These technologies require more sophisticated equipment and are more labor intensive than definitive methods such as LC-MS/MS. Currently, the reimbursement for the Current Procedural Terminology (CPT) code applied to drug screening is only \$60. This reimbursement was established for the historic immunoassay screens and the older ToxiLab thin-layer chromatography method. The newer

technologies identify over 1000 possible drugs, including designer drugs, but it is a labor-intensive approach to drug testing.³ The current reimbursement is too low to be financially viable for a commercial or hospital laboratory seeking to use more advanced technologies to detect drugs. There is a need to create a CPT code that pertains to use of the newer technologies for toxicological analysis so laboratories that wish to include designer drugs in their drug testing panels can be reasonably reimbursed. We believe there are enough data on overdose deaths from designer drugs to warrant testing for them in specific patient populations, such as those in drug rehabilitation facilities. Reimbursement would require medical necessity, and we propose the following guidelines:

Rationale (medical necessity for new CPT code and reimbursement):

1. Patient is in a pain clinic or drug rehabilitation facility
2. Clinical signs of impairment
3. Positive immunoassay screen, but negative by the usual targeted LC-MS/MS analysis of common drugs
4. Suspicion of designer drug use
5. Physician (provider) requests further testing

As an example, there are numerous fentanyl derivatives available to patients that we cannot identify with our current targeted testing, and a substantial portion of current opioid deaths are due to fentanyl.⁴ The use of TOF-based analytical methods would enable better detection of designer drug use. Current reimbursement makes this unworkable.

REFERENCES

1. What are designer drugs? (definition, examples & dangers). Accessed July 9, 2023. <https://americanaddictioncenters.org/designer-drugs-addiction>
2. Luethi D, Liechti ME. Designer drugs: mechanism of action and adverse effects. *Arch Toxicol*. 2020;94(4):1085–1133. <https://doi.org/10.1007/s00204-020-02693-7>
3. Krotulski AJ, Varnum SJ, Logan BK. Sample mining and data mining: combined real-time and retrospective approaches for the identification of emerging novel psychoactive substances. *J Forensic Sci*. 2020;65(2):550–562. <https://doi.org/10.1111/1556-4029.14184>
4. Kyle, P. Current trends in designer drug use. Ask The Expert: May 2023 *Clinical Laboratory News*. Accessed June 20, 2023. <https://www.aacc.org/cln/articles/2023/may/current-trends-in-designer-drug-use>

ABOUT THE AUTHOR

Amadeo J. Pesce, PhD, DABCC, is the Laboratory Director at Precision Diagnostics LLC in San Diego, CA. He has 45 years of experience in toxicology testing. He also holds the position of adjunct professor in the Department of Pathology and Laboratory Medicine at the UCSD School of Medicine. He obtained his bachelor's degree from MIT and his doctorate from Brandeis University. He was a National Institutes of Health postdoctoral fellow at the University of Illinois (Urbana) under the direction of Dr Gregorio Weber. Dr Pesce has published or edited more than 20 books or monographs in the field of Clinical Chemistry and is the author

or coauthor of more than 270 papers in the field of Clinical Chemistry and Clinical Toxicology.

Dr Pesce has been the recipient of several awards, including Established Investigator, American Heart Association New York, the Alvin Dubin Award from National Academy of Clinical Biochemistry, the Diploma of Honor from the Association of Clinical Scientists, and the Irving Sunshine Award from the International Association of Therapeutic Drug Monitoring and Clinical Toxicology.

Dr Pesce and his staff have been performing urine drug testing for many years, most recently focusing on the needs of pain patients and those undergoing addiction treatment.

Interprofessional Education in NAACLS MLT and MLS Programs: Results of a National Survey

Shafisha Bamfield-Cummings, MLS(ASCP),¹ Kendra Bufkin, MS, MHS, MLS(ASCP),² Stephanie Jones, BSN, MBA,³ Giti Bayhaghi, MHS, MLS(ASCP)^{CM},⁴ Hari Kashyap, MSOT, MBA, CLT-LANA, OTR/L,⁵ and Gianluca De Leo, PhD, MBA^{3,*}

¹Cytogenetic Department, ²Clinical Pathology—Core Hematology, ³College of Allied Health Sciences, ⁴Clinical Laboratory Program, and ⁵Georgia Cancer Center, Augusta University Medical Center, Augusta, GA, US. *To whom correspondence should be addressed: gdeleo@augusta.edu.

Keywords: interprofessional education, attitudes, beliefs, medical laboratory scientists, medical laboratory technicians, educational programs

Abbreviations: IPE, interprofessional education; IPEC, Interprofessional Education Collaborative Expert Panel; NAACLS, National Accreditation Agency for Clinical Laboratory Sciences; MLA, Medical Laboratory Assistant; MLS, Medical Laboratory Science; DCLS, Doctorate of Clinical Laboratory Scientist; MLT, Medical Laboratory Technician; CG, Cytogenetic Technologist; DMS, Diagnostic Molecular Scientist; HT, Histotechnician; HTL, Histotechnologist; Path A, Pathologists' Assistant; Phleb, Phlebotomist; HCP, health care professional; ACOTE, Accreditation Council for Occupational Therapy Education; APPs, advanced practice providers; EMS, emergency medical services; PA, physician assistant; NP, nurse practitioner; CRNA, certified registered nurse anesthetist

Laboratory Medicine 2023;54:555-561; <https://doi.org/10.1093/labmed/lmad006>

ABSTRACT

Background: Interprofessional education is essential for students enrolled in health care professional programs.

Objectives: We assessed the attitudes towards and the beliefs about interprofessional education (IPE) among program directors of medical laboratory science (MLS) and medical laboratory technician (MLT) programs accredited by the National Accrediting Agency for Clinical Laboratory Sciences (NAACLS). We also investigated the inclusion of IPE in the curricula of such programs.

Methods: We emailed the link to an anonymous 22-item cross-sectional survey to 468 program directors and tabulated the responses.

Results: Program directors who support the need to include IPE within the curricula of MLT and MLS programs showed a generally positive attitude towards IPE. The beliefs about IPE among our respondents were not homogeneous. Program directors who have not yet implemented IPE in the curriculum may not have had an opportunity to experience the practical benefits of IPE.

Conclusion: Although barriers to IPE implementation exist, half of the respondents reported having already implemented IPE within their curricula.

Interprofessional education (IPE) is defined as a model in which students from 2 or more disciplines acquire knowledge from each other to generate successful collaboration and improve patient care.¹ In 2011, the Interprofessional Education Collaborative Expert Panel (IPEC) identified 4 core domains of competency: values and ethics, roles and responsibilities, teamwork and team-based care, and interprofessional communication.² In 2016, IPEC decided to broaden its interprofessional competencies to improve the patient experience of care, improve the health of patient populations, and reduce the per capita cost of health care.³

The National Accreditation Agency for Clinical Laboratory Sciences (NAACLS) grants public recognition to education programs that meet established education standards in the following clinical laboratory science disciplines: Medical Laboratory Assistant (MLA), Medical Laboratory Science (MLS), Doctorate of Clinical Laboratory Scientist (DCLS), Medical Laboratory Technician (MLT), Cytogenetic Technologist (CG), Diagnostic Molecular Scientist (DMS), Histotechnician (HT), Histotechnologist (HTL), Pathologists' Assistant (Path A), and Phlebotomist (Phleb).

IPE is essential for students enrolled in health care professional (HCP) educational programs who will transition into clinical settings after graduation.⁴ An explanatory case study published in 2017⁵ reported that students in a clinical laboratory science program at a tertiary-care university hospital desire a curriculum that promotes respect, communication, and equality in their field of study. The study results also reported that clinical laboratory students felt less valued during clinical rotations than students in other HCP programs. IPE activities and earlier interactions with other HCPs may help medical laboratory students feel valued.⁶ Recurrent challenges for IPE integration in laboratory science programs are discipline-specific curricula, content saturation, and difficulties with fully integrating interprofessional experiences.⁵

Medical laboratory scientists and medical laboratory technicians play a crucial role in patient outcomes; they are essential in a team-based health care approach. They may work in various locations: hospitals, clinics, forensic laboratories, public health research laboratories, and

pharmaceutical laboratories. According to the United States Bureau of Labor, the number of jobs in 2020 for medical laboratory scientists and medical laboratory technicians totaled more than 335,500. The job outlook for 2020–2030 is expected to grow 11% faster than the national average for all occupations.⁷ Previous research study reports have highlighted faculty attitudes and beliefs about IPE among faculty members in nursing^{8,9} and in several allied HCP programs, such as respiratory therapy,^{10,11} nutrition,¹² occupational therapy,¹³ physical therapy,¹⁴ and dental hygiene.¹⁵

The goals of our research were to assess the inclusion of interprofessional education and collaboration in the curricula of NAACLS MLS and MLT programs, to determine IPE and collaboration attitudes and beliefs among NAACLS MLT and MLS program directors, and to identify differences among MLS/MLT programs and program directors based on the inclusion of IPE and collaboration in the curricula.

Methods

The target population of this research study was the program directors of NAACLS MLS and MLT programs in the United States. Using a Google Chrome plug-in called webscraper.io,¹⁶ we downloaded a listing of all program directors, their names, and their email addresses from the NAACLS website.¹⁷ The data were filtered to identify only MLS and MLT programs. MLT programs are associate degree-level programs only; MLS programs can be bachelor's or master's degree-level programs. Next, we performed data validation. We removed 13 duplicates because some program directors oversaw MLS and MLT programs. One program director was excluded from the survey because the NAACLS listed their program as being on administrative probation. The IRB office of our institution deemed this study as being exempt (IRB #1833916).

Survey Development

A 22-item survey was developed based on an extensive literature review and on previously used instruments.^{8,10–15} Questions were grouped into the following 6 sections: Section 1 asked questions about the rank of the program directors, their experience teaching, their experience in clinical settings, and the percentage of time they spent on program director activities. Section 2 solicited information about degree level, length of accreditation, current enrollment, institution type, and the current state of IPE in the curriculum. Sections 3 through 5 included questions that focused on the current implementation of IPE, the attitudes of the program directors toward IPE, and the beliefs of those individuals about IPE in the academic setting. Section 6 was created to identify what might prevent the implementation of IPE curricula.

We used Qualtrics XM software to develop the survey and to distribute it anonymously in January 2022. One reminder email was sent out 2 weeks after the initial contact to increase the return rate; the survey remained open for 5 weeks. The survey took less than 15 minutes to complete. Subjects were allowed to skip questions. Partial data were collected.

Data Repository and Data Analysis

The dataset¹⁸ used in this research is available on the secure cloud-based repository Mendeley Data. We used descriptive statistics and cross-tabulations to analyze the data. Then, we used the Mann-Whitney *U* test to compare the nonparametric questionnaire responses across

the different subgroups. We collectively reported data from MLS/MLT program directors and used SPSS software (IBM) to perform the data analysis.

Results

The survey was sent by email to 468 program directors. Four emails were returned as undeliverable. A total of 120 program directors completed the survey, for a response rate of 25.6%.

Program Director Demographics and Program Characteristics

All 120 program directors answered the questions in the demographic and program characteristics sections of the survey. **TABLE 1** provides detailed information about the demographics of the program directors and the characteristics of their programs. Of the 62 program directors who identified themselves with a rank of associate or full professor, 36 (58.1%) had already established IPE in their curriculum. Half of the respondents (61 [50.8%]) had more than 15 years of teaching experience, and slightly fewer than half of those people (28 [45.9%]) had implemented IPE in their curricula. Almost half of the respondents (57 [47.5%]) had more than 15 years of clinical experience, and slightly fewer than half of those people (26 [45.6%]) had implemented IPE in their curricula.

One-fifth of the respondents (25 [20.8%]) reported working on program director duties during half of their work time. The remaining respondents reported being equally split between working on program director duties less than half of their time (48 [40.0%]) and more than half of their time (47 [39.2%]).

Half of the program directors whose university awards a bachelor's level MLS degree (35 [53.8%]) have already implemented IPE in their curriculum. Most of the master's degree programs (14 [60.9%]) surveyed have also already implemented IPE in their curriculum. Approximately half of program directors of programs with more than 15 years of accreditation (43 [47.3%]) reported that they have already implemented IPE in their curriculum. Programs with more than 25 students (50 [41.7%]) have IPE established in their program more than half of the time (31 [62.0%]). More than three-quarters of respondents (95 [79.2%]) reported being program directors at a public institution, and slightly more than half of them (50 [52.6%]) have IPE currently implemented in their curriculum. Approximately three-fourths of respondents (84 [70.0%]) reported that their institution is not part of a health care center. Among those respondents, fewer than half (35 [41.7%]) already offer IPE in their curriculum. More than half of the program directors who have already implemented IPE (25 [62.5%]) reported having space in the curriculum to teach IPE. In comparison, more than half of the program directors who have not already implemented IPE (36 [65.5%]) reported not having space in the curriculum to teach IPE.

Using a 5-point Likert scale made up of the options never, rarely, most of the time, sometimes, and always, the program directors who had already implemented IPE in their curriculum were asked how often they use 4 instructional methods: case study, clinic, simulation, and a combination of methods to teach IPE. Case study was the method selected most often, followed by a combination of methods and simulation. Clinic was often selected rarely or never. More than three-fourths of program directors (97 [81.0%]) identified the following barriers to

TABLE 1. Program Director Demographics and Program Characteristics^a

Program Director Demographics (n = 120)	Total	IPE in Curriculum	No IPE in Curriculum
Faculty rank			
Lecture/instructor/adjunct	42 (35.0)	16 (38.1)	26 (61.9)
Assistant professor	16 (13.3)	5 (31.2)	11 (68.8)
Associate professor	25 (20.8)	16 (64.0)	9 (36.0)
Professor	37 (30.8)	20 (54.1)	17 (45.9)
Teaching experience, y			
<5	13 (10.8)	9 (69.2)	4 (30.8)
6-10	28 (23.3)	11 (39.3)	17 (60.7)
11-15	18 (15.0)	9 (50.0)	9 (50.0)
>15	61 (50.8)	28 (45.9)	33 (54.1)
Clinical experience, y			
0	2 (1.7)	2 (100)	0
<5	9 (7.5)	7 (77.8)	2 (22.2)
6-10	23 (19.2)	11 (47.8)	12 (52.2)
11-15	29 (24.2)	11 (37.9)	18 (62.1)
>15	57 (47.5)	26 (45.6)	31 (54.4)
Program Characteristics (n = 120)	Total	IPE in Curriculum	No IPE in Curriculum
Degree level ^b			
Associate MLT	45 (37.5)	16 (35.6)	29 (64.4)
Bachelor's MLS	65 (54.2)	35 (53.8)	30 (46.2)
Master's MLS	23 (19.2)	14 (60.9)	9 (39.1)
Accreditation, y			
<5	8 (6.7)	5 (62.5)	3 (37.5)
6-10	10 (8.3)	5 (50.0)	5 (50.0)
11-15	11 (9.2)	4 (36.4)	7 (63.6)
>15	91 (75.8)	43 (47.3)	48 (52.7)
No. of students in program			
<10	27 (22.5)	10 (37.0)	17 (63.0)
11-15	16 (13.3)	7 (43.8)	9 (56.3)
16-20	12 (10.0)	4 (33.3)	8 (66.7)
21-25	14 (11.7)	4 (28.6)	10 (71.4)
>25	50 (41.7)	31 (62.0)	19 (38.0)
Prefer not to answer	1 (0.8)	1 (100)	0
Type of institution			
Public	95 (79.2)	50 (52.6)	45 (47.4)
Private	16 (13.3)	4 (25.0)	12 (75.0)
Other	9 (7.5)	3 (33.3)	6 (66.7)
Is the institution part of a health care center?			
No	84 (70.0)	35 (41.7)	49 (58.3)
Yes	34 (28.3)	21 (61.8)	13 (38.2)
Prefer not to answer	2 (1.7)	1 (50.0)	1 (50.0)

IPE, interprofessional education; MLS, medical laboratory sciences; MLT, medical laboratory technician.

^aData are given as No. (%).^bSome programs have multiple degree options; total is >120.

implementing IPE in their curricula: logistics (77.3%), faculty resources (75.3%), curricular alignment and integration (64.9%), funding (58.8%), faculty buy-in (46.4%), credit for faculty time (44.3%), administrative support (40.2%), assessment of impact of IPE initiatives (18.6%), and accreditation limitation (19.6%).

TABLE 2 provides details on the current IPE collaborations of MLS and MLT programs surveyed. More than half of the program directors (80/117 [68.4%]) who answered the question about collaboration reported they would like to see a greater emphasis on IPE in their curricula. Among those program directors, approximately half (44 [55.0%]) reported they do not have IPE in their curriculum yet, and the other half (36 [45.0%]) reported they do. Program directors reported having active collaborations with other health care-related programs even when IPE has not been formally introduced in their curricula. Specifically, program directors reported they are currently collaborating with the departments of nursing (31 [25.8%]), pharmacy (18 [15.0%]), and physical therapy (17 [14.2%]), and the medical school (14 [11.7%]). Slightly less than half of program directors (48 [40.0%]) reported they do not collaborate with any other program.

Attitudes Towards IPE

TABLE 3 provides details on the attitudes of the program directors towards IPE. More than half of respondents somewhat disagreed or strongly disagreed (63 [64.3%]) that clinical problem-solving can only be learned effectively when students are taught within their individual departments or schools. Respondents who already have IPE implemented in their programs agreed less with the statement than those who have not implemented IPE ($P < .001$). More than half of the respondents somewhat agreed or strongly agreed (83 [84.7%]) that learning with students in other health care specialties helps MLS/MLT students become more effective members of a health care team. Respondents who are already offering IPE in their programs agreed more with the statement ($P = .02$). Most of the respondents somewhat agreed or strongly agreed (89 [90.8%]) that for small groups learning to work together, students need to trust and respect each other. Respondents already offering IPE in their programs agreed more with the statement ($P = .02$). Most of the respondents somewhat agreed or strongly agreed (90 [91.8%]) that implementing IPE will help students think positively about other professionals within their curriculum. Respondents already offering

TABLE 2. IPE Emphasis and Collaboration^a

Opinion (n = 117)	Total	IPE in Curriculum	No IPE in Curriculum
Would you like to see a greater emphasis on IPE in your curriculum?			
Yes	80 (68.4)	36 (45.0)	44 (55.0)
No	24 (20.5)	13 (54.2)	11 (45.8)
Prefer not to answer	13 (11.1)	6 (46.1)	7 (53.9)
Current Collaboration ^b	Total	IPE in Curriculum	No IPE in Curriculum
Which programs do you currently collaborate with?			
None	48 (40.0)	6 (12.5)	42 (87.5)
Nursing	31 (25.8)	25 (80.6)	6 (19.4)
Pharmacy	18 (15.0)	13 (72.2)	5 (27.8)
Physical therapy	17 (14.2)	14 (82.4)	3 (17.6)
Medical school	14 (11.7)	13 (92.9)	1 (7.1)
APPs ^c	13 (10.8)	11 (84.6)	2 (15.4)
Respiratory therapy	13 (10.8)	10 (76.9)	3 (23.1)
Occupational therapy	13 (10.8)	11 (84.6)	2 (15.4)
Dentistry	4 (3.3)	3 (75.0)	1 (25.0)
Social work	6 (5.0)	6 (100)	0
Speech and language	9 (7.5)	8 (88.9)	1 (11.1)
Dental hygiene	11 (9.2)	9 (81.8)	2 (18.2)
Prefer not to answer	0	0	0
Other ^d	21 (17.5)	18 (85.7)	3 (14.3)
Radiology	6 (28.6)	6 (100)	0
Public health	4 (19.1)	3 (75.0)	1 (25.0)
Nutrition	3 (14.3)	3 (100)	0
EMS	3 (14.3)	3 (100)	0

APPs, advanced practice providers; CRNA, certified registered nurse anesthetist; EMS, emergency medical services; IPE, interprofessional education; NP, nurse practitioner; PA, physician assistant.

^aData are given as No. (%).

^bn = 120. Some programs collaborate with multiple programs; total is >100%.

^cIncludes PA, NP, CRNA, etc.

^dOnly programs that were selected at least 3 times are shown.

TABLE 3. Attitudes of Program Directors Towards IPE^a

Statement	No.	Strongly Disagree	Somewhat Disagree	Neither Agree nor Disagree	Somewhat Agree	Strongly Agree
Clinical problem-solving can only be learned effectively when students are taught within their individual department/school ^b	98	20 (20.4)	43 (43.9)	23 (23.5)	8 (8.2)	4 (4.1)
IPE in curriculum	46	14 (30.4)	22 (47.8)	7 (15.2)	3 (6.5)	0
No IPE in curriculum	52	6 (11.5)	21 (40.4)	16 (30.8)	5 (9.6)	4 (7.7)
Learning with students in other health care professions helps MLS/MLT students become more effective members of a health care team ^c	98	1 (1.0)	3 (3.1)	11 (11.2)	29 (29.6)	54 (55.1)
IPE in curriculum	46	1 (2.2)	0	4 (8.7)	10 (21.7)	31 (67.4)
No IPE in curriculum	52	0	3 (5.8)	7 (13.5)	19 (36.5)	23 (44.2)
For a small group learning to work together, students need to trust and respect each other ^c	98	2 (2.0)	2 (2.0)	5 (5.1)	30 (30.6)	59 (60.2)
IPE in curriculum	46	1 (2.2)	0	1 (2.2)	11 (23.9)	33 (71.7)
No IPE in curriculum	52	1 (1.9)	2 (3.8)	4 (7.7)	19 (36.5)	26 (50.0)
Interprofessional learning will help students think positively about other HCPs ^b	98	0	1 (1.0)	7 (7.1)	35 (35.7)	55 (56.1)
IPE in curriculum	46	0	1 (2.2)	1 (2.2)	13 (28.3)	31 (67.4)
No IPE in curriculum	52	0	0	6 (11.5)	22 (42.3)	24 (46.2)
Patients would ultimately benefit if health care students work together to solve patient problems ^c	97	0	3 (3.1)	6 (6.2)	25 (25.8)	63 (64.9)
IPE in curriculum	46	0	1 (2.2)	0	11 (23.9)	34 (73.9)
No IPE in curriculum	51	0	2 (3.9)	6 (11.8)	14 (27.5)	29 (56.9)
Interprofessional learning integration with health care students will increase their ability to understand clinical problems	97	2 (2.1)	1 (1.0)	13 (13.4)	34 (35.1)	47 (48.5)
MLS students would benefit from working on small group projects with other health care students	98	0	6 (6.1)	11 (11.2)	42 (42.9)	39 (39.8)
Interprofessional learning will help students to understand their own professional limitations	98	2 (2.0)	2 (2.0)	18 (18.4)	42 (42.9)	34 (34.7)
Communication skills should be learned with integrated classes of health care students	98	2 (2.0)	3 (3.1)	14 (14.3)	39 (39.8)	40 (40.8)

HCPs, health care professionals; IPE, interprofessional education; MLS, medical laboratory sciences; MLT, medical laboratory technician.

^aData are given as No. (%).

^bStatistically significant at $P < .001$ between programs that have already IPE in the curriculum and programs that do not.

^cStatistically significant at $P < .05$ between programs that have already IPE in the curriculum and programs that do not.

IPE in their programs agreed more with the statement ($P = .03$). Most of the respondents somewhat agreed or strongly agreed (88 [90.7%]) that patients would ultimately benefit if health care students worked together to solve patient problems by implementing IPE within their curriculum. Respondents who are already offering IPE in their programs agreed more with the statement ($P = .04$).

We found no statistically significant difference between program directors who have already and those who have not yet implemented IPE in their curricula in the answers to the remaining questions related to attitudes towards IPE. In total, 81 respondents (83.6%) selected strongly agreed or somewhat agreed for the question that asked whether IPE integration with health care students will increase their ability to understand clinical problems. For the question asking whether students in MLS programs would benefit from working on small group projects with other health care students, 81 respondents (82.7%) selected strongly agreed or somewhat agreed. For the question of whether IPE will help students to understand their professional limitations, 76 respondents (77.6%) selected strongly agreed or somewhat agreed. For the question asking whether communication skills should be learned within integrated classes of health care students, 79 respondents (80.6%) selected strongly agreed or somewhat agreed.

Beliefs About IPE

TABLE 4 provides details on the beliefs of the program directors about IPE. More than half of the respondents somewhat agreed or strongly agreed (66 [68.8%]) that it is important for the academic health center campuses to provide IPE opportunities. Respondents who are already offering IPE in their programs agreed more with the statement ($P < .001$). Half of the respondents somewhat disagreed or strongly disagreed (49 [51.1%]) that NAACLS should mandate IPE in the CLS curriculum. Respondents who are already offering IPE in their programs agreed more with the statement ($P = .01$). Half of the respondents somewhat agreed or strongly agreed (48 [50.0%]) that their institutions have the resources to implement IPE. Respondents who are already offering IPE in their programs agreed more with the statement ($P = .01$). More than half of the respondents somewhat disagreed or strongly disagreed (55 [57.3%]) with the statement that their program has the resources and personnel to teach IPE courses. Respondents who are already offering IPE in their programs agreed more with the statement ($P = .03$).

No statistically significant difference between program directors who have already and those who have not yet implemented IPE in their curricula was found in the remaining questions related to beliefs about IPE. In total, 70 respondents (72.9%) selected strongly agreed

TABLE 4. Beliefs of Program Directors About IPE^a

Statement	No.	Strongly Disagree	Somewhat Disagree	Neither Agree nor Disagree	Somewhat Agree	Strongly Agree
It is important for academic health care center campuses to provide interprofessional learning opportunities ^b	96	0	5 (5.2)	25 (26.0)	45 (46.9)	21 (21.9)
IPE in curriculum	45	0	3 (6.7)	6 (13.3)	20 (44.4)	16 (35.6)
No IPE in curriculum	51	0	2 (3.9)	19 (37.3)	25 (49.0)	5 (9.8)
NAACLS should mandate IPE in the CLS curriculum ^b	96	30 (31.3)	19 (19.8)	25 (26.0)	15 (15.6)	7 (7.3)
IPE in curriculum	45	10 (22.2)	5 (11.1)	16 (35.6)	9 (20.0)	5 (11.1)
No IPE in curriculum	51	20 (39.2)	14 (27.5)	9 (17.6)	6 (11.8)	2 (3.9)
My institution has the resources to implement IPE ^b	96	10 (10.4)	24 (25.0)	14 (14.6)	26 (27.1)	22 (22.9)
IPE in curriculum	45	2 (4.4)	10 (22.2)	4 (8.9)	15 (33.3)	14 (31.1)
No IPE in curriculum	51	8 (15.7)	14 (27.5)	10 (19.6)	11 (21.6)	8 (15.7)
My program has the resources and personnel to teach IPE courses ^c	96	17 (17.7)	38 (39.6)	17 (17.7)	18 (18.8)	6 (6.3)
IPE in curriculum	45	6 (13.3)	15 (33.3)	8 (17.8)	12 (26.7)	4 (8.9)
No IPE in curriculum	51	11 (21.6)	23 (45.1)	9 (17.7)	6 (11.8)	2 (3.9)
Faculty should be encouraged to participate in IPE courses	96	0	6 (6.3)	20 (20.8)	49 (51.0)	21 (21.9)
IPE courses are logistically difficult	96	3 (3.1)	15 (15.6)	22 (22.9)	37 (38.5)	19 (19.8)
Faculty members like teaching with faculty members from other academic departments	95	0	15 (15.8)	49 (51.6)	28 (29.5)	3 (3.2)
IPE efforts weaken program content	95	33 (34.7)	33 (34.7)	22 (23.2)	6 (6.3)	1 (1.1)
Accreditation requirements limit IPE efforts	95	11 (11.6)	26 (27.4)	30 (31.6)	21 (22.1)	7 (7.4)
IPE efforts require support from campus administration	96	2 (2.1)	1 (1.0)	5 (5.2)	41 (42.7)	47 (49.0)
Certain current curriculum requirements could be removed to make room for additional IPE content	96	19 (19.8)	25 (26.0)	22 (22.9)	25 (26.0)	5 (5.2)
IPE better utilizes resources	96	2 (2.1)	13 (13.5)	40 (41.7)	32 (33.3)	9 (9.4)

CLS, clinical laboratory science; IPE, interprofessional education; NAACLS, National Accreditation Agency for Clinical Laboratory Sciences.

^aData are given as No. (%).

^bStatistically significant at $P < .001$ between programs that have already IPE in the curriculum and programs that do not.

^cStatistically significant at $P < .05$ between programs that have already IPE in the curriculum and programs that do not.

or somewhat agreed for the question that asked whether faculty should be encouraged to participate in IPE courses. For the question asking whether interprofessional courses are logistically difficult, 56 respondents (58.3%) selected strongly agreed or somewhat agreed. For the question asking if IPE efforts require support from campus administration, the number was 88 (91.7%).

In total, 66 respondents (69.4%) selected strongly disagree or somewhat disagree for the question asking whether IPE efforts weaken program content. For the question asking whether accreditation requirements limit IPE efforts, that number was 37 (39.0%). Almost half of the respondents selected the option “neither agree nor disagree” for the question of whether faculty members like teaching with faculty members from other academic departments (49 [51.6%]) and for the question of whether IPE better utilizes resources (40 [41.7%]).

Conclusion

Overall, the program directors of MLS and MLT programs showed a positive attitude towards IPE. However, the beliefs about IPE were not homogeneous. In particular, the program directors were not in agreement on how much the accreditation requirements limit IPE efforts, on the potential effect of a mandate by NAACLS to offer IPE in the curricula, and whether there are current curriculum requirements that could be removed to make room for additional IPE. Program directors who have

not yet implemented IPE in the curriculum may not have had an opportunity to experience the practical benefits of IPE.

Also, program directors of MLS and MLT programs reported challenges in implementing IPE, while recognizing that IPE is important within their curricula. This result is analogous to what respiratory therapy faculty members have reported in a previous study report.¹⁰ As in the report of a previous research study conducted among program directors of nutrition programs,¹² MLS and MLT program directors believe that patients would ultimately benefit if health care students worked together to solve patient problems.

More than half of program directors of occupational therapy programs reported¹³ that they strongly agreed or agreed that the Accreditation Council for Occupational Therapy Education (ACOTE) should mandate IPE in the occupational therapy curriculum. However, only half of the MLS and MLT program directors in our survey disagreed or strongly disagreed that NAACLS should mandate IPE in the CLS curriculum, and one-fourth of the respondents neither agreed nor disagreed with that statement. MLS and MLT program directors believe that some current curriculum requirements could be removed to make room for additional IPE education; more of those respondents believe this, compared with program directors of physical therapy programs.¹⁴ As in the report of a previous research study conducted among dental hygiene faculty members,¹⁵ MLS and MLT program directors strongly support the idea that faculty members should be encouraged to participate in IPE courses.

Among other health care professions, MLS and MLT program directors reported currently collaborating with the nursing department the most. The strong connection with the nursing programs may be explained by the fact that the nursing department handles most of the specimen collections for the medical laboratory. We also note that it appears that programs without IPE have active collaborations with other programs, such as nursing, but such collaborations are not considered by their program directors to be IPE activities.

We investigated whether there were any statistically significant differences in attitudes and beliefs among programs directors of programs housed or not housed in health care centers. We only found 1 statistically significant difference ($P = .01$) for the belief “My institution has the resources to implement IPE,” with program directors of programs not housed in health care centers strongly or somewhat disagreeing (29 [44.6%]) more than program directors of programs housed in health care centers (5 [16.9%]). We did not observe any statistically significant differences for attitudes and beliefs between programs directors of MLS or MLT programs.

This research project has 2 major limitations: the survey response rate may not represent all NAACLS program directors, and the findings were based on self-reporting. However, we report that a large majority of MLS and MLT programs strongly agree or somewhat agree that implementing IPE will help students think positively about other professionals within their curriculum. Also, more than 50% of the respondents would like to see a greater emphasis on IPE in their curricula.

Conflict of Interest Disclosure

The authors have nothing to disclose.

REFERENCES

1. World Health Organization (WHO). *Framework for Action on Interprofessional Education and Collaborative Practice*. WHO; 2010.
2. Interprofessional Education Collaborative Expert Panel. Core competencies for interprofessional collaborative practice: Report of an expert panel. Interprofessional Education Collaborative Expert Panel, American Association of Colleges of Nursing; 2011.
3. Interprofessional Education Collaborative Expert Panel. Core competencies for interprofessional collaborative practice: Report of an expert panel. Interprofessional Education Collaborative Expert Panel, American Association of Colleges of Nursing; 2016.
4. Buring SM, Bhushan A, Broeseker A, et al. Interprofessional education: definitions, student competencies, and guidelines for implementation. *Am J Pharm Educ*. 2009;73(4):59. doi:10.5688/aj730459
5. Salazar JH. Interprofessional education themes in a clinical laboratory sciences curriculum. *Am Soc Clin Lab Sci*. 2017;30(2):99–104.
6. Weber BW, Mirza K. Leveraging interprofessional education to improve physician/laboratory cooperation and patient outcomes. *Med Sci Educ*. 2022;32(1):239–241. doi:10.1007/s40670-021-01496-4
7. Bureau of Labor Statistics USDoL. *Occupational Outlook Handbook, Medical Scientists*, 2022. <https://www.bls.gov/ooh/life-physical-and-social-science/medical-scientists.htm>. Accessed January 21, 2023.
8. Curran VR, Sharpe D, Forristall J. Attitudes of health sciences faculty members towards interprofessional teamwork and education. *Med Educ*. 2007;41(9):892–896. doi:10.1111/j.1365-2923.2007.02823.x
9. Olenick M, Allen LR. Faculty intent to engage in interprofessional education. *J Multidiscip Healthc*. 2013;6:149–161. doi:10.2147/JMDH.S38499
10. Vernon MM, Moore NM, Cummins L-A, et al. Respiratory therapy faculty knowledge of and attitudes toward interprofessional education. *Respir Care*. 2017;62(7):873–881. doi:10.4187/respcare.05034
11. Vernon MM, Moore N, Mazzoli A, De Leo G. Respiratory therapy faculty perspectives on interprofessional education: findings from a cross-sectional online survey. *J Interprof Care*. 2018;32(2):235–238. doi:10.1080/13561820.2017.1389865
12. Patton Z, Vernon M, Haymond K, Anglin J, Heboyan V, De Leo G. Evaluation of interprofessional education implementation among nutrition program directors in the United States. *Top Clin Nutr*. 2018;33(3):196–204. doi:10.1097/tin.000000000000143
13. Hughes JK, Allen A, McLane T, Stewart JL, Heboyan V, De Leo G. Interprofessional education among occupational therapy programs: faculty perceptions of challenges and opportunities. *Am J Occup Ther*. 2019;73(1):7301345010p1–7301345010p6. doi:10.5014/ajot.2019.030304
14. Ramiscal L, Truelove C Jr, Heboyan V, De Leo G. Attitudes and beliefs of physical therapist and physical therapist assistant program directors in the United States towards interprofessional education. *Internet J Allied Health Sci Pract*. 2022;20(1):13.
15. Tolle SL, Vernon MM, McCombs G, De Leo G. Interprofessional education in dental hygiene: attitudes, barriers and practices of program faculty. *J Dent Hyg*. 2019;93(2):13–22.
16. Web Scraper. <https://webscraper.io/>. Accessed January 21, 2023.
17. *The National Accreditation Agency for Clinical Laboratory Sciences*. <https://www.nacls.org/about.aspx>. Accessed January 21, 2023.
18. De Leo G, Bamfield-Cummin S, Bayhaghi G, Bufkin K, Jones S, Kashyap H. Data from: status of Interprofessional Education among NAACLS MLS and MLT programs directors. 2022. doi:10.17632/345cygfv29.2

Identification of Differential Metabolites Between Type 2 Diabetes and Postchronic Pancreatitis Diabetes (Type 3c) Based on an Untargeted Metabolomics Approach

Liang Qi, PhD,^{1,a} Zheng Ye, PhD,² Hao Lin, PhD^{3,a,*}

¹Department of Endocrinology, Zhongda Hospital, School of Medicine, Southeast University, Nanjing, China, ²State Key Laboratory of Bioelectronics, School of Biological Science and Medical Engineering, Southeast University, Nanjing, China, ³Department of Clinical Science and Research, Zhongda Hospital, School of Medicine, Southeast University, Nanjing, China. *To whom correspondence should be addressed: haolin@seu.edu.cn. ^aFirst authors.

Keywords: type 3c diabetes, type 2 diabetes, chronic pancreatitis, metabolomics, LC-MS, biomarker

Abbreviations: T3cDM, type 3c diabetes mellitus; T2DM, type 2 DM; ROCs, receiver operating characteristics; ADA, American Diabetes Association; CP, chronic pancreatitis; BRAAs, branched-chain amino acids; GRS, genetic risk score; LC-MS, liquid chromatography-mass spectrometry; QC, quality control; PCA, principal component analysis; VIP, variable important for the projection; PLS-DA, partial least squares method-discriminant analysis; PC, principal component; FC, fold change; AUC, area under the curve; BPC, base peak chromatogram; CV, coefficient of variation; ARA-S, N-arachidonoyl-L-serine; TBA, total bile acid; TBIL, total bilirubin; ALT, alanine aminotransferase; AST, aspartate aminotransferase; BAs, bile acids; DCAs, deoxycholic acids; SFA, sphinganine; SFO, D-sphingosine; AP, acute pancreatitis; S1P, sphingosine-1-phosphate.

Laboratory Medicine 2023;54:562-573; <https://doi.org/10.1093/labmed/lmad004>

ABSTRACT

Objective: A nontargeted metabolomics approach was established to characterize serum metabolic profile in type 3c diabetes mellitus (T3cDM) secondary to chronic pancreatitis and compare with T2DM.

Methods: Forty patients were recruited for metabolite analysis based on liquid chromatography-mass spectrometry. Cluster heatmap and KEGG metabolic pathway enrichment analysis were used to analyze the specific and differential metabolites. The receiver operating characteristics (ROCs) were generated and correlation analysis with clinical data was conducted.

Results: Metabolites including sphingosine, lipids, carnitine, bile acid, and hippuric acid were found to be different between T2DM and

T3cDM, mainly enriched in bile acid biosynthesis, fatty acid biosynthesis, and sphingolipid metabolic pathways. The ROCs were generated with an area under the curve of 0.907 (95% confidence interval, 0.726–1) for the model with 15 metabolites.

Conclusion: T3cDM is characterized by increased sphingosine, carnitine, bile acid, and most lipids, providing novel biomarkers for clinical diagnosis and a future direction in research on pathophysiological mechanisms.

Diabetes due to general pancreatic dysfunction is classified as type 3c diabetes mellitus (T3cDM) according to the “Standards of Medical Care in Diabetes” published by the American Diabetes Association (ADA) in 2021.¹ Various exocrine pancreatic diseases can lead to T3cDM, including pancreatitis, pancreatic neoplasia, cystic fibrosis, and pancreatectomy. Chronic pancreatitis (CP) is one of the leading causes of T3cDM. Two large cohort studies have confirmed that postpancreatitis diabetes accounts for 76% to 79% of all cases.^{2,3} With the progression of CP, pancreatic endocrine function is impaired and leads to disorders of glucose metabolism; about 33% of CP patients will develop diabetes within 5 years.⁴ Currently, there are no recognized diagnostic criteria for T3cDM and its pathogenesis has not been elucidated, resulting in the misdiagnosis of and confusion with type 2 diabetes (T2DM) in the clinic. The first and only proposed diagnostic criteria were published in 2013 by Ewald and Bretzel,⁵ including the evidence of pancreatic exocrine disease, such as exocrine insufficiency, and pathological pancreatic imaging as well as potential alterations in pancreatic polypeptide or incretin secretion and low serum levels of fat-soluble vitamins (A, D, E, and K). However, these diagnostic criteria still face challenges due to the lack of extensive clinical validation. Our previous study identified metabolic differences between T2DM and T3cDM through postprandial pancreatic and gastrointestinal hormonal responses, but more comprehensive studies are needed to further summarize the metabolic profile of T3cDM.⁶ Recent data showed that the incidence of T3cDM is higher than generally thought, and due to the increased risk of pancreatic cancer in patients with T3cDM secondary to CP, early diagnosis and identification of this group is of great significance.

Metabolomics focuses on the qualitative and quantitative analysis of low-molecular-weight molecules in biological systems, and as the last link in the “omics” cascade, it can detect changes in metabolic pathways and reveal potential relationships between metabolites and physiological or pathological changes, thereby improving understanding of the origin and pathogenesis of the disease.^{7,8} Significant advances have been made in knowledge about pathophysiology of diabetes in recent years, benefitted by the application and progress of “omics” sciences.

Evidence had suggested that metabolites such as glucose, fructose, lipids, and amino acids are often altered in individuals with T1DM and T2DM, and these changes in metabolites are of great importance for identifying and analyzing these 2 types.⁹ The risk for T1DM increases with increases in concentrations of phenylalanine and branched-chain amino acids (BRAAs), and BRAAs worsen the disease state of T1DM.¹⁰ In addition, increased levels of lysophosphatidylcholine and low-carbon-number saturated lipids are associated with T1DM.¹¹ In patients with T2DM, the levels of BRAAs, aromatic amino acids, sugar metabolites, low-carbon lipids, mannose, glucose, and organic acids are increased.^{12–15} A genetic risk score (GRS) based on validated single nucleotide variants for T2DM was identified between groups with T3cDM and T2DM, but the research found that the two types are similar in terms of GRS.¹⁶

The early diagnosis of diabetes type and exploration of the potential pathophysiological mechanism of T3cDM are beneficial for optimized treatment strategies and better patient management. Due to different degrees of endocrine and exocrine disorders, metabolic levels of T3cDM and T2DM might be different and need to be verified. Therefore, the purpose of this study was to comprehensively investigate the differences in metabolites of T2DM and T3cDM by analyzing the changes in their serum metabolic profiles and to explore the potentially differential metabolic pathways, which can probably provide evidence for identification.

Materials and Methods

Participants and Study Design

In this study, 40 individuals of the Chinese Han population were recruited at the Zhongda Hospital of Southeast University, including 16 patients with T3cDM secondary to CP, 12 patients with T2DM, and 12 healthy controls. Patients with T2DM were diagnosed according to the diabetes criteria from ADA¹ and were excluded if they had a history of pancreatic exocrine diseases. Those patients who met the diagnostic criteria of diabetes after the definite diagnosis of CP were considered to have CP-associated T3cDM, and we excluded from the study those who were positive for T1DM-related-antibodies or those with potential risk factors of T2DM, such as obesity and family history of diabetes. The diagnosis of CP was based on clinical symptoms and radiological evidence including pancreatic calcifications, ductal dilatation, and atrophy visualized by imaging with computed tomography, magnetic resonance imaging, or both.¹⁷ CP-associated diabetes was also diagnosed by detection of fasting plasma glucose ≥ 126 mg dL⁻¹, 2-hour plasma glucose ≥ 200 mg/dL⁻¹ during an oral glucose tolerance test, and glycosylated hemoglobin $\geq 6.5\%$, according to ADA criteria. Healthy controls were age- and sex-matched with no unexplained upper abdominal pain or history of pancreatic diseases.

Blood samples for detection were collected by venipuncture in the morning after 8 to 10 hours fasting and centrifuged at 1000 rpm

TABLE 1. Demographic and Clinical Characteristics of Participants

	Control (n = 12)	T2DM (n = 12)	T3cDM (n = 16)	P Value
Age, y	50 (47, 52)	48 (41.5, 56)	52.5 (40.75, 63.5)	.801
Male, n (%)	12 (100)	12 (100)	15 (93.75)	.400 ^a
Total cholesterol, mmol/L	5.07 \pm 1.08	4.90 \pm 1.36	3.80 \pm 1.19	.015 ^b
Triglyceride, mmol/L	1.32 (0.96, 1.53)	2.53 (1.08, 4.06)	1.18 (0.83, 1.78)	.122
Uric acid, mmol/L	337.08 \pm 72.70	402.58 \pm 71.71	283.31 \pm 116.85	.007 ^c
Glucose, mmol/L	5.77 (4.97, 6.55)	8.16 (6.27, 11.96)	7.73 (5.87, 11.63)	.018 ^d

T2DM, type 2 diabetes mellitus.

^aUsing Fisher's Exact test

^bT3cDM group showed statistical difference compared with T2DM and healthy controls, $P < .05$.

^cExisting statistical difference between T2DM and T3cDM, $P < .05$

^dExisting statistical difference between T2DM and healthy controls, $P < .05$.

for 15 min at 4°C. The supernatants were immediately transferred to Eppendorf tubes and stored at -80°C until liquid chromatography-mass spectrometry (LC-MS) analysis. Detailed clinical information on the participants was collected and is summarized in **TABLE 1**. All procedures were conducted in accordance with the Declaration of Helsinki and were approved by the ethics committee of Zhongda Hospital of Southeast University (ethics number 2020ZDSYLL114-P01).

Materials and Reagents

Liquid chromatography-mass spectrometry grade chemicals included methanol and acetonitrile (A454-4 and A996-4 from Thermo Fisher Scientific), ammonia formate (17843-250G, Honeywell Fluka), and formic acid (50144-50ml, DIMKA). Water used in the experiments was obtained from a Milli-Q water purification system (Milli-Q Integral, Millipore)

Untargeted Metabolomics

Sample Preparation

After the samples were thawed slowly at 4°C, 100 μ L serum sample was placed in a 96-well plate and treated with 300 μ L extraction solution (methanol: acetonitrile = 2: 1, v: v, -20°C precooled). Then, 10 μ L internal standard 1 and internal standard 2 was added and placed at -20°C for 2 h after vortex mixing for 1 min. Then the samples were centrifuged at 4000 rpm for 20 min at 4°C, and 300 μ L of the supernatant was dried in a freezing vacuum concentrator (Maxi Vacbeta, Gene Company). Subsequently, 150 μ L reconstituted solution (methanol-water=1:1, v/v) was added to reconstitute, and followed by 1-min vortex and 30-min centrifugation at 4000 rpm. The supernatant was transferred to vials for LC-MS analysis. A quality control (QC) sample was prepared by mixing an equal aliquot (10 μ L) from all supernatant for the evaluation of repeatability and stability of the LC-MS analysis process.

LC-MS Experiments

Metabolic profiling analysis was performed using a Waters 2D UPLC (Waters) tandem Q Exactive HF high-resolution mass spectrometer (Thermo Fisher Scientific) system. Chromatographic analysis was performed using a BEH C18 column (1.7 μ m, 2.1 \times 100 mm, Waters). A 5- μ L aliquot of the prepared sample solution was injected onto a BEH C18 column; the flow rate was 0.35 mL/min and the column temperature was set at 45°C. The mobile phase in positive ion mode was

an aqueous solution containing 0.1% formic acid (liquid A) and 100% methanol containing 0.1% formic acid (liquid B). The mobile phase in negative ion mode was an aqueous solution containing 10 mM ammonia formate (liquid A) and 95% methanol containing 10 mM ammonia formate (liquid B). The following gradient was used for elution: 0 to 1 min, 2% liquid B; 1 to 9 min, 2%–98% liquid B; 9 to 12 min, 98% liquid B; 12 to 12.1 min, 98% to 2% liquid B; and 12.1 to 15 min, 2% B solution. The Q Exactive HF mass spectrometer (Thermo Fisher Scientific) was used for primary and secondary mass spectral data acquisition. The mass-to-nuclear ratio range for mass spectrometry scanning was 70 to 1050, the first-order resolution was 120,000, the AGC was 3e6, and the maximum injection time was 100 ms. According to the precursor ion intensity, the top 3 were selected for fragmentation and secondary information was collected. Secondary resolution was 30,000, AGC was 1e5, and maximum injection time was 50 ms. The optimal analysis conditions were set as follows: fragmentation energy (stepped nce), 20, 40, 60 eV; ion source (ESI) parameter settings, sheath gas flow rate: 40, auxiliary gas flow rate: 10, spray voltage (| KV |): 3.80 in positive mode and 3.20 in negative mode; ion transfer tube temperature (capillary temp): 320°C; auxiliary gas heater temperature (auxiliary gas heater temp): 350°C. The samples are randomly sorted where QC samples were interspersed every 10 samples to reduce system errors and provide more reliable experimental results.

Data Processing and Statistics Analysis

Statistical analyses for baseline information were performed using the SPSS statistical package version 23.0. All continuous variables were reported as mean \pm standard deviation, and categorical variables were expressed as percentages. Student's *t*-test or the Mann-Whitney *U* test were used as appropriate to analyze the continuous variables, and the χ^2 test was used to compare the related demographic data involved in the study. *P* < .05 was considered statistically significant.

Metabolite Identification and Metabolite Pathway Analysis

This project applied liquid chromatography-tandem mass spectrometry technology for nontargeted metabolomics analysis and used a high-resolution mass spectrometer Q Exactive HF (Thermo Fisher Scientific) to collect data in 2 modes, positive and negative, for improving metabolite coverage. Compound Discoverer 3.0 (Thermo Fisher Scientific) software was used for data processing, mainly for peak extraction, peak alignment, and compound identification. Metabolite identification combined multiple databases of BGI Library, mzCloud, and ChemSpider (HMDB, KEGG, LipidMaps). MetaboAnalyst 5.0 and the metabolomics information analysis process were used for data preprocessing, statistical analysis, metabolite classification annotation, and functional annotation. Principal component analysis (PCA) was used to reduce the dimensionality of multivariate raw data for analysis of the groups, trends (similarity and difference within and between sample groups), and outliers of the observed variables in the data set. The variable important for the projection (VIP) values of the first 2 principal components of the partial least squares method-discriminant analysis (PLS-DA) model were used in combination with the fold change (FC) and Student's *t*-test to screen for differential metabolites. Volcano plot, cluster heat map, and metabolic pathway enrichment analysis were used for visual display of differential metab-

olism. The area under the curve (AUC) was used to assess the predictive potential individually and in combination.

Results

Data Quality Assessment

The QC samples were added to the project to monitor the whole experiment, which equilibrated the chromatography-mass spectrometry system before the sample was tested and evaluated the stability of the system during the sample test. The onboard QC sample set was derived from the same sample, and we used 3 visualization methods including base peak chromatogram (BPC), PCA, and coefficient of variation (CV). The overlapped BPC of all QC samples showed that the spectrum overlapped well and the retention time and peak response intensity fluctuated little, indicating that the instrument was in good condition throughout the sample detection and analysis process and the signal was stable. During the experiment, QC samples were measured and PCA analysis was performed on the QC samples and the tested samples. The results showed that the QC samples formed a cluster and the measured samples did not have a significant shift, thus confirming that our metabolomics data have good repeatability and stability. A QC group with 60% of ions with a CV of less than 30% was considered satisfactory in our analysis.

Multidimensional Statistical Analysis of Metabolic Data *Metabolomic Data Analysis among Healthy Participants, T2DM, and T3cDM*

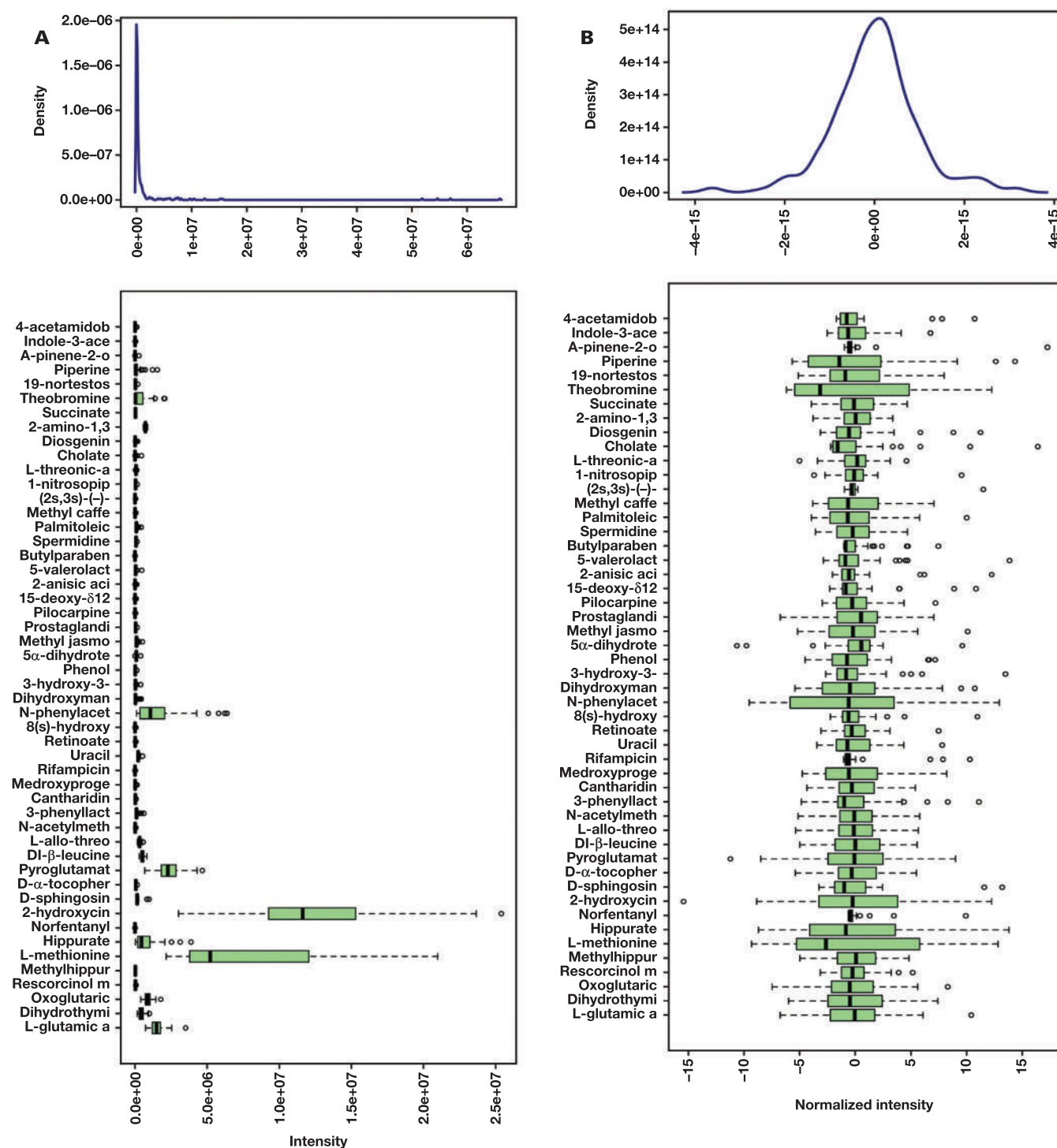
Intergroup PCA and PLS-DA analysis.—Before analysis, the original data was normalized. The effects before and after normalization are shown in **FIGURE 1**.

There were a total of 2345 compounds with identification information in positive mode and 707 in negative mode identified by LC-MS. After cubic root transformation and Pareto scaling, PCA was performed, which reflected the metabolic differences among the 3 groups and the variabilities in each group. The variance explained by principal components (PCs) is shown in **FIGURE 2A**, which showed the accumulated variance explained by PC1 to PC5. As shown in **FIGURE 2B**, the separation trend was not clear on the PC1 and PC2 dimension chart; additionally, the 3-dimensional score plot exhibited a separation trend between T2DM and T3cDM, indicating that the serum metabolic profiles of the 2 groups were different.

Unlike PCA, PLS-DA is a supervised multidimensional statistical method, which can reflect the differences between classification groups to the greatest extent, and clearly distinguished the 3 groups in this study (**FIGURES 2C** and **2D**). The model was evaluated by monitoring the interpretation ability and predictive ability values. The classification performance with different numbers of components is shown in **FIGURE 2E**, indicating that 3 to 5 components were better in distinguishing the serum metabolome among 3 groups by PLS-DA.

Identification of differential metabolites among the 3 groups.—The VIP scores were calculated to measure the impact strength and explanatory capability of each metabolite pattern on the classification and discrimination of each group, thereby assisting the screening of metabolic

FIGURE 1. Box plots and kernel density plots before (A) and after (B) normalization. The boxplots show at most 50 features due to space limitation. The density plots are based on all samples. Selected methods: row-wise normalization: N/A; data transformation: cubic root transformation; data scaling: Pareto scaling.



markers. The metabolites with $VIP > 2$ are shown in **FIGURE 2F**, with red and blue representing upregulated and downregulated metabolites, respectively.

One-way ANOVA and Fisher's least significant difference method were applied for exploratory data analysis. The important results

identified by ANOVA analysis are shown in **FIGURE 3A**, with the details supplemented in **TABLE S1**. There were 28 significant differentially expressed metabolites with P values lower than .005. Additionally, heatmap analysis of the top 50 differential metabolites is shown in **FIGURE 3B**.

FIGURE 2. A, Scree plot shows the variance explained by principal components (PCs). The top line on top shows the accumulated variance explained; the bottom line underneath shows the variance explained by individual PC. B, Principle component analysis (PCA) scores plot between the selected PCs. The explained variances are shown in brackets. C, Partial least squares method-discriminant analysis (PLS-DA) score plot between the selected PCs. The explained variances are shown in brackets. D, PLS-DA 3D score plot between the selected PCs. The explained variances are shown in brackets. E, PLS-DA classification using different number of components. The asterisk indicates the best classifier. F, Important features identified by PLS-DA. The colored boxes on the right indicate the relative concentrations of the corresponding metabolite in each group under study. Ctrl, control; T2DM, type 2 diabetes mellitus; T3cDM, type 3c DM.

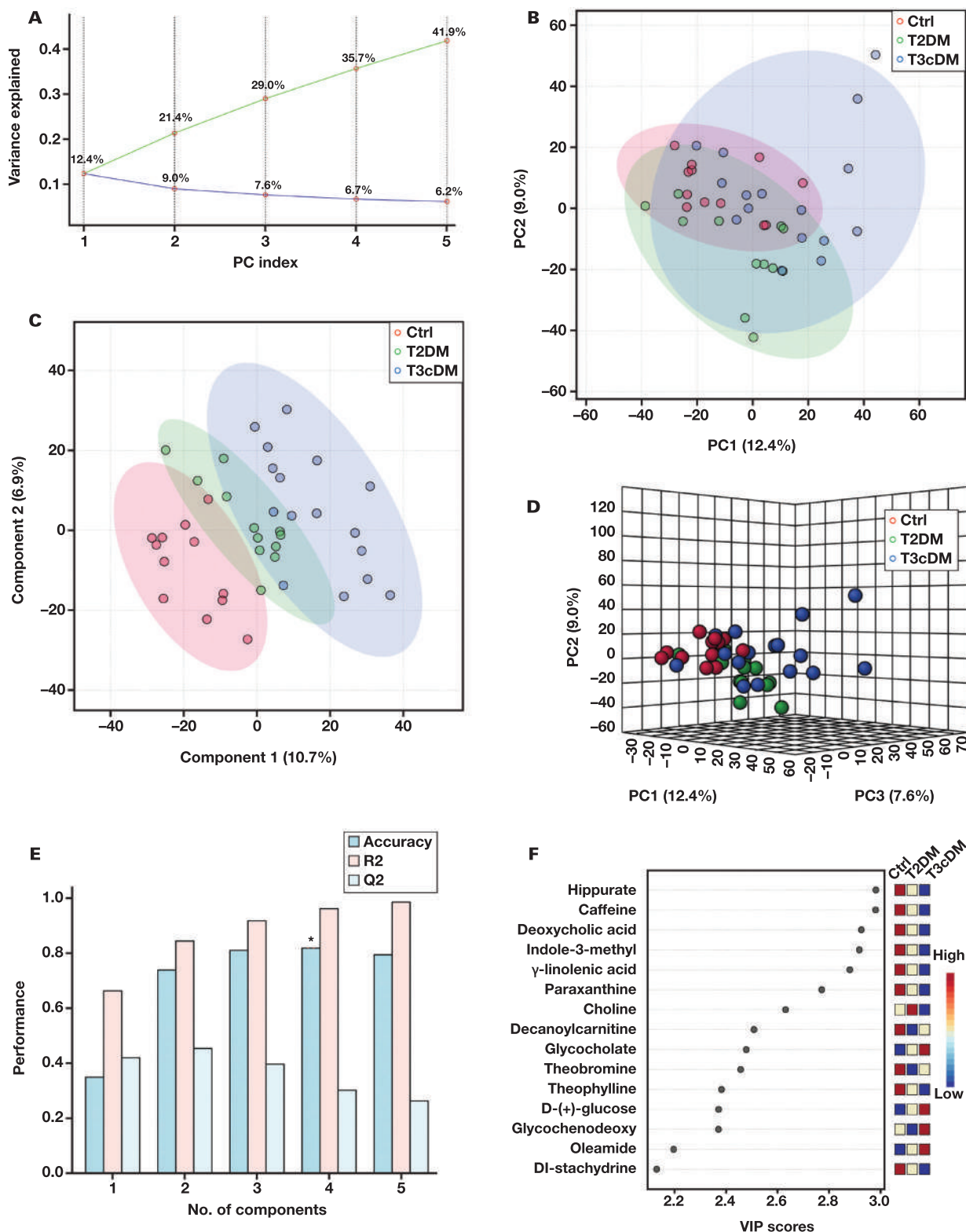
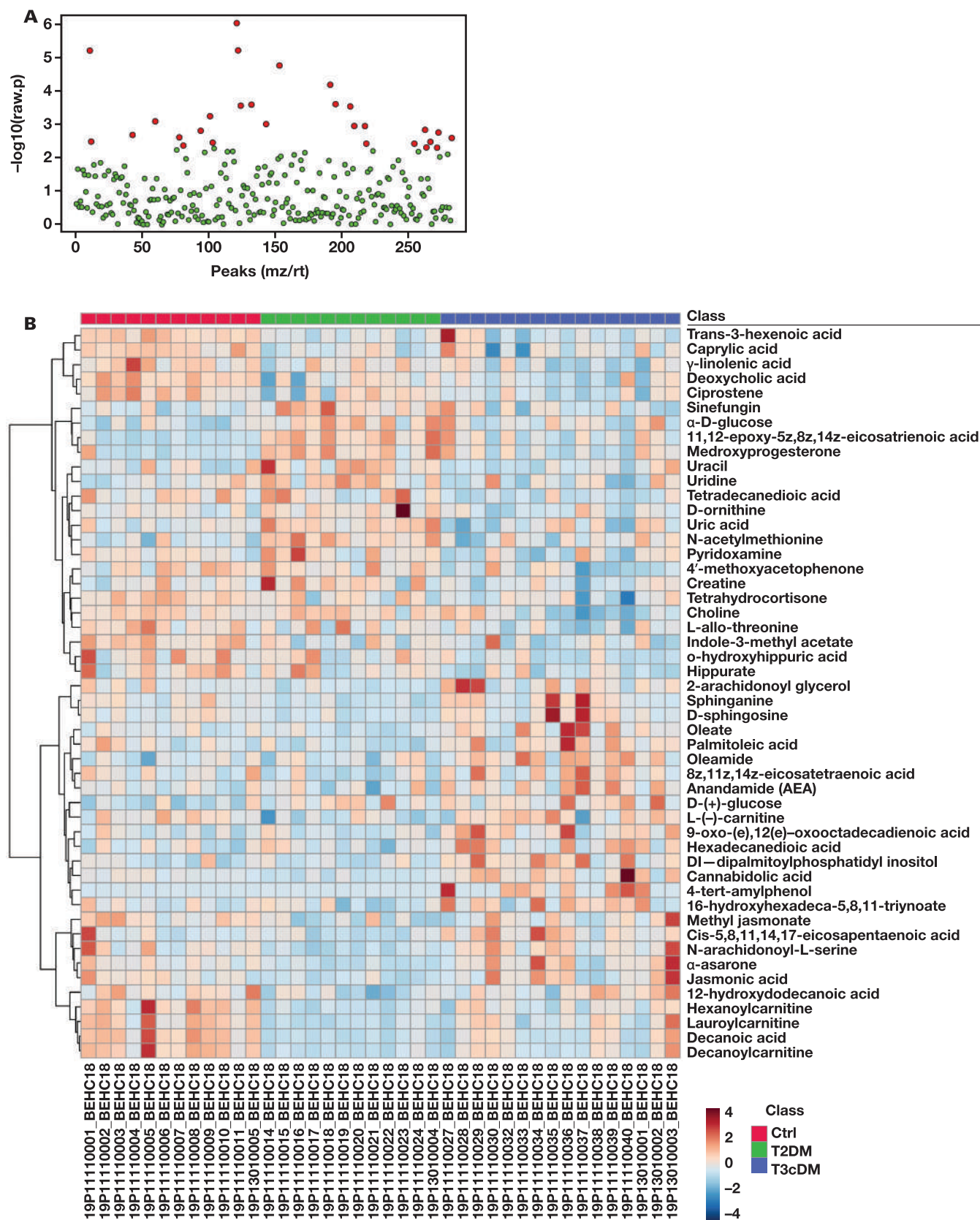


FIGURE 3. A, Important features selected by one-way ANOVA with threshold 0.01. The red circles represent features above the threshold. Note the P values are transformed by $-\log_{10}$ so that the more significant features (with smaller P values) will be plotted higher on the graph. B, Clustering result among 3 groups shown as heatmap (distance measure using Euclidean and clustering algorithm using ward D).



Metabolomic Data Analysis Between Type 2 and Type 3c Diabetes

Identification of differential metabolites between type 2 and type 3c diabetes.—We further analyzed differentially expressed metabolites between T2DM and T3cDM. Fold change and *t*-tests were applied to obtain information on important metabolites. First, the top 50 most important metabolites were selected for enrichment analysis (FIGURE 4A). The differential metabolites selected by volcano plot are shown in FIGURE 4B. The top 50 features identified by FC analysis are shown in TABLE S2 in detail. As shown by the bar chart in FIGURE 3C, the pathways of differential metabolites were mainly enriched in bile acid biosynthesis, beta oxidation of very long chain fatty acids, alpha linolenic acid and linolenic acid metabolism, fatty acid biosynthesis, and sphingolipid metabolism.

Biomarkers for distinguishing T3cDM from T2DM.—Preliminarily, the area under the receiver-operating characteristic (ROC) curves of the top 50 individual biomarkers were calculated, and they ranged from 0.75 to 0.932 (TABLE S3). N-arachidonoyl-L-serine (ARA-S) was identified as the most significant metabolite with an AUC of 0.932 (0.807–0.99), which increased in T3cDM and decreased in T2DM (FIGURES 4D–4E). Thereafter, the multivariate exploratory ROC curve analysis was used to evaluate the performance of biomarker models created through automated important feature identification. Support vector machines were applied for the ROC curves of 5, 10, 15, 25, 50, and 100 biomarkers model based on the average cross-validation performance (FIGURE 4F). According to the ROC curves, the combinations of 15 to 100 different biomarkers in multivariate models have discriminative power. The AUC for the model with 15 metabolites was 0.907 (95% confidence interval, 0.726–1), and the most important features of the selected model were ranked from most to least important (FIGURE 4G). The predictive accuracies of different features, shown in FIGURE 4H increases with the number of included metabolites. Based on the model with 15 metabolites, only 1 out of 12 T2DM samples were wrongly classified as T3cDM, whereas 2 out of 16 T3cDM samples were misclassified as T2DM (FIGURE 4I).

Correlation Analysis Between Differential Metabolites and Clinical Data

We also analyzed correlations between differential metabolites and the clinical data of T2DM and T3cDM (FIGURES 5A and 5B). Hippurate is inversely correlated with fasting serum glucose levels and total bile acid (TBA), and is positively correlated with uric acid in both types of diabetes. Glycochenodeoxycholate and glycocholate are both positively correlated with serum total bilirubin (TBIL), TBA, alanine aminotransferase (ALT), and aspartate aminotransferase (AST). Glycocholic acid and glycocholate are associated with liver dysfunction and impaired bile excretion, which showed significant correlation with ALT, AST, and TBA. The correlations between L (–) carnitine and mean corpuscular volume, mean corpuscular hemoglobin, TBIL, and direct bilirubin differ between T2 and T3, which showed significantly positive correlation in T2DM and negative correlation in T3cDM. Similarly, L-proline exhibited a positive correlation with neutrophil granulocyte, lymphocyte, and monocyte counts in T2DM, and a negative correlation with T3cDM.

Discussion

As an important metabolic disease, diabetes is closely related to a variety of metabolite disorders. Our study explored the metabolite

differences among T3cDM, T2DM, and healthy controls and ranked the important features that can be used to differentiate T2DM and T3cDM, providing areas for subsequent research in diagnosis and mechanisms of T3cDM.

Through the LC-MS/MS method, we initially identified several metabolites significantly differently expressed among healthy participants and those with T2DM and T3cDM, including hippuric acid, bile acid, and choline. According to the VIP score analysis of the 3 groups, hippurate was the most important metabolite, highest in the healthy group and lowest in the T3cDM group. Hippurate has been found to be positively associated with microbial diversity and negatively associated with visceral fat mass, blood pressure, and nonalcoholic fatty liver disease, suggesting its potential role in metabolic health.^{18–21} Recently, hippurate was shown to increase insulin-positive β cell mass and improve glucose homeostasis,²² which can be supported by our finding of a positive correlation between hippurate and serum glucose levels. As a marker of metabolic health, a reduced level of hippurate in T3cDM may indicate worse glucose metabolism. Bile acids (BAs) play a vital role in promoting digestion, absorption, and excretion of dietary lipids and are involved in several cellular signaling pathways, such as the inflammatory, activating apoptotic, and carcinogenic signaling pathways.^{23–25} Dysfunction of lipid metabolism is a major risk factor for T2DM, which has shown to be modulated by BAs via the signaling effect. It has been demonstrated that deoxycholic acids (DCAs) are significantly decreased in T2DM patients compared with healthy controls.²⁶ Our research showed a lower concentration of DCAs in T3cDM, suggesting the possibility that the pathophysiology of T3cDM may also be affected by alteration in BA synthesis. Choline is the nutrient in one-carbon metabolism, which has been suggested to be associated with obesity by increasing evidence.^{27,28} Recent study confirmed a positive relationship between higher plasma choline and higher fat mass or body weight.²⁹ Our results showed an elevated concentration of choline in T2DM but lower levels in T3cDM, which can be explained by T2DM being often associated with obesity, whereas T3cDM often accompanies CP-induced weight loss.

Subsequently, we identified the differential features between T2DM and T3cDM, which are mostly metabolites enriched in bile acid biosynthesis, beta oxidation of very-long-chain fatty acids, alpha linolenic acid and linolenic acid metabolism, fatty acid biosynthesis, and sphingolipid metabolism. Elevated lipid profiles were presented by the T3cDM group and constituted the first major differential features of T2DM/T3cDM-related metabolites. We identified ARA-S as one of the most important metabolites in distinguishing T3cDM from T2DM, with an AUC of 0.932. ARA-S is regarded as an endocannabinoid-like lipid, which acts as a proangiogenic factor and a vasorelaxant³⁰ with proneurogenic and neuroprotective properties.³¹ Subjects with T3cDM exhibited much higher concentrations of ARA-S, which may be attributed to its function in the protein phosphorylation of several signal transduction pathways of chronic inflammation and fibrosis in the pancreas.³²

Furthermore, we found elevated sphinganine (SFA) and D-sphingosine (SFO) levels in individuals with T3cDM. Sphingolipid dysregulation has been reported in T2DM, indicating decreased levels of SFA and SFO in T2DM compared with healthy controls.³³ By constructing a caerulein-induced acute pancreatitis (AP) model, it was found that the ceramide de novo synthesis pathway was characterized by remarkably increased SFA (the precursor of ceramide synthesis),

FIGURE 4. A, Heatmap of significantly different metabolites of type 2 diabetes mellitus (T2DM) and type 3c DM (T3cDM) groups (distance measure using Euclidean and clustering algorithm using ward D). B, Volcano plot of significantly different metabolites between T2DM and T3cDM. The x-axis is \log^2 (fold change), y-axis is $-\log_{10}$ (P value). C, The metabolites sets enrichment overview. D, The receiver operating characteristic (ROC) curve of an individual biomarker. The sensitivity is on the y-axis, and the specificity is on the x-axis. The area under the curve is in blue. Selected individual biomarker name: N-arachidonoyl-L-serine (ARA-S). E, Box plot of the concentrations of the selected feature between 2 groups within the dataset. F, Plot of ROC curves for all or a single biomarker model based on its average performance across all Manufacturers Council of the Central Valley (MCCV) runs. For a single biomarker, the 95% confidence interval can be computed and will appear as a band around the ROC curve. G, Plot of the most important features of a selected model ranked from most to least important, selected model including 15 metabolites. H, Plot of the predictive accuracy of biomarker models with an increasing number of features. The most accurate biomarker model will be highlighted with a red dot. I, Plot of predicted class probabilities for all samples using a single biomarker model. Due to balanced subsampling, the classification boundary is at the center ($x = 0.5$, dotted line), selected model including 15 metabolites.

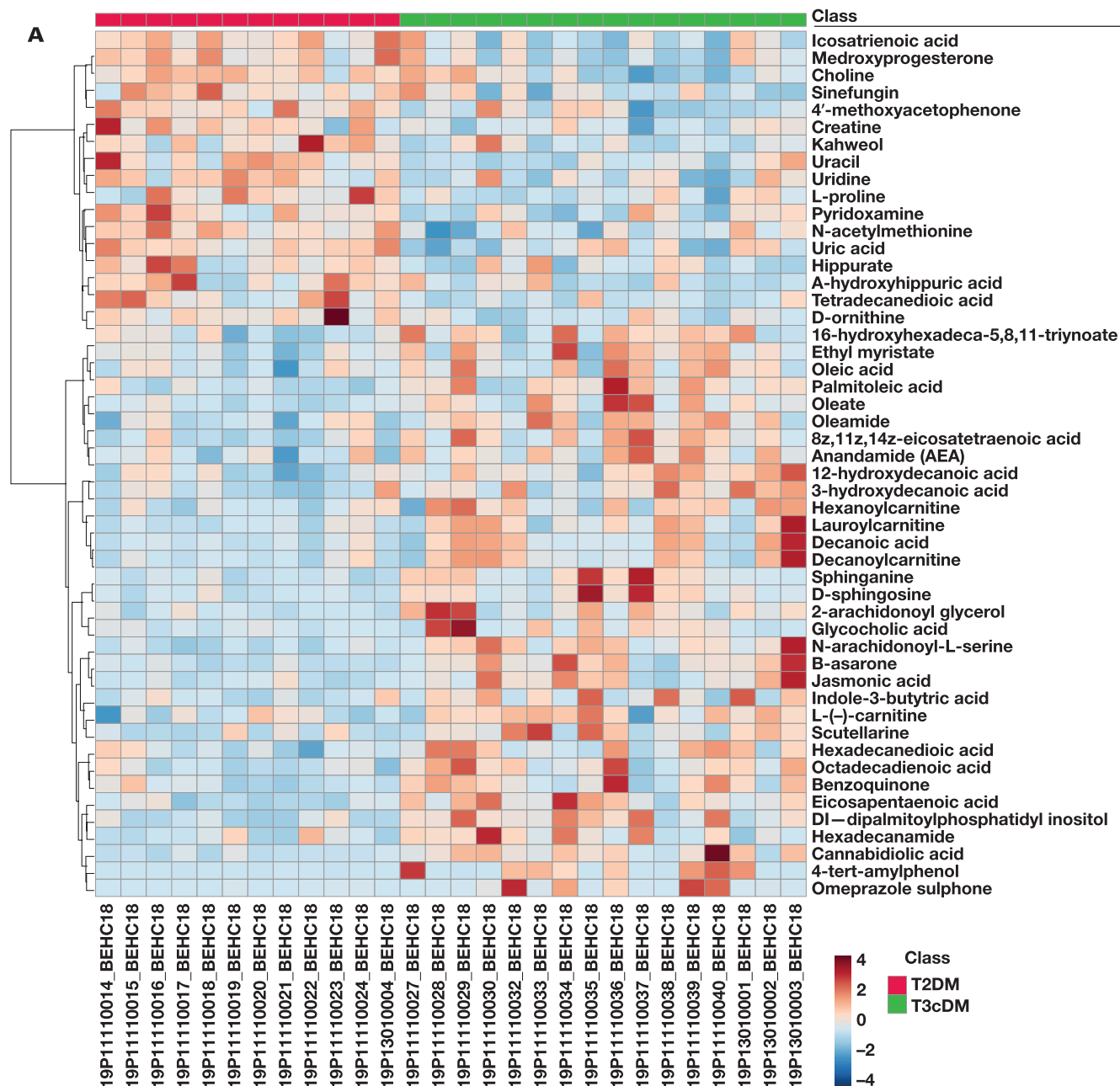


FIGURE 4. (cont)

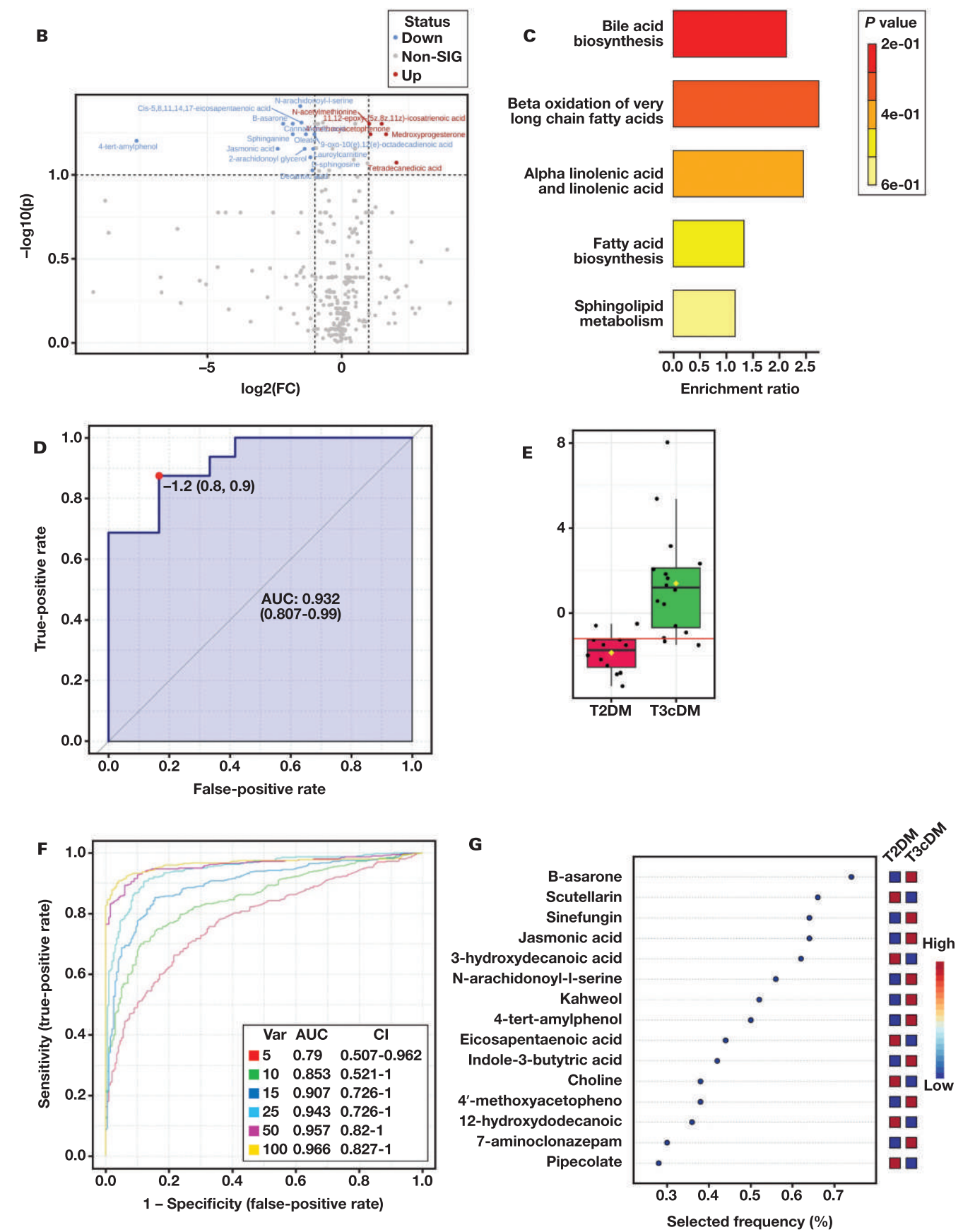
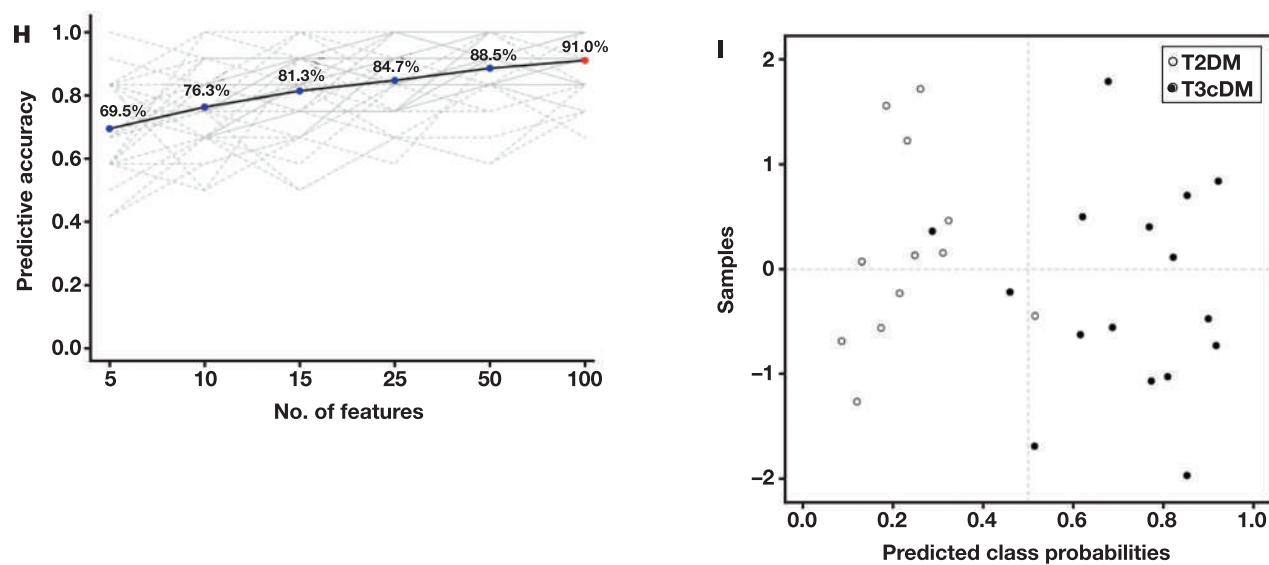
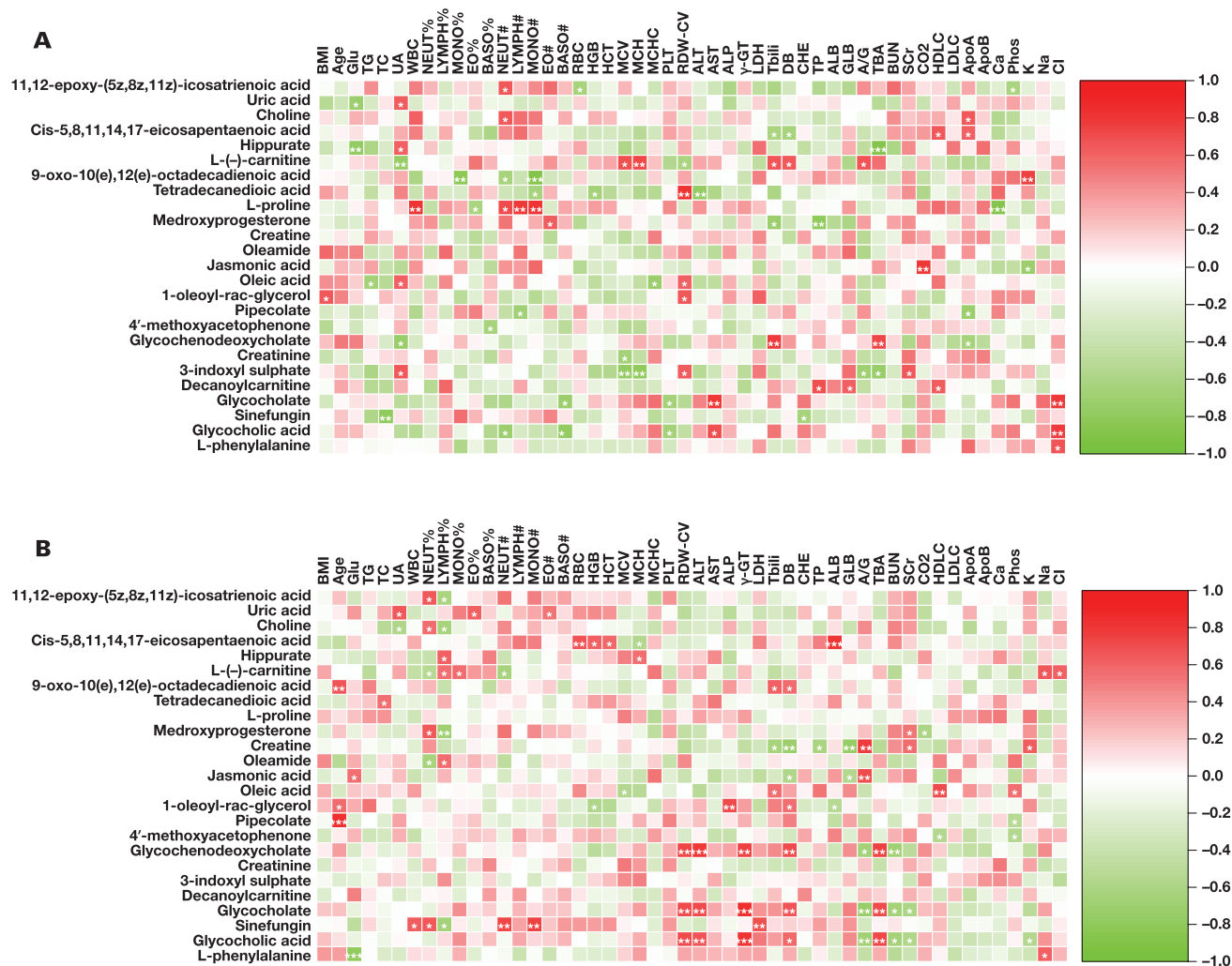


FIGURE 4. (cont)**FIGURE 5. Correlation analysis between differential metabolites and clinical data in T2DM (A) and T3cDM (B).**

SFO, or sphingosine-1-phosphate (S1P), which may protect against AP complications.³⁴ Also, of interest, SFO and S1P were elevated in pancreatic carcinoma with nodal disease, but unfortunately there has been no related research on CP or T3cDM patients so far. Disorders of fatty acid metabolism are related to many chronic diseases (obesity,³⁵ T2DM,³⁶ inflammation³⁷) and the abovementioned diseases non-alcoholic fatty liver and AP.³⁸ Palmitoleic acid was positively associated with homeostasis model assessment of insulin resistance and C-peptide concentration in T2DM regardless of region and race.^{39–41} Although higher levels of gamma-linolenic acid and dihomo- γ -linolenic acid have been identified in CP patients,⁴² elevated concentrations of palmitoleic acid were detected in the T3cDM group for the first time, and the related mechanism involved needs further exploration. Carnitine has 2 enantiomers: L- and D-carnitine, but only L-carnitine has physiological activity. Endogenous carnitine is distributed mostly in cardiac and skeletal muscle (98%) and only 1% within plasma. As low available carnitine may lead to impaired glucose tolerance, carnitine supplementation may improve metabolic flexibility in an impaired glucose tolerance group.⁴³ A significant protective effect of L-carnitine was verified in an AP model by adjusting the balance of oxidants/antioxidants and modulating the nitric oxide and myeloperoxidase systems.⁴⁴ A positive association was identified between cardiovascular disease risk in T2DM and increased acylcarnitine metabolites (decanoylcarnitine, lauroylcarnitine),⁴⁵ and lauroylcarnitine was related to alteration of proinflammatory metabolite and mitochondrial dysfunction.⁴⁶ Our results show that carnitine was higher in T3cDM than T2DM, which could provide a direction for future research after verification.

Recent research in White persons described 5 major metabolites that differed between T2DM and T3cDM, including L-tryptophan, palmitoylcarnitine, 7-HOCA, lysoPE (22:6), and biliverdin.⁴⁷ These metabolites were thought to be related to insulin resistance and have certain diagnostic value for new onset T2DM. However, the T2DM patients enrolled in our study had a diabetic course of 3 to 5 years, were mainly characterized by β -cell dysfunction, and insulin resistance was not obvious. Different stages of diabetes may be the cause of metabolic difference. Furthermore, our study was based on an Asian population, and the metabolites may be affected by race, living environment, and habits. As there were no baseline characteristics of participants showed in previous research, we suspect that the difference is due to different duration of diseases and race. Our work explored metabolic characteristics in T3cDM using the nontargeted metabolomic approach and compared healthy controls and persons with T2DM. Several metabolites involving sphingolipid metabolism, BAs, and fatty acid biosynthesis were discovered. The combination of 15 to 100 different biomarkers in multivariate models deliver discriminative results, with AUC ranging from 0.907 to 0.966, and the predictive accuracy with 15 features was 81.3%.

However, there are several limitations to our study. First, due to the relative low prevalence of CP and T3cDM, the sample size enrolled in the study is small. Males account for the majority in our samples, and some metabolites may be affected by sex-specific hormones. Also, the onset of diabetes in the diabetic participants was within 5 years, which may not represent the metabolic characteristics of the long-term diabetes population.

In conclusion, this cross-sectional study identified SFA, SFO, carnitine, choline, hippuric acid, and bile acid to be significantly different between T2DM and T3cDM and generated ROC curves for diagnosis based on differential metabolites. These differential metabolites

are mainly enriched in bile acid biosynthesis, beta oxidation of very-long-chain fatty acids, alpha linolenic acid and linolenic acid metabolism, fatty acid biosynthesis, and sphingolipid metabolic pathways and are closely related to clinical indicators reflecting liver and gallbladder function. Further targeted verification in a larger population could provide biomarkers for diagnosis and identification of CP-related T3cDM. Our results encourage further work to elucidate the pathophysiological mechanisms.

Acknowledgments

We are grateful to the staff in Biobank of Zhongda Hospital Affiliated to Southeast University for technical assistance.

This work was supported by National Natural Science Foundation of China (No. 81800571).

Supplementary Data

Supplemental figures and tables can be found in the online version of this article at www.labmedicine.com

Conflict of Interest Disclosure

The authors have nothing to disclose.

REFERENCES

1. American Diabetes Association. Classification and diagnosis of diabetes: standards of medical care indiabates-2021. *Diabetes Care*. 2021;44(Suppl 1):S15–S33.
2. Hardt PD, Brendel MD, Kloer HU, Bretzel RG. Is pancreatic diabetes (type 3c diabetes) underdiagnosed and misdiagnosed? *Diabetes Care*. 2008;31(Suppl 2):S165–S169. doi:10.2337/dc08-s244.
3. Hart PA, Bellin MD, Andersen DK, et al. Type 3c (pancreatogenic) diabetes mellitus secondary to chronic pancreatitis and pancreatic cancer. *Lancet Gastroenterol Hepatol*. 2016;1(3):226–237.
4. Zhu X, Liu D, Wei Q, et al. New-onset diabetes mellitus after chronic pancreatitis diagnosis: a systematic review and meta-analysis. *Pancreas*. 2019;48(7):868–875. doi:10.1097/mpa.0000000000001359.
5. Ewald N, Bretzel RG. Diabetes mellitus secondary to pancreatic diseases (type 3c)—are we neglecting an important disease? *Eur J Intern Med*. 2013;24(3):203–206.
6. Qi L, Wei Q, Ni M, et al. Pancreatic and gut hormone responses to mixed meal test in post-chronic pancreatitis diabetes mellitus. *Diabetes Metab*. 2022;48(3):101316. doi:10.1016/j.diabet.2021.101316.
7. Fiehn O. Metabolomics—the link between genotypes and phenotypes. *Plant Mol Biol*. 2002;48(1–2):155–171.
8. Madsen R, Lundstedt T, Trygg J. Chemometrics in metabolomics—a review in human disease diagnosis. *Anal Chim Acta*. 2010;659(1–2):23–33. doi:10.1016/j.aca.2009.11.042.
9. Arneth B, Arneth R, Shams M. Metabolomics of type 1 and type 2 diabetes. *Int J Mol Sci*. 2019;20(10):2467.
10. Bloomgarden Z. Diabetes and branched-chain amino acids: what is the link? *J Diabetes*. 2018;10(5):350–352. doi:10.1111/1753-0407.12645.
11. Han LD, Xia JF, Liang QL, et al. Plasma esterified and non-esterified fatty acids metabolic profiling using gas chromatography-mass spectrometry and its application in the study of diabetic mellitus and diabetic nephropathy. *Anal Chim Acta*. 2011;689(1):85–91. doi:10.1016/j.aca.2011.01.034.

12. Guasch-Ferré M, Hruby A, Toledo E, et al. Metabolomics in prediabetes and diabetes: a systematic review and meta-analysis. *Diabetes Care*. 2016;39(5):833–846. doi:10.2337/dc15-2251.
13. Roberts LD, Koulman A, Griffin JL. Towards metabolic biomarkers of insulin resistance and type 2 diabetes: progress from the metabolome. *Lancet Diabetes Endocrinol*. 2014;2(1):65–75. doi:10.1016/S2213-8587(13)70143-8.
14. Newgard CB. Interplay between lipids and branched-chain amino acids in development of insulin resistance. *Cell Metab*. 2012;15(5):606–614. doi:10.1016/j.cmet.2012.01.024.
15. Suhre K, Meisinger C, Döring A, et al. Metabolic footprint of diabetes: a multiplatform metabolomics study in an epidemiological setting. *PLoS One*. 2010;5(11):e13953. doi:10.1371/journal.pone.0013953.
16. Goodarzi MO, Nagpal T, Greer P, et al. Genetic risk score in diabetes associated with chronic pancreatitis versus type 2 diabetes mellitus. *Clin Transl Gastroenterol*. 2019;10(7):e00057.
17. Singh VK, Yadav D, Garg PK. Diagnosis and management of chronic pancreatitis: a review. *JAMA*. 2019;322(24):2422–2434. doi:10.1001/jama.2019.19411.
18. Holmes E, Loo RL, Stamler J, et al. Human metabolic phenotype diversity and its association with diet and blood pressure. *Nature*. 2008;453(7193):396–400. doi:10.1038/nature06882.
19. Elliott P, Posma JM, Chan Q, et al. Urinary metabolic signatures of human adiposity. *Sci Transl Med*. 2015;7(285):285ra28562.
20. Pallister T, Jackson MA, Martin TC, et al. Untangling the relationship between diet and visceral fat mass through blood metabolomics and gut microbiome profiling. *Int J Obes (Lond)*. 2017;41(7):1106–1113.
21. Hoyle L, Fernández-Real JM, Federici M, et al. Molecular phenomics and metagenomics of hepatic steatosis in non-diabetic obese women. *Nat Med*. 2018;24(7):1070–1080. doi:10.1038/s41591-018-0061-3.
22. Brial F, Chilloux J, Nielsen T, et al. Human and preclinical studies of the host-gut microbiome co-metabolite hippurate as a marker and mediator of metabolic health. *Gut*. 2021;70(11):2105–2114. doi:10.1136/gutjnl-2020-323314.
23. Bouscarel B, Kroll SD, Fromm H. Signal transduction and hepatocellular bile acid transport: cross talk between bile acids and second messengers. *Gastroenterology*. 1999;117(2):433–452. doi:10.1053/gast.1999.0029900433.
24. Nguyen A, Bouscarel B. Bile acids and signal transduction: role in glucose homeostasis. *Cell Signal*. 2008;20(12):2180–2197.
25. Gadaleta RM, Oldenburg B, Willemsen EC, et al. Activation of bile salt nuclear receptor FXR is repressed by pro-inflammatory cytokines activating NF- κ B signaling in the intestine. *Biochim Biophys Acta*. 2011;1812(8):851–858.
26. Lei S, Huang F, Zhao A, et al. The ratio of dihomog- γ -linolenic acid to deoxycholic acid species is a potential biomarker for the metabolic abnormalities in obesity. *FASEB J*. 2017;31(9):3904–3912. doi:10.1096/fj.201700055r.
27. Konstantinova SV, Tell GS, Vollset SE, Nygård O, Bleie O, Ueland PM. Divergent associations of plasma choline and betaine with components of metabolic syndrome in middle age and elderly men and women. *J Nutr*. 2008;138(5):914–920. doi:10.1093/jn/138.5.914.
28. Heianza Y, Sun D, Smith SR, Bray GA, Sacks FM, Qi L. Changes in gut microbiota-related metabolites and long-term successful weight loss in response to weight-loss diets: The POUNDS Lost Trial. *Diabetes Care*. 2018;41(3):413–419. doi:10.2337/dc17-2108.
29. Forth W, Schäfer SG. Absorption of di- and trivalent iron: experimental evidence. *Arzneimittelforschung*. 1987;37(1a):96–100.
30. Zhang X, Maor Y, Wang JF, Kunos G, Groopman JE. Endocannabinoid-like N-arachidonoyl serine is a novel pro-angiogenic mediator. *Br J Pharmacol*. 2010;160(7):1583–1594. doi:10.1111/j.1476-5381.2010.00841.x.
31. Cohen-Yeshurun A, Willner D, Trembovler V, et al. N-arachidonoyl-L-serine (AraS) possesses proneurogenic properties in vitro and in vivo after traumatic brain injury. *J Cereb Blood Flow Metab*. 2013;33(8):1242–1250. doi:10.1038/jcbfm.2013.75.
32. Kino T, Tomori T, Abutarboush R, et al. Effect of N-arachidonoyl-L-serine on human cerebrovascular endothelium. *Biochem Biophys Res*. 2016;8:254–260. doi:10.1016/j.bbrep.2016.09.002.
33. Sui J, He M, Wang Y, et al. Sphingolipid metabolism in type 2 diabetes and associated cardiovascular complications. *Exp Ther Med*. 2019;18(5):3603–3614.
34. Konończuk T, Łukaszuk B, Mikłosz A, Chabowski A, Żendzian-Piotrowska M, Kurek K. Cerulein-induced acute pancreatitis affects sphingomyelin signaling pathway in rats. *Pancreas*. 2018;47(7):898–903. doi:10.1097/mpa.0000000000001086.
35. Wahrensjö E, Ohrvall M, Vessby B. Fatty acid composition and estimated desaturase activities are associated with obesity and lifestyle variables in men and women. *Nutr Metab Cardiovasc Dis*. 2006;16(2):128–136.
36. Kröger J, Schulze MB. Recent insights into the relation of $\Delta 5$ desaturase and $\Delta 6$ desaturase activity to the development of type 2 diabetes. *Curr Opin Lipidol*. 2012;23(1):4–10. doi:10.1097/mol.0b013e32834d2dc5.
37. Martinelli N, Girelli D, Malerba G, et al. FADS genotypes and desaturase activity estimated by the ratio of arachidonic acid to linoleic acid are associated with inflammation and coronary artery disease. *Am J Clin Nutr*. 2008;88(4):941–949. doi:10.1093/ajcn/88.4.941.
38. Acharya C, Navina S, Singh VP. Role of pancreatic fat in the outcomes of pancreatitis. *Pancreatol*. 2014;14(5):403–408. doi:10.1016/j.pan.2014.06.004.
39. Patel PS, Sharp SJ, Jansen E, et al. Fatty acids measured in plasma and erythrocyte-membrane phospholipids and derived by food-frequency questionnaire and the risk of new-onset type 2 diabetes: a pilot study in the European Prospective Investigation into Cancer and Nutrition (EPIC)-Norfolk cohort. *Am J Clin Nutr*. 2010;92(5):1214–1222. doi:10.3945/ajcn.2010.29182.
40. Kotronen A, Velagapudi VR, Yetukuri L, et al. Serum saturated fatty acids containing triacylglycerols are better markers of insulin resistance than total serum triacylglycerol concentrations. *Diabetologia*. 2009;52(4):684–690. doi:10.1007/s00125-009-1282-2.
41. Kurotani K, Sato M, Ejima Y, et al. High levels of stearic acid, palmitoleic acid, and dihomog- γ -linolenic acid and low levels of linoleic acid in serum cholesterol ester are associated with high insulin resistance. *Nutr Res*. 2012;32(9):669–675.e3. doi:10.1016/j.nutres.2012.07.004.
42. Stevens T, Berk MP, Lopez R, et al. Lipidomic profiling of serum and pancreatic fluid in chronic pancreatitis. *Pancreas*. 2012;41(4):518–522. doi:10.1097/mpa.0b013e31823ca306.
43. Bruls YM, de Ligt M, Lindeboom L, et al. Carnitine supplementation improves metabolic flexibility and skeletal muscle acetylcarnitine formation in volunteers with impaired glucose tolerance: a randomised controlled trial. *EBioMedicine*. 2019;49:318–330. doi:10.1016/j.ebiom.2019.10.017.
44. Arafa HM, Hemeida RA, Hassan MI, et al. Acetyl-L-carnitine ameliorates caerulein-induced acute pancreatitis in rats. *Basic Clin Pharmacol Toxicol*. 2009;105(1):30–36.
45. Zhao S, Feng XF, Huang T, et al. The association between acylcarnitine metabolites and cardiovascular disease in Chinese patients with type 2 diabetes mellitus. *Front Endocrinol (Lausanne)*. 2020;11:212.
46. Sampey BP, Freemerman AJ, Zhang J, et al. Metabolomic profiling reveals mitochondrial-derived lipid biomarkers that drive obesity-associated inflammation. *PLoS One*. 2012;7(6):e38812. doi:10.1371/journal.pone.0038812.
47. Jimenez-Luna C, Martin-Blazquez A, Dieguez-Castillo C, et al. Novel biomarkers to distinguish between type 3c and type 2 diabetes mellitus by untargeted metabolomics. *Metabolites*. 2020;10(11):423. doi:10.3390/metabo10110423.

Application of the FMEA Method in Improving the Quality Management of Emergency Complete Blood Count Testing

Shuangshuang Lv, PhD^{1,*}, Yingqian Sun, PhD¹, Jian Zhang, PhD¹, Tingting Jin, PhD¹, Xiaxuan Hu, PhD¹

¹Clinical Laboratory, DongYang People's Hospital, Dongyang, China. *To whom correspondence should be addressed: 15958490336@139.com.

Keywords: FMEA, emergency complete blood count, laboratory turnaround time, phlebotomy skills, quality control, morphology training

Abbreviations: FMEA, failure mode and effects analysis; CBC, complete blood count; RPN, risk priority number; TAT, turnaround time; ISO, International Organization for Standardization; CRP, C-reactive protein; S, severity; O, probability of occurrence; D, fault detection; IQR, interquartile range

Laboratory Medicine 2023;54:574-581; <https://doi.org/10.1093/labmed/lmad002>

ABSTRACT

Objective: Failure mode and effects analysis (FMEA) was used to identify factors that contribute to quality management deficiencies in laboratory testing of emergency complete blood count (CBC).

Methods: Improvements included instrument updates, personnel training, and laboratory information system optimization. We used operational data from January 2021 (control group) and January 2022 (FMEA group) to compare the risk priority number (RPN) of FMEA, emergency CBC laboratory turnaround time (TAT), error report rate, and specimen failure rate.

Results: After the implementation of FMEA, the average RPN dropped from 36.24 ± 9.68 to 9.45 ± 2.25 , ($t = 20.89$, $P < .05$). Additionally, the median TAT for emergency CBCs decreased from 23 min to 11 min as did the interquartile distance (17-34 min to 8-16 min) ($P < .05$). The rate of emergency CBC error reports decreased from 1.39% to 0.71% ($P < .05$), and the specimen failure rate decreased from 0.95% to 0.32% ($P < .05$). Patient satisfaction also increased from 43% to 74% ($P < .05$), and the technician-performed morphology assessment pass rate increased from 16.7% to 100% ($P < .05$).

Conclusion: Improving the emergency CBC testing process with FMEA can shorten emergency CBC laboratory TAT and reduce

specimen failure rates and reporting error rates. The FMEA can be used to improve quality management in emergency CBC laboratories.

Emergency complete blood count (CBC) analysis is commonly requested during emergency medical care. Indicators such as hemoglobin, neutrophils, monocytes, and eosinophils can reflect early signs of many systemic diseases such as leukemia, anemia, systemic lupus erythematosus, tuberculosis, and acute aortic syndrome among others.¹⁻⁶ A CBC is usually the initial test of choice in emergency pediatric settings to differentiate between bacterial and viral infections.⁷ Recent studies have shown that CBCs also have had an early warning effect during the global COVID-19 pandemic.⁸⁻¹⁰ Timely and correct reporting is the basis for reliable medical disposition,¹¹ and establishing correct and effective laboratory quality indicators is the key to ensuring that test reports are timely and correct.

Quality indicators are one of the tools for quantifying the quality of a certain aspect of a laboratory's services. The International Organization for Standardization (ISO) 15189:2012 guidelines state "[L]aboratories should establish quality indicators to monitor and evaluate the key links in the pre-test, inspection and post-test process." The Chinese Health and Family Planning Commission issued 15 medical quality control indicators for clinical laboratory specialties (2015 edition). Using these 15 indicators combined with the characteristics of our laboratory, we selected 9 of them as the quality indicators for this emergency CBC laboratory. They are the specimen failure rate in the pretest process, laboratory turnaround time (TAT) during inspection, error reporting rate in the posttest process, and the rates of specimen type error, container error, specimen loss, specimen coagulation, hemolysis, and insufficient collection, which are the main reasons for specimen failure. Quantitative assessment of the errors in the entire process of testing was carried out using the above indicators. Although the use of quality indicators can help laboratories quantify and monitor risks throughout the workflow of emergency CBCs, the guidelines of ISO and the Chinese Health and Family Planning Commission do not provide specific methods for risk identification and management.

Failure mode and effects analysis (FMEA) is a management tool that proactively identifies potential failures and assesses their causes and effects, thereby preventing their occurrence.¹²⁻¹⁴ Liu et al¹⁴ showed that

FMEA has high utility in improving health care quality and reducing errors, and this method has already been widely used to improve health care processes in hospitals, including clinical practices¹⁵ such as chemotherapy,¹⁶ pediatrics,¹⁷ intensive care,¹⁸ paramedical technology,^{19,20} reproductive health medicine,²¹ hospital infection control,²² and others.

The FMEA has been successfully used to improve the quality of various clinical procedures and processes in hospital systems; however, its specific application to quality management in emergency CBC laboratories is rare, and it is not very common to use FMEA for process improvement to optimize laboratory quality management. At the same time, owing to the diversity of laboratory test lists and the consideration of time and effort costs, it is not easy to conduct extensive laboratory quality management assessments in this way. Therefore, we used emergency CBC as an example to conduct an FMEA study. The objective of this study was to (1) evaluate the effectiveness of improving emergency CBC quality management by applying the FMEA model, (2) identify improvement measures, and (3) provide a reference for quality management in other laboratories.

Materials and Methods

General Materials

The study was conducted at a 1700-bed general tertiary hospital in China. The selected emergency laboratory was certified by ISO15189 in 2014. We used operational data from all emergency CBC samples tested in emergency laboratories in January 2021 as the control group ($n = 9680$) and the same data in January 2022 as the FMEA group ($n = 10,352$). The FMEA improvement period was from February 2021 to December 2021. The data were obtained from the Emergency Laboratory Information System (LIS). Some emergency CBCs appeared in combination with C-reactive protein (CRP) level testing in the report. The original emergency CBC testing instrument was the BC 6800 Auto Hematology Analyzer (Mindray), which was replaced by the XN-2000 Hematology Analyzer (Sysmex) as part of the improvements. The CRP detection instrument used was the Aristo Specific Protein Analyzer (Goldsite), which was replaced by the PA990pro Specific Protein Analyzer (Lifotronic) after improvement. The study was approved by the hospital review board.

FMEA Team Formation

The FMEA team was multidisciplinary, consisting of 6 people—1 laboratory director, 1 FMEA guidance expert, 1 laboratory quality statistical analyst, 2 resident personnel of the emergency laboratory, and 1 specimen recipient—who were key to emergency CBC quality management. Under the auspices of the director, the FMEA guidance expert trained team members on FMEA models. The department regularly held FMEA meetings to analyze the quality defects in the emergency CBC process from reception to reporting, assessing risks, summarizing the causes, formulating improvement measures, and supervising implementation.

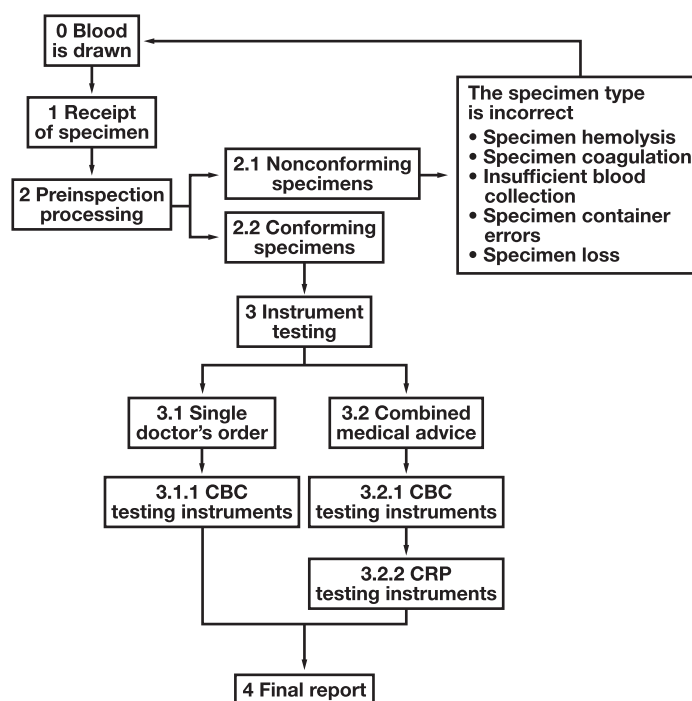
FMEA Analysis

Team members listed all the steps of emergency CBC analysis in detail, beginning from receipt of the sample in the laboratory to the issuance of the report, which was divided into receipt of specimen, preinspection processing, instrument testing, and final report based on the time recorded by the LIS (FIGURE 1). By consulting the literature and the

process characteristics of our hospital's emergency CBC,^{23,24} we listed 6 failure modes in the emergency CBC testing process that could cause quality defects, which were specimens not being processed in a timely manner after receipt, many unqualified specimens, congestion during peak periods, the instrument running slowly, reports not being sent in a timely manner, and error reporting. We discussed and analyzed the causes and outcomes of the failures, then scored them based on the severity (S), probability of occurrence (O), and fault detection (D), and summarized the scores of the 6 members, expressed as averages. To reduce subjective errors, we developed the scoring criteria of O, S, and D after discussion (TABLE 1). Based on the International Joint Commission guidelines of 2010,²¹ the risk priority number (RPN) was calculated as $O \times S \times D$. Finally, the risk was sorted according to the RPN, and the risks of failure were positively correlated with the RPN. Referring to the characteristics of this scoring and the introduction of the literature, we determined that an RPN ≥ 30 indicated a high-risk factor and prioritized a failure mode above $S \geq 4$ for improvement; if the RPN < 30 , but any of the values in O or D ≥ 4 , the factor was also considered to be high risk.^{25–27} According to the above rules, 6 failure modes were found in need of improvement. The risks from highest to lowest were as follows: the instrument running slowly, many unqualified specimens, congestion during peak periods, error reporting, specimens not being processed in a timely manner after receipt, and reports not being sent in a timely manner (TABLE 2).

FMEA Improvement Process

1. The instrument runs slowly (RPN: 46.24; S:4.00; O:4.33). This extended the laboratory TAT because of the high failure rate of CRP instruments; a single CBC instrument could not meet the daily workload. We therefore purchased the Sysmex blood routine assembly line, including 2 CBC detectors, a fully automatic staining instrument. We also updated and added 2 CRP detectors for alternative use to reduce failure rate.
2. There are many unqualified specimens of quality (RPN: 40.35; S:4.00; O:4.33). Here, the cause of the failure was the unqualified quality of specimens caused by insufficient phlebotomy skills. We created a phlebotomy training plan for all phlebotomists who had been trained and assessed every 6 months and set a monthly quality target for each phlebotomist. We then publicized the completions of the target. The Medical Department conducts a quarterly phlebotomy skills satisfaction survey.
3. Congestion during peak periods (RPN: 37.28; S:4.00; O:4.00), the failure was due to high specimen volume during peak periods; therefore, we increased the emergency laboratory staff during peak times (9:00 to 11:00 AM, 4:00 to 6:00 PM).
4. Error reporting (RPN: 21.36.28; S:4.00; O:2.67). Here, the cause of the failure was unfamiliar reporting rules. In response, we set the blood routine reexamination rules in the LIS: a report that does not trigger the reexamination rules is automatically sent by the system, the report that triggers the reexamination rules is sent after manual review, and the difficult results (such as leukemia) that cannot be automatically classified by the instrument are manually classified by microscopy. We also created a blood cell morphology training plan with a teaching group, and the morphology experts in the department served as teachers.

FIGURE 1. Emergency complete blood count laboratory turnaround process.**TABLE 1.** Scoring of Factors That Influence the Failure Modes and Effects Analysis Performance

Score	Description
Occurrence (O)	
1	Rarely occurs
2	Occurs quarterly
3	Occurs monthly
4	Occurs daily
5	Occurs continuously
Severity (S)	
1	No effect; processing time <5 min
2	Minor; processing time 5-10 min
3	Major; processing time 10-15 min
4	Serious; processing time 15-30 min
5	Very serious; processing time >30 min
Detection (D)	
1	When blood is drawn
2	Specimen collection phase
3	Before instrument testing
4	Inspection before report is issued
5	Unable to detect

Monthly morphology training and quarterly assessments were planned for young employees with less than 5 years of seniority, and employees with 5 to 10 years of seniority who had a certain morphological foundation were scheduled to be evaluated every 6 months. We set the qualifying score at 90 points. Employees

could stop the morphological assessments in advance if they passed the assessments 4 times in a row.

- Failure to process promptly after receipt (RPN: 24.56; S:2.83; O:4.00). This failure was caused by the fact that the specimen acceptance site was located at a distance from the laboratory, resulting in the extension of the reporting TAT. The improvement measures we took consisted of relocating the sampling site and setting up sampling points in the laboratory to shorten the time from specimen sampling to testing.
- Reports are not sent in a timely manner (RPN: 16.98; S:1.50; D:4.00). This failure was due to the large workload in the emergency laboratory, resulting in the extension of the laboratory TAT. To improve this, we set up a TAT reminder service on LIS to remind laboratory personnel to prioritize the processing of long reports of the TAT.

Finally, the team members then developed an emergency CBC test standard operating procedure based on the improvement measures for performance. Emergency department personnel were required to operate strictly according to these standardized procedures. These FMEA improvements were implemented between February 2021 and December 2021, followed by a second round of FMEA analysis of emergency CBC quality management in January 2022.

Evaluation

The RPN and changes in laboratory TAT were used to assess changes in processes before and after improvement. The specimen failure rate and the satisfaction of phlebotomy skills were used to evaluate phlebotomy skills; the error reporting rate and morphological assessment pass rate were used to evaluate the reporting ability.

TABLE 2. Risk Assessment Form for Quality Deficiencies in Emergency CBC Laboratory Management

Process Step	Potential Failure Mode	Cause	Impact on Quality Indicators	S	O	D	RPN	Prioritization	Improvement Measure
1. Receipt of specimen	Specimens are not processed in a timely manner after receipt	The specimen collection location is far from the detection location	Laboratory TAT increases	2.83	4.00	2.17	24.56	6	Relocation of sample collection sites; set the specimen collection point in the laboratory
2. Preinspection processing	There are many rejected specimens owing to quality	Insufficient phlebotomy skills	The quality failure rate increases, and the specimen is re-extracted	4.00	4.33	2.33	40.35	2	Train the phlebotomists in phlebotomy skills and set a target value for each person to pass the phlebotomy per month; finally, announce the completion of the target
3. Instrument testing	Congestion during peak periods	Large specimen volume	Laboratory TAT increases	4.00	4.00	2.33	37.28	3	Increased availability of personnel from 9:00 to 11:00 AM and from 4:00 to 6:00 PM to cope with the peak period of specimens
	The instrument runs slowly	Insufficient testing instruments	Laboratory TAT increases	4.00	4.33	2.67	46.24	1	The introduction of Sysmex blood routine assembly line, including 2 CBC detectors and an automatic dyeing instrument
4. Final report	Reports are not sent in a timely manner	Large specimen volume	Laboratory TAT increases	1.50	2.83	4.00	16.98	6	Set the TAT preset value in the LIS to detect when a report was unintentionally missed
	Error reporting	Lack of well-established reexamination system for reporting blood routines, and the morphological ability of the reporting was inadequate	Report recovery rates increased	4.00	2.67	2.00	21.36	4	We established a blood routine re-examination system and regularly train personnel in blood cell morphology

CBC, complete blood count; D, detectability of failure occurrence; LIS, laboratory information system; O, the possibility of the failure; RPN, risk priority number (1 to 6 from highest to lowest priority); S, the severity of the failure; TAT, turnaround time.

RPN

After the FMEA improvement, we obtained the RPN in the same way as before the improvement.

Laboratory TAT

We divided TAT into 4 subdivisions: (1) laboratory TAT, which was clock started when the specimen reached the laboratory and was first accessioned by the LIS and clock stopped when the result was finalized in the LIS; (2) peak hour TAT, that is, the laboratory TAT during the maximum specimen volume time period (9:00 to 11:00 AM, 4:00 to 6:00 PM); (3) single doctor's order TAT, which means a laboratory TAT that only contains a single item of the emergency CBC in the medical order; and (4) combination doctor's order TAT, which refers to the laboratory TAT, including emergency CBC and CRP level testing. We used median and interquartile range (IQR) to describe the changes in TAT before and after FMEA.

Error Report Rate

The error report rate was the number of emergency CBC error reports recovered by LIS divided by the total number of emergency CBC specimens in the month.

Specimen Failure Rate

The specimen failure rate is considered the number of rejected specimens divided by the total number of emergency CBC specimens in the month. The reasons for failure were divided into specimen type error, container error, specimen loss, hemolysis, coagulation, and insufficient collection amount, and the proportion of rejection reasons was compared.

Phlebotomy Skills Satisfaction

A questionnaire was compiled by the hospital medical department and distributed to patients every quarter. The satisfaction level was divided into unsatisfactory, average, satisfactory, and very satisfied. The content of the survey included the patient's satisfaction with environment, phlebotomy skills, infrastructure construction, and so on, and combined with the service attitude of the phlebotomists. Results were quantified thus: phlebotomy skills satisfaction = very satisfied + satisfied/total number of cases \times 100%. We compared the results of questionnaires in the fourth quarter of 2020 (control group, collected in January 2021) before and after improvement in the fourth quarter of 2021 (FMEA group, collected in January 2022) to identify changes in patient satisfaction.

Morphological Assessment Pass Rate

The assessment content was divided into theoretical examination and practical assessment. The theory consisted of 50 cell morphological maps. The practical assessment consisted of manually classifying 5 blood cell smears stained by Wright's staining within 30 min. The specimens used for the assessment were from healthy people, platelet aggregates, leukemia, inflammatory infection patients, and others. Results were quantified as pass rate = number of qualified people/total number of people assessed \times 100%. The total score was 100 points, and 90 points and above represented a passing grade.

Statistical Analysis

We used SPSS statistical software version 26.0 (IBM) for statistical analysis and processing. Continuous variables containing normally distributed data are expressed as the mean and standard deviation.

Nonnormally distributed data are represented as the median and interquartile range. We used χ^2 tests to compare categorical variables. We performed the Student's *t*-test and the Mann-Whitney *U* test to compare parametric and nonparametric continuous variables, respectively. A *P* value < .05 was considered statistically significant.

Results

There was no statistically significant difference (*P* > .05) in the sex and age or the proportion of disease types between the 2021 and 2022 groups (TABLE 3).

After the implementation of FMEA, the average RPN dropped from 36.24 ± 9.68 to 9.45 ± 2.25 , (*t* = 20.89, *P* < .05). (TABLE 4).

After FMEA improvements, the median TAT (11 min) and IQR (8-16 min) in the emergency CBC laboratories were significantly shorter than those before (23 min and 17-34 min), and the peak TAT, single doctor's order TAT, and combination doctor's order TAT were significantly (*P* < .01) shorter than those before (TABLE 5).

The error reporting rate decreased from 1.39% to 0.71% ($\chi^2 = 23.14$, *P* < .05) and the specimen failure rate decreased from 0.95% to 0.32% ($\chi^2 = 10.63$, *P* < .05), and the proportion of all causes of nonconformity decreased after improvement; especially of note was that the incidence of container error and specimen loss was 0, which was a significant improvement, as shown in TABLE 6.

After the phlebotomists received training, the patient satisfaction rate with regard to phlebotomy skills increased from 43% to 74%, ($\chi^2 = 19.79$, *P* < .05), which was statistically significant (TABLE 7).

During the morphology training of reporters, the pass rate of the assessment increased from 16.7% in the first quarter to 100% in the fourth quarter of 2021, and the difference was statistically significant (*P* < .05) (TABLE 8).

Discussion

In this study, we categorized the main processes involved in emergency CBC procedures into receipt of specimen, preinspection processing,

TABLE 3. Characteristics of Patients from Whom Samples Were Obtained

Item	Control Group	FMEA Group	χ^2/t	<i>P</i> Value
Sex (F/M)	4530/5150	4943/5409	1.81	.18
Age, y, $\bar{X} \pm SD$	46.31 ± 26.20	49.43 ± 23.48	-1.60	.112
Diagnostic categories	9680	10,352	14.27	.01
Presence of fever	3274	3409	1.78	.18
Surgical cases	3370	3818	9.29	<.05
Internal medicine cases	3036	3125	3.25	.07

FMEA, failure modes and effects analysis; SD, standard deviation; *X*, mean.

TABLE 4. Changes in RPN before and after FMEA

Potential Failure Mode	RPN		Reduction in RPN (%)
	Before	After	
The instrument runs slowly	46.24	10.68	76.90
Instrument congestion during peak periods	37.28	9.32	75.00
There are many rejected specimens due to quality	40.35	9.32	76.90
Error reporting	21.36	8.00	62.55
High review rate	42.47	12.75	69.98
Specimens are not processed in a timely manner after receipt	24.56	6.14	75.00
Reports are not sent in a timely manner	16.98	6.00	64.66
Average value ($\bar{X} \pm SD$)	36.24 ± 9.68	9.45 ± 2.25^a	71.57

FMEA, failure mode and effects analysis; RPN, risk priority number.

^aCompared with before, *t* = 20.89, *P* < .05.

TABLE 5. Decreases in Turnaround Time at Different Stages before and after FMEA

	Median (IQR), min		<i>Z</i> Value	<i>P</i> Value
	Control Group (2021)	FMEA Group (2022)		
Laboratory TAT	23 (17-34)	11 (8-16)	-63.79	<.05
Peak TAT	45 (37-71)	38 (33-49)	-3.95	<.05
Single doctor's order TAT	12 (7-27)	9 (6-15)	-67.08	<.05
Combination doctor's order TAT	24 (18-34)	11 (8-16)	-7.57	<.05

FMEA, failure mode and effects analysis; IQR, interquartile range; TAT, turnaround time.

^aLaboratory TAT is the TAT for laboratory from specimen receipt to report generation. T3 is the peak TAT, the lab TAT of maximum time period for specimen volume (9:00 to 11:00 AM, 4:00 to 6:00 PM). Single doctor's order TAT is the doctor's order includes only laboratory TAT at the time of emergency complete blood count (CBC) testing. The combination doctor's order TAT is the physician's order includes laboratory TAT for emergency CBC and C-reactive protein level testing.

TABLE 6. Emergency CBC Reporting Error Recovery Rate and Specimen Quality Analysis before and after FMEA

	No. (%)		χ^2	P Value
	Control Group (n = 9680)	FMEA Group (n = 10,352)		
Reporting error recovery rate	135 (1.39)	73 (0.71)	23.14 ^a	<.05
Total rejection rate of emergency CBC specimens	92 (1.12)	33 (0.41)	10.63 ^b	.04
The specimen type is incorrect	17 (0.17)	9 (0.09)	3.03 ^a	<.05
Specimen container errors	10 (0.10)	0 (0)	10.70 ^b	<.05
Specimen loss	7 (0.07)	0 (0)	7.49 ^b	<.05
Specimen hemolysis	18 (0.18)	11 (0.11)	29.99 ^a	<.05
Specimen coagulation	34 (0.35)	8 (0.07)	17.95 ^a	<.05
Insufficient blood collection	23 (0.24)	11 (0.1)	5.09 ^a	.02

CBC, complete blood count; FMEA, failure mode and effects analysis.

^aPearson χ^2 .

^bFisher exact probability.

TABLE 7. Patient Satisfaction of Blood Collection before and after Improvement^a

	Not Satisfied	Generally	Satisfied	Very Satisfied	Satisfaction
Control group (n = 200)	50 (25%)	64 (32%)	64 (32%)	22 (11%)	43%
FMEA group (n = 200)	16 (8%)	36 (18%)	94 (47%)	54 (27%)	74%

^aThe control group shows the results of a blood collection satisfaction survey for the fourth quarter of 2020. The failure mode and effects analysis (FMEA) group shows the results of a blood collection satisfaction survey for the fourth quarter of 2021. Satisfaction is calculated as very satisfied + satisfied/total number of cases \times 100%. $\chi^2 = 19.79$; $P < .05$.

TABLE 8. Changes in Morphology Test Pass Rates^a

Employees with Less than 10 Years of Service	Examination Score			
	1st Quarter	2nd Quarter	3rd Quarter	4th Quarter
A	72	89	98 (pass)	100 (pass)
B	68	84	92 (pass)	98 (pass)
C	82	90 (pass)	92 (pass)	100 (pass)
D	90 (pass)	95 (pass)	100 (pass)	100 (pass)
E	78	96 (pass)	100 (pass)	98 (pass)
F	77	86	92 (pass)	100 (pass)
G		88		92 (pass)
H		90 (pass)		96 (pass)
J		91 (pass)		94 (pass)
Pass rate	16.7%	55.6% ^b	100% ^b	100% ^b

^aA to F indicates employees within 5 years of seniority who are evaluated quarterly in morphology. G to J indicates employees with 5 to 10 years of seniority who had a certain morphological foundation and were scheduled to be evaluated every 6 months. A score of 90 or more will be awarded a pass. The pass rate is the number of passes/total number of people taking the exam \times 100%.

^bCompared with the first quarter, $P < .05$.

instrument testing, preliminary examination, and final report. Failure patterns that caused laboratory quality defects at each step were investigated, and interventions were developed to address them. Using FMEA, we identified 6 failure modes that could lead to emergency CBC quality defects and sorted them by rectification priority. These failure modes were divided into the following: the instrument runs slowly, there are many unqualified specimens of quality, congestion during peak periods, error reporting, specimens are not processed in a timely manner after receipt, and reports are not sent in a timely manner.

The instrument runs slowly had the largest RPN in our risk assessment, in which the failure mode was instrument detection in the

inspection; therefore, we updated and increased the number of our testing instruments for CBC and CRP level. We purchased the Sysmex XN2800 pipeline system, which included 2 XN2000 blood cell detectors and a fully automatic staining instrument to replace the previously improved single blood cell detection mode. Additionally, as emergency CBC and CRP level testing often exist in combination orders, we also added new CRP detectors to increase the speed of our analysis. After this improvement, both the laboratory TAT and the combined doctor's order TAT were shortened by half, and the single doctor's order TAT was also significantly shortened. Although we did not compare instrument characteristics of CBC and CRP before and after the improvement, the

significantly shortened TAT illustrated the benefits of replacing the instrument. Updating and adding testing equipment also solved the problem of specimen accumulation caused by insufficient equipment. However, congestion due to large specimen volumes during peak periods remained a problem. The failure mode of congestion during peak periods, which was the same as specimens are not processed in a timely manner after receipt, would lead to the extension of laboratory TAT. The causes of failure also overlapped partially, mainly owing to the large number of specimens and insufficient manpower during peak hours. In particular, the specimens are not processed in a timely manner after receipt failure category had an additional cause: the specimen acceptance site was located at a distance from the laboratory. Therefore, the relocation of the specimen receiving area to the laboratory effectively solved the problem. To improve congestion during peak periods we increased the emergency laboratory staff during peak times (9:00 to 11:00 AM, 4:00 to 6:00 PM). As the peak period TAT was shortened significantly after improvement, the effectiveness of the measure was demonstrated. However, the changes in this TAT were not as obvious as other TAT changes, possibly because of other fault factors, such as the occupation of resources by nonemergency specimens, which was also mentioned in the 738 Chinese laboratory surveys conducted by Zhang et al.²⁸

Another important indicator of the quality of emergency CBC laboratories was the specimen failure rate, which was manifested in several aspects: specimen type error, container error, specimen coagulation, hemolysis, insufficient collection, and specimen loss. We implemented further training in phlebotomy skills while setting each phlebotomist a monthly target for quality qualification and the completion of the target value was publicized. Owing to the continuous enhancement of phlebotomy skills, simple collection errors, such as container errors, were directly avoided and dropped to zero after improvements. The specimen coagulation, hemolysis, and insufficient amount of collection were also significantly reduced. However, in the process of phlebotomy, it is difficult to avoid the phenomenon of unqualified specimens due to the fact that some patients' blood vessels are relatively hidden, or the patient's blood itself is in a hypercoagulable state and incorrect pretreatment process outside the laboratory. For the improvement of specimen loss, the solution was to separate the placement areas for inspected and uninspected specimens. This stopped the phenomenon of random placement of uninspected specimens with the completed specimens, and the incidence of specimen loss after improvement decreased to zero, which shows that a reasonable laboratory layout can reduce the frequency of adverse events. This was similar to the conclusions of Tsai et al.²⁹

To address the error reporting failure category, we rectified both LIS and personnel. We also added blood routine review rules to LIS, which could be automatically issued for normal reports that do not trigger the rules, whereas reports that trigger retest rules need to be manually reviewed. Reports that cannot be automatically sorted by the instrument would be sent through manual classification. At the same time, regular blood cell morphology training was carried out for personnel to improve the detection and accuracy of difficult blood cell reports. Although the decline in the error reporting rate showed that this rectification was effective, the application of the automatic report sending system requires further improvements and supervision in the later stage. Finally, to address the reports are not sent in a timely manner failure category, we set up a TAT reminder service on the LIS, which effectively reminds the staff to review and deliver the report on time.

Similar to other efforts to employ FMEAs, our analysis may be subjective and depends on the experience and skills of the team members. We only targeted process improvements within the emergency CBC laboratory and did not address the relevant process factors outside the laboratory, which should be investigated in future research.

In summary, we optimized the testing process of emergency CBC laboratory from the aspects of instrument update, personnel training, and LIS optimization and improved their quality management capabilities.

Conclusion

Improving the emergency CBC testing process through FMEA can shorten laboratory TAT and reduce specimen failure rates and report recovery rates, thereby improving laboratory quality management.

Conflict of Interest Disclosure

The authors have nothing to disclose.

REFERENCES

1. Lee E, Kim M, Jeon K, et al. Mean platelet volume, platelet distribution width, and platelet count, in connection with immune thrombocytopenic purpura and essential thrombocytopenia. *Lab Med*. 2019;50(3):279–285.
2. Park CH, Yun JW, Kim HY, et al. Myelodysplastic syndrome/ myeloproliferative neoplasm with ring sideroblasts and thrombocytosis with cooccurrent SF3B1 and MPL gene mutations: a case report and brief review of the literature. *Lab Med*. 2020;51(3):315–319.
3. Jeon YL, Lee WI, Kang SY, et al. Neutrophil-to-monocyte-plus-lymphocyte ratio as a potential marker for discriminating pulmonary tuberculosis from nontuberculosis infectious lung diseases. *Lab Med*. 2019;50(3):286–291.
4. Peirovy A, Malek Mahdavi A, Khabbazi A, et al. Clinical usefulness of hematologic indices as predictive parameters for systemic lupus erythematosus. *Lab Med*. 2020;51(5):519–528.
5. Moon SY, Lee HS, Park MS, Kim I-S, Lee SM. Evaluation of the barricor tube in 28 routine chemical tests and its impact on turnaround time in an outpatient clinic. *Ann Lab Med*. 2021;41(3):277–284. doi:10.3343/alm.2021.41.3.277.
6. Morello F, Cavalot G, Giachino F, et al. White blood cell and platelet count as adjuncts to standard clinical evaluation for risk assessment in patients at low probability of acute aortic syndrome. *Eur Heart J Acute Cardiovasc Care*. 2017;6(5):389–395.
7. Tamelytė E, Vaičekauskienė G, Dagys A, et al. Early blood biomarkers to improve sepsis/bacteremia diagnostics in pediatric emergency settings. *Medicina (Kaunas)*. 2019;55(4):E99.
8. Urrechaga E, Ponga C, Fernández M, et al. Diagnostic potential of leukocyte differential and cell population data in prediction of COVID-19 among related viral and bacterial infections at emergency department. *Clin Chem Lab Med*. 2022;60(5):e104–e107.
9. Cabitza F, Campagner A, Ferrari D, et al. Development, evaluation, and validation of machine learning models for COVID-19 detection based on routine blood tests. *Clin Chem Lab Med*. 2021;59(2):421–431.
10. Ye W, Chen G, Li X, et al. Dynamic changes of D-dimer and neutrophil-lymphocyte count ratio as prognostic biomarkers in COVID-19. *Respir Res*. 2020;21(1):169.
11. Huang Y, Zhang X, Fei Y, et al. Investigation on the turnaround time of the whole process of clinical testing blood projects. *J Clin Examination*. 2018;36(7):528–531.
12. Woodhouse S. Engineering for safety: use of failure mode and effects analysis in the laboratory. *Lab Med*. 2005;36(1):16–18.

13. Hammerling JA. A review of medical errors in laboratory diagnostics and where we are today. *Lab Med*. 2012;43(2):41–44.
14. Liu HC, Zhang LJ, Ping YJ, Wang L. Failure mode and effects analysis for proactive healthcare risk evaluation: a systematic literature review. *J Eval Clin Pract*. 2020;26(4):1320–1337.
15. Lee H, Lee H, Baik J, et al. Failure mode and effects analysis drastically reduced potential risks in clinical trial conduct. *Drug Des Devel Ther*. 2017;11(19):3035–3043.
16. Cheng CH, Chou CJ, Wang PC, et al. Applying HFMEA to prevent chemotherapy errors. *J Med Syst*. 2012;36(3):1543–1551.
17. Anjalee JAL, Rutter V, Samaranyake NR. Application of failure mode and effects analysis (FMEA) to improve medication safety in the dispensing process—a study at a teaching hospital, Sri Lanka. *BMC Public Health*. 2021;21(1):1430.
18. Lin L, Wang R, Chen T, et al. Failure mode and effects analysis on the control effect of multi-drug-resistant bacteria in ICU patients. *Am J Transl Res*. 2021;13(9):10777–10784.
19. Wexler A, Gu B, Goddu S, et al. FMEA of manual and automated methods for commissioning a radiotherapy treatment planning system. *Med Phys*. 2017;44(9):4415–4425. doi:[10.1002/mp.12278](https://doi.org/10.1002/mp.12278).
20. Jiang Y, Jiang H, Ding S, Liu Q. Application of failure mode and effects analysis in a clinical chemistry laboratory. *Clin Chim Acta*. 2015;448(25):80–85. doi:[10.1016/j.cca.2015.06.016](https://doi.org/10.1016/j.cca.2015.06.016).
21. Rienzi L, Bariani F, Dalla Zorza M, et al. Comprehensive protocol of traceability during IVF: the result of a multicentre failure mode and effect analysis. *Hum Reprod*. 2017;32(8):1612–1620. doi:[10.1093/humrep/dex144](https://doi.org/10.1093/humrep/dex144).
22. Xu Y, Wang W, Li Z, et al. Effects of healthcare failure mode and effect analysis on the prevention of multi-drug resistant organisms infections in oral and maxillofacial surgery. *Am J Transl Res*. 2021;13(4):3674–3681.
23. Duan M, Kang F, Zhao H, et al. Analysis and evaluation of the external quality assessment results of quality indicators in laboratory medicine all over China from 2015 to 2018. *Clin Chem Lab Med*. 2019;57(6):812–821.
24. Biljak VR, Lapić I, Vidranski V, et al. Policies and practices in the field of laboratory hematology in Croatia—a current overview and call for improvement. *Clin Chem Lab Med*. 2022;60(2):271–282.
25. Karadağ C, Demirel NN. Continual improvement of the pre-analytical process in a public health laboratory with quality indicators-based risk management. *Clin Chem Lab Med*. 2019;57(10):1530–1538.
26. Hoof VV, Bench S, Soto AB, et al. Failure mode and effects analysis (FMEA) at the preanalytical phase for POCT blood gas analysis: proposal for a shared proactive risk analysis model. *Clin Chem Lab Med*. 2022;60(8):1186–1201.
27. Donald M. Powers, PhD. Laboratory quality control requirements should be based on risk management principles. *Lab Med*. 2005;36(10):633–638.
28. Zhang X, Fei Y, Wang W, et al. National survey on turnaround time of clinical biochemistry tests in 738 laboratories in China. *J Clin Lab Anal*. 2018;32(2):e22251.
29. Tsai ER, Tintu AN, Demirtas D, et al. A critical review of laboratory performance indicators. *Crit Rev Clin Lab Sci*. 2019;56(7):458–471.

Evaluation of Serum Creatinine Levels with Reference Change Value in Patients Receiving Colistin Treatment

Havva Yasemin Cinpolat, MD,^{1,*} Sevil Alkan, MD,² Hatice Betül Altınışık, MD,³ Dilek Ulker Cakir, MD,¹ Hamdi Oguzman, MD⁴

¹Department of Medical Biochemistry, Faculty of Medicine, Canakkale Onsekiz Mart University, Canakkale, Turkey, ²Department of Infectious Diseases, Faculty of Medicine, Canakkale Onsekiz Mart University, Canakkale, Turkey, ³Department of Anesthesiology and Reanimation, Faculty of Medicine, Canakkale Onsekiz Mart University, Canakkale, Turkey, ⁴Department of Medical Biochemistry, Faculty of Medicine, Hatay Mustafa Kemal University, Antakya, Hatay, Turkey. *To whom correspondence should be addressed: drcinpolat@gmail.com.

Keywords: biological variation, colistin, adverse effects, toxicity, clinical chemistry, reference values

Abbreviations: SCr, serum creatinine; RCV, reference change value; CVw, intra-individual biological variation; CVg, inter-individual biological variation; EFLM, European Federation of Clinical Chemistry and Laboratory Medicine; RIFLE, Risk, Injury, Failure, Lost, End Stage Renal Disease; AKIN, Acute Kidney Injury Network; KDIGO, Kidney Disease: Improving Global Outcomes; AKI, acute kidney injury; IV, intravenously; SD, standard deviation; CLSI, Clinical and Laboratory Standards Institute; CKD, chronic kidney disease

Laboratory Medicine 2023;54:582-586; <https://doi.org/10.1093/labmed/lmad009>

ABSTRACT

Objective: In this study, we aimed to evaluate the serum creatinine (SCr) levels with the reference change value (RCV) in patients receiving colistin treatment.

Methods: We retrospectively recorded the SCr levels of 47 patients receiving colistin treatment before treatment and on days 3 and 7 after treatment. RCV was calculated with the asymmetrical RCV formula ($Z = 1.64$, $P < .05$). Percent (%) increase in the SCr results of the patients was compared with RCV and values exceeding RCV were regarded as statistically significant.

Results: The RCV was calculated as 15.6% for SCr. Compared with pretreatment values, SCr value on day 3 was 32/47 and on day 7 it was 36/47; as these results exceeded RCV, they were considered statistically significant.

Conclusion: Use of RCV in the interpretation of results between serial measurements will provide a more rapid and sensitive method when making decisions.

Population-based reference ranges are obtained from the distribution of the results of individuals with emphasis on different age groups, sex, time of sample collection, position of sample collection (supine or upright), smoking habits, pregnancy, etc, by using direct or indirect methods. When previous results for an individual cannot be obtained or if test results are being interpreted for the first time, these ranges become very useful.¹ In instances where consecutive measurements are needed, the changes in results for a person can be due to the progression of disease, or it may as well be due to intra-individual biological variation (CVw) and analytical variation. In addition to population based reference ranges, using reference change values (RCVs) that include analytical variation and biological variation will increase the precision of interpretation of the results.² By CVw with inter-individual biological variation (CVg), individuality index is calculated. If the individuality index is <0.6 , population-based reference ranges would include only a limited number of subjects.^{3,4}

Serum creatinine (SCr) is a cheap, accessible, and fast parameter for the assessment of nephrotoxicity, so it is a frequently preferred test. However, the individuality index calculated for SCr is 0.31 based on data obtained from the European Federation of Clinical Chemistry and Laboratory Medicine (EFLM) database, and it demonstrates high level of individuality.⁵ This means that the population-based reference range does not cover all the results. Although a patient's results may be within the reference range, when a comparison is made between later and initial results of the same person, the difference can be significant. Thus, RCV gains further importance in routine patient follow-ups.⁶

Depending on the increase in SCr, RIFLE (Risk, Injury, Failure, Lost, End Stage Renal Disease), AKIN (Acute Kidney Injury Network) and KDIGO (Kidney Disease: Improving Global Outcomes) criteria are used in the classification of acute kidney injury (AKI).⁷⁻⁹ The RIFLE classification is based on a proportional increase in SCr or a decrease in glomerular filtration rate, whereas the AKIN classification is based on a proportional or an absolute increase in SCr and decrease in urine output. The KDIGO criteria was formed by combining with these 2 criteria.

Colistin is an antibiotic used in the 1960s that lost its place to other antibiotics with fewer side effects, as it was found to cause nephrotoxicity. During the last 10 to 15 years, with the emergence of multiple antibiotic resistance to Gram-negative bacteria, colistin use has increased.¹⁰

The most common and important side effect of colistin is nephrotoxicity. It develops within a week after initiation of treatment. This side effect is dose dependent and mostly reversible. Permanent kidney damage

can rarely develop.¹¹ The mechanism of nephrotoxicity for colistin is similar to its antibacterial effect. Colistin increases the membrane permeability of tubular cells. Increases in the permeability of anions, cations, and water result in the swelling and destruction of tubular cells. This then leads to acute tubular necrosis. The SCr levels of the person increase, and decreases in creatinine clearance, proteinuria, cylindruria, or oliguria may be seen.^{12,13}

In this study, we aimed to calculate the RCV for SCr measured in our laboratory, evaluate serial SCr measurements of patients receiving colistin treatment to demonstrate the development of nephrotoxicity with RCV, and investigate diagnostic accuracy of RCV by comparison with KDIGO criteria.

Materials and Methods

The study was carried out retrospectively by obtaining data from medical reports at the university hospital between 2018 and 2021. Included subjects were over 18 years of age, had infections with Gram-negative bacteria that showed multiple antibiotic resistance, and had received colistin for 10 to 14 days at the dose that was prescribed according to their renal function (colistimethate sodium 150 mg intravenously [IV]; Kolistipol). Patients under 18 years of age, who were pregnant, had a history of rhabdomyolysis, received renal replacement therapy, had history of previous colistin use, used nephrotoxic medications other than colistin, or were given radiocontrast material were excluded. By performing electronic archive screening, SCr values before the start of colistin treatment and 3 and 7 days after and demographic data like age, sex, indication for administering colistin, and underlying diseases were recorded.

The approval of Canakkale Onsekiz Mart University Medical School Clinical Research Ethical Committee (date 09.06.2021 number 06-17) was obtained.

The population-based reference interval for SCr was defined as 0.70 to 1.20 mg/dL for males and 0.50 to 0.90 mg/dL for females.

The increase in SCr more than ≥ 0.3 mg/dL within 48 hours or the increase in SCr more than 1.5-fold from the baseline was defined as colistin nephrotoxicity.⁹

SCr was measured with the kinetic alkaline picrate method on a cobas 8000 autoanalyzer (Roche Diagnostics). For calculating within-laboratory precision, 2-level internal quality control (Precicontrol 1 [lot No. 41011000] and Precicontrol 2 [lot No. 41003200]; Roche Diagnostics) material was used. The same operator measured each level of material for 20 testing days, 2 runs per testing day and 2 replicate measurements per run, and Westgard multirules were used to accept or reject these runs.¹⁴

Statistical Analysis

The SPSS v.18.0 software was used for statistical analysis. The normality of data distribution was determined using the Shapiro-Wilk test. Continuous data that did not have a normal distribution was expressed as median (interquartile range), those with normal distribution as mean plus or minus standard deviation (SD), and categorical variables as proportions. The difference between SCr at different time points was compared by one-way analysis of variance with repeated measures and Bonferroni was used for post hoc analysis. Exact *P* value was given and *P* values of $< .05$ were considered as statistically significant.

Within-laboratory precision was calculated according to the Clinical and Laboratory Standards Institute (CLSI) document EP05:A3.¹⁴ The CVw was obtained by using the biological variation database published on the EFLM website.⁵ The RCV was calculated according to the asymmetrical RCV formula¹⁵:

$$RCV = 100\% * \left[\exp(Z * 2^{1/2} * (\ln(1 + CV_a^2) + \ln(1 + CV_w^2)^{1/2} - 1)) \right]$$

As the increase in SCr level (unidirectional) was evaluated, *Z* coefficient with 95% probability (*P* < .05) was 1.64.

Based on the pretreatment SCr levels of the patients individually, percent change on days 3 and 7 were compared with RCV. Results exceeding RCV increase value were considered significant.

Results

Median age of the 47 patients included in the study was 74 (60–84) years and 32 of them were male. The indication to start administering colistin was ventilator-associated pneumonia in 37 of the patients, 3 had blood circulation infections, 4 had urinary system infection, and 3 had surgical site infections. There were 11 patients with pretreatment SCr levels exceeding the upper reference limit, 16 patients within the reference interval, and 20 patients below the lower reference limit.

When pretreatment SCr levels were compared with day 3 and day 7 levels after treatment, the increase in SCr levels was found to be statistically significant (*P* < .001). Also, there was a statistically significant

FIGURE 1. SCr levels at pretreatment, after dose on day 3, and after dose on day 7 in patients undergoing treatment with colistin.

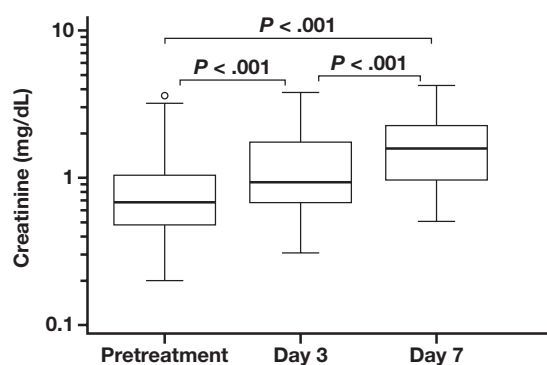


TABLE 1. Calculation of the Within-Laboratory Precision for Serum Creatinine

Sample	Mean (mg/dL)	Repeatability		Within-Laboratory Precision	
		SD	CV	SD	CV
Precicontrol 1 (lot No. 41011000)	1.05	0.01	1.0%	0.03	2.5%
Precicontrol 2 (lot No. 41003200)	3.97	0.05	1.1%	0.14	3.6%

CV, coefficient of variation; SD, standard deviation.

difference between SCr levels at day 3 and day 7 ($P < .001$) (FIGURE 1). The number of patients developing nephrotoxicity after colistin treatment was 22 of 47 on day 3 and 35 of 47 on day 7.

According to data obtained from the EFLM biological variation database, for SCr, CV_w was 4.4 and CV_g was 14.1. Mean, SD, and CV values

FIGURE 2. The rate of acute kidney injury (AKI) according to the reference interval on day 3. KDIGO, Kidney Disease: Improving Global Outcomes; RCV, reference change value.

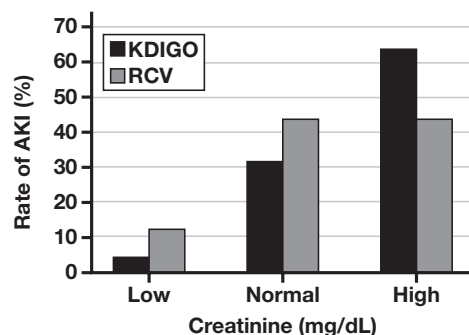
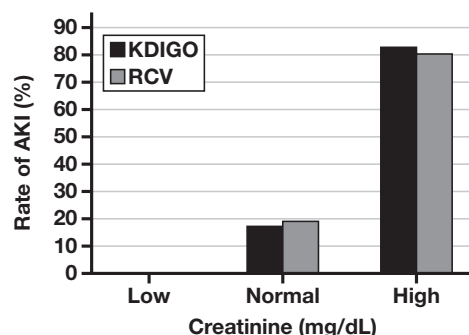


FIGURE 3. The rate of acute kidney injury (AKI) according to the reference interval on day 7. KDIGO, Kidney Disease: Improving Global Outcomes; RCV, reference change value.



calculated for SCr are summarized in TABLE 1. The RCV was calculated as 15.6%.

When the percent increase in SCr levels after treatment was compared with pretreatment SCr levels, on day 3 there were 32 patients whose values exceeded RCV and on day 7 there were 36. RCV had 100% sensitivity and 60% specificity on day 3 and 97.1% sensitivity and 83.3% specificity on day 7 for colistin nephrotoxicity. Of the 47 patients, 10 with a false-positive rate on day 3 progressed to colistin nephrotoxicity on day 7.

On day 3, the number of patients with SCr values exceeding the upper reference limit and developing AKI according to the RCV and KDIGO was 14 and 16, respectively, whereas the SCr values were within or below the reference interval, although AKI developed in 18 patients according to RCV and 21 patients according to KDIGO. There were 28 patients with SCr levels exceeding both the RCV and the upper reference limit on day 7, whereas the SCr levels of 8 patients were within or below the reference interval although they exceeded the RCV. In a similar manner, although 30 patients exceeded the upper reference limit and were considered as having AKI according to KDIGO, the SCr of 7 patients with AKI did not exceed the upper reference limit on day 7. The distribution of patients developing AKI according to the reference interval is given in FIGURES 2 and 3.

Patient evaluation by using RCV is given in TABLE 2 as an example.

Discussion

In this study, serial SCr measurements were evaluated with RCV to show the development of nephrotoxicity in patients using colistin treatment. First, our laboratory's RCV value for SCr was calculated, and for SCr unidirectional $P < .05$, we found it to be 15.6%. In a study where CV_w was obtained from the Westgard website, SCr unidirectional RCV $P < .05$ was calculated as 15.03%.¹⁶ Reinhard et al¹⁷ conducted a study on 20 healthy volunteers and 19 patients with impaired renal function. For SCr, CV_w of healthy volunteers was 4.7% and RCV was 13.6%; for patients with impaired renal function, CV_w was 8.9% and RCV was 25%. In another study on CKD patients, SCr CV_w was reported as 5.7% and RCV as 17%.¹⁸ The difference in RCV values is due to the within-laboratory precision,

TABLE 2. Example of the Interpretation of the Creatinine Levels Using RCV

		Patient 1	Patient 2	Patient 3	Patient 4
Predose	mg/dL	0.78	0.65	0.56	0.64
After dose on day 3	mg/dL	1.79	0.89	0.45	0.66
	Change (%) ^a	129.49	36.92	-19.64	3.13
After dose on day 7	mg/dL	2.37	2.23	0.52	1.41
	Change (%) ^b	203.85	243.08	-7.14	120.31
RCV ^c	3rd day	15.6<129.49 ^d	15.6<36.92 ^d	— ^e	15.6<3.13 ^f
	7th day	15.6<203.85 ^d	15.6<243.08 ^d	— ^e	15.6<120.31 ^f

RCV, reference change value.

^a $(\text{creatinine}_{\text{after dose 3rd day}} - \text{creatinine}_{\text{predose}}) / \text{creatinine}_{\text{predose}} \times 100$.

^b $(\text{creatinine}_{\text{after dose 7th day}} - \text{creatinine}_{\text{predose}}) / \text{creatinine}_{\text{predose}} \times 100$.

^cReference change value, calculated as 15.6%.

^dThe percent change in creatinine on 3rd day and 7th day exceeded RCV and the change is significant.

^eAs the increase in creatinine level (unidirectional) was evaluated, the change is insignificant on 3rd day and 7th day.

^fThe percent change in creatinine predose on 3rd day is below the RCV and the change is insignificant but the percent change in creatinine on 7th day exceeded RCV and the change is significant.

the use of different RCV formulas and Z coefficients, and obtaining CVW from previously published studies in the literature or from samples from healthy volunteers as well as a specific patient population.

We evaluated the SCr levels of patients receiving colistin treatment and analyzed their SCr levels before treatment and on days 3 and 7 after treatment. On day 3 and 7 after treatment, SCr levels were found to be significantly high compared with pretreatment levels. We found the risk for developing nephrotoxicity as 22 of 47 on day 3 and 35/47 on day 7. Hartzell et al¹⁹ evaluated 66 patients who had received colistin treatment for at least 3 days in their study, showing that 30 of 66 patients developed nephrotoxicity. In another study on patients receiving colistin treatment, 53.5% of the patients developed colistin-associated kidney damage.²⁰ In a study evaluating 30 adult patients receiving intravenous colistin, 10 of 30 patients were found to develop nephrotoxicity during the first 5 days of treatment.²¹ In a case-control study comparing aerosolized and IV forms of colistin for the treatment of ventilator-associated pneumonia, the risk of developing nephrotoxicity was found to be 50% for both forms.²² Spapen et al¹¹ conducted a review on the side effects of colistin, stating that the risk for developing nephrotoxicity changed from 0% to 53.5%. We think that different rates are found due to differences in patient groups in the conducted studies, presence or absence of a history of renal dysfunction, differences in age, sex, obesity, underlying diseases, other medications in use, or different criteria in use. Despite the fact that different criteria were used, the studies all make classifications based on the changes in SCr levels.

In our study, when day 3 SCr levels were compared with basal SCr levels, the ratio of patients with percent increases that exceeded the RCV was 32 of 47, whereas on day 7 this figure was 36 of 47. Nephrotoxicity developed on day 7 in 9 of 10 patients with a false-positive rate on day 3. Therefore, RCV can provide a warning for possible nephrotoxicity before SCr reaches the identified level by monitoring patient results on a daily basis. The second patient in **TABLE 2** can be given as an example of this situation. Before colistin treatment, SCr was 0.65 mg/dL, and SCr on day 3 was measured as 0.89 mg/dL. As the increase in the patient's SCr did not exceed 50% of the basal level and there was a lack of increase of 0.3 mg/dL in SCr on day 3, this patient was evaluated as not having developed nephrotoxicity. However, when SCr increase on day 3 was compared with the RCV, the increase in this patient's result was significant. On day 7, the patient's SCr was increased to 2.23 mg/dL showing developing nephrotoxicity; the increase in SCr was significant when compared with RCV as well.

Patients are expected to show an increase in SCr due to the use of nephrotoxic agents; however, SCr might remain within the reference interval, leading to mistaken interpretation.²³ In many previous biological variation studies, the index of individuality of SCr was shown to be <0.6.^{24–26} It is recommended to use the percentage of the change from baseline or in serial measurements.²⁷ In this study, if SCr was only evaluated according to the reference interval, 18 of 47 patients on day 3 and 8 on 47 patients on day 7 who were diagnosed AKI using the RCV would be incorrectly considered non-AKI.

One of the limitations of this study was the inaccessibility of the records of preanalytical factors interfering with SCr, as it was designed as a retrospective study. In addition, although persons with CKD were included in the study, the value of RCV could not be shown in patients above the upper reference limit because of an insufficient number of patients. Although RCV was compatible with KDIGO in 10 patients

with SCr levels exceeding the upper reference limit before treatment, AKI could not be detected in 1 patient with an SCr level that was approximately 3.3-fold the upper reference limit with RCV on day 3 nor on day 7. A study with a larger patient group is needed to demonstrate the diagnostic accuracy of RCV in the patients that developed AKI with underlying CKD.

Conclusion

This study provided an example of the clinical use of RCV. As shown in the results, small but significant changes in SCr level can be detected with RCV. Even if this increases the false positivity rate, it will provide early detection of the development of AKI, especially by follow-up assessment of SCr levels caused by treatments such as colistin that have nephrotoxic side effects. We think including RCV using KDIGO criteria would be a more accurate and faster approach for decision making.

Conflict of Interest Disclosure

The authors have nothing to disclose.

REFERENCES

- Fraser CG. Reference change values. *Clin Chem Lab Med*. 2011;50(5):807–812.
- Bugdayci G, Polat M, Oguzman H, Cinpolat HY. Interpretation of biochemical tests using the reference change value in monitoring adverse effects of oral Isotretinoin in 102 ethnic Turkish patients. *Lab Med*. 2016;47(3):213–219. doi:10.1093/labmed/lmw024.
- Fraser CG. *Biological Variation: From Principles to Practice*. Washington, DC: AACC Press; 2001.
- Harris EK. Statistical aspects of reference values in clinical pathology. *Prog Clin Pathol*. 1981;8:45–66.
- Aarsand AK, Fernandez-Calle P, Webster C, et al. The EFLM biological variation database. <https://biologicalvariation.eu>. Accessed June 30, 2022.
- Ozturk OG, Paydas S, Balal M, et al. Biological variations of some analytes in renal posttransplant patients: a different way to assess routine parameters. *J Clin Lab Anal*. 2013;27(6):438–443. doi:10.1002/jcla.21625.
- Van Biesen W, Vanholder R, Lameire N. Defining acute renal failure: RIFLE and beyond. *Clin J Am Soc Nephrol*. 2006;1(6):1314–1319. doi:10.2215/cjn.02070606.
- Mehta RL, Kellum JA, Shah SV, et al. Acute Kidney Injury Network: report of an initiative to improve outcomes in acute kidney injury. *Crit Care*. 2007;11(2):R31. doi:10.1186/cc5713.
- Khwaja A. KDIGO clinical practice guidelines for acute kidney injury. *Nephron Clin Pract*. 2012;120(4):c179–c184. doi:10.1159/000339789.
- Prasannan BK, Mukthar FC, Unni VN, Mohan S, Vinodkumar K. Colistin Nephrotoxicity-age and baseline kidney functions hold the key. *Indian J Nephrol*. 2021;31(5):449–453. doi:10.4103/ijn.ijn_130_20.
- Spapen H, Jacobs R, Van Gorp V, Troubleyn J, Honoré PM. Renal and neurological side effects of colistin in critically ill patients. *Ann Intensive Care*. 2011;1(1):14.
- Falagas ME, Kasiakou SK. Toxicity of polymyxins: a systematic review of the evidence from old and recent studies. *Crit Care*. 2006;10(1):R27.
- Mendes CA, Burdmann EA. Polymyxins - review with emphasis on nephrotoxicity. *Rev Assoc Med Bras*. 2009;55(6):752–759.

14. Clinical and Laboratory Standards Institute. *Evaluation of Precision Performance of Quantitative Measurement Methods, Approved Guideline. CLSI EP05-A*. 3rd ed. Wayne, PA: Clinical and Laboratory Standards Institute; 2014.
15. Fokkema MR, Herrmann Z, Muskiet FA, Moecks J. Reference change values for brain natriuretic peptides revisited. *Clin Chem*. 2006;52(8):1602–1603. doi:[10.1373/clinchem.2006.069369](https://doi.org/10.1373/clinchem.2006.069369).
16. Bugdayci G, Oguzman H, Arattan HY, Sasmaz G. The use of reference change values in clinical laboratories. *Clin Lab*. 2015;61(3-4):251–257.
17. Reinhard M, Erlandsen EJ, Randers E. Biological variation of cystatin C and creatinine. *Scand J Clin Lab Invest*. 2009;69(8):831–836. doi:[10.3109/00365510903307947](https://doi.org/10.3109/00365510903307947).
18. Carter JL, Parker CT, Stevens PE, et al. Biological variation of plasma and urinary markers of acute kidney injury in patients with chronic kidney disease. *Clin Chem*. 2016;62(6):876–883. doi:[10.1373/clinchem.2015.250993](https://doi.org/10.1373/clinchem.2015.250993).
19. Hartzell JD, Neff R, Ake J, et al. Nephrotoxicity associated with intravenous colistin (colistimethate sodium) treatment at a tertiary care medical center. *Clin Infect Dis*. 2009;48(12):1724–1728. doi:[10.1086/599225](https://doi.org/10.1086/599225).
20. Kwon JA, Lee JE, Huh W, et al. Predictors of acute kidney injury associated with intravenous colistin treatment. *Int J Antimicrob Agents*. 2010;35(5):473–477. doi:[10.1016/j.ijantimicag.2009.12.002](https://doi.org/10.1016/j.ijantimicag.2009.12.002).
21. Deryke CA, Crawford AJ, Uddin N, Wallace MR. Colistin dosing and nephrotoxicity in a large community teaching hospital. *Antimicrob Agents Chemother*. 2010;54(10):4503–4505. doi:[10.1128/aac.01707-09](https://doi.org/10.1128/aac.01707-09).
22. Kofteridis DP, Alexopoulou C, Valachis A, et al. Aerosolized plus intravenous colistin versus intravenous colistin alone for the treatment of ventilator-associated pneumonia: a matched case-control study. *Clin Infect Dis*. 2010;51(11):1238–1244. doi:[10.1086/657242](https://doi.org/10.1086/657242).
23. Delanaye P, Cavalier E, Pottel H. Serum creatinine: not so simple! *Nephron*. 2017;136(4):302–308. doi:[10.1159/000469669](https://doi.org/10.1159/000469669).
24. Mercan H, Orhan B, Bercik-Inal B. Estimation of reference change value and biological variation of creatinine measurements in healthy individuals. *Clin Lab*. 2022;68(9).
25. Bandaranayake N, Ankrah-Tetteh T, Wijeratne S, Swaminathan R. Intra-individual variation in creatinine and cystatin C. *Clin Chem Lab Med*. 2007;45(9):1237–1239.
26. Carobene A, Marino I, Coşkun A, et al. The EuBIVAS project: within- and between-subject biological variation data for serum creatinine using enzymatic and alkaline picrate methods and implications for monitoring. *Clin Chem*. 2017;63(9):1527–1536. doi:[10.1373/clinchem.2017.275115](https://doi.org/10.1373/clinchem.2017.275115).
27. Sottas PE, Kapke GF, Leroux JM. Adaptive Bayesian analysis of serum creatinine as a marker for drug-induced renal impairment in an early-phase clinical trial. *Clin Chem*. 2012;58(11):1592–1596. doi:[10.1373/clinchem.2012.193698](https://doi.org/10.1373/clinchem.2012.193698).

Oxidative Stress Levels and Dynamic Thiol-Disulfide Balance in Preterm Newborns with Bronchopulmonary Dysplasia

Mehmet Semih Demirtas,^{1,*} Fatih Kilicbay,² Huseyin Erdal,³ Gaffari Tunc²

¹Department of Pediatrics, Aksaray University, Faculty of Medicine, Aksaray, Turkey, ²Division of Neonatology, Department of Pediatrics, Sivas Cumhuriyet University Faculty of Medicine, Sivas, Turkey, ³Department of Medical Genetics, Aksaray University Faculty of Medicine, Aksaray, Turkey. *To whom correspondence should be addressed: md.semihdemirtas@gmail.com.

Keywords: newborn, bronchopulmonary dysplasia, thiol-disulfide homeostasis, oxidative stress

Abbreviations: BPD, bronchopulmonary dysplasia; OS, oxidative stress; TOS, total oxidant status; TAS, total antioxidant status; OSI, OS index; NT, native thiol; FIO₂, fraction of inspired oxygen; ELBW, extremely low birth weight; NICU, neonatal intensive care unit; GA, gestational age; RNS, reactive nitrogen species; IUGR, intrauterine growth restriction; TT, total thiol; RDS, respiratory distress syndrome; ROS, reactive oxygen species; SGA, small gestational age; SOD, superoxide dismutase

Laboratory Medicine 2023;54:587-592; <https://doi.org/10.1093/labmed/lmad010>

ABSTRACT

Objective: The aim of this study was to assess the oxidative stress (OS) levels and dynamic thiol-disulfide balance in preterm newborns with bronchopulmonary dysplasia (BPD).

Methods: This prospective study included newborns separated into 2 groups, those with BPD (case) or without BPD (control). The 2 groups were compared by clinical and laboratory findings. The OS parameters total oxidant status (TOS), total antioxidant status (TAS), OS index (OSI), native thiol (NT), and total thiol were measured within the first day after birth. Oxygen requirements were measured using the fraction of inspired oxygen (FIO₂) recorded in the first hour after birth/admission and the average FIO₂ within 28 days of the birth.

Results: Infants diagnosed with BPD had a significantly lower gestational age and birth weight and a lower 5-min Apgar score ($P < .05$). Infants with BPD also had a higher rate of respiratory distress syndrome, rate of use of surfactant therapy, duration of ventilation therapy, and duration of hospital stay compared with control ($P = .001$,

$P = .001$, $P = .001$, and $P = .001$, respectively). Plasma TAS and NT levels of newborns with BPD were significantly lower than newborns without BPD ($P < .05$). In the BPD group, plasma TOS and OSI levels were significantly higher than in the control group.

Conclusion: We found that OS was increased in newborns with BPD. The clinical significance of this study will provide the clinician with a different perspective on BPD by determining the dynamic thiol disulfide balance.

Bronchopulmonary dysplasia (BPD) is one of the important causes of chronic lung disease in preterm newborns and one of the leading causes of mortality.¹ Despite changes in the diagnostic criteria for BPD in recent years, there is still no consensus on the definition. Bronchopulmonary dysplasia is most often diagnosed based on the need for respiratory support at 36 weeks postmenstrual age (PMA).^{2,3} Bronchopulmonary dysplasia is detected in approximately 40% of extremely low birth weight (ELBW) infants. Although there have been important developments in the follow-up, care, and treatment of premature infants, no significant progress has been made in reducing the incidence of BPD in recent years. This may be due to the increased life expectancy of ELBW infants.³

The impairment of lung development in preterm infants, damage in the alveoli during the intrauterine and postnatal periods, and abnormal repair process play a role in the pathophysiology of BPD. Multiple pathologies in the respiratory system, epithelial surfaces, mesenchyme, and pulmonary vascular systems that cause early pulmonary damage play a role in the classification of BPD.⁴ Exposure to high oxygen pressure and volume in the necessary ventilation support for insufficient lung capacity of a premature infant can cause damage to the lungs. Ventilation and oxygen-induced damage at first activate inflammatory pathways, which can amplify preexisting lesions (chorioamnionitis) or be amplified by continuous exposure to oxygen and ventilation-induced lesions.⁵ Chorioamnionitis may cause inflammation of the lungs before delivery, intrauterine growth restriction may interfere with the structural development of the lung, and maternal vascular diseases such as preeclampsia may disturb the vascular development of fetal lungs, thereby increasing the risk of BPD.⁴ High levels of lipid and protein

oxidation products and proinflammatory cytokines in the first days of life in premature infants have been associated with adverse lung development, suggesting that oxidative stress (OS) and inflammatory mediators play a role in the pathogenesis of BPD. However, a perfect marker to predict BPD risk has not yet been identified.⁶

Dynamic thiol-disulfide homeostasis plays an essential role in anti-oxidant protection, detoxification, signal transduction, apoptosis, regulation of enzyme activity and transcription factors, and cellular signaling mechanisms.⁷ Increased OS in blood is shown by a deterioration in the total oxidant status (TOS) and total antioxidant capacity balance and an increase in OS index (OSI).^{7,8} Increased OS is known to cause negative effects on macromolecules such as lipid, protein, and DNA. There are different enzyme and nonenzyme defense mechanisms against the harmful effects of reactive oxygen types.⁹ One of these antioxidant mechanisms is the presence of thiols. It is known that these compounds containing the sulfhydryl group play an important role in the prevention of OS in cells.¹⁰ The primary target of intracellularly produced reactive oxygen species (ROS) is thiol groups in sulfur-containing amino acids in proteins. These thiol groups interact with ROS to form reversible disulfide bonds. These disulfide bonds are then reduced to thiol groups again by antioxidant mechanisms. Thus, a dynamic thiol/disulfide balance is achieved.^{11,12} The ratio of thiol to disulfide is increasingly studied for many disorders; a growing body of evidence indicates that abnormal homeostasis of thiol disulfide is involved in the pathogenesis of various disorders.¹³

To the best of our knowledge, thiol-disulfide homeostasis has not been previously investigated in BPD. The aim of this study was to evaluate thiol-disulfide hemostasis in newborns with BPD.

Material and Methods

Patients and Method

This prospective case-control research was conducted in a level III neonatal intensive care unit (NICU) in Sivas Cumhuriyet University Medical Faculty Hospital in Sivas, Turkey, between February 2021-2022.

Study Groups

Preterm neonates of less than 34 weeks gestational age (GA), were enrolled in this study. Newborns of greater than 34 weeks GA and those with congenital heart diseases, meconium aspiration, or major congenital anomalies were excluded from the study. The parents of eligible infants were invited to participate in the study in the first hours after birth. On agreement of the parents, the infant was enrolled in the study. Newborns born before the 34th week and who did not develop BPD at the 36th gestational week were included as the control group (FIGURE 1). All newborns in the patient and control groups were followed up and treated by the same neonatology specialist.

Resuscitation Practice and Administering Oxygen

The resuscitation practice in the NICU at the time of the study conformed to the 2010 American Heart Association guidelines.¹⁴ In accordance with the neonatal resuscitation program in the delivery room, infants of greater than 34 weeks GA were given blended oxygen therapy with the necessary adjustments made to obtain target saturation at 85%

to 95%.¹⁵ Supplemental oxygen administration following that provided in the delivery room was titrated to maintain saturation levels between 85% and 95%.

Measurements

Demographic and medical data were retrieved from the infant's medical record, including gender, birth weight (g), GA at birth (weeks), rate of respiratory distress syndrome (RDS), use of surfactant therapy, small gestational age (SGA), early-onset sepsis, 5-min Apgar score, delivery mode, labor, complicated pregnancy, antenatal steroid administration, first blood gas pH, mode of ventilation therapy, duration of ventilation, FIO₂ level on admission, duration of hospital stay, and in-hospital mortality.

Lung Disease

The definition of BPD was made for newborns who received oxygen for at least 28 days. The BPD classification was made according to the need for oxygen and respiratory support in the 36th gestational week.¹⁶

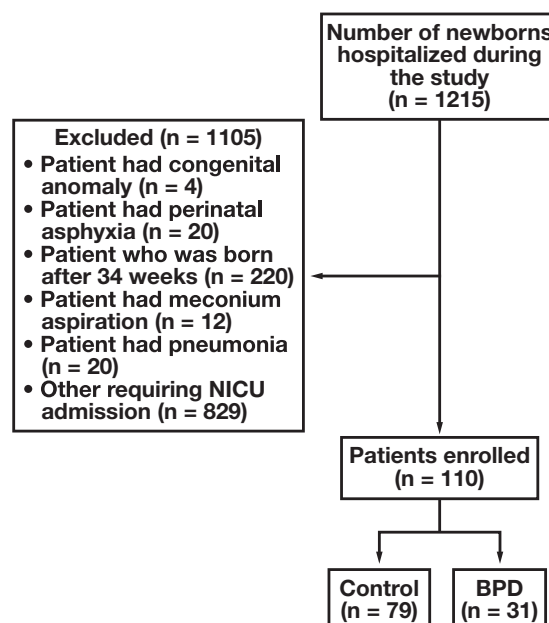
Samples

At 24-h post partum, a 2 mL blood sample was collected from a postnatal peripheral vein of the infant. The sample was centrifuged at 3000 rpm for 10 minutes, and the supernatants were stored in an Eppendorf tube at -80°C until they were analyzed. The serum samples were labeled by the laboratory biochemistry technician by the name of the newborn. The researcher who conducted the assays on the labeled samples was blinded to newborn information.

Measurement of Thiol-Disulfide Homeostasis

In this study, total antioxidant status (TAS) and total oxidant concentrations were measured by spectrophotometry using the method developed by Erel. A new spectrophotometric method developed by Erel and Neselioglu allowed the measurement of native and total thiol concentrations.¹¹ The disulfide levels and ratios of disulfide to native

FIGURE 1. Flow diagram of the study



thiol, disulfide to total thiol, and native to total thiol percentages were calculated using the following formulas: disulfide levels ($\mu\text{mol/L}$) = (total thiol – native thiol)/2.

$$\text{disulfide/native thiol percentage (\%)} = (\text{disulfide} \times 100) / \text{native thiol}$$

In the calculation of OSI, the TAS unit was converted to mol/L and the OSI unit was obtained with TOS/TAS.^{17,18}

The dynamic thiol-disulfide homeostasis of newborn blood samples in 2 groups (with BPD and without BPD = control) were compared.

Statistical Analysis

The study data were analyzed statistically using IBM SPSS 23 software. Data were examined with descriptive statistical tests. The normality of numerical variables was examined with the Shapiro-Wilk test. Descriptive measurements were expressed as numbers and percentages for categorical variables and as median with interquartile range values for continuous variables not showing normal distribution. Nonparametric tests were applied to data that were not consistent with normal distribution; the Mann-Whitney *U* test for numerical data and the χ^2 test for categorical data. As the BPD stage values were not normally distributed, the Kruskal-Wallis test was applied. In the power

analysis, when $\alpha = 0.05$, $\beta = 0.10$, $1-\beta = 0.90$, and *R* (simple) allocation = 2.4, it was deemed necessary to include 31 subjects in the patient group and 79 in the control group, and the power of the test was determined to be 0.9867. A value of $P < .05$ was considered statistically significant.

Results

A total of 110 infants of less than 34 weeks GA were enrolled in the study between February 2021 and 2022, and 10 infants died on day 8. Demographic and medical variables for the whole sample and infants with and without BPD are shown in **TABLE 1**. At 36 weeks corrected GA, 28% ($n = 31$) of the 110 infants were diagnosed with BPD. There was no statistically significant difference between the BPD and control groups with respect to gender, SGA, early-onset sepsis, delivery mode, labor, FIO_2 , admission level, or in-hospital mortality ($P > .05$). The BPD group had significantly lower GA ($P = .004$), birth weight ($P = .001$), and 5-min Apgar score. Those in the BPD group also had a higher rate of RDS, more frequent need for surfactant therapy, higher first pH levels, longer duration of ventilation therapy, and longer duration of hospital stay compared with the control group. The OS levels and dynamic thiol-disulfide balance parameters of infants with BPD and control group are shown in **TABLE 2**. In the newborns who developed BPD, plasma TAS [1.33 1.1–1.67] nmol

TABLE 1. Demographic and Medical Features for the Whole Sample, and for Infants with BPD and Controls^a

Characteristic	BPD (n = 31) ^b	Control (n = 79) ^b	P Value ^c
Sex, n (%)			
Male	17 (55)	40 (51)	.427
Female	14 (45)	39 (49)	
Birth weight, g	1181 (870–1640)	1850 (1480–2150)	.001
Gestational age, wk	28 (27–31)	33 (31–33)	.004
Respiratory distress syndrome, n (%)	20 (64)	23 (29)	.001
Use of surfactant, n (%)	22 (71)	28 (35)	.001
SGA, n (%)	1 (3.2)	6 (7.6)	.401
Early-onset sepsis, n (%)	5 (16.1)	1 (1.3)	.200
Apgar score, 5 min	7 (6–8)	8 (7–9)	.002
Delivery mode			
Cesarean, %	31 (100)	77 (97)	.514
Birth action, n (%)	11 (35)	19 (24)	.823
Presence of complicated pregnancy, n (%)	6 (19.4)	10 (17)	.001
Antenatal steroid administration, n (%)	28 (90)	46 (58)	.001
First pH ^d	7.38 (7.34–7.41)	7.34 (7.30–7.38)	.004
Mode of ventilation therapy, n (%)			
CPAP	12 (39)	46 (58)	
NIPPV	19 (61)	33 (42)	.016
Duration of ventilation, d	6 (3–20)	2 (2–4)	.001
FIO_2 admission	40 (30–40)	30 (30–40)	.267
Duration of hospital stay, d	47 (39–65)	18 (13–33)	.001
Intrahospital death, n (%)	4 (13)	6 (7.6)	.386

BPD, bronchopulmonary dysplasia; CPAP, continuous positive airway pressure; LGA, large for gestational age; NIPPV, nasal intermittent positive pressure ventilation; SGA, small for gestational age.

^aMann-Whitney *U* test or *t*-test was used for data analyses. Data are stated as median with interquartile range values unless indicated otherwise.

^bA total of 31 patients were diagnosed with BPD at 36 weeks of gestation.

^cBold values indicate significance $P < .05$.

^dThe pH first recorded in the medical record from venous, capillary, and arterial samples.

^eThe mean inhaled oxygen fraction (FIO_2) recorded in the first hour after admission to the neonatal intensive care unit.

TABLE 2. Oxidative Stress Levels and Dynamic Thiol-Disulfide Balance in Infants with BPD and Controls^a

Oxidative Stress Parameters	BPD (n = 31) ^b	Control (n = 79) ^b	P Value ^c
TAS, nmol Trolox/L	1.33 (1.1–1.67)	1.80 (1.4–1.95)	.001
TOS, $\mu\text{mol H}_2\text{O}_2$ Equiv/L	7.3 (6.65–8.9)	6.4 (4.62–8.67)	.028
OSI	0.55 (0.46–0.69)	0.42 (0.25–0.55)	.001
Total thiol, $\mu\text{mol/L}$	432 (403–498)	478 (422–512)	.127
Native thiol, $\mu\text{mol/L}$	392 (366–432.5)	440 (380–468.5)	.046
Disulfide, $\mu\text{mol/L}$	21 (17.5–27.75)	20 (15.6–25)	.183
Disulfide/native thiol ratio, %	5.39 (4.59–6.75)	4.87 (3.58–6.63)	.060
Disulfide/total thiol ratio, %	4.87 (4.20–5.95)	4.44 (3.34–5.86)	.060
Native thiol/total thiol ratio, %	90.27 (88.1–91.58)	91.12 (88.29–93.31)	.059

BPD, bronchopulmonary dysplasia; OSI, oxidative stress index; TAS, total antioxidant status; TOS, total oxidant status.

^aMann-Whitney U test or t-test was used for data analyses. Data are stated as median with interquartile range values.

^bA total of 31 patients were diagnosed with BPD at 36 weeks of gestation.

^cBold values indicate significance $P < .05$.

TABLE 3. Oxidative Stress Levels and Dynamic Thiol-Disulfide Balance in Infants with BPD According to Grade^a

Oxidative Stress Parameters	Grade 1 (n = 13)	Grade 2 (n = 9)	Grade 3 (n = 9)	P Value
TAS, nmolTrolox/L	1.25 (1.05–1.68)	1.40 (1.31–1.71)	1.30 (1.13–1.60)	.457
TOS, $\mu\text{mol H}_2\text{O}_2$ Equiv/L	7.5 (6.7–9.3)	7.4 (6.55–8.95)	7.2 (6.3–10.1)	.912
OSI	0.58 (0.45–0.82)	0.52 (0.42–0.67)	0.55 (0.49–0.7)	.778
Total thiol, $\mu\text{mol/L}$	415 (403–524)	432 (406–475)	467 (389.5–518.5)	.912
Native thiol, $\mu\text{mol/L}$	385 (358–445)	392 (369–426)	415 (354–449.5)	.966
Disulfide, $\mu\text{mol/L}$	22.5 (15–30)	20 (18.25–25)	24 (17.25–27.75)	.851
Disulfide/native thiol ratio, %	5.93 (3.90–8.61)	5.1 (4.59–6.83)	5.34 (4.75–6.68)	.967
Disulfide/total thiol ratio, %	5.30 (3.61–7.35)	4.63 (4.20–6)	4.83 (4.34–5.89)	.960
Native thiol/total thiol ratio	89.4 (85.3–92.7)	90.74 (87.99–91.58)	90.35 (88.22–91.31)	.967

BPD, bronchopulmonary dysplasia; OSI, oxidative stress index; TAS, total antioxidant status; TOS, total oxidant status.

^aData are median with interquartile range values. As the BPD stage values were not normally distributed, the Kruskal-Wallis test was applied.

Trolox/L), and NT (392 [366–432.5] $\mu\text{mol/L}$) levels were significantly lower than in the control group ($P < .05$). Plasma TOS (7.3 [6.65–8.9] $\mu\text{mol H}_2\text{O}_2$ Equiv/L) and OSI (0.55 [0.46–0.69]) levels were significantly higher in the BPD group than in the control group ($P < .05$). There was no difference between the 2 groups in terms of TT, disulfide, disulfide/NT ratio, disulfide/TT ratio, and NT/TT ratios, which are the other parameters of OS.

The relationship between BPD stages and levels of dynamic thiol-disulfide balance parameters is summarized in **TABLE 3**. When the levels of TAS, TOS, OSI, TT, NT, disulfide, and disulfide/NT, disulfide/TT, and NT/TT ratios were evaluated according to BPD level, no statistically significant difference was found (**TABLE 3**).

Discussion

To the best of our knowledge, this is the first study to have evaluated serum thiol/disulfide homeostasis in newborns with BPD. This prospective study shows that infants in the BPD group had significantly lower GA, birth weight, and 5-min Apgar score than those in the control group ($P = .004$, $P = .001$, $P = .002$, respectively). In addition, newborns with BPD had longer durations of ventilation therapy and hospital stay, more surfactant use, and a higher ratio of RDS than the control group (the P value among all compared parameters was $P = .001$). Plasma TAS and NT levels measured in newborns with BPD were significantly lower than in the control group ($P = .001$ and $P = .046$, respectively). Plasma TOS and

OSI levels were also significantly higher in the newborns with BPD than controls ($P = .028$ and $P = .001$, respectively).

Thiol-disulfide homeostasis is an important indicator of OS in the body, and different results can be obtained depending on the etiopathogenesis of diseases.¹⁸ In studies conducted between adult diseases and thiol disulfide, disulfide level was found to be high in degenerative diseases (such as diabetes, pneumonia, and obesity), whereas it was found to be lower in proliferative diseases (such as colon cancer, multiple myeloma, and urinary bladder).^{7,19,20} Infants and children vary from adults because of the ongoing growth in organs and systems, such as the gastrointestinal and central nervous systems, from the period of conception until they reach adulthood.²¹ Events such as infections, teratogens, and stress that children are exposed to during growth can cause a wide range of conditions, from congenital anomalies to diseases such as transient tachypnea of the newborn and RDS, depending on the exposure time.²¹ Recent thiol studies on diseases in children are especially important for understanding the oxidative balance in these children.^{11,18,22,23}

Newborns, especially premature infants, are exposed to more biochemical and enzymatic reactions due to deterioration of oxidative balance.^{11,18} In studies of OS in the neonatal period, it has been shown that OS is not only increased by ROS but also by reactive nitrogen species (RNS) and other radicals.^{17,24} The presence of an increasing number of RNS and ROS in the body causes damage to biochemical functions in vital organs, such as cell progression and the immune system.^{24,25}

In a study evaluating the relationship between postpartum cord clamping time and thiol disulfide hemostasis, it was reported that OS increased in newborns who underwent early cord clamp, whereas plasma thiol levels decreased.²⁶ Ulubaş et al¹³ investigated the effect of the mode of delivery on the thiol disulfide balance and showed that vaginal deliveries affected OS and thiol disulfide balance less than cesarean deliveries. Ozler et al²⁷ found that decreased antioxidant total thiol/disulfide levels were associated with intrauterine growth restriction (IUGR). It has been suggested that the increase in oxidant levels as a result of the decrease in antioxidant mechanisms in newborns with IUGR is the reason for this. In previous studies of the respiratory system of pediatric asthma patients, the dissolved level and dissolved NT ratio of the patient groups were determined to be higher than those of the control groups.^{28,29} In recent years, there has been increasing evidence that OS plays a role in the development of BPD.^{30,31} Premature newborns are more exposed to OS damage due to immaturity of lungs, exposure to oxygen therapy and hyperoxia, and inadequate antioxidant mechanisms, and this situation makes premature neonates more prone to inflammation.³²

Newborns, especially premature, have insufficient detoxification capacity against free radicals. A number of therapeutic strategies have been proposed to prevent damage caused by OS and to improve antioxidant capacity.^{11,18} It has been reported that with the development of antioxidant capacity in newborns, OS-related diseases can be prevented, the immune system will be strengthened, and stillbirths can be reduced.¹⁸ Therefore, studies have been conducted on many therapeutic antioxidants such as melatonin, glutathione peroxidase, superoxide dismutase (SOD), and N-acetylcysteine, which are thought to play a role in neonatal diseases.³³ Melatonin and its metabolites are powerful antioxidants that play an important role in preventing free radicals from mutilating critical molecules. In experimental models of excessive ROS, melatonin has been shown to reduce all aspects of the damage resulting from ischemia and subsequent reperfusion of the heart, kidney, liver, intestine, and brain.³⁴ Gitto et al⁹ demonstrated that melatonin therapy may reduce the severity of RDS in preterm infants by reducing inflammation. In addition, melatonin has been shown to be available for the treatment of hypoxic-ischemic encephalopathy in newborns. Endotracheal administration of melatonin and surfactant substitute recombinant human SOD may reduce pulmonary lesions in premature infants who receive mechanical ventilation for RDS.³⁵ Exogenous antioxidants like vitamins A and E and recombinant human SOD are considered capable of preventing BPD.³⁶ The results of this evaluation of thiol-disulfide homeostasis in preterm newborns demonstrated that the plasma levels of TAS and NTL were significantly lower in the BPD group than in the control group. At the same time, plasma TOS and OSI levels were higher in the infants with BPD. Decreased TAS levels and increased TOS and OSI levels may explain the susceptibility to oxidative damage in infants with BPD. These results also support the findings of previous studies on BPD OS damage.

Vatansever et al²⁶ reported that thiol levels in cord blood were not significantly different between male and female newborns. Ulubaş et al¹³ observed that cord blood thiol levels were higher in female infants than in male infants. In a study conducted in newborns who received phototherapy for indirect hyperbilirubinemia, it was shown that it did not cause a change in the gender factor.¹⁸ In line with the literature, no significant difference in terms of gender factor was found in newborns with BPD in this study ($P = .427$).

Limitations

Despite the limitations of the low number of subjects and sample sizes of the included tests, these results can be considered of value to aid in the selection of interventions that could be assessed in future high-quality randomized controlled trials on this topic with larger samples.

Conclusion

Neonatal cells, organs, and systems are susceptible to OS due to their rapid growth, and this makes newborns vulnerable to the damage of free radicals. There remains a lack of information about the possible role of oxidative balance in the pathophysiology of neonatal diseases. In addition, there are very few studies in the literature regarding OS and antioxidant biomarkers and their functions in newborns. The decrease in plasma TAS and NTL levels and increased plasma TOS and OSI levels reflect increased OS in BPD. Therefore, there is a need for cohort studies that include new strategies to prevent the development of oxidative damage to prevent BPD.

Conflict of Interest Disclosure

The authors have nothing to disclose.

REFERENCES

1. Gilfillan M, Bhandari A, Bhandari V. Diagnosis and management of bronchopulmonary dysplasia. *BMJ*. 2021;375:n1974. doi:10.1136/bmj.n1974.
2. Arsan S, Korkmaz A, Oguz S. Turkish Neonatal Society guideline on prevention and management of bronchopulmonary dysplasia. *Turk Pediatri Ars*. 2018;53(suppl 1):S138–S150. doi:10.5152/TurkPediatriArs.2018.01814.
3. Mammel D, Kemp J. Prematurity, the diagnosis of bronchopulmonary dysplasia, and maturation of ventilatory control. *Pediatr Pulmonol*. 2021;56(11):3533–3545. doi:10.1002/ppul.25519.
4. Jobe AH. Mechanisms of lung injury and bronchopulmonary dysplasia. *Am J Perinatol*. 2016;33(11):1076–1078. doi:10.1055/s-0036-1586107.
5. Hillman NH, Kallapur SG, Jobe AH. Physiology of transition from intrauterine to extrauterine life. *Clin Perinatol*. 2012;39(4):769–783. doi:10.1016/j.clp.2012.09.009.
6. Madoglio RJ, Rugolo LM, Kurokawa CS, Sa MP, Lyra JC, Antunes LC. Inflammatory and oxidative stress airway markers in premature newborns of hypertensive mothers. *Braz J Med Biol Res*. 2016;49(9):e5160. doi:10.1590/1414-431X20165160.
7. Erel O, Neselioglu S. A novel and automated assay for thiol/disulphide homeostasis. *Clin Biochem*. 2014;47(18):326–332. doi:10.1016/j.clinbiochem.2014.09.026.
8. Millan I, Pinero-Ramos JD, Lara I, Parra-Llorca A, Torres-Cuevas I, Vento M. Oxidative stress in the newborn period: useful biomarkers in the clinical setting. *Antioxidants*. 2018;7(12). doi:10.3390/antiox7120193.
9. Gitto E, Reiter RJ, Cordaro SP, et al. Oxidative and inflammatory parameters in respiratory distress syndrome of preterm newborns: beneficial effects of melatonin. *Am J Perinatol*. 2004;21(4):209–216. doi:10.1055/s-2004-828610.
10. Cakirca G, Çelik M, Erdal H, et al. Investigation of thiol/disulfide homeostasis in familial Mediterranean fever patients. *J Clin Med*. 2018;9(3).
11. Huseyin E, Mehmet SD, Sibel CT, Oguzhan O. Thiol/disulfide homeostasis as a new oxidative stress marker in patients with neonatal transient tachypnea. *Clin Anal Med*. 2022. doi:10.4328/ACAM.21457.

12. Ravarotto V, Carraro G, Pagnin E, et al. Oxidative stress and the altered reaction to it in fabry disease: a possible target for cardiovascular-renal remodeling? *PLoS One*. 2018;13(9):e0204618. doi:10.1371/journal.pone.0204618.
13. Ulubas ID, Akdas RY, Bas AY, et al. The effect of the modes of delivery on the maternal and neonatal dynamic thiol-disulfide homeostasis. *J Matern Fetal Neonatal Med*. 2019;32(23):3993–3997. doi:10.1080/14767058.2018.1481028.
14. Kattwinkel J, Perlman JM, Aziz K, et al. Neonatal resuscitation: 2010 American Heart Association guidelines for cardiopulmonary resuscitation and emergency cardiovascular care. *Pediatrics*. 2010;126(5):e1400–e1413. doi:10.1542/peds.2010-2972e.
15. Escrig R, Arruza L, Izquierdo I, et al. Achievement of targeted saturation values in extremely low gestational age neonates resuscitated with low or high oxygen concentrations: a prospective, randomized trial. *Pediatrics*. 2008;121(5):875–881. doi:10.1542/peds.2007-1984.
16. Jobe AH, Bancalari E. Bronchopulmonary dysplasia. *Am J Respir Crit Care Med*. 2001;163(7):1723–1729. doi:10.1164/ajrccm.163.7.2011060.
17. Celik E, Tayşi S, Sucu S, Ulusal H, Sevinçler E, Celik A. Urotensin 2 and oxidative stress levels in maternal serum in pregnancies complicated by intrauterine growth restriction. *Medicina*. 2019;55(7). doi:10.3390/medicina55070328.
18. Demirtas MS, Erdal H. Evaluation of thiol–disulfide homeostasis and oxidative stress parameters in newborns receiving phototherapy. *J Investig Med*. 2023. doi:10.1177/10815589221140594.
19. Ergin M, Aydin C, Yurt EF, Cakir B, Erel O. The variation of disulfides in the progression of type 2 diabetes mellitus. *Exp Clin Endocrinol Diabetes*. 2020;128(2):77–81. doi:10.1055/s-0044-100376.
20. Guney T, Kanat IF, Alkan A, et al. Assessment of serum thiol/disulfide homeostasis in multiple myeloma patients by a new method. *Redox Rep*. 2017;22(6):246–251. doi:10.1080/13510002.2016.1180100.
21. Demirtaş MS. The pathogenesis of congenital anomalies: roles of teratogens and infections. In: *Congenital Anomalies in Newborn Infants-Clinical and Etiopathological Perspectives*. IntechOpen; 2020.
22. Demirtas MS, Erdal H. Evaluation of thiol disulfide balance in adolescents with vitamin B12 deficiency. *Ital J Pediatr*. 2023;49(1):3. doi:10.1186/s13052-022-01396-2.
23. Yasar Durmus S, Sahin NM, Ergin M, Neselioglu S, Aycan Z, Erel O. How does thiol/disulfide homeostasis change in children with type 1 diabetes mellitus? *Diabetes Res Clin Pract*. 2019;149:64–68. doi:10.1016/j.diabres.2019.01.027.
24. Tayşi S, Tascan AS, Ugur MG, Demir M. Radicals, oxidative/nitrosative stress and preeclampsia. *Mini Rev Med Chem*. 2019;19(3):178–193. doi:10.2174/1389557518666181015151350.
25. Yucel A, Sucu M, Al-Taesh H, Ulusal H, Ertosun FM, Tayşi S. Evaluation of oxidative DNA damage and thiol-disulfide homeostasis in patients with aortic valve sclerosis. *Echocardiogr*. 2018.
26. Vatansever B, Demirel G, Ciler Eren E, et al. Is early cord clamping, delayed cord clamping or cord milking best? *J Matern Fetal Neonatal Med*. 2018;31(7):877–880. doi:10.1080/14767058.2017.1300647.
27. Ozler S, Oztas E, Guler BG, et al. Dynamic thiol/disulfide homeostasis in predicting adverse neonatal outcomes in fetal growth restriction. *Fetal Pediatr Pathol*. 2020;39(2):132–144. doi:10.1080/15513815.2019.1644686.
28. Erel O, Erdogan S. Thiol-disulfide homeostasis: an integrated approach with biochemical and clinical aspects. *Turk J Med Sci*. 2020;50(SI-2):1728–1738. doi:10.3906/sag-2003-64.
29. Kaya BK, Aydin M, Donma MM, Demirkol M, Bicer C, Erel O. Association of thiol disulfide homeostasis with childhood asthma. *J Pediatr Biochem*. 2016;6(03):152–155.
30. Perrone S, Tataranno ML, Buonocore G. Oxidative stress and bronchopulmonary dysplasia. *J Clin Neonatol*. 2012;1(3):109–114. doi:10.4103/2249-4847.101683.
31. Wang J, Dong W. Oxidative stress and bronchopulmonary dysplasia. *Gene*. 2018;678:177–183. doi:10.1016/j.gene.2018.08.031.
32. Saugstad OD. Bronchopulmonary dysplasia-oxidative stress and antioxidants. *Semin Neonatol*. 2003;8(1):39–49. doi:10.1016/s1084-2756(02)00194-x.
33. Lee JW, Davis JM. Future applications of antioxidants in premature infants. *Curr Opin Pediatr*. 2011;23(2):161–166. doi:10.1097/mop.0b013e3283423e51.
34. Ozsürekci Y, Aykac K. Oxidative stress related diseases in newborns. *Oxid Med Cell Longev*. 2016;2016:2768365. doi:10.1155/2016/2768365.
35. Poggi C, Dani C. Antioxidant strategies and respiratory disease of the preterm newborn: an update. *Oxid Med Cell Longev*. 2014;2014:721043. doi:10.1155/2014/721043.
36. Suresh GK, Davis JM, Soll RF. Superoxide dismutase for preventing chronic lung disease in mechanically ventilated preterm infants. *Cochrane Database Syst Rev*. 2001;2001(1):CD001968. doi:10.1002/14651858.CD001968.

Diagnostic Performance of 10 Mathematical Formulae for Identifying Blood Donors with Thalassemia Trait

Egarit Noulisri, PhD,^{1,*} Surada Lerdwana, BSc,² Duangdao Palasuwan, PhD,³ and Attakorn Palasuwan, PhD³

¹Research Division, ²Biomedical Research Incubator Unit, Faculty of Medicine Siriraj Hospital, Mahidol University, Bangkok, Thailand, ³Oxidation in Red Cell Disorders Research Unit, Department of Clinical Microscopy, Faculty of Allied Health Sciences, Chulalongkorn University, Bangkok, Thailand. *To whom correspondence should be addressed: egarit.nou@mahidol.ac.th; egarit@hotmail.com.

Keywords: thalassemia trait, RBC indices, complete blood count, blood donor, transfusion medicine, basic science

Abbreviations: IDA, iron deficiency anemia; Hb CS, Hb constant spring; G6PD, glucose-6-phosphate dehydrogenase; HCT, hematocrit

Laboratory Medicine 2023;54:593-597; <https://doi.org/10.1093/labmed/lmad011>

ABSTRACT

Objective: To compare the diagnostic performance of 10 mathematical formulae for identifying thalassemia trait in blood donors.

Methods: Complete blood counts were conducted on peripheral blood specimens using the UniCel DxH 800 hematology analyzer. Receiver operating characteristic curves were used to evaluate the diagnostic performance of each mathematical formula.

Results: In the 66 donors with thalassemia and 288 subjects with no thalassemia analyzed, donors with thalassemia trait had lower values for mean corpuscular volume and mean corpuscular hemoglobin than subjects without thalassemia donors (77 fL vs 86 fL [$P < .001$]; 25 pg vs 28 pg [$P < .001$]). The formula developed by Shine and Lal in 1977 showed the highest area under the curve value, namely, 0.9. At the cutoff value of <1812, this formula had maximum specificity of 82.35% and sensitivity of 89.58%.

Conclusions: Our data indicate that the Shine and Lal formula has remarkable diagnostic performance in identifying donors with underlying thalassemia trait.

Thalassemia is an inherited hematological disorder that has been reported in many countries.¹ Patients can have thalassemia in different

degrees of severity, ranging from asymptomatic to severe anemia.² Patients with severe anemia require blood transfusions, whereas silent carriers of thalassemia trait have no symptoms and do not require therapy. In several countries, individuals with thalassemia trait can still donate blood if their hemoglobin levels meet the minimum criteria established in blood donor selection guidelines.³

Certain study reports^{4,5} have stated that the spectrum of β gene mutations varies among ethnic groups. Given the wide range of independent mutations that affect different populations regionally and donor selection criteria, blood donors with underlying thalassemia trait may have little effect in some areas, such as the United States and North America. In Thailand, a previous study⁶ examined the prevalence of donors with thalassemia, and the investigators found that 20% of transfusion donors were carriers of this trait. Despite advanced research on donors with thalassemia trait, a recent published review⁷ noted that studies would be required to investigate the quality of blood products prepared from these donors, as well as the quality of life of healthy donors who have underlying thalassemia trait. Given the prevalence of thalassemia in selected geographic locations, an approach to identifying thalassemia is required. This strategy will help to minimize adverse donor events during and after blood donations.

A variety of approaches have been used to identify individuals with thalassemia, such as the use of CBC parameters or hemoglobin typing using high-performance liquid chromatography (HPLC), which is the criterion standard.^{8,9} In addition to these strategies, mathematical formulae have been used to identify individuals suspected of carrying β -thalassemia or those with hypochromic microcytic anemia. Sinvastava¹⁰ and Mentzer¹¹ published reports of the first attempt, which used algorithms to calculate mean corpuscular hemoglobin (MCH), mean corpuscular volume (MCV), and red blood cell (RBC) concentration. Subsequently, Shine and Lal¹² developed another calculation by multiplying MCV by MCH and then dividing the result by 100; they reported that this approach could detect 137 heterozygous thalassemia traits. The findings of several studies¹³⁻¹⁶ have confirmed the reliability of the Shine and Lal formula.

Later, other formulae were proposed to improve the accuracy and reliability of the mathematical formulae by including other complete blood count (CBC) parameters in the calculations.¹⁷⁻²⁰ Bordbar et al²¹ applied the formula $|80 - \text{MCV}| \times |27 - \text{MCH}|$ to screen couples who had children younger than 18 years who had β -thalassemia and reported that the formula had high sensitivity and specificity in differentiating people carrying β -thalassemia (thalassemia carriers) from individuals with microcytic hypochromic anemia.

Further, Schoorl et al²² incorporated 4 hematological parameters, including hemoglobin (Hb), RBC, and mean corpuscular hemoglobin concentration (MCHC), into a mathematical formula for distinguishing iron deficiency anemia (IDA) from thalassemia. Their findings showed that the algorithm has sensitivity and specificity of 79% and 97%, respectively. Several studies, such as Roth et al¹³ and Bordbar et al,²¹ have evaluated these formulae, and the results regarding the detection of thalassemia carriers in the general population have varied. However, little is known about the performance of these formulae in transfusion laboratories in identifying donors with thalassemia. In the current study, we performed CBC and thalassemia screening tests on 354 blood donors to assess the practical use of the proposed mathematical formulae for identifying donors with thalassemia trait.

Materials and Methods

Ethics Statement

This study was approved by the International Review Board of the Faculty of Medicine Siriraj Hospital, Mahidol University, Bangkok, Thailand (COA No. Si395/2016). The donors who participated in the current study were referred by the Department of Transfusion. All experimental procedures were performed in accordance with the ethics standards of the Declaration of Helsinki.

Blood Specimen Collection and Thalassemia Screening

The following were our requirements for recruiting blood donors: donors must be between the ages of 17 and 70 years and weigh more than 45 kg; volunteer donors must have a minimum Hb concentration of 13 g/dL for males and 12.5 g/dL for females; and donors were screened for Hb using a copper sulfate (CuSO_4)-specific gravity approach, and those who had a drop of blood that floated or took too long to sink in CuSO_4 solution were deferred and excluded from the current study.

After written informed consent was obtained from each participant, 3 mL of peripheral blood was collected into a BD Vacutainer tube (Becton Dickinson) containing the anticoagulant K_2EDTA . Hemoglobin typing was performed using HPLC. The percentage of Hb was determined, and patients whose HbA2 levels were $>3.5\%$ were identified as having β -thalassemia trait. The multiplex gap-polymerase chain reaction was used to detect α -globin gene variants.

Automated Hematology Analyzer

The CBCs were determined using a UniCel DxH 800 hematology analyzer (Beckman Coulter) according to the routine procedure of the Department of Transfusion, Faculty of Medicine, Siriraj Hospital. Before being used to analyze the specimens, the instrument underwent inter- and intralaboratory validation. The CBC data set obtained included RBC, Hb, hematocrit (HCT), MCV, MCH, MCHC, red cell distribution width (RDW), white blood cell (WBC) count, and platelet (PLT) count.

Mathematical Calculations

The hematological data from each donor were incorporated into each formula used, which included the following mathematical formulae: the Srivastava formula¹⁰: MCH/RBC ; the Mentzler formula¹¹: MCV/RBC ; the Shine and Lal formula¹²: $(\text{MCV}^2 \times \text{MCH})/100$; the Green and King formula¹⁷: $(\text{MCV}^2 \times \text{RDW})/(\text{Hb} \times 100)$; the D'Onofrio et al

formula¹⁸: MCV/MCH ; the Ehsani et al formula¹⁹: $(\text{MCV} - 10 \times \text{RBC})$; the Sirdah et al formula²³: $(\text{MCV} - \text{RBC} - 3 \times \text{Hb})$; the Sirachainan et al formula²⁰: $1.5 \times \text{Hb} - 0.05 \times \text{MCV}$; the Bordbar et al formula²¹: $|80 - \text{MCV}| \times |27 - \text{MCH}|$; and the Schoorl et al formula²²: $(\text{Hb} \times \text{RDW} \times 100)/(\text{RBC}^2 \times \text{MCHC})$.

Statistical Analysis

The data were analyzed and graphed using GraphPad Prism software, version 5.0. The Kolmogorov-Smirnov normality test was used to assess the distribution of the variables. The results were expressed as mean, SE, and range (minimum–maximum). For each formula, a receiver operating characteristic (ROC) curve was plotted to calculate the area under the curve (AUC), sensitivity, and specificity, all of which were considered when determining the optimal cutoff values. The AUC is represented as a value between 0 and 1, and the ideal ROC curve has an AUC of 1.0, indicating the outstanding ability of the test to distinguish between patients with and without the disease. The optimal cutoff value is determined by the maximum sensitivity and specificity of the model. An unpaired *t* test was used to compare the differences in hematological data between the 2 groups. $P \leq .05$ was considered statistically significant.

RESULTS

Donor Characteristics, Hemoglobin Analysis, and CBC Parameters

In the current cross-sectional study, we examined data from 354 transfusion donors, 66 of whom had thalassemia trait, and 288 of whom did not have thalassemia trait. The mean age of the donors with thalassemia trait was 35 (1.4) years, and the mean age of the donors without thalassemia was 36 (0.69) years. In the thalassemia group, the female/male (F/M) ratio was 26/40, and in the non-thalassemia group, it was 147/141. The donors with thalassemia were classified as having hemoglobin E trait ($n = 34$); 3.7-kb deletion ($n = 20$); Hb constant spring (Hb CS) ($n = 5$); β -thalassemia trait ($n = 3$); and other Hb types, which included 4.2-kb deletion ($n = 1$), homozygous Hb E ($n = 1$), Southeast Asian (SEA) deletion ($n = 1$), and Hb Pakse ($n = 1$).

TABLE 1 summarizes the hematological parameters of donors with and without thalassemia trait. Those with thalassemia trait had MCV and MCH values significantly lower than those without thalassemia. However, donors with thalassemia trait had higher RDW and RBC values than donors without thalassemia. A slight but statistically significant difference in MCHC was found between the donor groups. There were no statistically significant differences between the groups in the levels of Hb, HCT, WBC, or PLT.

AUC, Sensitivity, and Specificity of Each Mathematical Formula

The CBC parameters were incorporated into each mathematical formula, and diagnostic performance was compared using ROC analysis. **TABLE 2** summarizes the results regarding AUC values, sensitivities, and specificities. Five formulae had an AUC >0.8 , with the Shine and Lal formula having the highest AUC value: 0.9. The Shine and Lal formula also had the highest sensitivity, 83.58%, and specificity, 82.35%, at a cutoff value of 1812; the other formulae had sensitivities and specificities ranging from 70%–81%.

TABLE 1. Hematological Parameters of Donors with and without Thalassemia Trait

Parameter	Mean (SE) (Minimum–Maximum)		P Value
	Donors with Thalassemia Trait (n = 66)	Donors without Thalassemia Trait (n = 288)	
Hb (g/dL)	14 (0.12) (12–16)	14 (0.07) (11–18)	.08
RBCs ($\times 10^6$ cells/ μ L)	5.4 (0.06) (4.36–7.17)	4.92 (0.02) (3.98–6.84)	<.001 ^a
HCT (%)	42 (0.35) (36–47)	42 (0.21) (34–54)	.24
MCV (fL)	77 (0.71) (57–87)	86 (0.34) (56–96)	<.001 ^a
MCH (pg)	25 (0.24) (20–29)	28 (0.13) (18–33)	<.001 ^a
MCHC (g/dL)	33 (0.1) (30–35)	33 (0.05) (30–36)	.05 ^a
RDW (%)	15 (0.13) (13–18)	14 (0.06) (12–21)	<.001 ^a
WBCs ($\times 10^3$ cells/ μ L)	7.55 (0.21) (4.27–12.54)	7.31 (0.09) (3.77–13.97)	.29
PLTs ($\times 10^3$ cells/ μ L)	252 (7) (141–413)	266 (3.66) (33–415)	.09

Hb, hemoglobin; HCT, hematocrit; MCH, mean corpuscular hemoglobin; MCHC, mean corpuscular hemoglobin concentration; MCV, mean corpuscular volume; PLT, platelet; RBC, red blood cell; RDW, red cell distribution width; WBC, white blood cell.

^aIndicates statistically significant difference.

TABLE 2. Area Under the Curve (AUC) Values, Cutoff, Sensitivity, and Specificity of Mathematical Formulae

Formula	Mean (95% CI)			
	AUC	Cutoff Value	Sensitivity, %	Specificity, %
Srivastava ¹⁰	0.85 (0.8–0.9)	<5.29	80.6 (69.58–88.29)	74.05 (68.7–78.76)
Mentzer ¹¹	0.84 (0.8–0.89)	<15.62	73.13 (61.48–82.28)	80.97 (76.05–85.08)
Shine and Lal ¹²	0.9 (0.87–0.93)	<1812	83.58 (72.94–90.58)	82.35 (77.54–86.32)
Green and King ¹⁷	0.74 (0.67–0.8)	<68.94	64.18 (52.22–74.6)	67.13 (61.52–72.29)
D'Onofrio et al ¹⁸	0.58 (0.5–0.65)	>3.05	56.72 (44.81–67.9)	55.02 (49.25–60.65)
Ehsani et al ¹⁹	0.86 (0.82–0.91)	<30.45	74.63 (63–83.51)	79.93 (74.93–84.14)
Sirdah et al ²³	0.82 (0.77–0.88)	<34.51	73.13 (61.48–82.28)	80.62 (75.68–84.77)
Sirachainan et al ²⁰	0.52 (0.45–0.6)	<16.39	52.24 (40.49–63.75)	52.25 (46.5–57.94)
Bordbar et al ²¹	0.61 (0.54–0.69)	>7.17	59.7 (47.74–70.61)	61.94 (56.22–67.34)
Schoorl et al ²²	0.76 (0.7–0.82)	<22.73	68.66 (56.80–78.49)	67.82 (62.23–72.94)

Discussion

The current study investigated the diagnostic performance of 10 mathematical equations used to identify donors with thalassemia trait. Among these formulae, the Shine and Lal algorithm had the best diagnostic performance in identifying donors with underlying thalassemia that had not yet been recognized.

Our main findings are as follows. First, there were no statistically significant differences in Hb values between donors with and without thalassemia. This finding confirmed the thalassemia trait characteristics of the individuals recruited into the current study and implied that traditional practices, such as the CuSO₄ method, may be unable to identify donors with thalassemia trait.²⁴ Second, the Shine and Lal formula had the highest AUC, at 0.9, which suggests a strong capacity for discrimination between donors with and without thalassemia. Third, the Shine and Lal formula demonstrated the highest sensitivity and specificity—each more than 80%—which means that this formula produces few false-negative and false-positive results.

Taken together, our findings suggest that the Shine and Lal formula could be useful as an initial indicator of the need for further extensive investigation of a specific donor, to protect donors from undue harm during blood donation.²⁵ Given that automatic CBC analysis is less expensive than HPLC testing, this simple technique could lower the cost of identifying large numbers of transfusion donors in transfusion laboratories.

Another finding of ours was that donors with thalassemia trait had lower MCV and MCH levels than donors without thalassemia. This observation is consistent with those of earlier studies^{26,27} that examined the most commonly used erythrocyte indices and concluded that MCV and MCH are the most essential criteria for identifying thalassemia trait. This finding is also consistent with our previous observation regarding the Shine and Lal formula having the highest performance. This formula multiplies MCV by MCH, resulting in a noticeable difference when compared to the results of formulas that lack similar qualities in their formulations. Although MCV and MCH values may be used to differentiate between donors with and without thalassemia, multiplying these parameters may increase the strength of the discrimination and minimize erroneous results compared to using MCV or MCH by themselves. Previously, Carlos et al²⁸ reported decreased RBC values, including those for Hb, MCV, MCH, MCHC, and RDW, in patients with IDA who also had thalassemia. Other studies^{29,30} assessing the prevalence of IDA in blood donors found sensitivity and specificity of more than 80% when using the Mentzer algorithm to screen these groups of blood donors. The variability in the performance of each formula might be explained by interpopulation variances, various mutations, and the degree of anemia affecting RBC parameters.

Despite the good performance of the Shine and Lal formula, the variations between our study findings and those of other studies regarding

the detected sensitivity and specificity might be due to a distinct mutation that influences the pathophysiology of thalassemia or the use by other studies of different criteria to group individuals.^{23,31} Further, the discrepancies in performance suggest that each laboratory should determine its own cutoff level for identifying donors with thalassemia trait.

It is also worth mentioning that RBC levels were higher in donors with thalassemia than in healthy volunteer donors in the study. However, both levels were within normal ranges.³² In addition to the formulae examined in this study, algorithms that have diagnostic performance regarding IDA and thalassemia carriers have been reported in the general population.^{26,33} As a result, further studies should be conducted to analyze these proposed equations to find better algorithms for identifying donors with thalassemia.

In terms of cutoff values, a previous study¹² reported the performance of the Shine and Lal formula for diagnosing thalassemia with a cutoff value of 1530. Another study found that the Shine and Lal formula had excellent diagnostic performance (AUC = 0.94) for diagnosing thalassemia with a cutoff value of 1110.²¹ Variability in cutoff values, sensitivity, and specificity may be attributed to various gene mutations in different geographical groups or an underlying cause of anemia, such as iron or B12 deficiency, which affects RBC indices.^{4,5} Also, variation in cutoff levels implies that each laboratory should determine its own values. It might also be argued that screening requires a high-sensitivity approach. However, other underlying diseases, such as IDA, may be associated with hematological characteristics that were not included in the current investigation. Given this context, a reliable screening strategy is necessary to minimize false positives and false negatives. As a result, we chose the optimal cutoff values for maximum sensitivity and specificity.

The current study has several limitations. First, we examined only donors with thalassemia. However, 2 previous study reports^{6,34} stated that glucose-6-phosphate dehydrogenase (G6PD) deficiency was common in transfusion donors. Therefore, because our investigation might have included donors with G6PD deficiency, additional studies should examine the application of mathematical formulae to identify donors who are deficient in G6PD.

The second drawback is that we did not test for IDA. Given its prevalence in various countries, including Thailand, the presence of IDA might have been a factor in the decreased levels of MCV and MCH we observed in this study.^{35,36}

Third, we examined conventional RBC parameters. Earlier study reports^{37,38} have stated that expanded RBC characteristics from multiple automated hematological analyzers may be used to detect individuals who are carriers of thalassemia. Further studies should be conducted to identify whether these extended RBC measures surpass conventional RBC parameters in identifying blood donors with thalassemia. Finally, the reliability of the mathematical calculations could have been limited if the donors had mutations that had no effect on their RBC characteristics.^{39,40}

Our findings support the reliability and accuracy of the Shine and Lal formula in identifying donors with thalassemia trait. Implementing this easy, low-cost technique can help to assure the safety of voluntary donors, particularly those with undisclosed underlying thalassemia.

Acknowledgments

This research was funded by Chulalongkorn University (CU-GE60-05-30-01). The authors thank the Faculty of Medicine of Siriraj Hospital, Mahidol University, for supporting this research project.

Conflicts of Interest

The authors have nothing to disclose.

REFERENCES

- Clegg JB, Weatherall DJ. Thalassemia and malaria: new insights into an old problem. *Proc Assoc Am Physicians*. 1999;111(4):278–282. doi:10.1046/j.1525-1381.1999.99235.x
- Olivieri NF, Pakbaz Z, Vichinsky E. Hb E/beta-thalassaemia: a common & clinically diverse disorder. *Indian J Med Res*. 2011;134(4):522–531.
- World Health Organization: Guidelines Review Committee. *Blood Donor Selection: Guidelines on Assessing Donor Suitability for Blood Donation*. World Health Organization; 2012.
- De Sanctis V, Kattamis C, Canatan D, et al. β -Thalassemia distribution in the Old World: an ancient disease seen from a historical standpoint. *Mediterr J Hematol Infect Dis*. 2017;9(1):e2017018. doi:10.4084/MJHID.2017.018
- Rezaee AR, Banoei MM, Khalili E, Houshmand M. Beta-thalassemia in Iran: new insight into the role of genetic admixture and migration. *Sci World J*. 2012;2012:635183. doi:10.1100/2012/635183
- Kittisares K, Palasuwan D, Nulsri E, Palasuwan A. Thalassemia trait and G6PD deficiency in Thai blood donors. *Transfus Apher Sci*. 2019;58(2):201–206. doi:10.1016/j.transci.2019.03.009
- Nulsri E, Lerdwana S. Blood donors with thalassemic trait, glucose-6-phosphate dehydrogenase deficiency trait, and sickle cell trait and their blood products: current status and future perspective. *Lab Med*. 2023;54(1):6–12. doi:10.1093/labmed/lmac061
- Brancaleoni V, Di Pierro E, Motta I, Cappellini MD. Laboratory diagnosis of thalassemia. *Int J Lab Hematol*. 2016;38(Suppl 1):32–40. doi:10.1111/ijlh.12527
- Khera R, Singh T, Khuana N, Gupta N, Dubey AP. HPLC in characterization of hemoglobin profile in thalassemia syndromes and hemoglobinopathies: a clinicohematological correlation. *Indian J Hematol Blood Transfus*. 2015;31(1):110–115.
- Srivastava PC. Differentiation of thalassaemia minor from iron deficiency. *Lancet*. 1973;2(7821):154–155. doi:10.1016/s0140-6736(73)93104-8
- Mentzer WC Jr. Differentiation of iron deficiency from thalassaemia trait. *Lancet*. 1973;1(7808):882. doi:10.1016/s0140-6736(73)91446-3
- Shine I, Lal S. A strategy to detect β -thalassaemia minor. *Lancet*. 1977;1(8013):692–694. doi:10.1016/S0140-6736(77)92128-6
- Roth IL, Lachover B, Koren G, Levin C, Zalman L, Koren A. Detection of β -thalassaemia carriers by red cell parameters obtained from automatic counters using mathematical formulas. *Mediterr J Hematol Infect Dis*. 2018;10(1):e2018008. doi:10.4084/MJHID.2018.008
- Sahli CA, Bibi A, Ouali F, et al. Red cell indices: differentiation between β -thalassaemia trait and iron deficiency anemia and application to sickle-cell disease and sickle-cell thalassaemia. *Clin Chem Lab Med*. 2013;51(11):2115–2124. doi:10.1515/ccclm-2013-0354
- Beyan C, Kaptan K, Ifran A. Predictive value of discrimination indices in differential diagnosis of iron deficiency anemia and beta-thalassaemia trait. *Eur J Haematol*. 2007;78(6):524–526. doi:10.1111/j.1600-0609.2007.00853.x
- Rathod DA, Kaur A, Patel V, et al. Usefulness of cell counter-based parameters and formulas in detection of beta-thalassaemia trait in areas of high prevalence. *Am J Clin Pathol*. 2007;128(4):585–589. doi:10.1309/R1YL4B4BT2WCQDGV
- Green R, King R. A new red cell discriminant incorporating volume dispersion for differentiating iron deficiency anemia from thalassaemia minor. *Blood Cells*. 1989;15(3):481–491; discussion 492–485.
- d'Onofrio G, Zini G, Ricerca BM, Mancini S, Mango G. Automated measurement of red blood cell microcytosis and hypochromia in iron deficiency and beta-thalassaemia trait. *Arch Pathol Lab Med*. 1992;116(1):84–89.

19. Ehsani MA, Shahgholi E, Rahiminejad MS, Seighali F, Rashidi A. A new index for discrimination between iron deficiency anemia and beta-thalassemia minor: results in 284 patients. *Pak J Biol Sci.* 2009;12(5):473–475. doi:[10.3923/pjbs.2009.473.475](https://doi.org/10.3923/pjbs.2009.473.475)
20. Sirachainan N, Iamsirirak P, Charoenkwan P, et al. New mathematical formula for differentiating thalassemia trait and iron deficiency anemia in thalassemia prevalent area: a study in healthy school-age children. *Southeast Asian J Trop Med Public Health.* 2014;45(1):174–182.
21. Bordbar E, Taghipour M, Zucconi BE. Reliability of different RBC indices and formulas in discriminating between β -thalassemia minor and other microcytic hypochromic cases. *Mediterr J Hematol Infect Dis.* 2015;7(1):e2015022. doi:[10.4084/mjhid.2015.022](https://doi.org/10.4084/mjhid.2015.022)
22. Schoorl M, Schoorl M, van Pelt J, Bartels PCM. Application of innovative hemocytometric parameters and algorithms for improvement of microcytic anemia discrimination. *Hematol Rep.* 2015;7(2):5843.
23. Sirdah M, Tarazi I, Al Najjar E, Al Haddad R. Evaluation of the diagnostic reliability of different RBC indices and formulas in the differentiation of the beta-thalassaemia minor from iron deficiency in Palestinian population. *Int J Lab Hematol.* 2008;30(4):324–330. doi:[10.1111/j.1751-553x.2007.00966.x](https://doi.org/10.1111/j.1751-553x.2007.00966.x)
24. Antwi-Baffour S, Annor DK, Adjei JK, Kyeremeh R, Kpentey G, Kyei F. Anemia in prospective blood donors deferred by the copper sulphate technique of hemoglobin estimation. *BMC Hematol.* 2015;15:15. doi:[10.1186/s12878-015-0035-3](https://doi.org/10.1186/s12878-015-0035-3)
25. Figueiredo MS. Anemia and the blood donor. *Rev Bras Hematol Hemoter.* 2012;34(5):328–329. doi:[10.5581/1516-8484.20120085](https://doi.org/10.5581/1516-8484.20120085)
26. Hoffmann JJML, Urrechaga E, Aguirre U. Discriminant indices for distinguishing thalassemia and iron deficiency in patients with microcytic anemia: a meta-analysis. *Clin Chem Lab Med.* 2015;53(12):1883–1894. doi:[10.1515/cclm-2015-0179](https://doi.org/10.1515/cclm-2015-0179)
27. Clarke GM, Higgins TN. Laboratory investigation of hemoglobinopathies and thalassemias: review and update. *Clin Chem.* 2000;46(8 Pt 2):1284–1290.
28. Carlos AM, Souza BMB, Souza RAV, Resende GAD, Pereira GA, Moraes-Souza H. Causes of microcytic anaemia and evaluation of conventional laboratory parameters in the differentiation of erythrocytic microcytosis in blood donors candidates. *Hematology.* 2018;23(9):705–711. doi:[10.1080/10245332.2018.1446703](https://doi.org/10.1080/10245332.2018.1446703)
29. Tiwari AK, Chandola I, Ahuja A. Approach to blood donors with microcytosis. *Transfus Med.* 2010;20(2):88–94. doi:[10.1111/j.1365-3148.2009.00980.x](https://doi.org/10.1111/j.1365-3148.2009.00980.x)
30. Sundh A, Kaur P, Palta A, Kaur G. Utility of screening tools to differentiate beta thalassemia trait and iron-deficiency anemia - do they serve a purpose in blood donors? *Blood Res.* 2020;55(3):169–174. doi:[10.5045/br.2020.2020219](https://doi.org/10.5045/br.2020.2020219)
31. Nienhuis AW, Nathan DG. Pathophysiology and clinical manifestations of the β -thalassemias. *Cold Spring Harb Perspect Med.* 2012;2(12):a011726. doi:[10.1101/cshperspect.a011726](https://doi.org/10.1101/cshperspect.a011726)
32. Besarab A, Frinak S, Yee J. What is so bad about a hemoglobin level of 12 to 13 g/dL for chronic kidney disease patients anyway? *Adv Chronic Kidney Dis.* 2009;16(2):131–142. doi:[10.1053/j.ackd.2008.12.007](https://doi.org/10.1053/j.ackd.2008.12.007)
33. Hoffmann JJML, Urrechaga E. Verification of 20 mathematical formulas for discriminating between iron deficiency anemia and thalassemia in microcytic anemia. *Lab Med.* 2020;51(6):628–634. doi:[10.1093/labmed/lmaa030](https://doi.org/10.1093/labmed/lmaa030)
34. Noulis E, Lerdwana S, Palasuwan D, Palasuwan A. Cell-derived microparticles in blood products from blood donors deficient in glucose-6-phosphate dehydrogenase. *Lab Med.* 2021;52(6):528–535. doi:[10.1093/labmed/lmab007](https://doi.org/10.1093/labmed/lmab007)
35. Brimson S, Suwanwong Y, Brimson JM. Nutritional anemia predominant form of anemia in educated young Thai women. *Ethn Health.* 2019;24(4):405–414. doi:[10.1080/13557858.2017.1346188](https://doi.org/10.1080/13557858.2017.1346188)
36. Jamnok J, Sanchaisuriya K, Sanchaisuriya P, Fucharoen G, Fucharoen S, Ahmed F. Factors associated with anaemia and iron deficiency among women of reproductive age in Northeast Thailand: a cross-sectional study. *BMC Public Health.* 2020;20(1):102. doi:[10.1186/s12889-020-8248-1](https://doi.org/10.1186/s12889-020-8248-1)
37. Urrechaga E. The new mature red cell parameter, low haemoglobin density of the Beckman-Coulter LH750: clinical utility in the diagnosis of iron deficiency. *Int J Lab Hematol.* 2010;32(1 pt 1):e144–e150. doi:[10.1111/j.1751-553X.2008.01127.xCitations](https://doi.org/10.1111/j.1751-553X.2008.01127.xCitations)
38. Ng EHY, Leung JHW, Lau YS, Ma ESK. Evaluation of the new red cell parameters on Beckman Coulter DxH800 in distinguishing iron deficiency anaemia from thalassaemia trait. *Int J Lab Hematol.* 2015;37(2):199–207. doi:[10.1111/ijlh.12262](https://doi.org/10.1111/ijlh.12262)
39. Maragoudaki E, Kanavakis E, Traeger-Synodinos J, et al. Molecular, haematological and clinical studies of the -101 C → T substitution in the beta-globin gene promoter in 25 β -thalassaemia intermedia patients and 45 heterozygotes. *Br J Haematol.* 1999;107(4):699–706. doi:[10.1046/j.1365-2141.1999.01788.x](https://doi.org/10.1046/j.1365-2141.1999.01788.x)
40. Perseu L, Satta S, Moi P, et al. *KLF1* gene mutations cause borderline HbA_{1c}. *Blood.* 2011;118(16):4454–4458. doi:[10.1182/blood-2011-04-345736](https://doi.org/10.1182/blood-2011-04-345736)

Evaluation of methods to eliminate analytical interference in multiple myeloma patients with spurious hyperphosphatemia

Xin Tian, MD,^{1,*} Li Zhao, MD,^{1,*} Jin Ma, MD,¹ Jie Lu, MD,¹ Tian-yi Zhu, MD,¹ Yan Liu, MD,¹ Hong-xun Sun, MD¹

¹Department of Laboratory Medicine, The Third Hospital of Hebei Medical University, Shijiazhuang, China. Corresponding author: Hong-xun Sun; 18533112710@163.com. *First authors.

Keywords: paraprotein interference, spurious hypophosphate, multiple myeloma

Abbreviations: TCA, trichloroacetic acid; H₂O, deionized water, NS, normal saline; bias%, bias percentage; Ig, immunoglobulin; MM, multiple myeloma

Laboratory Medicine 2023;54:598-602; <https://doi.org/10.1093/labmed/lmad012>

ABSTRACT

Objective: The acid/molybdate assay performed on the Beckman Coulter AU5821 could be subject to paraprotein interference, which potentially results in spurious hyperphosphatemia. We attempted to find a reliable solution to eliminate paraprotein interference in laboratory test results and discuss the causes of paraprotein interference.

Methods: We observed 50 multiple myeloma patients with serum paraproteins. We used the trichloroacetic acid (TCA) deproteinizing method to confirm that paraproteins indeed interfered with phosphate detection in the serum acid/molybdate assay. Furthermore, we used the dry chemical method (Vitros 5.1 FS, Johnson) and deionized water (H₂O), normal saline (NS), and healthy human serum as alternative diluents. We assessed the clinical acceptability of the 4 methods by evaluating a bias percentage (bias%) lower than 10% under the premise of TCA treatment as a serum phosphate reference method.

Results: In total, comparing the results of the TCA treatment on the Beckman Coulter AU5821, 3/50 (6%) multiple myeloma patients exhibited phosphate pseudo-elevation (bias% >10%). Additionally, we found pseudo-hypophosphate only in immunoglobulin (Ig)G-kappa paraprotein samples, and all were above 50 g/L. The bias% between TCA and dry chemical method for the 3 patients was below 10%. The maximum acceptable dilutions for patient 22 were 8-fold H₂O, 4-fold H₂O, and 2-fold serum; those for patient 45 were 16-fold H₂O, 16-fold

H₂O, and 2-fold serum. However, the bias% of patient 40 was beyond the acceptable range in all 3 dilution groups.

Conclusion: High concentrations of IgG kappa-type paraproteins are more likely to interfere with serum phosphorous detection. Both the TCA and dry chemical method can effectively eliminate paraprotein interference.

Paraproteins are monoclonal immunoglobulins (Igs) or immunoglobulin fractions present in the blood or urine produced by a clonal population of B-cell lineage cells, most commonly plasma cells. The presence of paraproteins may signify a variety of underlying conditions, ranging from a benign process known as monoclonal gammopathy of unknown significance to plasma cell malignancy, that is, multiple myeloma (MM).¹ It has been reported that paraproteins often interfere with biochemical immunoassays and result in inaccurate test results.^{2,3} In particular, there have been several reports indicating that serum phosphate concentrations may be erroneously high in patients with paraproteinemia if the method of phosphate measurement is based on a direct reaction with molybdate in an acid medium.⁴ However, the method information sheet accompanying the current phosphate method kit does not explicitly mention the possibility of interference by paraproteins. Therefore, the presence of pseudo-hyperphosphorus interference by paraprotein effects could be more widespread than realized due to current laboratory testing method limitations.

Hyperphosphatemia occurs in hypoparathyroidism, acute rhabdomyolysis, and metabolic acidosis. Hyperphosphatemia also occurs in secondary renal damage caused by B-cell neoplasia, such as MM or Waldenström's macroglobulinemia.⁵ If incorrect serum phosphate results are reported to clinicians, they could lead to unnecessary investigations and changes to patient treatment. Therefore, in the current study, serum phosphate concentrations were measured in 50 MM patients with serum paraproteins to study how paraproteins interfered with phosphate detection in the serum direct acid/molybdate method. We attempted to find a reliable and simple solution to eliminate paraprotein interference for laboratory serum phosphate examination and further explore the causes of paraprotein interference by using the trichloroacetic acid (TCA) deproteinizing method to remove paraproteins to accurately assay the serum phosphate and used deionized water (H₂O), normal saline (NS), and healthy low-value human serum as alternative diluents.

Materials and Methods

Ethics Statement

All procedures performed in the study involving human participants were in accordance with the ethical standards of the institutional and/or national research committee and with the 1964 Helsinki Declaration and its later amendments or comparable ethical standards. The study protocol was approved by Hebei Medical University ethical committee (W2021-095-1). Written informed consent was obtained from each participant.

Study Subjects

Subjects meeting the following criteria were enrolled in the study: (1) Chinese patients who met the diagnosis standard for MM according to the Revised International Myeloma Working Group criteria (IMWG 2014)⁶; and (2) MM patients with a monoclonal immunoglobulin band identified by serum protein electrophoresis. Patients whose serum samples were lipemic, icteric, or hemolytic or those who were treated with phosphate therapy were excluded.

Paraprotein Typing and Concentration Detection

Identified paraproteins were typed by immunofixation electrophoresis as IgM, IgG, IgE, IgA, or IgD, and light chain type (kappa or lambda). The paraprotein concentration was detected by the immunoturbidimetric method on the Beckman Coulter IMMAGE 800 Specific Protein Analyzer.

Methods for Serum Phosphate Concentration Detection

Beckman Coulter AU5821 Determination Method

Serum phosphate concentrations were analyzed using a Beckman Coulter AU5821 and an ammonium molybdate-based method in which inorganic phosphorus reacted with ammonium molybdate in the presence of sulfuric acid to form an unreduced phosphomolybdate complex, which was measured as an end-point reaction at 340 nm (reference interval: 0.85–1.51 mmol/L).

TCA Deproteinizing Method

Samples were deproteinized using TCA (Deproteinizing Sample Preparation Kit, Bio Vision). The protocol included: (1) Protein precipitation, in which 150 μ L sample was mixed with 15 μ L cold TCA in a 1.5 mL microcentrifuge tube. The sample was kept on ice for 15 min, then centrifuged at 12,000g for 5 min. Supernatant was carefully transferred to another tube. (2) Sample neutralization, in which 10 μ L cold neutralization solution was added to the collected supernatant. The sample was placed on ice for 5 min and directly measured with the Beckman Coulter AU5821 analyzer for the phosphate concentrations. We defined the serum phosphate results by the TCA deproteinizing method and removal of paraproteins as the true result and compared them with the original results to confirm whether there were pseudo-hyperphosphatemia test results in patients with MM with paraproteins, where the relative bias (bias%) between the 2 assays was more than 10%. We analyzed the relationship between paraprotein-interfered serum phosphate determination samples and paraprotein concentrations and immunoglobulin typing.

Methods for Removing Paraprotein Interference

Vitros 5.1 FS Detection Method

Serum phosphate concentrations were analyzed using the dry chemical method (Vitros 5.1 FS, Johnson). Vitros 5.1 FS analysis requires the use

of a slide-based method for the reaction of inorganic phosphorus with ammonium molybdate to form a phosphomolybdate complex. This complex was then reduced by p-methyl-aminophenol sulfate, an organic reductant, to form a stable heteropoly molybdenum blue chromophore. The phosphate concentration was then estimated by reflectance spectrophotometry at 670 nm.

Dilution Methods

Diluents included H₂O, NS, and healthy low-value serum phosphorus samples; the original serum samples containing paraproteins were diluted by the various diluents, and serum phosphate was remeasured on the AU5821 analyzer.

Separately, we compared the results by the multiple methods for removing paraprotein interference with the results by TCA treatment, where a bias% <10% was the judgment criterion, to determine the most desirable method to detect serum phosphorus interference by paraproteins in daily practice.

Statistical Methods

Continuous variables conforming to a normal distribution are described as mean \pm SD; otherwise, they are described as median and interquartile range (P_{25} – P_{75}). Categorical variables are described as frequencies and percentages (%).

The absolute bias was defined by the difference between the serum phosphate results by the TCA deproteinizing method and the original serum phosphate concentrations by AU5821. The relative bias (bias%) denoted the absolute bias divided by the original serum phosphate concentrations by AU5821. If the bias% was more than 10%, there was a difference; that is, there was pseudo-hyperphosphorus interference by paraprotein effects in the AU5821 analyzer.

Results

Patient Characteristics and Paraprotein Typing

In the current study, 50 different MM patients were included, 23 females and 27 males. The median age was 63 years (interquartile range, 43–80 years). Of the study patients, 27 had IgG typing paraproteins (9 IgG lambda and 18 IgG kappa), 18 had IgA paraproteins (10 IgA lambda and 8 IgA kappa), and 5 had IgM paraproteins (4 IgM kappa and 1 IgM lambda). The paraprotein concentration range was 5.62 to 74.90 g/L with a median of 23.9 (12.06–40.31) g/L (TABLE 1).

Original Serum Phosphate Results and TCA Treatment Results

Of the 50 paraprotein-positive samples, 3 (6%) showed a bias% greater than 10% and phosphate pseudo-elevation. In addition, we found pseudo-hyperphosphate only in IgG kappa-type paraprotein samples. The concentrations of paraproteins in the 3 cases were all above 50 g/L, and serum total protein was above 100 g/L (TABLE 1 and TABLE 2).

Comparison of the Results of the Dilution Group and Vitros Group with TCA

The maximum dilutions of patient 22 were 8-fold H₂O, 4-fold NS, and 2-fold low-value phosphate serum; those for patient 45 were 16-fold

TABLE 1. Basic Characteristics of 50 Patients with Multiple Myeloma

Patient No.	AU5821	TCA	Bias%	Paraprotein type	Paraprotein concentration (g/L)	Patient No.	AU5821	TCA	Bias%	Paraprotein type	Paraprotein concentration (g/L)
1	1.41	1.38	2%	IgG kappa	18.64	26	0.91	0.93	-2%	IgM kappa	8.26
2	1.50	1.46	3%	IgG lambda	8.53	27	1.34	1.39	-4%	IgG lambda	11.82
3	1.29	1.21	6%	IgA kappa	5.62	28	0.92	0.91	1%	IgG lambda	31.27
4	2.28	2.18	5%	IgM lambda	7.15	29	1.27	1.30	-2%	IgG lambda	17.16
5	1.34	1.45	-8%	IgG kappa	43.85	30	0.90	0.93	-3%	IgA lambda	34.20
6	0.99	0.92	7%	IgA lambda	31.90	31	1.18	1.20	-2%	IgG kappa	23.70
7	1.33	1.24	7%	IgG kappa	31.3	32	1.18	1.23	-4%	IgA lambda	55.70
8	1.48	1.34	10%	IgG kappa	38.39	33	1.32	1.26	4%	IgG kappa	25.47
9	1.31	1.28	3%	IgG kappa	13.54	34	0.92	0.99	-7%	IgA kappa	23.90
10	1.42	1.33	7%	IgA lambda	38.91	35	1.26	1.26	0%	IgA kappa	25.00
11	1.04	1.00	4%	IgA lambda	15.3	36	0.96	1.00	-4%	IgG kappa	8.70
12	1.79	1.61	10%	IgA lambda	57.4	37	1.00	1.00	0%	IgG kappa	15.40
13	1.34	1.25	7%	IgA kappa	60.42	38	0.69	0.63	9%	IgM kappa	7.5
14	1.05	1.13	-7%	IgG lambda	16.73	39	0.93	0.96	-3%	IgG kappa	8.9
15	0.83	0.88	-5%	IgA kappa	10.77	40	5.50	2.25	59%	IgG kappa	73.90
16	1.63	1.61	1%	IgA lambda	13.78	41	1.27	1.38	-8%	IgA kappa	60.3
17	1.34	1.35	-1%	IgA lambda	12.62	42	1.61	1.54	5%	IgA lambda	37.1
18	1.35	1.43	-6%	IgG kappa	74.90	43	0.74	0.75	-1%	IgG lambda	19.09
19	1.30	1.23	6%	IgA lambda	26.28	44	1.49	1.44	4%	IgG kappa	53.9
20	1.50	1.48	2%	IgM kappa	38.12	45	3.19	1.56	51%	IgG kappa	50.10
21	1.83	1.86	-2%	IgG lambda	34.20	46	1.41	1.46	-4%	IgG kappa	6.97
22	2.96	1.56	47%	IgG kappa	59.90	47	1.45	1.46	-1%	IgA kappa	12.3
23	2.50	2.26	10%	IgG kappa	46.65	48	1.46	1.36	7%	IgG kappa	41.7
24	1.42	1.43	0%	IgM kappa	8.07	49	1.53	1.41	8%	IgA kappa	9.5
25	1.35	1.26	6%	IgG lambda	22.79	50	1.47	1.46	1%	IgG lambda	49.3

AU5821, the serum phosphate concentration(mmol/L) result measured on the AU5821 analyzer; TCA, the serum phosphate concentration(mmol/L) result measured on AU5821 after TCA precipitation method.

TABLE 2. Patient Characteristics Associated with Spurious Hyperphosphatemia and Results After Dilution

Characteristic	Patient No.		
	22	40	45
Sex	M	M	M
Age (y)	57	62	66
Monoclonal component type	IgG kappa	IgG kappa	IgG kappa
Monoclonal component (g/L)	59.90	73.90	50.10
Serum total protein (g/L)	118.09	121.29	118.56
Serum creatinine (mmol/L)	57.16	544.79	99.92
Serum calcium (mmol/L)	2.18	2.88	2.17
Serum phosphorus by AU5821 (mmol/L)	2.96	5.50	3.19
Serum phosphorus by TCA (mmol/L)	1.56	2.25	1.75
Serum phosphorus by Vitros (mmol/L)	1.69	2.43	1.81

IgG, immunoglobulin.

H₂O, 16-fold NS, and 2-fold serum. However, the bias% of patient 40 was beyond the acceptable range in the 3 dilution groups. The bias% of the Vitros 5.1 FS method compared with the TCA method was less than 10% in these 3 cases (TABLE 3).

Discussion

Hyperphosphatemia is usually secondary to hypoparathyroidism or advanced renal failure. Pseudo-hyperphosphatemia, a rare condition, is most commonly associated with paraproteinemia but is also seen in other conditions, such as hyperlipidemia, hyperbilirubinemia, and hemolysis. Pseudo-hyperphosphatemia is found in MM samples, caused by the interaction of the paraprotein with molybdate reagent in the acid molybdate-based assay.^{7–11} Indeed, in the current study, we discovered 3 cases of pseudo-hyperphosphatemia in our laboratory from April 2021 to January 2022, all of them IgG kappa-type MM. However, the available studies do not suggest that the pseudo-increased serum phosphorus has a significant correlation with paraprotein types. Sinclair et al¹² reported IgA and IgG with pseudo-increased blood phosphorus in MM patients. In 2007, Kiki et al⁹ reported another pseudo-elevation in serum phosphorus in IgG MM. In 2015, Made et al¹³ found pseudo-hyperphosphatemia in an IgA kappa MM patient. Additionally, the study results are discrepant about whether the paraprotein concentration is related to the spurious increase in phosphorus. In the current study, we found that the paraprotein concentration of 3 cases was more than 50 g/L, indicating that high concentrations of paraprotein are more likely to cause interference. Some experts also believe that paraprotein interference is more likely to occur at high paraprotein concentrations.¹⁴

TABLE 3. Recovery Rate of Serum Phosphate on the AU 5821 Analyzer at Various Dilutions

	Dilution	H ₂ O				NS				Serum			
		Expected value (mmol/L)	Obtained value (mmol/L)	Bias (%)	Expected value (mmol/L)	Expected value (mmol/L)	Obtained value (mmol/L)	Bias (%)	Expected value (mmol/L)	Obtained value (mmol/L)	Bias (%)	Expected value (mmol/L)	Bias (%)
Patient 22	Original	1.56	—	—	1.56	—	—	—	1.56	—	—	—	—
	2×	0.78	0.78	0.00 ^a	0.78	0.85	0.85	8.97 ^a	0.78	0.82	5.13 ^a	0.82	5.13 ^a
	4×	0.39	0.37	-5.13 ^a	0.39	0.36	0.36	-7.69 ^a	0.39	0.34	-12.82	0.34	-12.82
	8×	0.20	0.18	-7.69 ^a	0.20	0.16	0.16	-17.95	0.20	0.16	-17.95	0.16	-17.95
	16×	0.10	0.08	-17.95	0.10	0.08	0.08	-17.95	0.10	0.07	-28.21	0.07	-28.21
Patient 40	Original	2.25	—	—	2.25	—	—	—	2.25	—	—	—	—
	2×	1.13	3.16	180.89	1.13	3.34	3.34	196.89	1.13	3.97	252.89	3.97	252.89
	4×	0.56	2.20	291.11	0.56	1.19	1.19	111.56	0.56	1.16	105.99	1.16	105.99
	8×	0.28	0.76	170.22	0.28	0.74	0.74	163.11	0.28	0.66	133.29	0.66	133.29
	16×	0.14	0.18	28.00	0.14	0.18	0.18	28.00	0.14	0.16	14.13	0.16	14.13
Patient 45	Original	1.75	—	—	1.75	—	—	—	1.75	—	—	—	—
	2×	0.88	0.96	9.71 ^a	0.88	0.95	0.95	8.57 ^a	0.88	0.94	7.43 ^a	0.94	7.43 ^a
	4×	0.44	0.46	5.14 ^a	0.44	0.43	0.43	-1.71 ^a	0.44	0.39	-10.86	0.39	-10.86
	8×	0.22	0.20	-8.57 ^a	0.22	0.20	0.20	-8.57 ^a	0.22	0.18	-17.71	0.18	-17.71
	16×	0.11	0.10	-8.57 ^a	0.11	0.10	0.10	-8.57 ^a	0.11	0.09	-17.71	0.09	-17.71

^aIndicates that the bias% is within the acceptable range.

However, Roy¹ insisted that there is no significant correlation between paraprotein interference and concentration or type.

Furthermore, it has been reported that artifactual laboratory abnormalities are uncommon; percentage of abnormalities were found to be 1.2% and 1.5% in 2 studies.^{10,11} We found that of the 50 paraprotein-positive samples, 3 (6%) exhibited phosphate pseudo-elevation. The incidence of such a phenomenon is not accurately known and may be even higher than generally appreciated. It is important for clinicians to be aware of the possibility and recognize artifactual errors in laboratory parameters so that unnecessary tests and erroneous conclusions can be avoided. The wide variation in reported incidences of pseudo-hyperphosphatemia may be due to different definitions of the phenomenon in different studies. We defined any phosphate value measured on the AU5821 that was 10% different from the result obtained on TCA as being pseudo-hyperphosphatemia. Because TCA could completely eliminate the paraproteins, we treated the TCA result as the real result. There was no significant difference in the serum phosphate values between the TCA treatment and the Vitros 5.1 FS dry chemical analyzer method, indicating that both methods had a similar ability to resist paraprotein interference in the clinical laboratory. The Vitros 5.1 FS method is reported to be interference-free because the sample has to penetrate several slide layers before reaching the reaction layer, although the method is based on the reaction of phosphate with ammonium molybdate. This may therefore have the effect of filtering out any interfering compounds.¹⁵ Finally, we attempted the dilution method commonly used in eliminating analytical interference and compared it with the TCA method. The maximum acceptable dilutions of patient 22 were 8-fold H₂O, 4-fold NS, and 2-fold low-value phosphate serum and those of patient 45 were 16-fold H₂O, 16-fold NS, and 2-fold serum. The only exception was patient 40, whose results lacked linearity. This patient's phosphate concentrations measured on the AU5821 system were 5.5 mmol/L and the overestimated values were absurdly high. In addition, the patient had severe renal impairment (creatinine: 544.79 mmol/L). As a result, this sample is not linear with the TCA method regardless of dilution method. However, the TCA treatment result of this sample was 2.25 mmol/L, and the dry chemical result was 2.43 mmol/L. These results are a more realistic reflection of the patient's physiological state.

The purpose of the current study was to analyze the clinical laboratory abnormalities caused by paraproteins to improve awareness of the possibility of such interference and avoid unnecessary erroneous conclusions in practical work. When suspicious results appear, the TCA method is preferred for processing samples. If a laboratory does not have a deproteinizing reagent, the dry chemical (Vitros) method is reliable. Through a series of dilutions, the results were also close to the real results except for an unexpectedly high concentration of phosphorus. It is very important to provide clinicians and patients with more accurate results, which can assist clinicians in making accurate diagnoses.

Conclusion

A high concentration of paraproteins is more likely to cause interference, and IgG kappa-type paraproteins are more likely to interfere with phosphorous detection. Both the TCA and dry chemical methods can effectively eliminate paraprotein interference. Paraprotein interference cannot be completely eliminated by dilution, especially with very high paraprotein concentrations.

Funding

This work was supported by the Health Commission of Hebei Province (20211034) and the Hebei Education Department (ZD2015040).

Conflict of Interest Disclosure

The authors have nothing to disclose.

Data Availability

The datasets used and/or analyzed during the current study are available from the corresponding author on reasonable request.

REFERENCES

1. Roy V. Artfactual laboratory abnormalities in patients with paraproteinemia. *South Med J*. 2009;102(2):167–170.
2. Oren S, Feldman A, Turkot S, Lugassy G. Hyperphosphatemia in multiple myeloma. *Ann Hematol*. 1994;69:41–43. doi:10.1007/BF01757346
3. Sinclair D, Smith H, Woodhead P. Spurious hyperphosphataemia caused by an IgA paraprotein: a topic revisited. *Ann Clin Biochem*. 2004;41(pt 2):119–124. doi:10.1258/000456304322879999
4. McClure D, Lai LC, Cornell C. Pseudohyperphosphataemia in patients with multiple myeloma. *J Clin Pathol*. 1992;45:731–732. doi:10.1136/jcp.45.8.731
5. Endres DB, Rude RK. Bone and mineral metabolism. In: Burtis CA, Ashwood ER, Bruns DE, eds. *Tietz Textbook of Clinical Chemistry and Molecular Diagnostics*. 4th ed. St Louis, MO: Elsevier; 2006:1905–1909.
6. Rajkumar SV, Dimopoulos MA, Palumbo A, et al. International Myeloma Working Group updated criteria for the diagnosis of multiple myeloma. *Lancet Oncol*. 2014;15:e538–e548. doi:10.1016/S1470-2045(14)70442-5
7. Lee Y, Koo T, Yi JH, et al. Pseudohyperphosphatemia in a patient with multiple myeloma. *Electrolyte Blood Press*. 2007;5:131–135. doi:10.5049/EBP.2007.5.2.131
8. Umeda M, Okuda S, Izumi H, et al. Prognostic significance of the serum phosphorus level and its relationship with other prognostic factors in multiple myeloma. *Ann Hematol*. 2006;85:469–473. doi:10.1007/s00277-006-0095-3
9. Kiki I, Gundogdu M, Kaya H. Spuriously high phosphate level which is promptly resolved after plasmapheresis in a patient with multiple myeloma. *Transfus Apher Sci*. 2007;37:157–159. doi:10.1016/j.transci.2007.07.005
10. Izzedine H, Camous L, Bourry E, Azar N, Leblond V, Deray G. Make your diagnosis: multiple myeloma associated with spurious hyperphosphatemia. *Kidney Int*. 2007;72:1035–1036. doi:10.1038/sj.ki.5002485
11. Mavrikakis M, Vaiopoulos G, Athanassiades P, Antoniadis L, Papamichael C, Dimopoulos MA. Pseudohyperphosphatemia in multiple myeloma. *Am J Hematol*. 1996;51:178–179. doi:10.1002/(SICI)1096-8652(199602)51:2<178::AID-AJH22>3.0.CO;2-D
12. Sinclair D, Smith H, Woodhead P. Spurious hyperphosphataemia caused by an IgA paraprotein: a topic revisited. *Ann Clin Biochem*. 2004;41(pt 2):119–124. doi:10.1258/000456304322879999
13. Maden M, Emel Pamuk G, Asoglu V, Nuri Pamuk O. The rapid resolution of pseudohyperphosphatemia in an IgA κ multiple myeloma patient after therapy with a bortezomib-containing regimen: report of the first case. *J Cancer Res Ther*. 2015;11(4):1043.
14. García-González E, González-Tarancón R, Aramendía M, Rello L. Analytical interference by monoclonal immunoglobulins on the direct bilirubin AU Beckman Coulter assay: the benefit of unsuspected diagnosis from spurious results. *Clin Chem Lab Med*. 2016;54:1329–1335. doi:10.1515/cclm-2015-0608
15. Sonntag O. Dry chemistry analysis with carrier-bound reagents. In: Van der Vliet PC, ed. *Laboratory Techniques in Biochemistry and Molecular Biology*. Vol 25. London, UK: Elsevier; 1993:57–59.

The importance of the trisomy 21 local cutoff value evaluation for prenatal screening in the second trimester of pregnancy

Yiming Chen, MBBS^{1,2,*}, Yijie Chen, MD^{2,*}, Long Sun, MD³, Liyao Li, MM¹, Wenwen Ning, MM, MS²

¹Departments of Prenatal Diagnosis and Screening Center and ³Clinical Laboratory, Hangzhou Women's Hospital (Hangzhou Maternity and Child Health Care Hospital), Hangzhou, China, ²Department of the Fourth School of Clinical Medical, Zhejiang Chinese Medical University, Hangzhou, China. Corresponding author: Yiming Chen; cxy40344@163.com. *Contributed equally.

Key words: alpha-fetoprotein; free beta subunit of human chorionic gonadotropin; trisomy 21; the local cutoff value; the inline cutoff value; second-trimester

Abbreviations: LCV, local cutoff value; ICV, the inline cutoff value; DS, Down syndrome; ROC, receiver operating characteristic; AFP, alpha-fetoprotein; free β -hCG, free beta human chorionic gonadotropin; uE3, unconjugated estriol; FPR, false-positive rate; MoM, multiple of the median; AUC, area under the curve; SEN, sensitivity; PRs, positive rates; PPV, positive predictive value.

Laboratory Medicine 2023;54:603-607; <https://doi.org/10.1093/labmed/lmad015>

ABSTRACT

Objective: The aim of this work was to compare different local cutoff values (LCV) and inline cutoff values (ICV) in pregnant women in the second trimester at high risk for carrying fetuses with trisomy 21.

Methods: This retrospective cohort study analyzed prenatal screening outcomes in pregnant women ($n = 311,561$). The receiver operating characteristic curve was used to evaluate the diagnostic significance of the trisomy 21 risk value, alpha-fetoprotein, and free beta human chorionic gonadotropin multiple of the median for predicting trisomy 21 risk. The cutoff value corresponding to the maximal Youden index was taken as the LCV. The screening efficiency of both cutoff values was compared.

Results: The LCV cutoff value was lower than the ICV cutoff value (1/643 vs 1/270). The sensitivity increased by 19.80%, the positive predictive value decreased by 0.20%, and the false-positive rate increased by 6.50%.

Conclusion: The LCV should be used to determine trisomy 21 risk, which can increase the detection rate of trisomy 21 in the second trimester.

Aneuploidy is the presence or the absence of one or more extra chromosomes.¹ Persons who have an extra chromosome 21 are diagnosed with Down syndrome (DS), one of the most common fetal chromosomal abnormalities, with a prevalence of approximately 1/800 to 1/600 live births.² Most individuals with trisomy 21 cannot take care of themselves due to severe mental and physical disabilities. The risk of a pregnant woman giving birth to a newborn with trisomy 21 increases from 1/1480 at 20 years of maternal age to 1/85 at 40 years of maternal age. As there is no treatment for trisomy 21, individuals with DS can create serious economic burdens on families and health care systems. As such, all pregnant women should undergo prenatal screening and counseling,³⁻⁵ which can help patients and families decide whether or not to continue the pregnancy. Furthermore, counseling should be nondirective in nature, and clinicians should support patients and families, regardless of the decision that is made.⁶

Comprehensive indicator screening between 10 and 13 weeks of gestation can detect approximately 82% to 87% of fetuses with trisomy 21, whereas screening between 15 and 21 weeks of gestation can detect approximately 81% of fetuses with the abnormality. The positive detection rate of trisomy 21 is higher in women in early pregnancy that underwent serum panel testing or integrated screening (ie, ultrasound combined with serum panel testing) than that in women that underwent single biomarker testing.⁷ Noninvasive prenatal testing, a high-performance screening approach for determining trisomy 21 risk with a detection rate of 99%, can be used initially or subsequently in the follow-up of abnormal results in the first or second trimester of pregnancy.⁸ Diagnostic testing to confirm positive results includes chorionic villus sampling at 10 to 13 weeks of gestation or amniocentesis after 15 weeks of gestation.⁷ Triple screening of serum indicators, namely, alpha-fetoprotein (AFP), free beta human chorionic gonadotropin (free β -hCG), and unconjugated estriol (uE3), is routinely carried out in pregnant women in the second trimester, which usually yields the lowest positive detection rate and the highest false-positive rate (FPR). Another advantage of triple screening is that it can detect neural tube defects when screening for trisomy 21 and 18.^{9,10}

Presently, there is no agreement on the cutoff value for predicting trisomy 21 risk in the second trimester of pregnancy. The cutoff value is 1/250 in France and Finland,^{11,12} 1/300 in the UK and Germany,^{13,14} and 1/270 in China and other Asian countries.^{15,16} As such, it is important to establish the trisomy 21 cutoff value in prenatal screening.

The aim of our study was to explore the diagnostic significance of the local cutoff value (LCV) in dual-marker prenatal screening of trisomy 21 in the second trimester. This retrospective cohort study analyzed 311,561 young pregnant women, including 136 cases of trisomy 21, and compared the diagnostic significance of the LCV with the inline cutoff value (ICV) for predicting trisomy 21 risk.

Materials and Methods

Participants

This was a retrospective study of young women undergoing routine second trimester aneuploidy screenings (15 to 20 weeks and 6 days of gestation) at 48 prenatal health community centers in Hangzhou Women's Hospital (Hangzhou Maternity and Child Health Care Hospital) China, from January 2015 to October 2019. There were 136 pregnant women carrying fetuses with trisomy 21, including high-risk and low-risk cases, and 311,425 pregnant women carrying healthy fetuses. The fetuses with trisomy 21 were diagnosed according to results of karyotype analysis of amniotic fluid cells and ultrasound examinations.

Inclusion and Exclusion Criteria

The inclusion criteria were as follows: pregnant women at 15 to 20 weeks and 6 days of gestation, with a singleton pregnancy, voluntarily undergoing prenatal screening for determining trisomy 21 risk in the second trimester. The exclusion criteria were as follows: patients with a history of smoking, diabetes mellitus, chromosomal abnormalities and congenital malformations, pregnancy complications or other related conditions, fetuses conceived in vitro, or plural gestations. This study was approved by the Medical Ethics Committee of Hangzhou Women's Hospital [2021] Medical Ethics Review A (3) - 02.

Reagents and Instruments

The 1235 Automatic Immunoassay System (Perkin Elmer) and double labeling kit (AFP/free β -hCG, catalog number 644147, Wallac Oy) were used in this study.

Detection Methods

Materials and Test Indicators

Fasting venous blood (2–3 mL) was collected from pregnant women at 15 to 20 weeks and 6 days of gestation. Serum specimens were stored in a refrigerator at 2°C to 8°C and transported to the Prenatal Screening Laboratory of Hangzhou Women's Hospital (Hangzhou Maternity and Child Health Hospital) within 1 week from collection.

MoM Calculation

AFP and free β -hCG were expressed as the multiple of the median (MoM) for variables, such as gestational age and maternal weight, as previously reported.¹⁷

Quality Control

Quality control serum specimens (catalog number 39180; Bio-Rad) were classified as low value, medium value, or high value. The certificate of

conformity, which describes the activities organized by the Clinical Laboratory Center of the National Health Commission of China 3 times a year, was obtained. All personnel received training and obtained certification from the relevant health authorities before the start of testing and analysis.

Inline Cutoff Value

Life Cycle 4.0 software (Wallac Oy) was used to calculate the ICV of trisomy 21 after adjusting for maternal age, maternal weight, and gestational age at testing. If the trisomy 21 risk value was $\geq 1:270$, then the fetus was at high risk of trisomy 21, with all other values indicating that the fetus was at low risk of the abnormality.¹⁸ According to the ROC, the cutoff value corresponding to the maximal Youden index was taken as the LCV with the largest area under the curve (AUC) and the best screening efficacy.

Prenatal Diagnosis

Pregnant women underwent ultrasound-guided amniocentesis at 17 to 20 weeks of gestation after providing written informed consent. In brief, the amniotic tank was positioned and <30 mL of amniotic fluid was collected by puncture through the abdomen with a 20-gauge needle and transferred to a sterile centrifuge tube. Specimens were centrifuged at 2500 rpm for 10 min. Cells were resuspended in medium and cultured in an incubator at 37°C with 5% CO₂, and cell proliferation was observed. Thirty mitotic phases were counted under a microscope, and 5 karyotypes were analyzed. Additionally, chromosomal G-banding and karyotype analyses were performed according to the International Nomenclature System of Human Genetics. The number of abnormal karyotypes was increased, adding C and N banding, if necessary.¹⁹

Data Analysis

IBM SPSS 24.0 software (IBM Corp) was used for statistical analysis. The one-sample Kolmogorov-Smirnov test was used to assess the normality. The maternal age, gestational age at testing, and maternal weight in the second trimester of pregnancy were expressed as percentiles [M (P_{2.5}, P_{97.5})]. Skewed data were compared within or between groups using the Mann-Whitney *U* test. The positive rates (PRs) of the 2 methods were compared using the χ^2 test. To assess the diagnostic significance of AFP MoM and free β -hCG MoM, as well as the trisomy 21 risk calculation, cutoff values and AUCs were determined using receiver operator characteristic (ROC) curves. The sensitivity (SEN) and the FPR were used to evaluate the efficacy of trisomy 21 screening. The SEN was calculated as follows: number of true positives/(number of true positives + number of false negatives) \times 100%. The FPR was calculated as follows: number of false positives/(number of true negatives + number of false positives) \times 100% \div number of gold standard. *P* < .05 was considered statistically significant.

Results

Comparison of Patient Characteristics

The maternal age at testing in the second trimester was significantly higher in the trisomy 21 group than in the control group (*Z* = 9.470, *P* < .001), whereas the gestational age at testing was lower in the trisomy 21 group than in the control group (*Z* = 2.579, *P* = 0.010). No significant difference in the maternal weight between the groups was noted (*P* > 0.05) (TABLE 1).

TABLE 1. Comparison of Clinical Data Between the Control and the Trisomy 21 Group^a

Variable	Control (n = 311,425)	Trisomy 21 (n = 136)	Z	P
Maternal age (y)	28.80 (21.62–37.61)	33.34 (23.43–44.35)	9.470	<.001
Maternal weight (kg)	55.00 (43.00–75.00)	55.10 (45.00–75.00)	0.745	.456
Gestational age (d)	118.00 (109.00–133.00)	117.00 (109.00–131.00)	2.579	.010
Trisomy 21 risk value	1/4377 (1/121–1/68176)	1/132 (1/5–1/7983)	16.422	<.001
Trisomy 18 risk value	1/56,383 (1/2303–1/100,000)	1/18,498 (1/442–1/100,000)	7.820	<.001
AFP MoM	0.98 (0.54–1.86)	0.73 (0.40–1.51)	9.310	<.001
Free β -hCG MoM	0.99 (0.33–3.62)	2.23 (0.44–12.64)	11.994	<.001

AFP, alpha-fetoprotein; free β -hCG, free beta subunit of human chorionic gonadotropin; MoM, multiple of the median.

^aData are presented as median ($P_{2.5}$ – $P_{97.5}$).

TABLE 2. Diagnostic Significance of the Trisomy 21 Risk Value, AFP MoM, and Free β -hCG MoM for Predicting Trisomy 21 Risk

Screening Indicator	AUC	95% CI	P	SEN	SPE	Youden Index	LCV Cutoff	High Risk (n)	PR	ICV Cutoff	High Risk (n)	PR	χ^2	P
Trisomy 21 risk value	0.907	0.878–0.935	<.001	0.816	0.880	0.697	1/643	37357	0.120	1/270	17171	0.055	8189.394	<.001
AFP MoM	0.730	0.683–0.778	<.001	0.559	0.819	0.378	0.75	56419	0.181	0.50	4781	0.015	48315.275	<.001
Free β -hCG MoM	0.797	0.755–0.839	<.001	0.713	0.774	0.488	1.56	70370	0.226	2.50	22798	0.073	28560.839	<.001

AFP, alpha-fetoprotein; free β -hCG, free beta subunit of human chorionic gonadotropin; ICV, inline cutoff value; LCV, local cutoff value; MoM, multiple of the median; PR, positive rate; SEN, sensitivity; SPE, specificity.

Determination of the Trisomy 21 Risk Value, AFP MoM, and Free β -hCG MoM

The trisomy 21 risk value (1/132) was significantly higher in the trisomy 21 group than in the control group ($Z = 16.442$, $P < .001$), whereas the trisomy 18 risk value (1/18498) was significantly higher in the trisomy 21 group than in the control group ($Z = 7.820$, $P < .001$). The AFP MoM was 0.73 in the trisomy 21 group, which was significantly lower than in the control group (0.98, $Z = 9.310$, $P < .001$). The free β -hCG MoM was 2.23 in the trisomy 21 group, which was significantly higher than in the control group (0.99, $Z = 11.994$, $P < .001$) (TABLE 1).

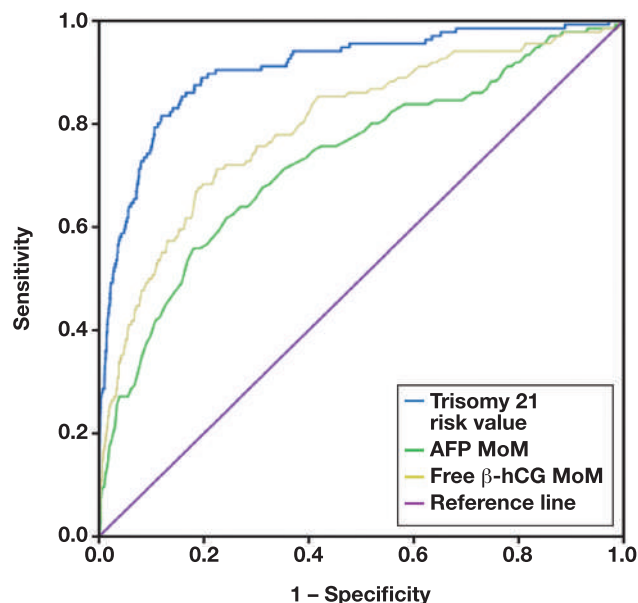
Diagnostic Value of the Trisomy 21 Risk Value, AFP MoM, and Free β -hCG MoM for Predicting Trisomy 21 Risk Using Local and Inline Cutoff Values

The LCV for predicting trisomy 21 risk, the AUC, the cutoff value and SEN of the trisomy 21 risk calculation, AFP MoM, and free β -hCG MoM were 0.907, 1/643 and 0.816; 0.730, 0.75 MoM and 0.559; 0.797, 1.56 MoM and 0.713, respectively (TABLE 2 and FIGURE 1).

The PRs of the LCVs for predicting the trisomy 21 risk value, AFP MoM, and free β -hCG MoM were all higher than those of the ICVs (0.120, 0.181, and 0.226 vs 0.055, 0.015, and 0.073, respectively), and differences were statistically significant ($\chi^2 = 8189.394$, $\chi^2 = 48315.275$, and $\chi^2 = 28560.839$, all $P < .001$) (TABLE 2). The LCV cutoff value was lower than the ICV cutoff value (1/643 vs 1/270), whereas the SEN increased by 19.80% (0.816 vs 0.618), the positive predictive value (PPV) decreased by 0.20% (0.005 vs 0.003), and the FPR increased by 6.50% (0.120 vs 0.055) (TABLE 3).

Discussion

The main findings of our study were as follows: differences in the trisomy 21 risk value, AFP MoM, and free β -hCG MoM between trisomy 21 and control groups were statistically significant ($P < .001$), and the PRs of the LCVs for predicting the trisomy 21 risk value, AFP MoM, and

FIGURE 1. Receiver operating characteristic curve for predicting trisomy 21 risk. AFP, alpha-fetoprotein; free β -hCG, free beta subunit of human chorionic gonadotropin; MoM, multiple of the median.

free β -hCG MoM were all higher than the PRs of the respective ICVs ($P < .001$). The LCV cutoff value was 1/643, the SEN increased by 19.80% (0.816 vs 0.618), the PPV decreased by 0.20% (0.005 vs 0.003), and the FPR increased by 6.50% (0.120 vs 0.055), which was lower than the ICV cutoff value (1/270).

Prenatal screening, a safe, simple, and economical approach used in prenatal health centers worldwide, is critical in pregnant women at risk for carrying fetuses with congenital defects such as trisomy 21. In Europe, the prevalence of trisomy 21 is 22/10,000.²⁰ Our study

TABLE 3. Diagnostic Significance of LCV and ICV for Predicting Trisomy 21 Risk

Screening Model	Cutoff	SEN	SPE	PPV	NPV	FPR	FNR
ICV	1/270	0.618	0.945	0.005	1.000	0.055	0.382
LCV	1/643	0.816	0.88	0.003	1.000	0.120	0.184

FNR, false negative rate; FPR, false positive rate; ICV, inline cutoff value; LCV, local cutoff value; NPV, negative predictive value; PPV, positive predictive value; SEN, sensitivity; SPE, specificity.

shows statistically significant differences in the PRs of cutoff values for predicting trisomy 21 risk. We wanted to understand whether LCV is suitable in the local laboratory and the prenatal screen value of LCV for trisomy 21 fetuses. In our study, LCV reduced the misdiagnosis rate compared with ICV and improved the detection rate. Furthermore, our results showed that the AUC of the trisomy 21 risk value was higher than that of AFP MoM and free β -hCG MoM alone (0.907 vs 0.704 and 0.797). The SEN of the trisomy 21 risk value was 0.816, which was higher than that of AFP MoM (0.559) and free β -hCG MoM (0.713), consistent with previous studies.²¹ Liu et al²¹ demonstrated that the AUC of AFP MoM + free β -hCG MoM was 0.748 (95% CI: 0.635–0.860), whereas Guo et al²² illustrated that the AUC of the trisomy 21 risk value was 0.935 (95% CI: 0.879–0.991), indicating that the screening efficacy of AFP MoM + free β -hCG MoM was better than that of AFP MoM and free β -hCG MoM alone. Guo et al²² also reported that when the FPR was 0.047, the cutoff value and the SEN were 1/265 and 0.778, respectively. However, when the FPR was 0.223, the cutoff value and the SEN were 1/1000 and 0.889.

Hwa et al²³ showed that when the FPR was 0.178, the cutoff value of the ROC was 1/499 and the SEN was 0.900. However, when the FPR was 0.120, the cutoff value was 1/332 and the SEN was 0.800.^{23, 24} In our study, the PRs of the LCVs for predicting the trisomy 21 risk value, AFP MoM, and free β -hCG MoM were all higher than those of the respective ICVs.

As such, a reasonable FPR is key to determining the cutoff value. However, our results illustrated that trisomy 21 risk value, AFP MoM, and free β -hCG MoM were variable with different FPRs. Therefore, the LCV should be used to determine the trisomy 21 risk in different settings. In addition, we acknowledge the limitations of our study. First, there were only 136 cases of trisomy 21 among 311,561 pregnant women. Although the incidence of trisomy 21 in our study was too low to bias the results, compared with the prevalence of 1/800 to 1/600 fetuses, additional studies with a larger population of trisomy 21 cases are needed. Second, the FPR increased by 6.50% (0.120 vs 0.055) compared with the previous screening (3% to 5%), and the former required the next prenatal diagnosis. Finally, from 2015 to 2019, the local medical system in China only paid for AFP and free β -hCG double screening; uE3 is not included in medical insurance. Therefore, this study only uses data from double screening instead of a AFP, free β -hCG, and uE3 triple screening.

In summary, prenatal health centers should use LCV to determine the trisomy 21 risk in the second trimester of pregnancy, which can reduce the misdiagnosis rate, increase the detection rate, and eliminate unnecessary interventions, thereby increasing the efficacy of prenatal screening.

Acknowledgments

The authors are grateful to all participants and contributors. We thank Songhe Chen from Hangzhou Women's Hospital for assistance in

collecting the data. We also thank Xiao Lu and Shaolei Lv of the Data Analysis Department of Zhejiang Biosan Biochemical Technologies for their contribution to data matching and model building. We also thank International Science Editing (<http://www.internationalscienceediting.com>) for editing this manuscript. The datasets used and/or analyzed during the current study are available from the corresponding author on reasonable request.

Funding

This study was supported by The Joint Fund Project of Zhejiang Provincial Natural Science Foundation of China under Grant No. LB23H200009.

Conflicting of Interest Disclosure

The authors have nothing to disclose.

REFERENCES

- Chitayat D, Langlois S, Wilson RD. No. 261-Prenatal screening for fetal aneuploidy in singleton pregnancies. *J Obstet Gynaecol Can*. 2017;39(9):e380–e394.
- The American College of Obstetricians and Gynecologists' Committee on Practice Bulletins—Obstetrics, Committee on Genetics, and the Society for Maternal–Fetal Medicine, Nancy CR, Brian MM. Practice bulletin No. 163 summary: screening for fetal aneuploidy. *Obstet Gynecol*. 2016;127(5):979–981.
- Webster A, Schuh M. Mechanisms of aneuploidy in human eggs. *Trends Cell Biol*. 2017;27(1):55–68.
- Li T, Zhao H, Han X, et al. The spontaneous differentiation and chromosome loss in iPSCs of human trisomy 18 syndrome. *Cell Death Dis*. 2017;8(10):e3149.
- Wang S, Hassold T, Hunt P, et al. Inefficient crossover maturation underlies elevated aneuploidy in human female meiosis. *Cell*. 2017;168(6):977–989.
- Johnston J, Farrell RM, Parens E. Supporting women's autonomy in prenatal testing. *N Engl J Med*. 2017;377(6):505–507.
- LeFevre NM, Sundermeyer RL. Fetal aneuploidy: screening and diagnostic testing. *Am Fam Physician*. 2020;101(8):481–488.
- Cheng Y, Leung WC, Leung TY, et al. Women's preference for non-invasive prenatal DNA testing versus chromosomal microarray after screening for Down syndrome: a prospective study. *BJOG*. 2018;25(4):451–459.
- Metcalfe A, Hippman C, Pastuck M, Johnson JA. Beyond trisomy 21: additional chromosomal anomalies detected through routine aneuploidy screening. *J Clin Med*. 2014;3(2):388–415.
- Palomaki GE, Bupp C, Gregg AR, Norton ME, Oglesbee D, Best RG. Laboratory screening and diagnosis of open neural tube defects, 2019 revision: a technical standard of the American College of Medical Genetics and Genomics (ACMG). *Genet Med*. 2020;22(3):462–474.
- Royère D. The impact of introducing combined first-trimester trisomy 21 screening in the French population. *Eur J Public Health*. 2016;26(3):492–497.

12. Peuhkurinen S, Laitinen P, Honkasalo T, Ryyanen M, Marttala J. Comparison of combined, biochemical and nuchal translucency screening for Down syndrome in first trimester in Northern Finland. *Acta Obstet Gyn Scan.* 2013;92(7):769–774.
13. Snijders RJ, Noble P, Sebire N, Souka A, Nicolaides KH. UK multicentre project on assessment of risk of trisomy 21 by maternal age and fetal nuchal-translucency thickness at 10–14 weeks of gestation. Fetal medicine foundation first trimester screening group. *Lancet (London).* 1998;352(9125):343–346.
14. Hörmansdörfer C, Scharf A, Golatta M, et al. Comparison of prenatal risk calculation (PRC) with PIA fetal database software in first-trimester screening for fetal aneuploidy. *Ultrasound Obstet Gynecol.* 2009;33(2):147–151.
15. Lan RY, Chou CT, Wang PH, Chen RC, Hsiao CH. Trisomy 21 screening based on first and second trimester in a Taiwanese population. *Taiwan J Obstet Gynecol.* 2018;57(4):551–554.
16. Shaw SW, Lin SY, Lin CH, et al. Second-trimester maternal serum quadruple test for Down syndrome screening: a Taiwanese population-based study. *Taiwan J Obstet Gynecol.* 2010;49(1):30–34.
17. Bock JL. Current issues in maternal serum alpha-fetoprotein screening. *Am J Clin Pathol.* 1992;97(4):541–554.
18. Huang T, Alberman E, Wald N, Summers AM. Triploidy identified through second-trimester serum screening. *Prenatal Diag.* 2005;25(3):229–233.
19. Ordulu Z, Wong KE, Currall BB, Ivanov AR, Pereira S, Althari S, Gusella JF, Talkowski ME. Describing sequencing results of structural chromosome rearrangements with a suggested next-generation cytogenetic nomenclature. *Am J Hum Genet.* 2014;94(5):695–709.
20. Loane M, Morris JK, Addor MC, et al. Twenty-year trends in the prevalence of Down syndrome and other trisomies in Europe: impact of maternal age and prenatal screening. *Eur. J. Hum. Genet.* 2013;21(1):27–33.
21. Liu F, Liang H, Jiang X, et al. Second trimester prenatal screening for Down's syndrome in mainland Chinese subjects using double-marker analysis of α -fetoprotein and β -human chorionic gonadotropin combined with measurement of nuchal fold thickness. *Ann Acad Med Singap.* 2011;40(7):315–318.
22. Guo F, Xiao KC, Lin LH, et al. Assessment of risk cut-off values for Down syndrome screening in midtrimester. *Chin J Eugen Genet.* 2014;22(02):50–51.
23. Hwa HL, Ko TM, Hsieh FJ, Yen MF, Chou KP, Chen TH. Risk prediction for Down's syndrome in young pregnant women using maternal serum biomarkers: determination of cutoff risk from receiver operating characteristic curve analysis. *J Eval Clin Pract.* 2007;13(2):254–258.
24. Yu D Y, Fu P, Zhang Z H, et al. Evaluation of Down's syndrome screening methods using maternal serum biochemistry in the second trimester pregnancy. *Zhonghua Yi Xue Yi Chuan Xue Za Zhi.* 2011;28(3):332–335.

Serum aspartate aminotransferase is an adverse prognostic indicator for patients with resectable pancreatic ductal adenocarcinoma

Meifang He, MD^{1,2,*}, Yin Liu, MS^{1,*}, Hefei Huang, MS¹, Jiali Wu, MS¹, Juehui Wu, MS¹, Ruizhi Wang, MD¹, Dong Wang, MD¹

¹Division of Laboratory Medicine and ²Laboratory of General Surgery, the First Affiliated Hospital of Sun Yat-sen University, Guangzhou, China. Corresponding author: Dong Wang; cwdong@mail.sysu.edu.cn. *Contributed equally.

Key words: aspartate aminotransferase; prognosis; overall survival; nomogram; TNM stage; pancreatic ductal adenocarcinoma

Abbreviations: OS, overall survival; ALT, alanine aminotransferase; AST, aspartate aminotransferase; PDAC, pancreatic ductal adenocarcinoma; GGT, γ -glutamyltransferase; ALP, alkaline phosphatase; LDH, lactate dehydrogenase; HR, hazard ratio

Laboratory Medicine 2023;54:608-612; <https://doi.org/10.1093/labmed/lmad014>

ABSTRACT

Objective: In this study, the association between preoperative levels of serum liver enzymes and overall survival (OS) was evaluated in patients with resectable pancreatic cancer.

Methods: Preoperative serum levels of alanine aminotransferase (ALT), aspartate aminotransferase (AST), γ -glutamyltransferase, alkaline phosphatase, and lactate dehydrogenase of 101 patients with pancreatic ductal adenocarcinoma (PDAC) were collected. Univariate and multivariate Cox hazard models were used to identify independent variables associated with OS in this cohort.

Results: Patients with elevated AST levels had significantly worse OS than patients with lower AST levels. A nomogram was created using TNM staging and AST levels and was shown to be more accurate in prediction than the American Joint Committee on Cancer 8th edition standard method.

Conclusion: Preoperative AST levels could be a novel independent prognostic biomarker for patients with PDAC. The incorporation of AST levels into a nomogram with TNM staging can be an accurate predictive model for OS in patients with resectable PDAC.

Pancreatic cancer has a high mortality rate and is the fourth leading cause of cancer-related deaths globally, and the incidence has been increasing year after year. Pancreatic ductal adenocarcinoma (PDAC) is the most common type of pancreatic cancer. The 5-year overall survival rate for patients with PDAC is less than 9%, and median survival is less than 1 year.¹ Although 20% to 30% of patients with resectable PDAC receive active therapeutic interventions, postoperation survival periods vary from patient to patient. The median survival among surgically resected cases is less than 2 years, and the 5-year survival rate is only around 20% to 25%.² Therefore, it is imperative to identify biomarkers that facilitate improved disease prognosis for these patients.

As routine clinical indexes, serum levels of liver enzymes, including alanine aminotransferase (ALT), aspartate aminotransferase (AST), γ -glutamyltransferase (GGT), alkaline phosphatase (ALP), and lactate dehydrogenase (LDH), are informative biomarkers of liver injury and predictors of all-cause mortality. Aspartate aminotransferase is a key enzyme of amino acid metabolism that catalyzes the reversible transfer of the amine group from L-aspartate to 2-oxoglutarate. Aspartate aminotransferase is primarily expressed in mitochondria and is present in all tissues except bone, with the highest expression levels in liver and skeletal muscle. When liver cells are damaged, the mitochondria disintegrate, causing AST to be released into the circulation. Aspartate aminotransferase is a specific indicator of abnormal liver function and has prognostic value for different types of hepatitis, cancer, and other diseases.

Recently, it has been reported that liver enzymes might serve as biomarkers for prognostic monitoring and recurrence in different cancers, including metastatic colorectal cancer,³ metastatic breast cancer,⁴ advanced urothelial carcinoma,⁵⁻⁸ and advanced PDAC.^{9,10} Serum levels of GGT, LDH, ALP, and ALT have been shown to be independent prognostic indicators of advanced PDAC,¹⁰⁻¹³ and preoperative serum levels of LDH and ALP have been identified as independent prognostic factors for disease-free survival and overall survival for patients with resectable PDAC.¹⁴ Nevertheless, the contributions of other liver enzymes, such as ALT and AST, to disease prognosis for patients with resectable PDAC have yet to be established.⁹ Therefore, the relationship between the serum liver enzymes, including AST and ALT, and prognosis of early stage PDAC merits elucidation.

In this study, we performed a retrospective analysis to explore the feasibility of using serum liver enzymes as prognostic biomarkers to predict patient survival in PDAC. We constructed a prognostic nomogram for

resectable PDAC based on clinicopathological parameters and evaluated whether use of this model resulted in a more accurate prediction of outcome for patients with PDAC.

Materials and Methods

Patients

This study was approved by the Human Research Ethics Committees of the First Affiliated Hospital of Sun Yat-sen University (approval No. [2020]339), in accordance with the Helsinki Declaration.

A total of 101 adult patients diagnosed with PDAC (62 males and 39 females) who underwent curative resection at the First Affiliated Hospital of Sun Yat-sen University from 2003 to 2011 and received standard treatment with no chemotherapy or radiotherapy before or after surgery were enrolled and analyzed retrospectively in this study. Follow-up was based on electronic hospital charts and physician records. In general, patients were followed up every 3 months in the first year, every 6 months for the next 2 years, and annually thereafter. Recurrence was defined as disease recurrence locally or in distant organs. Patients who did not experience recurrence, cancer-specific death, or any-cause death were censored at last follow-up. The inclusion and exclusion criteria were as follows: (1) pathological diagnosis of PDAC; (2) no radiotherapy, chemotherapy, or medication before surgery; (3) complete clinical data and follow-up data present; (4) did not receive any drugs known to affect indicators of liver function or surgery before enrollment; (5) not diagnosed with liver disease, cardiovascular disease, diabetes, or metabolic syndrome; (6) no history or concurrence of other cancers; and (7) no concurrence of other severe diseases. Routine clinic data including sex, age, tumor size, histological differentiation, and TNM stage were collected from patient records.

Laboratory Measurements

Serum biochemical tests were performed on the first visit to the hospital. Blood was collected between 7 AM and 8 AM and centrifuged at 3500 rpm for 5 minutes to collect serum samples. The serum levels of ALT, AST, GGT, ALP, and LDH were evaluated by enzyme method (such as the malate dehydrogenase method for AST and LDH method for ALT) on an AU5800 automated analyzer (Beckman Coulter) and the corollary reagents. Accuracy and precision of all methods were performed in accordance with the relevant guidelines and regulations.

Statistical Analysis

Statistical analyses were performed by SPSS software version 22 (IBM). Overall survival was calculated from the date of tumor resection to the time of death. Patients who were lost to follow-up or died from causes unrelated to PDAC were treated as censored events. Cox proportional-hazard regression model was used for univariate and multivariate analysis. Significant prognostic factors identified by univariate analysis were further evaluated by multivariate Cox regression analysis. Survival curves were plotted using the Kaplan-Meier method, and differences between survival curves were analyzed using the log rank test. The χ^2 test was used to analyze the correlation between AST and clinical characteristics. The prognostic nomogram was performed using the R package. The predictive performance of the prognostic nomogram was assessed by C-index and receiver operating characteristic curve for overall survival (OS). All

statistical tests were 2-sided, and a *P* value of $\leq .05$ was considered to be statistically significant.

Results

Clinical Pathological Characteristics

A cohort of 101 patients with pathologically confirmed PDAC was enrolled in this study. Patient characteristics are listed in **TABLE 1**. There were 62 males and 39 females with an average age of 59.5 years. The median follow-up time was 32 months with a range from 1 to 56 months. Regarding tumor differentiation, 25 patients had tumors with poor differentiation and 76 patients had tumors with moderate or well-defined differentiation. The number of patients diagnosed at stage I-II and III-IV were 66 (65.3%) and 35 (34.7%), respectively.

Prognostic Significance of AST in PDAC

The clinical data above and levels of serum liver enzymes (ALT, AST, ALP, GGT, and LDH) were included in Cox regression analysis for evaluation of OS. Univariate analysis indicated that higher levels of ALT (hazard

TABLE 1. Baseline Characteristics in Patients with PDAC

Characteristic	No. of Cases (%)
Sex	101
Male	62 (61.4)
Female	39 (38.6)
Age, y	101
≤60	47 (46.5)
>60	54 (53.5)
Tumor size, cm	101
≤2	14 (13.9)
>2	87 (86.1)
Differentiation	101
Poor	25 (24.8)
Moderate/well	76 (75.2)
TNM stage	101
I-II	66 (65.3)
III-IV	35 (34.7)
Lymphatic spread	101
Yes	37 (36.6)
No	64 (63.4)
Metastasis	101
Yes	14 (13.9)
No	87 (86.1)
CEA, μg/L	94
≤3.1	46 (48.9)
>3.1	48 (51.1)
CA125, U/mL	87
≤19.5	49 (56.3)
>19.5	38 (43.7)
CA199, U/mL	95
≤371.5	55 (57.9)
>371.5	40 (42.1)

ratio [HR]: 1.002, 95% CI = 1.001–1.004, $P = .007$) and AST (HR: 1.003, 95% CI = 1.001–1.005, $P = .003$) were significantly associated with higher mortality in PDAC patients (TABLE 2). Variables with $P < .05$ in the univariate analysis were further evaluated in multivariate analysis to

TABLE 2. Univariate and Multivariate Analysis of Factors Associated with OS^a

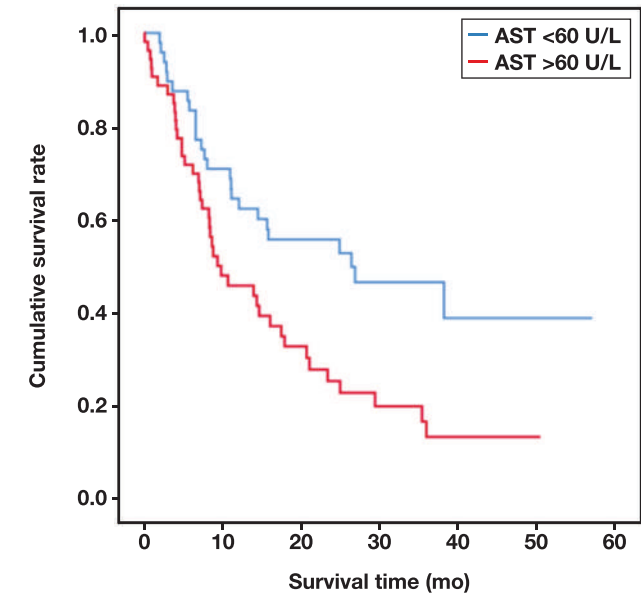
Clinical variables	No. of cases	HR (95% CI) ^b	P value ^b
Univariate analysis			
Sex (M vs F)	62/39	1.211 (0.733–2.002)	.455
Age (>60 y vs ≤60 y)	54/47	1.497 (0.811–2.761)	.197
Tumor size (>3 cm vs ≤3 cm)	87/14	1.031 (0.745–1.426)	.853
Differentiation (poor vs well and moderate)	25/86	1.409 (1.090–1.823)	.009
TNM stage (III/IV vs I/II)	45/66	1.344 (1.052–1.715)	.018
Lymphatic spread (yes vs no)	30/71	1.304 (1.020–1.667)	.034
Metastasis (yes vs no)	40/61	1.425 (1.050–1.934)	.023
Serum ALT	NA	1.002 (1.001–1.004)	.007
Serum AST	NA	1.003 (1.001–1.005)	.003
Serum GGT	NA	1.000 (1.000–1.001)	.519
Serum ALP	NA	1.001 (1.000–1.002)	.177
Serum LDH	NA	1.002 (1.000–1.005)	.065
Multivariate analysis			
TNM stage (III/IV vs I/II)	45/66	1.736 (1.064–2.833)	.027
Serum AST	NA	1.003 (1.001–1.005)	.005

ALP, alkaline phosphatase; ALT, alanine aminotransferase; AST, aspartate aminotransferase; GGT, γ -glutamyltransferase; LDH, lactate dehydrogenase; NA, not applicable; OS, overall survival; PDAC, pancreatic ductal adenocarcinoma.

^aAnalysis was conducted on 101 cases.

^bHR (hazard ratio) and P values were calculated using univariate or multivariate Cox proportional hazards regression. P values < .05 are shown in bold.

FIGURE 1. Overall survival curve of patients with pancreatic ductal adenocarcinoma according to aspartate aminotransferase (AST) levels ($P = .005$). Kaplan-Meier survival curves indicated that higher AST level was significantly related to shorter survival.



exclude the confounder effect, confirming that TNM stage (HR: 1.736, 95% CI = 1.064–2.833, $P = .027$) and AST (HR: 1.003, 95% CI = 1.001–1.005, $P = .005$) were independent predictors for OS. These data suggest that serum AST levels are a reliable prognostic indicator for PDAC.

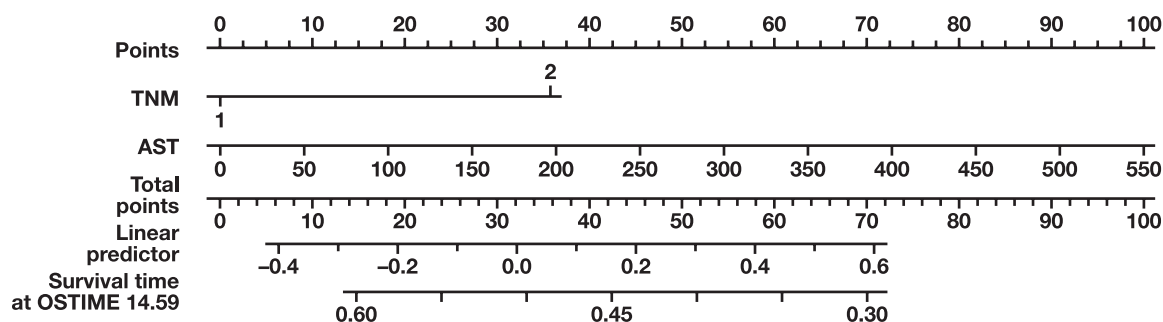
TABLE 3. Relationship between AST Levels and Clinical Characteristics in Patients with PDAC

Variable	AST (U/L)		Total cases	P value ^a
	≤60	>60		
Sex				
Male	28	34	62	.683
Female	20	19	39	
Age, y				
≤60	24	23	47	.553
>60	24	30	54	
Tumor size, cm				
≤2	5	9	14	.398
>2	43	44	87	
Differentiation				
Poor	7	15	22	.147
Moderate/well	41	38	79	
TNM stage				
I–II	31	35	66	1.000
III–IV	17	18	35	
Lymphatic spread				
Yes	12	25	37	.024
No	36	28	64	
Metastasis				
Yes	11	15	26	.650
No	37	38	75	
CEA, μg/L				
≤3.1	23	23	46	.680
>3.1	21	27	48	
CA125, U/mL				
≤19.5	20	29	49	.288
>19.5	20	18	38	
CA199, U/mL				
≤371.5	27	28	55	.540
>371.5	17	23	40	
Death				
Yes	25	41	66	.012
No	23	12	35	
ALT	48	53	101	.000
AST	48	53	101	.000
GGT	48	53	101	.000
ALP	48	53	101	.160
LDH	48	53	101	.879

ALP, alkaline phosphatase; ALT, alanine aminotransferase; AST, aspartate aminotransferase; CEA, carcinoembryonic antigen; GGT, γ -glutamyltransferase; LDH, lactate dehydrogenase; PDAC, pancreatic ductal adenocarcinoma.

^aP values of nominal variables and continuous variables were calculated using the χ^2 test and t-test, respectively. P values < .05 are shown in bold.

FIGURE 2. Prognostic nomogram for pancreatic ductal adenocarcinoma (PDAC). The nomogram predicts overall survival (OS) in patients with PDAC. A patient's value for each variable is located on the respective axis; the top axis is used to measure the score of each variable. The sum of these scores is located on the total points axis, and the bottom line is the survival axes to determine the likelihood of 14.59-month OS.



Next, X-tile software was used to determine the optimal cut-off value of 60 U/L AST levels in the Kaplan-Meier survival analysis. Based on this cut-off value, the associations between serum AST levels and clinical pathologic factors in patients were analyzed (TABLE 3). The χ^2 test revealed that higher AST levels (>60 U/L) were associated with histological differentiation ($P = .042$) and death ($P = .006$). Moreover, Kaplan-Meier analysis revealed that higher AST level (>60 U/L) was significantly associated with decreased OS (FIGURE 1). The OS in patients with lower AST levels was 13.8 months longer than in patients with higher AST levels.

Nomogram Construction and Prognostic Value in PDAC

To predict the mortality of patients with PDAC, a prognostic nomogram was constructed using multivariate Cox regression model analysis, which integrated the 2 independent prognostic indicators for OS, AST, and TNM (FIGURE 2). The Harrell's C-index for mortality prediction was 0.802 (95% CI = 0.66–0.82), which was significantly higher than TNM stage alone (0.756). The calibration plot for the probability of mortality demonstrates an optimal agreement between the prediction by nomogram and actual observation.

Discussion

Pretreatment serum AST level and its relative indexes are significantly associated with OS of patients with advanced PDAC.^{9,15} However, the relationship between the pretreatment serum AST levels and survival of patients with resectable early-stage PDAC has not previously been reported. Therefore, the aim of this study was to explore the role of serologic AST levels in disease prognosis for patients with resectable PDAC. Here, we attempted to identify serum liver enzymes that could be informative prognostic indicators for patients with resectable PDAC. We analyzed data from routine blood test results of liver enzymes from 101 patients with PDAC. We used univariate and multivariate analysis to determine that serum AST levels and TNM stage were independent prognostic factors for patients with surgically treated PDAC. We found that higher AST levels are generally associated with shorter survival time. To evaluate the prognostic power of AST, we established a predictive nomogram model for patients with PDAC. The C-index of the nomogram model predicted OS with an accuracy of 0.802 (95% CI, 0.66–0.82). Interestingly, this nomogram displayed improved accuracy compared to the current TNM classification system (C-index = 0.756).

We suggest a potential mechanism for how the established nomogram based on AST can improve prognostic assessment of patients

with PDAC. First, in pancreatic cancer, tumor cells invading the adjacent biliopancreatic ducts obstruct bile and damage hepatocytes, which impairs liver function and contributes to elevated AST levels. In addition, PDAC is usually accompanied by a proinflammatory state. Inflammation is an essential promoter of pancreatic cancer development and is involved in PDAC initiation, progression, and metastasis.^{16,17} A prolonged state of inflammation can cause lasting damage to the pancreas and release AST into the blood. In addition to the release of cellular content caused by tissue damage, AST itself plays a key role in cancer cell metabolism in PDAC. Cancer cells are often adapted to glycolytic metabolism as a principle mode of energy production. In addition, PDAC cancer cells strongly depend on glutamine to supply biomass and energy for cell growth and replication. Aspartate derived from glutamine is transported to the cytoplasm and converted to oxaloacetate by AST (GOT1), which is subsequently converted to malic acid and, finally, pyruvate. Aspartate aminotransferase is an important regulator in this metabolic pathway, which increases the nicotinamide adenine dinucleotide phosphate hydrogen/nicotinamide adenine dinucleotide phosphate ratio and maintains reactive oxygen species balance in PDAC cells.^{18,19}

Prognostic biomarkers are needed to better understand the progression of PDAC and to develop personalized treatment strategies for early stage disease. It is necessary to identify readily assessable and efficient prognostic biomarkers for PDAC. Liver function tests are common laboratory tests, and previous studies have noted the association between AST and the risk of malignancy.^{20–23} Based on the function of AST in PDAC development and the value of serum AST level in prognosis of advanced PDAC,^{9,15} we therefore hypothesized that serum AST levels might also be a prognostic marker for patients with resectable early stage PDAC. Our data confirming that TNM stage and differentiation are significant prognostic factors for PDAC are consistent with other reports.^{24,25} In addition, among the 101 patients in our study cohort, patients with high preoperative serum AST levels had significantly poorer OS than patients with low serum AST levels. This finding suggests a possible prognostic role for AST in predicting survival for patients with resected early-stage PDAC.

The established nomogram based on serum AST levels could predict survival more precisely for patients with resectable PDAC than current methods. However, there are several limitations to this study. First, this was a retrospective study carried out in a single center in China. A large-scale and multicenter prospective study is needed to eliminate selectivity bias and validate the conclusion. Further studies using another dataset to verify this prognostic model may shed more light on

the clinical application of serum AST levels for prognostic prediction in PDAC. Second, the AST cut-off value in this study may not be applicable in other studies, and it may be necessary to determine the most appropriate AST cut-off value through a meta-analysis that includes various AST validated studies. Despite these limitations, this model provides an effective tool for predicting OS of patients with PDAC and can be helpful when making individualized treatment decisions for patients.

In summary, our data indicated that preoperative serum AST levels, but not levels of ALT, LDH, ALP or GGT, are an independent prognostic factor of resectable PDAC. Aspartate aminotransferase is an effective and available serum biomarker and may be a reliable prognostic predictor for survival in patients with resected early-stage PDAC. Compared to the TNM staging system alone, a prognostic monogram composed of serum AST and TNM stage could provide more accurate prognostic prediction for patients with resectable PDAC.

Data Availability

The datasets generated for this study are available on reasonable request to the corresponding author.

Funding

This work was financially supported by the National Natural Science Foundation of China (No. 81972750) to Ruizhi Wang.

Conflict of Interest Disclosure

The authors have nothing to disclose.

REFERENCES

1. Siegel RL, Miller KD, Jemal A. Cancer statistics, 2020. *CA Cancer J Clin*. 2020;70(1):7–30. doi:10.3322/caac.21590.
2. Hackert T, Buchler MW. Pancreatic cancer: advances in treatment, results and limitations. *Dig Dis*. 2013;31(1):51–56. doi:10.1159/000347178.
3. Wei Y, Xu H, Dai J, et al. Prognostic significance of serum lactic acid, lactate dehydrogenase, and albumin levels in patients with metastatic colorectal cancer. *Biomed Res Int*. 2018;2018:1804086. doi:10.1155/2018/1804086.
4. Staudigl C, Concin N, Grimm C, et al. Prognostic relevance of pretherapeutic gamma-glutamyltransferase in patients with primary metastatic breast cancer. *PLoS One*. 2015;10(4):e0125317. doi:10.1371/journal.pone.0125317.
5. Takemura K, Fukushima H, Ito M, et al. Prognostic significance of serum gamma-glutamyltransferase in patients with advanced urothelial carcinoma. *Urol Oncol*. 2019;37(2):108–115. doi:10.1016/j.urolonc.2018.11.002.
6. Lakshmanan M, Kumar V, Chaturvedi A, et al. Role of serum HE4 as a prognostic marker in carcinoma of the ovary. *Indian J Cancer*. 2019;56(3):216–221. doi:10.4103/ijc.IJC_305_18.
7. McCartney A, Biagioni C, Schiavon G, et al. Prognostic role of serum thymidine kinase 1 activity in patients with hormone receptor-positive metastatic breast cancer: analysis of the randomised phase III Evaluation of Faslodex versus Exemestane Clinical Trial (EFFECT). *Eur J Cancer*. 2019;114:55–66. doi:10.1016/j.ejca.2019.04.002.
8. Wan Z, Zhang X, Yu X, Hou Y. Prognostic significance of serum soluble DR5 levels in small-cell lung cancer. *Int J Med Sci*. 2019;16(3):403–408. doi:10.7150/ijms.28814.
9. Riedl JM, Posch F, Prager G, et al. The AST/ALT (De Ritis) ratio predicts clinical outcome in patients with pancreatic cancer treated with first-line nab-paclitaxel and gemcitabine: post hoc analysis of an Austrian multicenter, noninterventional study. *Ther Adv Med Oncol*. 2020;12:1758835919900872. doi:10.1177/1758835919900872.
10. Xiao Y, Lu J, Chang W, et al. Dynamic serum alkaline phosphatase is an indicator of overall survival in pancreatic cancer. *BMC Cancer*. 2019;19(1):785. doi:10.1186/s12885-019-6004-7.
11. Xiao Y, Yang H, Lu J, Li D, Xu C, Risch HA. Serum gamma-glutamyltransferase and the overall survival of metastatic pancreatic cancer. *BMC Cancer*. 2019;19(1):1020. doi:10.1186/s12885-019-6250-8.
12. Xiao Y, Chen W, Xie Z, et al. Prognostic relevance of lactate dehydrogenase in advanced pancreatic ductal adenocarcinoma patients. *BMC Cancer*. 2017;17(1):25. doi:10.1186/s12885-016-3012-8.
13. Deng QL, Dong S, Wang L, et al. Development and validation of a nomogram for predicting survival in patients with advanced pancreatic ductal adenocarcinoma. *Sci Rep*. 2017;7(1):11524. doi:10.1038/s41598-017-11227-8.
14. Ji F, Fu SJ, Guo ZY, et al. Prognostic value of combined preoperative lactate dehydrogenase and alkaline phosphatase levels in patients with resectable pancreatic ductal adenocarcinoma. *Medicine (Baltimore)*. 2016;95(27):e4065e4065. doi:10.1097/md.00000000000004065.
15. Stocken DD, Hassan AB, Altman DG, et al. Modelling prognostic factors in advanced pancreatic cancer. *Br J Cancer*. 2008;99(6):883–893. doi:10.1038/sj.bjc.6604568.
16. Yamada S, Fujii T, Yabusaki N, et al. Clinical implication of inflammation-based prognostic score in pancreatic cancer: Glasgow prognostic score is the most reliable parameter. *Medicine (Baltimore)*. 2016;95(18):e3582e3582. doi:10.1097/md.00000000000003582.
17. Lu H, Ouyang W, Huang C. Inflammation, a key event in cancer development. *Mol Cancer Res*. 2006;4(4):221–233. doi:10.1158/1541-7786.MCR-05-0261.
18. Son J, Lyssiotis CA, Ying H, et al. Glutamine supports pancreatic cancer growth through a KRAS-regulated metabolic pathway. *Nature*. 2013;496(7443):101–105. doi:10.1038/nature12040.
19. Holt MC, Assar Z, Beheshti Zavareh R, et al. Biochemical characterization and structure-based mutational analysis provide insight into the binding and mechanism of action of novel aspartate aminotransferase inhibitors. *Biochemistry*. 2018;57(47):6604–6614. doi:10.1021/acs.biochem.8b00914.
20. Yuk HD, Jeong CW, Kwak C, Kim HH, Ku JH. De Ritis ratio (aspartate transaminase/alanine transaminase) as a significant prognostic factor in patients undergoing radical cystectomy with bladder urothelial carcinoma: a propensity score-matched study. *Dis Markers*. 2019;2019:6702964. doi:10.1155/2019/6702964.
21. Miyake H, Matsushita Y, Watanabe H, et al. Significance of De Ritis (aspartate transaminase/alanine transaminase) ratio as a significant prognostic but not predictive biomarker in Japanese patients with metastatic castration-resistant prostate cancer treated with cabazitaxel. *Anticancer Res*. 2018;38(7):4179–4185. doi:10.21873/anticancer.12711.
22. Kang M, Yu J, Sung HH, et al. Prognostic impact of the pretreatment aspartate transaminase/alanine transaminase ratio in patients treated with first-line systemic tyrosine kinase inhibitor therapy for metastatic renal cell carcinoma. *Int J Urol*. 2018;25(6):596–603. doi:10.1111/iju.13574.
23. Lee H, Lee SE, Byun SS, Kim HH, Kwak C, Hong SK. De Ritis ratio (aspartate transaminase/alanine transaminase ratio) as a significant prognostic factor after surgical treatment in patients with clear-cell localized renal cell carcinoma: a propensity score-matched study. *BJU Int*. 2017;119(2):261–267. doi:10.1111/bju.13545.
24. Imamura T, Yamamoto Y, Sugiura T, et al. The prognostic relevance of the new 8th edition of the Union for International Cancer Control Classification of TNM Staging for ampulla of Vater carcinoma. *Ann Surg Oncol*. 2019;26(6):1639–1648. doi:10.1245/s10434-019-07238-6.
25. Wen S, Zhan B, Feng J, et al. Non-invasively predicting differentiation of pancreatic cancer through comparative serum metabolomic profiling. *BMC Cancer*. 2017;17(1):708. doi:10.1186/s12885-017-3703-9.

Serum expression of tumor marker CA242 in patients with different gynecological diseases

Jing Zhu, BS¹, Huidan Li, PhD²

¹Department of Laboratory Medicine, Jiading Branch of Shanghai General Hospital, Shanghai Jiao Tong University School of Medicine, Shanghai, China,

²Department of Clinical Laboratory, Shanghai General Hospital, Shanghai, China. Corresponding author: Huidan Li; lhdlucky@163.com

Key words: tumor marker; CA242; gynecological diseases; clinical diagnosis

Abbreviations: ROC, receiver operating characteristic; AUC, area under the curve; CIN, cervical intraepithelial neoplasia

Laboratory Medicine 2023;54:613-617; <https://doi.org/10.1093/labmed/lmad017>

ABSTRACT

Objective: The aim of this study was to investigate the serum levels of CA242 in different types of gynecological diseases and its clinical significance.

Methods: A total of 1021 patients with gynecological diseases and 499 healthy female controls were included in the study. The serum CA242 levels were detected and median value, $-\log_{10} P$ value, and positive rate were calculated. Serum CA125 and HE4 levels of patients with ovarian lesions were measured, and the predictive value for ovarian cancer was statistically analyzed.

Results: Higher serum CA242 levels were observed in patients with mature teratoma, ovarian cancer, and other gynecological tumor diseases than in healthy controls. In contrast, the CA242 levels in patients with cervical intraepithelial neoplasia, uterine polyps, or endometrial hyperplasia were comparable to that of controls. Moreover, serum CA242 expression was increased in malignant uterine and ovarian diseases compared with benign ones ($P < .05$). Specifically, combining CA242, CA125, and HE4 yielded a higher area under the receiver operating characteristic curve than single biomarkers ($P < .05$).

Conclusion: Heterogeneous increases in tumor marker CA242 expression levels are observed in different gynecological diseases, suggesting its potential value for clinical diagnosis.

Tumor-associated antigen CA242 is a new sialic acid-containing carbohydrate, present on the cell surface as a glycoprotein/glycolipid or in the

serum as an O-linked enriched glycoprotein (mucin). Elevated CA242 levels have long been used clinically as serological diagnostic markers for intestinal diseases, especially pancreatic cancer.¹⁻³ However, given its high expression in some gynecologic tumors,⁴⁻⁷ an increasing body of evidence suggests that CA242 has significant value as a screening marker for cancer in females.⁸ To the best of our knowledge, few reports have hitherto compared serum CA242 levels in different populations of female tumor and nontumor patients. Therefore, this study sought to analyze serum CA242 levels in female patients with different gynecological diseases and assess its diagnostic value.

Materials and Methods

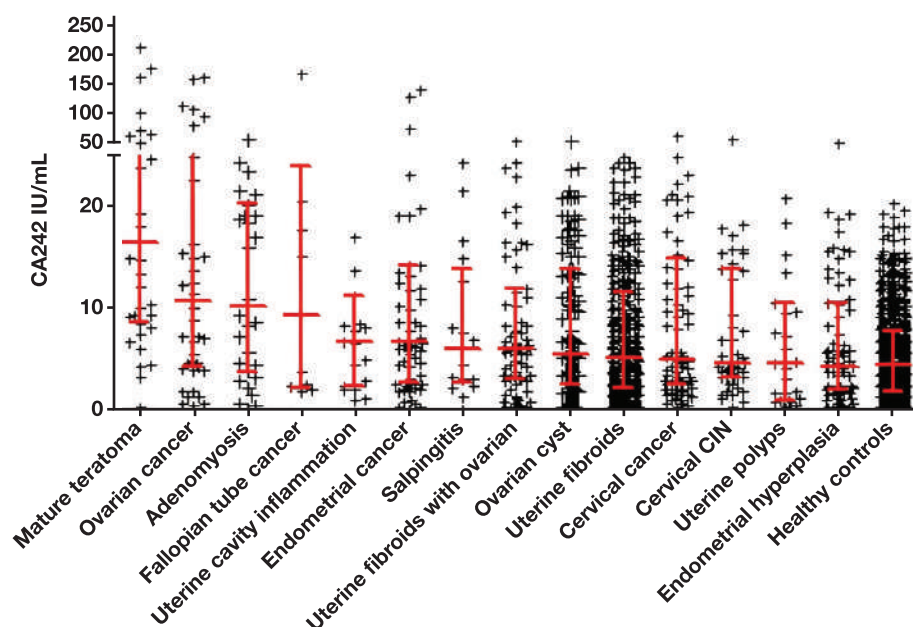
All clinical data were collected from 1371 patients admitted to the gynecological ward of Shanghai General Hospital from March 2019 to November 2019. All patients were informed of the study and agreed to undergo serum CA242 quantitative analysis before diagnosis.

All included tumor patients had newly diagnosed cases and had not received chemotherapy, radiotherapy, or other antitumor treatments. The diagnosis was confirmed by postoperative histopathology. Patients with other benign diseases were confirmed by pathology, imaging, and laboratory examinations. We excluded patients with comorbidities such as autoimmune diseases, mental disorders, severe liver and kidney dysfunction, and other cancers (pancreatic cancer, colorectal cancer, etc). Using these inclusion and exclusion criteria, 1021 patients were enrolled and divided into 14 groups according to the disease type. In addition, 499 healthy females that underwent blood testing during the same period were included in the control group.

All blood samples were collected 1 day after admission. The serum was separated by centrifugation at 3000 rpm for 10 min. The serum CA242 was detected using the Beijing Kemei CHEMCLIN1500 Immunoassay System. The serum CA125 and HE4 in the ovarian cancer group were measured using the Beckman Coulter's Dxl 800 Immunoassay System and the Roche E170 Immunoassay System, respectively. The CA242 reference range was 0 to 25 U/mL, CA125 reference range was 0 to 35 U/mL, and the HE4 reference range was 0 to 140 pmol/L. A finding of CA242 >25 U/mL is regarded as positive.

All data were analyzed by IBM SPSS Statistics for Windows, version 21. The Kolmogorov-Smirnov test was used to test for normality. Because the data were nonnormally distributed, pairwise comparisons between groups were statistically analyzed using the Mann-Whitney U test with $P < .05$ being considered as statistically significant. The $-\log_{10} P$ value was used to compare the difference in P values between diseases. The receiver

FIGURE 1. The expression levels of serum CA242 in 14 different gynecological diseases. The data are sorted in descending order of median value. The concentration of CA242 within the range of lower quartile (25%), median (50%), and upper quartile (75%) in each type are shown.



operating characteristic (ROC) curve was used to calculate the sensitivity and specificity of the biomarkers and determine their diagnostic efficacy.

Results

After statistical analysis of the data, we calculated and listed the median value, $-\log_{10} P$ value, and positive rate of serum CA242 levels in 14 gynecological diseases and healthy controls. The median serum CA242 values were higher in 9 diseases than in healthy controls. The highest median serum CA242 value (16.57 U/mL) was observed in mature teratoma. The median serum CA242 levels were higher in patients with ovarian cancer (10.80 U/mL), adenomyosis (10.25 U/mL), and fallopian tube cancer (9.46 U/mL) than in other gynecological diseases and healthy controls. The median serum CA242 values in patients with cervical intraepithelial neoplasia (CIN) (4.71 U/mL), uterine polyps (4.64 U/mL), and endometrial hyperplasia (4.45 U/mL) did not increase significantly compared with healthy controls (**FIGURE 1**). Among the 4 gynecological malignancies (ovarian, fallopian tube, endometrial, and cervical cancers), the median and positive rates of serum CA242 were higher in fallopian tube and ovarian cancers. In contrast, the median (5.15 U/mL) and the positive rate (8.97%) of serum CA242 in cervical cancer was relatively low (**TABLE 1**).

Compared with healthy controls, the CA242 $-\log_{10} P$ value level heat map of 14 different diseases showed a $-\log_{10} P$ value >1.3 for 9 diseases, suggesting that $-\log_{10} P$ value has a significant diagnostic value for at least 8 gynecological diseases, such as teratoma, ovarian cancer, ovarian cyst, and adenomyosis (**FIGURE 2**).

The highest positive rate was observed in mature teratoma (38.89%) followed by ovarian and endometrial cancers. The positive rates of serum CA242 in ovarian cysts and adenomyosis were also relatively high. In contrast, the positive rate of serum CA242 in uterine fibroids with ovarian cysts (8%) was lower than in ovarian cysts (8.81%) but higher

than in simple uterine fibroids (4.37%). Among them, the positive rates of serum CA242 in CIN, uterine fibroids, endometrial diseases, and uterine polyps were relatively low (**TABLE 1**).

As shown in **TABLE 2**, a comparison of serum CA242 levels between benign and malignant lesions of the same site showed that serum CA242 levels in malignant uterine lesions were higher than in benign lesions. Also, the serum CA242 levels in malignant ovarian lesions were higher than in benign ovarian lesions. There was a significant difference between benign/malignant lesions of the uterus and ovary ($P < .05$).

The area under the ROC curve for the diagnosis of ovarian cancer using CA242, CA125, and HE4 was 0.631 (sensitivity 64.3% and specificity 59.7%), 0.703 (sensitivity 78.6% and specificity 59.1%), and 0.839 (sensitivity 66.7% and specificity 90.6%) (**TABLE 3**), respectively. The area under the ROC curve of the combination of CA125 and CA242 in the diagnosis of ovarian cancer was 0.759 (sensitivity 83.3% and specificity 60.4%), which yielded better diagnostic performance than single biomarkers. The area under the ROC curve of CA125 combined with HE4 for the diagnosis of ovarian cancer was 0.858 (sensitivity 71.4% and specificity 88.7%). When CA242 was added to the above combination, the area under the curve (AUC) was 0.887, yielding a relatively higher sensitivity of 78.6% than CA125 combined with HE4 detection and high specificity of 86.8% (**FIGURE 3**).

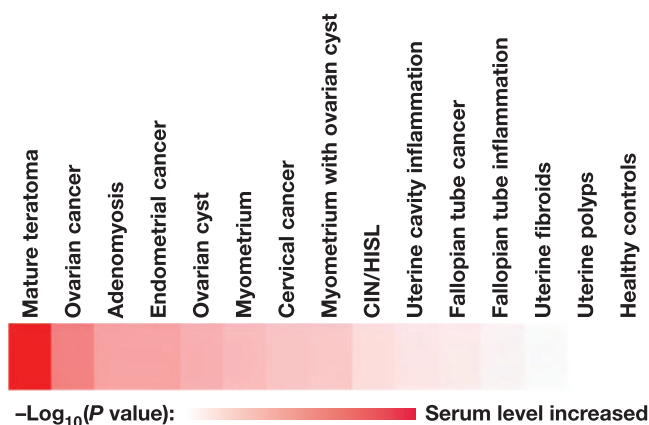
Discussion

In 1985, Lindholm isolated the sialylated glycoprotein CA242 by immunizing mice with the human colorectal cancer cell line COLO205, which has similar antigenic determinant epitopes to CA199 and CA50 both. However, its antigenic determinant structure differs from CA199 and CA50 and cannot react with sialylated galactosides.⁹ With its low expression levels in healthy people and benign diseases,

TABLE 1. Comparison of Serum CA242 Levels in Between 14 Different Gynecological Diseases and Healthy Controls

Group	n	M (P25, P75)	Median difference (95% CI)	$-\log_{10}$ (P value)	Positive rate, n (%) ^a
Mature teratoma	36	16.57 (9.05, 39.93)	12.08 (7.77–19.39)	12.11	14 (38.89)
Ovarian cancer	42	10.80 (4.45, 27.59)	6.31 (2.89–9.11)	5.54	11 (26.19)
Adenomyosis	30	10.25 (4.15, 19.89)	5.76 (2.55–10.49)	4.01	3 (10.00)
Fallopian tube cancer	10	9.46 (2.46, 19.85)	4.97 (–0.62–14.01)	0.99	2 (20)
Uterine cavity inflammation	19	6.85 (2.75, 9.91)	2.36 (–0.22–4.41)	1.08	2 (10.53)
Endometrial cancer	63	6.76 (2.96, 14.27)	2.27 (1.25–4.44)	3.99	10 (15.87)
Salpingitis	17	6.18 (3.18, 12.71)	1.69 (–0.75–3.98)	0.71	0 (0)
Uterine fibroids with ovarian cyst	75	6.12 (3.30, 11.90)	1.63 (0.43–2.90)	2.25	6 (8.00)
Ovarian cyst	159	5.64 (2.72, 13.78)	1.15 (0.61–2.36)	3.34	14 (8.81)
Uterine fibroids	343	5.17 (2.38, 11.69)	0.68 (0.35–1.59)	2.84	15 (4.37)
Cervical cancer	78	5.15 (2.69, 14.59)	0.66 (0.48–2.91)	2.42	7 (8.97)
Cervical intraepithelial neoplasia	47	4.71 (3.32, 13.83)	0.22 (0.04–2.55)	1.38	3 (6.38)
Uterine polyps	27	4.64 (1.21, 10.18)	0.15 (1.30–2.32)	0.09	2 (7.41)
Endometrial hyperplasia	75	4.45 (2.16, 10.57)	–0.04 (–0.61–1.26)	0.31	3 (4.00)
Healthy controls	499	4.49 (1.94, 7.89)			

^aPositive rate: CA242 >25 U/mL is regarded as positive.

FIGURE 2. The $-\log_{10}$ P values of CA242 in 14 different gynecological diseases compared with the normal control group.

CA242 is a relatively new tumor marker extensively used in clinical practice.¹⁰ Overwhelming evidence substantiates that serum CA242 is a good diagnostic marker for pancreatic and colorectal cancers.^{11–13} Lei et al¹⁴ reported that the CA242 value has the highest specificity (80.14%) and positive predictive value (69.71%) in diagnosing pancreatic cancer. Moreover, when CA242 is combined with CA199, CEA, and CA125, the diagnostic sensitivity and specificity for pancreatic cancer were improved to 90.4% and 93.8%, respectively, which is significantly higher than single tumor markers.¹⁵ Further studies confirmed that the positive detection rate of CA242 was high and assisted in diagnosing lung, breast, and other cancers.^{16–19} Meanwhile, numerous studies^{5,20–22} reported that the combination of CA242, CA199, and CA125 has high application value in the differential diagnosis of ovarian cancer, cervical cancer, and other gynecological cancers, as well as in dynamic observation during tumor treatment.

This study showed that the serum levels of CA242 in ovarian, cervical, and other gynecological tumor diseases were high, consistent with previous reports.^{5,23} The median value and positive rate of CA242 in ovarian, endometrial, and fallopian tube cancer were significantly higher than in cervical cancer, followed by nonmalignant diseases such as adenomyosis, uterine cavity inflammation, and ovarian cysts. The me-

dian and $-\log_{10}$ P values of serum CA242 levels in ovarian cancer were significantly higher than those of ovarian cysts. Moreover, the serum CA242 levels in endometrial and cervical cancers were higher than in endometrial hyperplasia and CIN respectively. These results indicate that the higher the degree of malignancy of the gynecological disease, the higher the serum CA242 level. We used $-\log_{10}$ P value to show the CA242 serum levels of 14 gynecological diseases. Mature teratomas and ovarian cancer exhibited the highest expression levels compared with healthy controls, followed by ovarian cysts, adenomyosis, and endometrial cancer. Eight diseases had $-\log_{10}$ P values > 1.3, indicating that CA242 expression can be used as a tumor marker for these 8 diseases. However, there was no significant difference in intrauterine inflammation, fallopian tube cancer, tubal inflammation, endometrial hyperplasia and uterine polyps ($P > .05$).

According to the grouping of benign and malignant lesions at the same sites, the results showed that serum CA242 was significantly higher in serum of malignant lesions at uterine and ovarian sites than at benign sites ($P < .05$). For the fallopian tube site, although the median value of CA242 was higher in the serum of malignant lesions compared with benign lesions ($P > .05$), there was no significant difference between the two, probably due to the small number of cases of tubal lesions in this study. We also analyzed the diagnostic performance of CA242, CA125, and HE4 alone and in combination for ovarian cancer. The area under the ROC curve of CA242 combined with CA125 in diagnosing ovarian cancer was 0.759, with a sensitivity of 83.3% and a specificity of 60.4%, higher than the single marker. The AUC of CA125 combined with HE4 in the diagnosis of ovarian cancer was 0.858, with a sensitivity of 71.4%, which was inferior to that of CA242 combined with CA125. In contrast, its specificity of 88.7% was significantly higher than that of CA242 combined with CA125. The AUC of the combination of the three tumor markers in the diagnosis of ovarian cancer was 0.887, with a sensitivity of 78.6% and a specificity of 86.8%, which was higher than the combination of CA125 and HE4. However, the sensitivity was inferior to that of the combination of CA242 and CA125, indicating that the sensitivity of CA242 combined with the other two indicators was significantly higher. A good specificity was also observed, suggesting the combination of CA242, CA125, and HE4 has diagnostic value for ovarian cancer.

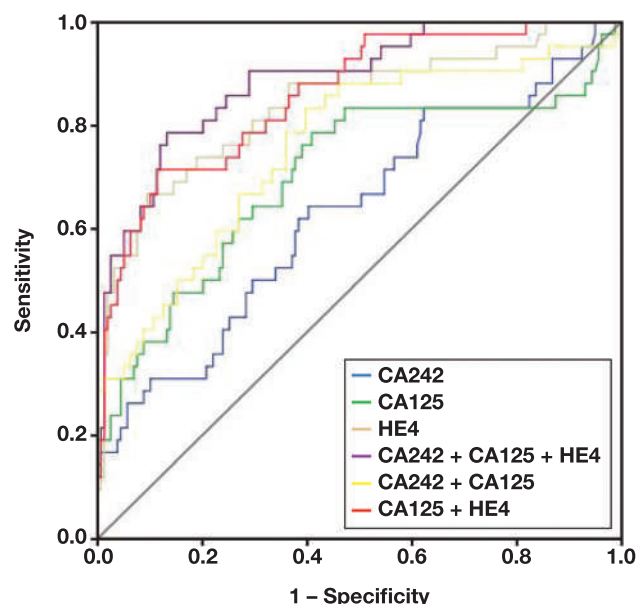
In this study, we also found that the median value, positive rate, and $-\log_{10}$ P value of serum CA242 in patients with mature teratoma were

TABLE 2. The Expression Levels of CA242 in Benign and Malignant Lesions of the Same Site

Group ^a	n	Median (25%, 75%) (U/mL)
Uterine benign lesions	475	5.17 (2.24, 11.97)
Uterine malignant lesions	63	6.67 (2.78, 14.31) ^b
Ovarian benign lesions	159	5.64 (2.67, 13.91)
Ovarian malignant lesions	42	10.80 (4.35, 28.52) ^b
Cervical benign lesions	47	4.71 (3.31, 13.84)
Cervical malignant lesions	78	5.14 (2.64, 14.89)
Benign fallopian tube lesions	17	6.18 (2.78, 13.87)
Malignant fallopian tube lesions	10	9.46 (2.30, 23.96)

^aBenign uterine lesions include adenomyosis, uterine polyps, endometrial hyperplasia, and uterine fibroids. Uterine malignant lesions include endometrial cancer. Ovarian benign lesions include ovarian cysts. Ovarian malignant lesions include ovarian cancer. Cervical benign lesions include cervical intraepithelial neoplasia (CIN). Cervical malignant lesions include cervical cancer. Benign fallopian tube lesions include salpingitis. Malignant fallopian tube lesions include fallopian tube cancer. Comparison of benign and malignant lesions is at the same site.

^bP < .05.

FIGURE 3. The receiver operating characteristic curve of CA242, CA125, and HE4 alone and in combination for the diagnosis of ovarian cancer.**TABLE 3.** Comparison of the Diagnostic Efficacy of CA242, CA125, and HE4 Alone and in Combination for Ovarian Cancer

Tumor marker	AUC	95% CI	Sensitivity	Specificity	P value
CA242	0.631	0.531~0.731	0.643	0.597	<.05
CA125	0.703	0.600~0.805	0.786	0.591	<.05
HE4	0.839	0.764~0.915	0.667	0.906	<.05
CA242+CA125	0.759	0.671~0.847	0.833	0.604	<.05
CA125+HE4	0.858	0.794~0.922	0.714	0.887	<.05
CA242+CA125+HE4	0.887	0.831~0.944	0.786	0.868	<.05

AUC, area under the curve.

the highest among the 14 gynecological diseases. Teratoma is a germ cell tumor, and mature teratomas correlate with a lower risk of malignant transformation. In contrast, relatively immature teratomas are usually associated with higher levels of necrotic components.^{24,25} Interestingly, Wang et al²⁴ and Suh et al²⁶ founded that the combination of CA199 and CA125 can differentiate mature cystic teratoma from other malignant tumors. Chen et al²⁷ and Gomes et al²⁸ showed that the combination of tumor markers has significant value in the differential diagnosis of immature and mature ovarian teratomas. However, few studies have assessed the value of CA242 in the clinical diagnosis of teratoma. Our future studies will focus on more in-depth stratified study with a larger sample size to provide more valuable laboratory data for clinical practice.

In summary, heterogeneous increases in tumor marker CA242 expression levels are observed in different gynecological diseases. The CA242 levels are increased in chronic diseases and malignant tumors of the uterus and ovary. Further studies are warranted to assess its clinical application value.

Funding

This study was supported by the National Natural Science Foundation of China (Grant No. 81801582) and the Key Medical Discipline of Shanghai Jiading District (Grant No. 2020-jdyxzdxx-13).

Conflict of Interest Disclosure

The authors have nothing to disclose.

REFERENCES

1. Su J, Wang Y, Shao H, You X, Li S. Value of multi-detector computed tomography combined with serum tumor markers in diagnosis, preoperative, and prognostic evaluation of pancreatic cancer. *World J Surg Oncol.* 2022;20(1):323. PMID: 36175918.
2. Ge L, Pan B, Song F, et al. Comparing the diagnostic accuracy of five common tumour biomarkers and CA19-9 for pancreatic cancer: a protocol for a network meta-analysis of diagnostic test accuracy. *BMJ Open.* 2017;7(12):e018175. PMID: 29282264.
3. Sun LQ, Peng LS, Guo JF, et al. Validation of serum tumor biomarkers in predicting advanced cystic mucinous neoplasm of the pancreas. *World J Gastroenterol.* 2021; 27(6): 501–512. PMID: 33642824.
4. Luo H, Shen K, Li B, Li R, Wang Z, Xie Z. Clinical significance and diagnostic value of serum NSE, CEA, CA19-9, CA125 and CA242 levels in colorectal cancer. *Oncol Lett.* 2020;20(1):742–750. PMID: 32566000.
5. Dou H, Sun G, Zhang L. CA242 as a biomarker for pancreatic cancer and other diseases. *Prog Mol Biol Transl Sci.* 2019;162:229–239. PMID: 30905452.
6. Zhu Y, Chen N, Chen M, et al. Circulating tumor cells: a surrogate to predict the effect of treatment and overall survival in gastric

- adenocarcinoma. *Int J Biol Markers* 2021;36(1): 28–35. PMID: 33499715.
7. Wang YF, Feng FL, Zhao XH, et al. Combined detection tumor markers for diagnosis and prognosis of gallbladder cancer. *World J Gastroenterol* 2014;20(14): 4085–4092. PMID: 24744600.
 8. Zhang Y, Li C, Luo S, et al. Retrospective study of the epidemiology, pathology, and therapeutic management in patients with mucinous ovarian tumors. *Technol Cancer Res Treat*. 2020;19: 1533033820946423 PMID: 32783505.
 9. Gui JC, Yan WL, Liu XD. CA19-9 and CA242 as tumor markers for the diagnosis of pancreatic cancer: a meta-analysis. *Clin Exp Med*. 2014;14(2):225–233. PMID: 23456571.
 10. Dong D, Jia L, Zhang L, et al. Periostin and CA242 as potential diagnostic serum biomarkers complementing CA19.9 in detecting pancreatic cancer. *Cancer Sci*. 2018;109(9): 2841–2851 PMID: 29945294.
 11. Zhang Y, Yang J, Li H, Wu Y, Zhang H, Chen W. Tumor markers CA19-9, CA242 and CEA in the diagnosis of pancreatic cancer: a meta-analysis. *Int J Clin Exp Med*. 2015;8(7):11683–11691. PMID: 26380005.
 12. Liu Y, Chen J. Expression levels and clinical significance of serum miR-497, CEA, CA24-2, and HBsAg in patients with colorectal cancer. *Biomed Res Int*. 2022;2022:3541403. PMID: 35993056.
 13. Tao L, Zhou J, Yuan C, et al. Metabolomics identifies serum and exosomes metabolite markers of pancreatic cancer. *Metabolomics*. 2019;15(6):86. PMID: 31147790.
 14. Lei XF, Jia SZ, Ye J, et al. Application values of detection of serum CA199, CA242 and CA50 in the diagnosis of pancreatic cancer. *J Biol Regul Homeost Agents*. 2017;31(2): 383–388. PMID: 28685541.
 15. Gu YL, Lan C, Pei H, Yang SN, Liu YF, Xiao LL. Applicative value of serum CA19-9, CEA, CA125 and CA242 in diagnosis and prognosis for patients with pancreatic cancer treated by concurrent chemoradiotherapy. *Asian Pac J Cancer Prev*. 2015;16(15):6569–6573. PMID: 26434876.
 16. Wang X, Zhang Y, Sun L, et al. Evaluation of the clinical application of multiple tumor marker protein chip in the diagnostic of lung cancer. *J Clin Lab Anal* 2018;32(8): e22565. PMID: 29736949.
 17. Xu MX, Cui HJ, Yao TL, Gui YF. Clinical value of combined tests for tumor markers for gastric cancer. *J Biol Regul Homeost Agents*. 2018;32(2):263–268. PMID: 29685004.
 18. Liang L, Fang J, Han X, et al. Prognostic value of CEA, CA19-9, CA125, CA724, and CA242 in serum and ascites in pseudomyxoma peritonei. *Front Oncol*. 2021;11:594763. PMID: 34733775.
 19. Zhao H, Lu B. Prediction of multiple serum tumor markers in hepatolithiasis complicated with intrahepatic cholangiocarcinoma. *Cancer Manag Res*. 2022;14:249–255. PMID: 35082529.
 20. Deng H, Chen M, Guo X, et al. Comprehensive analysis of serum tumor markers and BRCA1/2 germline mutations in Chinese ovarian cancer patients. *Mol Genet Genomic Med*. 2019;7(6):e672. PMID: 30972954.
 21. Li X, Li S, Zhang Z, Huang D. Association of multiple tumor markers with newly diagnosed gastric cancer patients: a retrospective study. *PeerJ*. 2022;10:e13488. PMID: 35611170.
 22. Ge L, Wang S, Liu H, Shi X, Shi J, Feng R. Intralobar pulmonary sequestration with aspergillus infection and elevated serum CA19-9 and CA242: a case report. *Transl Cancer Res*. 2021;10(2):1169–1176. PMID: 35116444.
 23. Bian J, Li B, Kou XJ, Wang XN, Sun XX, Ming L. Clinical applicability of multi-tumor marker protein chips for diagnosing ovarian cancer. *Asian Pac J Cancer Prev*. 2014;15(19):8409–8411. PMID: 25339038.
 24. Wang YQ, Xia WT, Wang F, Zhuang XX, Zheng FY, Lin F. Use of cancer antigen 125, cancer antigen 19-9, and the neutrophil-to-lymphocyte ratio to diagnose mature cystic teratoma with torsion. *Int J Gynaecol Obstet*. 2017;137(3):332–337. PMID: 28273351.
 25. Fan JT, Yan HQ, Malla S, et al. The clinical significance of CA19-9 in ovarian mature cystic teratoma. *Clin Exp Obstet Gynecol*. 2016;43(4): 522–525. PMID: 29734540.
 26. Suh DS, Moon SH, Kim SC, Joo JK, Park WY, Kim KH. Significant simultaneous changes in serum CA19-9 and CA125 due to prolonged torsion of mature cystic teratoma of the ovary. *World J Surg Oncol*. 2014;12:353. PMID: 25416055.
 27. Chen JM, Gao HY, Wang Q, Li Q. Expression and clinical significance of tumor markers in ovarian mature cystic teratoma. *Clin Exp Obstet Gynecol*. 2016;43(3):397–400. PMID: 27328499.
 28. Gomes TA, Campos EA, Yoshida A, Sarian LO, Andrade L, Derchain SF. Preoperative differentiation of benign and malignant non-epithelial ovarian tumors: clinical features and tumor markers. *Rev Bras Ginecol Obstet*. 2020;42(9):555–561. PMID: 32992358.

A population-based characterization study of anti-mitochondrial M2 antibodies and its consistency with anti-mitochondrial antibodies

En-yu Liang, MD,^{1,2} Miao Liu, MBBS,¹ Pei-feng Ke, MM,¹ Guang Han, MM,¹ Cheng Zhang, MM,¹ Li Deng, MBBS,¹ Yun-xiu Wang, MM,¹ Hui Huang, MM,¹ Wu-jiao Huang, MM,¹ Rui-ping Liu, MBBS,¹ Guo-hua Li, MM,¹ Ze-min Wan, MM,¹ Yi-ting He, MD,³ Min He, MD,^{1,2,4,*} Xian-zhang Huang, MD^{1,2,4,*}

¹Department of Laboratory Medicine, ²State Key Laboratory of Dampness Syndrome of Chinese Medicine, ³Intellectual Property Management and Transfer Center, and ⁴Guangdong Provincial Key Laboratory of Chinese Medicine for Prevention and Treatment of Refractory Chronic Diseases, the Second Affiliated Hospital of Guangzhou University of Chinese Medicine, Guangzhou, China. Corresponding author: Min He; minhe@gzucm.edu.cn. *Contributed equally.

Keywords: antimitochondrial antibody subtype M2 (AMA-M2); primary biliary cholangitis; population characteristics; risk factors

Abbreviations: AMA, antimitochondrial antibody; AMA-M2, AMA M2 subtype; PBC, primary biliary cholangitis; EASL, European Association for the Study of the Liver; ACG, American College of Gastroenterology; ALP, alkaline phosphatase; IIF, indirect immunofluorescence; ELISA, enzyme-linked immunosorbent assay; ALT, alanine aminotransferase; AST, aspartate aminotransferase; GGT, gamma-glutamyl transferase; ALB, albumin; TP, total protein; TBIL, total bilirubin; PA, prealbumin; Ig, immunoglobulin; C3/C4, complement 3/4; RF, rheumatoid factor; ASO, antistreptolysin O; BMI, body mass index; CHE, cholinesterase; ULN, upper limit of normal; DBIL, direct bilirubin

Laboratory Medicine 2023;54:618–625; <https://doi.org/10.1093/labmed/lmad018>

ABSTRACT

Objective: This study aims to estimate the prevalence of anti-mitochondrial antibody subtype M2 (AMA-M2) and assess its consistency with AMA in a general population.

Methods: A total of 8954 volunteers were included to screen AMA-M2 using enzyme-linked immunosorbent assay. Sera with AMA-M2 >50 RU/mL were further tested for AMA using an indirect immunofluorescence assay.

Results: The population frequency of AMA-M2 positivity was 9.67%, of which 48.04% were males and 51.96% were females. The AMA-M2 positivity in males had a peak and valley value of 7.81% and 16.88% in those aged 40 to 49 and ≥70 years, respectively, whereas it showed a balanced age distribution in females. Transferrin and immunoglobulin

M were the risk factors for AMA-M2 positivity and exercise was the only protective factor. Of 155 cases with AMA-M2 >50 RU/mL, 25 cases were AMA-positive, with a female-to-male ratio of 5.25:1. Only 2 people, with very high AMA-M2 of 760 and >800 RU/mL, met the diagnostic criteria of primary biliary cholangitis (PBC), making the prevalence of PBC 223.36 per million in southern China.

Conclusion: We found that AMA-M2 has a low coincidence rate with AMA in the general population. A new decision-making point for AMA-M2 is needed to improve consistency with AMA and diagnostic accuracy.

Introduction

Primary biliary cholangitis (PBC), previously named primary biliary cirrhosis, is a chronic autoimmune cholestatic liver disease with progressive histological lesions as nonsuppurative lymphocytic or granulomatous interlobular bile duct cholangitis.^{1,2} Primary biliary cholangitis has been reported to be more prevalent in Europe and North America than in the Asia Pacific region.^{3–5} During the last decade, there has been a marked increase in the number of PBC cases in China.⁶ This may be largely attributed to the awareness and availability of early screening of PBC, especially for the application of autoantibody testing like antimitochondrial antibodies (AMA). However, most of the reported prevalence of PBC was based on the combined case-finding and case ascertainment strategy,⁷ which probably underestimated the PBC prevalence in the whole population and neglected preclinical and asymptomatic persons. Thus, epidemiological data on the prevalence of PBC based on the general population strategy in China is desirable.

Primary biliary cholangitis typically progresses slowly and insidiously to cirrhosis, hepatobiliary malignancies, and eventually to liver-related mortality. Therefore, early diagnosis and intervention are essential for delaying the development of this disease. Antimitochondrial antibodies are serological hallmarks of PBC and are present in more than 95% of PBC patients.⁸ They may antedate other biochemical markers, histological changes, and clinical manifestations for several years and persist throughout the whole course of the disease.⁹ As suggested by the European Association for the Study of the Liver (EASL)¹⁰ and the American College of Gastroenterology (ACG),¹¹ a diagnosis of PBC can be made

with the presence of AMA and elevated alkaline phosphatase (ALP), even without a liver biopsy. This makes the AMA test particularly attractive for assessing the extent of the PBC spectrum on a population scale. Currently, the standard method for detecting AMA in many clinical laboratories is indirect immunofluorescence (IIF), which is based on tissue sections. However, the costly, lengthy process and observer dependence limit its large-scale clinical application. Recently, quantitative detection of its specific subtype, M2 (AMA-M2), by enzyme-linked immunosorbent assay (ELISA) is widely used in clinical practice, especially those using recombinant proteins such as MIT3 targeting immunodominant portions of PDC-E2, BCOADC-E2, and OGDC-E2.¹² However, increasing research has reported that ELISA is slightly more sensitive but less specific than IIF in biopsy-proven PBC. Its application can turn 90% of the PBC-negative tests for AMA by the conventional IIF method into positives.¹³ As suggested by a large-scale characterization study, nearly half of prospectively detected AMA in clinical practice was not related to a diagnosis of PBC.⁹ Because AMA-M2 and AMA have advantages and disadvantages, the issue is whether they share the same prevalence in the general population.

Herein, we report on a population-based epidemiological study to estimate the prevalence of PBC and analyze the natural distribution of AMA-M2 in both sampled populations and individuals undergoing health checkups. Moreover, the related risk factors of AMA-M2, including biochemical, immunological, and lifestyles, were analyzed. Our rationale was that the natural distribution and sources of variations of AMA-M2 in the general population would promote the efficiency of early screening and accurate diagnosis of PBC.

Methods

Subjects

This was a cross-sectional study conducted in Guangzhou from August 2010 to June 2014, including 2 cohorts. The volunteers in cohort 1 (n = 3755) were recruited using a stratified sampling method based on the regional population distribution and the proportion of urban and rural residents from the sixth national census data of the Guangzhou resident population. Adult citizens who lived in Guangzhou for at least 5 years and lived at the sampling points for at least 1 year were included in this study. The participants were invited to complete a questionnaire on medical history before they were enrolled. General information, living habits, health status, and physical examinations were recorded

in a secure database with restricted access. Participants in cohort 2 (n = 5197) were consecutively enrolled from those who underwent a health checkup at the Second Affiliated Hospital of Guangzhou University of Chinese Medicine. Overall, of the 8952 volunteers recruited in the study, 4582 (51.2%) were males and 4354 (48.8%) were females. The age of participants ranged from 18 to 93 years with a male-to-female ratio of 1.05:1, which reflects the general sex distribution in Guangzhou (1.08:1) as reported in the sixth national census data of the Guangzhou resident population.

Ethical Approval

This study followed the tenets of the Helsinki Declaration. All human subjects signed informed consent about using their medical data and blood specimens for research purposes before they were enrolled in this study. This study was approved by the hospital ethical committee (2013-127-2).

Laboratory Testing

The laboratory indices included clinical chemical analytes, immunoassay, and infection markers. The clinical chemical analytes included alanine aminotransferase (ALT), aspartate aminotransferase (AST), ALP, gamma-glutamyl transferase (GGT), albumin (ALB), total protein (TP), and total bilirubin (TBIL), which were measured by Roche Modular P 800 automatic biochemical analyzer (Roche Diagnostics). The immunoassays included prealbumin (PA), immunoglobulin (Ig)G, IgA, IgM, complement 3 (C3), C4, rheumatoid factor (RF), antistreptolysin O (ASO), and transferrin and were quantified by Roche Modular P or Siemens BNII. The serum infection markers of hepatitis B or hepatitis C viruses were detected using the cobas e602 analyzer (Roche Diagnostics).

Detection of AMA-M2

Antimitochondrial antibody subtype M2 was measured using an ELISA kit (Shanghai Kexin Biotech). The manufacturer's cutoff was established at 25 RU/mL.¹⁴ According to the resulting concentrations of AMA-M2, patients were categorized into three subgroups for further analysis: group 1, AMA-M2 ≤25 RU/mL; group 2, 25 < M2 ≤50 RU/mL; and group 3, AMA-M2 >50 RU/mL (twice the cutoff value).

IIF Assay for AMA

Sera with AMA-M2 >50 RU/mL were additionally tested for AMA (the quadruple tissue matrix; Euroimmun).¹⁵ Positivity and patterns were evaluated by 2 independent evaluators using fluorescence microscopy, and titer equal to or higher than 1:100 was considered positive.

TABLE 1. Positive Rates of AMA-M2 by Sex and Age Groups

Age, y	Cohort 1 (n = 3755)		Cohort 2 (n = 5197)		Total (n = 8952)	
	Male	Female	Male	Female	Male	Female
18-29	29/290 (10.00%) ^{a,b}	41/337 (12.17%)	98/1086 (9.02%)	78/777 (10.04%)	127/1376 (9.23%) ^{a,b}	119/1114 (10.68%)
30-39	23/286 (8.04%) ^{a,b}	37/298 (12.41%)	67/653 (10.26%)	58/559 (10.38%)	90/939 (9.58%) ^{a,b,c}	95/857 (11.09%)
40-49	25/320 (7.81%) ^b	45/403 (11.17%)	27/436 (6.19%)	37/455 (8.13%)	52/756 (6.88%) ^b	82/858 (9.56%) ^d
50-59	35/399 (8.77%) ^{a,b}	35/413 (8.47%)	25/378 (6.61%)	34/308 (11.04%)	60/777 (7.72%) ^{a,b}	69/721 (9.57%)
60-69	34/295 (11.53%) ^{a,b}	33/335 (9.85%)	16/167 (9.58%)	14/181 (7.73%)	50/462 (10.82%) ^{a,c}	47/516 (9.11%)
≥70	27/160 (16.88%) ^a	31/219 (14.16%)	10/112 (8.93%)	7/69 (10.14%)	37/272 (13.60%) ^c	38/288 (13.19%)
Total	173/1750 (9.89%)	222/2005 (11.07%)	243/2832 (8.58%)	228/2349 (9.71%)	416/4582 (9.08%)	450/4354 (10.34%)

^{a,b,c}Compared with the different age groups in the same cohort and with the same sex, no statistically significant difference exists between the 2 groups with any identical superscript footnote.

^aCompared with males in the same age group, P < .01.

TABLE 2. Physical and Laboratory Characteristics of 3755 Participants Categorized with AMA-M2 Concentrations^a

Measurement parameters	Group 1 M2 ≤25 RU/mL (n = 3360)	Group 2 25 RU/mL < M2 ≤50 RU/mL (n = 240)	Group 3 M2 >50 RU/mL (n = 155)	P1 ^b	P2 ^b	P3 ^b
Age (y)	47.74 ± 15.78	49.38 ± 16.95	47.6 ± 17.16	NS	NS	NS
Height (m)	1.62 ± 0.08	1.62 ± 0.09	1.61 ± 0.08	NS	NS	NS
Weight (kg)	59.78 ± 10.65	59.38 ± 10.76	57.6 ± 10.76	NS	.017	NS
BMI (kg/m ²)	22.79 ± 3.13	22.64 ± 2.98	22.07 ± 3.06	NS	.010	NS
Waistline (cm)	81.51 ± 23.19	80.47 ± 9.03	78.70 ± 9.29	NS	.004	NS
Hipline (cm)	94.42 ± 7.13	94.30 ± 6.68	93.14 ± 7.44	NS	.040	NS
ALT (U/L)	20.42 ± 15.35	21.49 ± 31.67	19.6 ± 17.05	NS	NS	NS
AST (U/L)	22.26 ± 8.11	24.50 ± 28.02	23.2 ± 13.51	NS	NS	NS
ALP (U/L)	72.24 ± 21.43	71.64 ± 20.33	78.3 ± 65.59	NS	NS	NS
GGT (U/L)	28.26 ± 27.92	34.23 ± 75.99	31.8 ± 61.37	NS	NS	NS
CHE (U/L)	9268.32 ± 1799.03	9271.32 ± 1730.66	8629.8 ± 1566.07	NS	.040	.016
TP (g/L)	76.70 ± 4.49	77.27 ± 4.83	76.95 ± 4.96	NS	NS	NS
ALB (g/L)	47.63 ± 2.84	47.75 ± 3.40	47.38 ± 3.05	NS	NS	NS
TBIL (μmol/L)	10.83 ± 5.02	10.81 ± 5.51	10.94 ± 7.62	NS	NS	NS
DBIL (μmol/L)	3.47 ± 2.02	3.48 ± 1.75	3.93 ± 6.02	NS	NS	NS
IgA (g/L)	2.55 ± 1.04	2.52 ± 0.96	2.60 ± 1.01	NS	NS	NS
IgG (g/L)	13.08 ± 2.47	13.39 ± 2.37	13.60 ± 3.33	NS	NS	NS
IgM (g/L)	1.23 ± 0.63	1.29 ± 0.71	1.58 ± 1.41	NS	.002	.030
C3 (g/L)	1.09 ± 0.18	1.11 ± 0.16	1.10 ± 0.20	NS	NS	NS
C4 (g/L)	0.28 ± 0.09	0.29 ± 0.09	0.28 ± 0.13	NS	NS	NS
RF (IU/mL)	12.09 ± 27.64	12.38 ± 12.69	16.0 ± 53.51	NS	NS	NS
ASO (IU/mL)	69.12 ± 78.76	56.70 ± 53.65	77.0 ± 83.14	NS	NS	NS
Transferrin (mg/L)	2.60 ± 0.38	2.59 ± 0.35	2.74 ± 0.44	NS	.045	.009
PA (mg/L)	282.03 ± 53.51	286.74 ± 56.24	283.9 ± 56.95	NS	NS	NS
Questionnaire survey						
Sex						
Male	1577 (46.93)	112 (46.67)	61 (39.35)	NS	NS	NS
Female	1783 (53.07)	128 (53.33)	94 (60.65)			
Habitation						
Urban	2470 (73.51)	165 (68.75)	112 (72.26)	NS	NS	NS
Rural	890 (26.49)	75 (31.25)	43 (27.74)			
Exercise						
Less	1921 (57.17)	127 (52.92)	106 (68.39)	NS	.008	.008
More	1439 (42.83)	113 (47.08)	49 (31.61)			
Fatigue						
No	2450 (72.92)	180 (75.00)	112 (72.26)	NS	NS	NS
Yes	910 (27.08)	60 (25.00)	43 (27.74)			
Smoke						
Nonsmoking	2621 (78.01)	183 (76.25)	126 (81.29)	NS	NS	NS
Abstinence	221 (6.58)	15 (6.25)	4 (2.58)			
Smoker	518 (15.42)	42 (17.50)	25 (16.13)			
Drink						
Teetotaler	2647 (78.78)	187 (77.92)	127 (81.94)	NS	NS	NS
Abstinence	411 (12.23)	30 (12.50)	17 (10.97)			
Alcoholic	302 (8.99)	23 (9.58)	11 (7.10)			

ALB, albumin; ALP, alkaline phosphatase; ALT, alanine aminotransferase; AMA, antimitochondrial antibody; ASO, antistreptolysin O; AST, aspartate aminotransferase; BMI, body mass index; CHE, cholinesterase; DBIL, direct bilirubin; GGT, gamma-glutamyl transferase; NS, nonsignificant; PA, prealbumin; RF, rheumatoid factor; TBIL, total bilirubin; TP, total protein.

^aData are given as mean ± SD or No. (%).

^bP1, P2, and P3 were the P values for M2 ≤25 RU/mL vs 25 RU/mL < M2 ≤50 RU/mL, M2 ≤25 RU/mL vs M2 >50 RU/mL, 25 RU/mL < M2 ≤50 RU/mL vs M2 >50 RU/mL, respectively.

FIGURE 1. Forest plot of various risk factors. A, The risk factors and odds ratio (OR) between M2 ≤ 25 RU/mL and M2 > 50 RU/mL groups. B, The risk factors and OR between 25 RU/mL $< M2 \leq 50$ RU/mL and M2 > 50 RU/mL group. BMI, body mass index; CHE, cholinesterase.

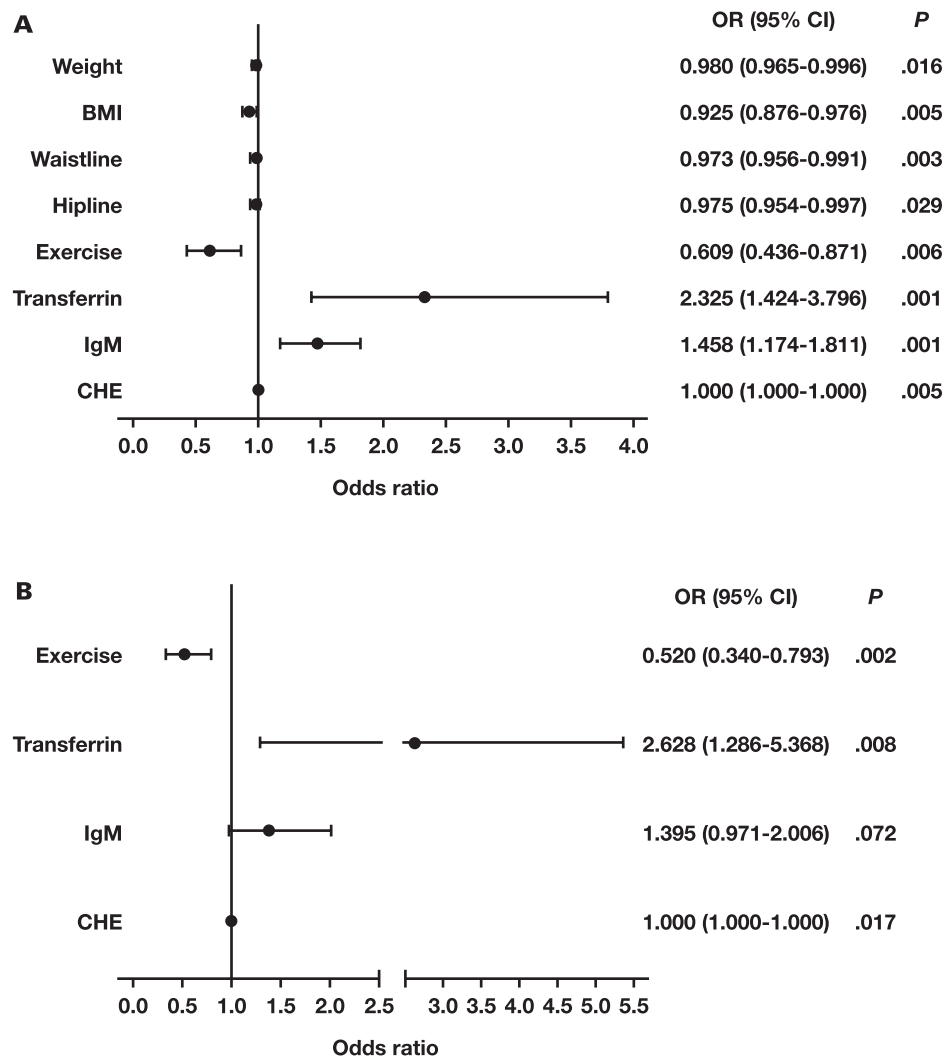


FIGURE 2. The distribution characteristics of the antimitochondrial antibody (AMA)-positive population. A, The positive rates of AMA were categorized by sex and age groups. B, The correlation of AMA with quantitative AMA-M2, sex, and age. The black circles around the dots represented that the participant had an elevated alkaline phosphatase (ALP) up to 2 \times the upper limit of normal. The numbers above or next to the dots represented the concentration of AMA-M2 in cases with positive AMA.

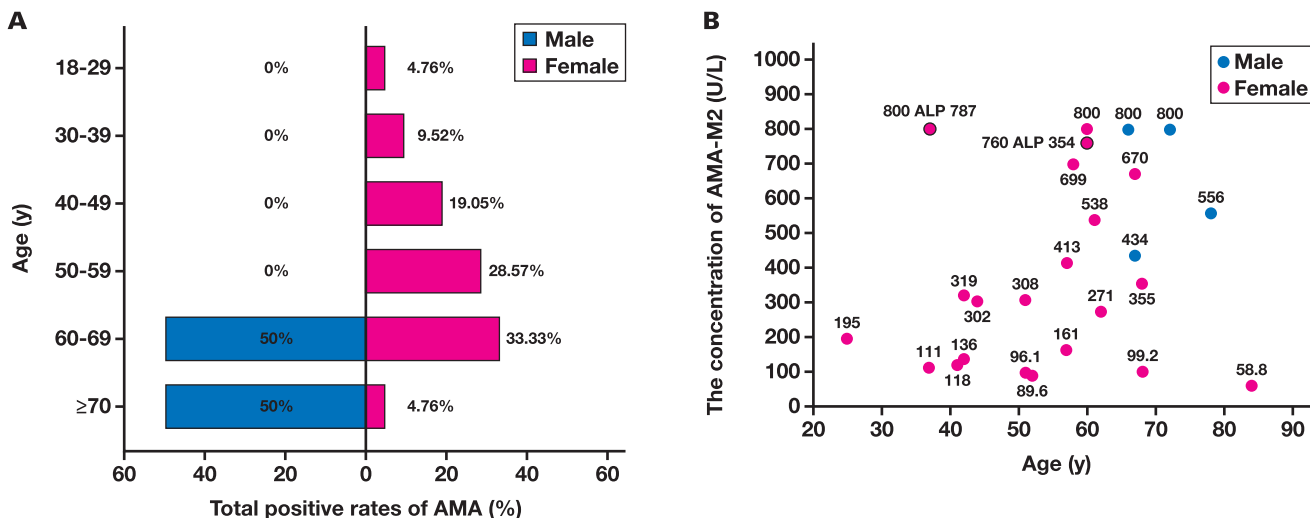


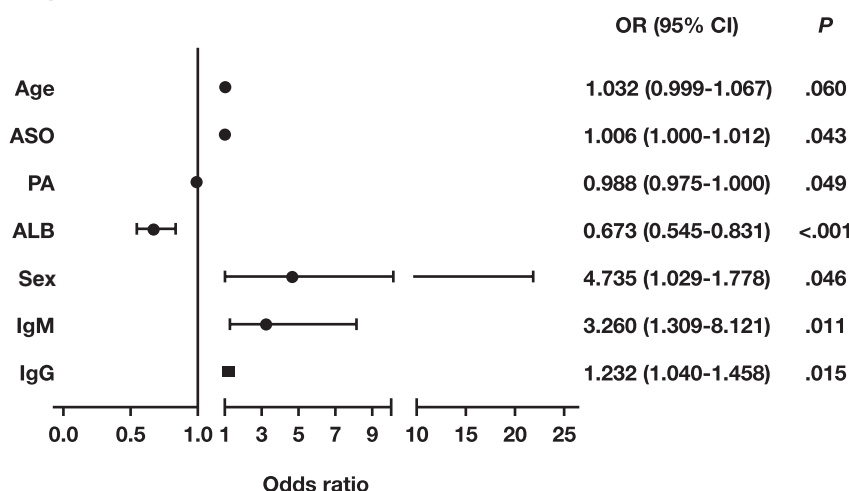
TABLE 3. Physical and Laboratory Characteristics of 155 Participants Categorized by AMA^a

Measurement parameters	AMA– (n = 140)	AMA+ (n = 15)	P
Age (y)	46.78 ± 17.27	55.73 ± 14.24	.041
Height (m)	1.62 ± 0.08	1.57 ± 0.07	.054
Weight (kg)	58.09 ± 10.86	52.18 ± 6.94	.138
BMI (kg/m ²)	22.11 ± 3.09	21.16 ± 2.28	.670
Waistline (cm)	78.86 ± 9.51	76.57 ± 6.85	.600
Hipline (cm)	93.27 ± 7.19	90.21 ± 7.49	.391
ALT (U/L)	19.12 ± 16.16	24.71 ± 24.87	.213
AST (U/L)	22.18 ± 8.73	33.93 ± 34.71	.235
ALP (U/L)	72.50 ± 22.40	135.43 ± 203.51	.259
GGT (U/L)	25.37 ± 22.92	96.86 ± 183.64	.440
CHE (U/L)	8699.78 ± 1583.71	7580.75 ± 782.26	.100
TP (g/L)	76.77 ± 4.45	79.11 ± 8.43	.419
ALB (g/L)	47.72 ± 2.78	44.49 ± 3.75	<.001
TBIL (μmol/L)	10.42 ± 4.90	16.23 ± 19.86	.444
DBIL (μmol/L)	3.38 ± 1.65	9.48 ± 18.99	.560
IgA (g/L)	2.50 ± 0.92	3.35 ± 1.45	.095
IgG (g/L)	13.24 ± 2.67	16.37 ± 6.18	.033
IgM (g/L)	1.37 ± 0.62	3.28 ± 3.58	.001
C3 (g/L)	1.09 ± 0.19	1.17 ± 0.28	.869
C4 (g/L)	0.29 ± 0.13	0.24 ± 0.05	.125
RF (IU/mL)	16.91 ± 57.05	9.75 ± 3.48	.942
ASO (IU/mL)	69.97 ± 77.67	108.78 ± 87.85	.025
Transferrin (mg/L)	2.71 ± 0.39	3.00 ± 0.67	.473
PA (mg/L)	288.35 ± 56.57	253.74 ± 53.18	.044
Questionnaire survey			
Sex			
Male	59 (42.14)	2 (13.33)	.048
Female	81 (57.86)	13 (86.67)	
Habitation			
Urban	100 (71.43)	12 (80.00)	.558
Rural	40 (28.57)	3 (20.00)	
Exercise			
Less	99 (70.71)	7 (46.67)	.078
More	41 (29.29)	8 (53.33)	
Fatigue			
No	104 (74.29)	8 (53.33)	.125
Yes	36 (25.71)	7 (46.67)	
Smoke			
Nonsmoking	112 (80.00)	14 (93.33)	.325
Abstinence	4 (2.86)	0 (0.00)	
Smoker	24 (17.14)	1 (6.67)	
Drink			
Teetotaler	113 (80.71)	14 (93.33)	1.000
Abstinence	16 (11.43)	1 (6.67)	
Alcoholic	11 (7.86)	0 (0.00)	

ALB, albumin; ALT, alanine aminotransferase; ALP, alkaline phosphatase; AMA, antimitochondrial antibody; ASO, antistreptolysin O; AST, aspartate aminotransferase; BMI, body mass index; CHE, cholinesterase; DBIL, direct bilirubin; GGT, gamma-glutamyl transferase; PA, prealbumin; RF, rheumatoid factor; TBIL, total bilirubin; TP, total protein.

^aData are given as mean ± SD or No. (%).

FIGURE 3. Forest plot of risk factors with odds ratio (OR) in the antimitochondrial antibody-positive population. ALB, albumin; ASO, antistreptolysin O; PA, prealbumin.



Statistical Analysis

Descriptive statistics were expressed as mean \pm SD and percentage (%). The continuous variables were compared by 1-way analysis of variance or Mann-Whitney *U* test according to the distributions of the data, whereas the categorical variables were compared using the χ^2 or Fisher exact test. The significant variables were submitted to logistic regression analysis to calculate the odds ratio (OR) and the 95% CI. The forest plots of various risk factors were drawn using GraphPad Prism 8.0. The statistical analysis was performed using SPSS 19.0 with a 2-sided statistically significant *P* value < .05.

Results

Demographic Characteristics of AMA-M2 Antibody

To improve representativeness and investigate the prevalence of AMA-M2, 3755 participants recruited by stratified sampling (cohort 1) and 5197 participants enrolled from health checkups (cohort 2) were included in our study. The quantitative distribution of positive results for males and females in each age group is shown in **TABLE 1**. The AMA-M2 positive rate of cohort 1 was a little higher than that of cohort 2 (10.52% vs 9.06%). In cohort 1, only the positive rates of AMA-M2 of males showed a different age distribution with the peak and valley values being 7.81% and 16.88% in those 40 to 49 years old and ≥ 70 years old, respectively (**TABLE 1**). There was no other difference between age groups, sex, and cohorts. Overall, the population frequency of AMA-M2 was 9.67% (866/8952), accounting for 9.08% of males and 10.34% of females. The age distribution of abnormal AMA-M2 displayed a parabolic model with the lowest point at 40 to 49 years where the positive rates of AMA-M2 in females (82/858) were 28.03% higher than that in males (52/756) (*P* = .006) (**TABLE 1**).

Risk Factors for Quantitative AMA-M2

Complete laboratory data and lifestyle parameters were available for cohort 1. Thus, a subgroup analysis was performed based on AMA-M2 concentrations to define the risk factors. All variables of the participants did not differ between group 1 ($M_2 \leq 25$ RU/mL) and group 2 (25 RU/mL < $M_2 \leq 50$ RU/mL) but a significant difference was found when

compared with group 3 ($M_2 > 50$ RU/mL). The volunteers in group 3 ($M_2 > 50$ RU/mL) had a significantly lower weight, smaller body mass index (BMI), waistline, hipline, and a lower exercise frequency, whereas cholinesterase (CHE), IgM, and transferrin were markedly increased (**TABLE 2**). Unexpectedly, no sex differences were found among these 3 groups (**TABLE 2**). Finally, the variables with statistical significance were included in the next risk assessments. The results showed that transferrin was the most significant risk factor in group 3, with an OR of 2.325 and 2.628 when compared with group 1 and 2, respectively. Immunoglobulin M was a significant risk factor for group 3, with an OR of 1.458 when compared with group 1, whereas it was unremarkable between group 2 and group 3. The ORs of weight, BMI, waistline, and hipline were too close to 1 to be defined as a protective factor. Exercise was the only protective factor in group 3 (**FIGURE 1**).

Correlation of Quantitative AMA-M2 with AMA

The population characteristics in group 3 were remarkably different from those in group 1 and group 2. Therefore, sera with AMA-M2 > 50 RU/mL (155 cases from cohort 1 and 180 cases from cohort 2) were further tested for AMA using an IIF assay. There were 25 cases (15 cases from cohort 1 and 10 cases from cohort 2) in the AMA-M2-positive population that were concurrently AMA-positive, in which 21 cases were female and 4 cases were male, accounting for the high female-to-male ratio of 5.25:1. The females with positive AMA showed an increasing trend with age and more than 80% of these cases were found at 40 to 69 years old. The males with positive AMA were over 60 years old (**FIGURE 2A**). In these 25 cases, only 2 cases had an elevated ALP up to 2 times upper limit of normal who had a very high AMA-M2, 760 RU/mL and >800 RU/mL (**FIGURE 2B**). According to EASL¹⁰ and ACG,¹¹ these 2 individuals (2/8936, 0.022%) met the diagnostic criteria of PBC, increasing speculation about the approximate prevalence of PBC, which was 223.81 per million in southern China.

Characteristic and Risk Factor Assessment of Various Parameters Categorized by AMA

We also explored whether population characteristics were more distinctive when categorized by AMA. First, the patients in cohort 1

with AMA-M2 concentrations >50 RU/mL were further categorized into 2 groups: AMA+/M2+ and AMA-/M2+. Unlike the characteristics categorized with AMA-M2 concentrations, the populations differed significantly when classified by AMA. The AMA-positive population tended to have low ALB and PA, increased IgG and IgM, and a sex ratio imbalance. The female-to-male ratio was 6.5:1 with an OR of 4.735 (TABLE 3, FIGURE 3). Also, the increased IgG and IgM were significant high-risk factors, with OR of 1.232 and 3.260, respectively, whereas ALB was a protective factor for the AMA-positive population (FIGURE 3).

Discussion

We conducted a population-based study to screen for PBC with its specific autoantibodies in representative Guangzhou residents. We started from the natural distribution of quantitative AMA-M2 and semi-quantitative AMA to their associated risk factors.

It is reported that PBC displayed substantial geographical disparity. In the Asia-Pacific region, the estimated overall prevalence of PBC was 204.87 per million in China, 221.01 per million in Japan, 99.6 per million in New Zealand, and 39.09 per million in Australia and South Korea.⁵ Even in China, the prevalence of PBC varied greatly, ranging from 56.4 to 492 per million inhabitants.^{16–18} The apparent inconsistency between different studies is due not only to geographical variations but to the research methodologies. Some of these studies were based on the case-finding and case ascertainment strategy and included only diagnosed patients, which might have underestimated the prevalence.¹⁹ Some studies were conducted on people who came to a hospital for a health checkup, which might not be the same as the general population and may have overestimated PBC prevalence. In this study, we recruited 2 cohorts of volunteers, a sampled population and those attending health checkups. The recruited individuals were almost equally distributed by age and sex, which represent the local population. Finally, 2 cases were diagnosed as PBC patients, which led to a point prevalence of PBC in southern China as 223.36 per million. These 2 cases were found in the sampled population, not in the health checkup group. However, this point prevalence was much lower than that in another Chinese report conducted only on people who came to a hospital for a health checkup.¹⁷

Although AMA-M2 is one of the serological markers of PBC, it is not disease-specific. The elevation of AMA-M2 had been found in various disorders, such as chronic hepatitis C virus infection,²⁰ autoimmune hepatitis,²¹ Sjögren syndrome,²² and hematological malignancies.²³ Thus, the population frequencies of AMA-M2 remained to be clarified. In this study, both cohorts showed similar distributions of AMA-M2 (10.52% vs 9.06% in cohort 1 vs cohort 2). The total positivity rate was much higher than that reported by a Chinese study as 0.73%.¹⁴ The assay methods and the selected population are the main reasons. It is noteworthy that the AMA-M2 levels of the 2 diagnostic PBC patients were 760 RU/mL and >800 RU/mL. These results are much higher than the cut-off value. Therefore, it seems that the currently used reference interval for AMA-M2 is not proper for the screen of PBC, let alone the diagnosis. As recommended by the American Association for the Study of Liver Diseases, liver biopsies were performed only in the presence of high titers of autoantibodies with signs suggestive of autoimmune liver disease.²⁴ Concerning the low prevalence of PBC, the application of AMA-M2 to the general population would lead to a very low positive predictive value. Thus, our study highlights the necessity to establish a diagnostic level for AMA-M2 for PBC diagnosis.

Primary biliary cholangitis predominantly affects women in their fifties and sixties.^{25,26} Unexpectedly, female predominance was not prominent when categorized with AMA-M2 concentrations. However, a sex ratio imbalance emerged when the AMA-M2-positive population was further categorized with AMA (male-to-female ratio, 1:6.5). Of note, the positive reactivity for AMA in this study was close to another study conducted in Guangzhou.¹⁷ Therefore, these findings imply that AMA-M2 (ELISA) and AMA (IIF) had tremendously different screening performances in different populations. Hu et al²⁷ suggested that although both AMA and AMA-M2 have favorable accuracy for the diagnosis of PBC, AMA would be a better and more comprehensive test than AMA-M2. Nevertheless, Han et al²⁸ suggested the use of IIF with high specificity as a first-line screening test for AMA detection and the use of a sensitive AMA-M2 assay as a confirmatory test. The combination of AMA-M2 and AMA was not only useful for IIF AMA-negative patients but also useful for low-titer AMA-positive patients.

Several prognostic models have been developed and validated for survival in untreated PBC patients, such as the Mayo score. Other than age and sex, several potential and significant risk factors for PBC have been included, such as IgM, ALB, IgG, etc. We tried to explore the risk factors related to elevated AMA-M2. Three subgroups were categorized according to serum AMA-M2 concentrations in cohort 1. Group 3 (AMA-M2 >50 RU/mL) exhibited a different population character, including lower weight, smaller BMI, waistline, hipline, higher transferrin, and IgM. Logistic regression analysis showed that transferrin had the highest OR, which was consistent with the findings of an early study that the serum level of transferrin in PBC was higher than in healthy blood donors, alcoholic cirrhosis, and fatty liver.²⁹ The significant elevation of transferrin in PBC patients might be caused by increased efflux through the disruptive cell membrane.³⁰ In addition, we also confirmed that ALB and exercise were protective factors for the AMA-M2-positive population. The ALB reduction in PBC is a signature of impaired liver synthesis, which usually indicates the development of cirrhosis.¹⁰ In the AMA-positive population, the risk effects of sex and IgM were more prominent than in the AMA-M2-positive population. Despite smoking cessation and limited or no alcohol consumption being recommended in the primary care guidelines for PBC,¹¹ our results indicated that the demographics of smoking and alcohol consumption had little association with AMA-M2 and AMA.

One of the strengths of our study is that the data are based on a population-based cohort of inhabitants that is representative of the southern China population. As one of the main limitations of this study, AMA-2 was not the only disease-specific autoantibody for PBC.³¹ Other autoantibodies, such as antinuclear antibodies to sp-100 or gp-210, are often identified in patients with PBC. Thus, a screening started from AMA-M2 might lead to underestimated prevalence. Second, we could not obtain follow-up data to learn about development or outcome of the participants with different concentrations of AMA-M2. Third, although PBC is reported to be almost exclusively a disease of adults,³² it would be more thorough to study all ages. Thus, further multicenter research to learn disease prevalence, geographic variations, heterogeneity, and differences in the sex ratio of PBC in China is desirable.

This study highlights different characteristics and reports on a risk assessment of the populations defined by AMA-M2 and AMA. These results indicate that more research should focus on the decision-making point for AMA-M2 to improve consistency with AMA and accuracy of diagnosis.

Funding

The study was supported by Science and Technology Projects in Guangzhou [202102021139]; Science and technology research project of traditional Chinese Medicine of Guangdong Provincial Hospital of Chinese Medicine [YN2019QL06]; Guangdong Basic and Applied Basic Research Foundation [2020A1515110329]; State Key Laboratory of Dampness Syndrome of Chinese Medicine [SZ2021ZZ24]; Guangdong Provincial Key Laboratory of Chinese Medicine for Prevention and Treatment of Refractory Chronic Diseases [2018B030322012].

Conflict of Interest Disclosure

The authors have nothing to disclose.

REFERENCES

- Shah RA, Kowdley KV. Current and potential treatments for primary biliary cholangitis. *Lancet Gastroenterol Hepatol*. 2020;5(3):306–315. doi:10.1016/S2468-1253(19)30343-7.
- Lv T, Chen S, Li M, Zhang D, Kong Y, Jia J. Regional variation and temporal trend of primary biliary cholangitis epidemiology: a systematic review and meta-analysis. *J Gastroenterol Hepatol*. 2021;36(6):1423–1434. doi:10.1111/jgh.15329.
- Yoshida EM, Mason A, Peltekian KM, et al. Epidemiology and liver transplantation burden of primary biliary cholangitis: a retrospective cohort study. *CMAJ Open*. 2018;6(4):E664–E670. doi:10.9778/cmajo.20180029.
- Boonstra K, Beuers U, Ponsioen CY. Epidemiology of primary sclerosing cholangitis and primary biliary cirrhosis: a systematic review. *J Hepatol*. 2012;56(5):1181–1188. doi:10.1016/j.jhep.2011.10.025.
- Zeng N, Duan W, Chen S, et al. Epidemiology and clinical course of primary biliary cholangitis in the Asia-Pacific region: a systematic review and meta-analysis. *Hepatol Int*. 2019;13(6):788–799. doi:10.1007/s12072-019-09984-x.
- Wang L, Gershwin ME, Wang FS. Primary biliary cholangitis in China. *Curr Opin Gastroenterol*. 2016;32(3):195–203. doi:10.1097/MOG.0000000000000257.
- Lleo A, Colapietro F. Changes in the epidemiology of primary biliary cholangitis. *Clin Liver Dis*. 2018;22(3):429–441. doi:10.1016/j.cld.2018.03.001.
- Lindor KD, Bowlus CL, Boyer J, Levy C, Mayo M. Primary biliary cholangitis: 2018 practice guidance from the American Association for the Study of Liver Diseases. *Hepatology*. 2019;69(1):394–419. doi:10.1002/hep.30145.
- Dahlqvist G, Gaouar F, Carrat F, et al; French Network of Immunology Laboratories. Large-scale characterization study of patients with antimitochondrial antibodies but nonestablished primary biliary cholangitis. *Hepatology*. 2017;65(1):152–163. doi:10.1002/hep.28859.
- European Association for the Study of the Liver. EASL clinical practice guidelines: the diagnosis and management of patients with primary biliary cholangitis. *J Hepatol*. 2017;67(1):145–172.
- Younossi ZM, Bernstein D, Shiffman ML, et al. Diagnosis and management of primary biliary cholangitis. *Am J Gastroenterol*. 2019;114(1):48–63. doi:10.1038/s41395-018-0390-3.
- Moteki S, Leung PS, Coppel RL, et al. Use of a designer triple expression hybrid clone for three different lipoyl domain for the detection of antimitochondrial autoantibodies. *Hepatology*. 1996;24(1):97–103. doi:10.1002/hep.510240117.
- Patel D, Egner W, Gleeson D, Wild G, Ward A. Detection of serum M2 anti-mitochondrial antibodies by enzyme-linked immunosorbent assay is potentially less specific than by immunofluorescence. *Ann Clin Biochem*. 2002;39(Pt 3):304–307. doi:10.1258/0004563021902008.
- Chen BH, Wang QQ, Zhang W, Zhao LY, Wang GQ. Screening of anti-mitochondrial antibody subtype M2 in residents at least 18 years of age in an urban district of Shanghai, China. *Eur Rev Med Pharmacol Sci*. 2016;20(10):2052–2060.
- Li X, Liu X, Cui J, et al. Epidemiological survey of antinuclear antibodies in healthy population and analysis of clinical characteristics of positive population. *J Clin Lab Anal*. 2019;33(8):e22965. doi:10.1002/jcla.22965.
- Trivedi PJ, Hirschfield GM. Recent advances in clinical practice: epidemiology of autoimmune liver diseases. *Gut*. 2021;70(10):1989–2003. doi:10.1136/gutjnl-2020-322362.
- Liu H, Liu Y, Wang L, et al. Prevalence of primary biliary cirrhosis in adults referring hospital for annual health check-up in Southern China. *BMC Gastroenterol*. 2010;10:100. doi:10.1186/1471-230X-10-100.
- Cheung KS, Seto WK, Fung J, Lai CL, Yuen MF. epidemiology and natural history of primary biliary cholangitis in the Chinese: a territory-based study in Hong Kong between 2000 and 2015. *Clin Transl Gastroenterol*. 2017;8(8):e116. doi:10.1038/ctg.2017.43.
- French J, van der Mei I, Simpson S Jr, et al. Increasing prevalence of primary biliary cholangitis in Victoria, Australia. *J Gastroenterol Hepatol*. 2020;35(4):673–679.
- Ramos-Casals M, Pares A, Jara LJ, et al., HISPAMEC Study Group. Antimitochondrial antibodies in patients with chronic hepatitis C virus infection: description of 18 cases and review of the literature. *J Viral Hepat*. 2005;12(6):648–654. doi:10.1111/j.1365-2893.2005.00642.x.
- Tomizawa M, Shinozaki F, Fugo K, et al. Anti-mitochondrial M2 antibody-positive autoimmune hepatitis. *Exp Ther Med*. 2015;10(4):1419–1422. doi:10.3892/etm.2015.2694.
- Zamfir O, Briaud I, Dubel L, Ballot E, Johanet C. Anti-pyruvate dehydrogenase autoantibodies in extrahepatic disorders. *J Hepatol*. 1999;31(5):964–965. doi:10.1016/S0168-8278(99)80302-x.
- Wakabayashi SI, Kimura T, Tanaka N, et al. Emergence of anti-mitochondrial M2 antibody in patient with angioimmunoblastic T-cell lymphoma. *Clin J Gastroenterol*. 2018;11(4):302–308. doi:10.1007/s12328-018-0831-y.
- Ravi S, Shoreibah M, Raff E, et al. Autoimmune markers do not impact clinical presentation or natural history of steatohepatitis-related liver disease. *Dig Dis Sci*. 2015;60(12):3788–3793. doi:10.1007/s10620-015-3795-5.
- Lleo A, Jepsen P, Morenghi E, et al. Evolving trends in female to male incidence and male mortality of primary biliary cholangitis. *Sci Rep*. 2016;6:1–8. doi:10.1038/srep25906.
- Asselta R, Paraboschi EM, Gerussi A, et al; Canadian-US PBC Consortium. X Chromosome contribution to the genetic architecture of primary biliary cholangitis. *Gastroenterology*. 2021;160(7):2483–2495. e26. doi:10.1053/j.gastro.2021.02.061.
- Hu C, Deng C, Song G, et al. Prevalence of autoimmune liver disease related autoantibodies in Chinese patients with primary biliary cirrhosis. *Dig Dis Sci*. 2011;56(11):3357–3363. doi:10.1007/s10620-011-1756-1.
- Han E, Jo SJ, Lee H, et al. Clinical relevance of combined anti-mitochondrial M2 detection assays for primary biliary cirrhosis. *Clin Chim Acta*. 2017;464:113–117. doi:10.1016/j.cca.2016.11.021.
- Teppo AM, Maury CP. Serum prealbumin, transferrin and immunoglobulins in fatty liver, alcoholic cirrhosis and primary biliary cirrhosis. *Clin Chim Acta*. 1983;129(3):279–286. doi:10.1016/0009-8981(83)90030-x.
- Grytczuk A, Bauer A, Gruszevska E, Cylwik B, Chrostek L. Changed profile of serum transferrin isoforms in primary biliary cholangitis. *J Clin Med*. 2020;9(9):2894.
- Hu S, Zhao F, Wang Q, Chen WX. The accuracy of the anti-mitochondrial antibody and the M2 subtype test for diagnosis of primary biliary cirrhosis: a meta-analysis. *Clin Chem Lab Med*. 2014;52(11):1533–1542. doi:10.1515/cclm-2013-0926.
- Kitic I, Boskovic A, Stankovic I, Prokic D. Twelve-year-old girl with primary biliary cirrhosis. *Case Rep Pediatr*. 2012;2012:937150. doi:10.1155/2012/937150.

Serum Ribonucleotide Reductase Subunit M2 in Patients with Chronic Liver Diseases and Hepatocellular Carcinoma

Xuehang Jin, PhD,¹ Wei Yu, MD,¹ Ange Wang, MM,² and Yunqing Qiu, MM^{1,*}

¹State Key Laboratory for Diagnosis and Treatment of Infectious Disease, National Clinical Research Center for Infectious Diseases, Collaborative Innovation Center for Diagnosis and Treatment of Infectious Diseases, Zhejiang Provincial Key Laboratory for Drug Clinical Research and Evaluation, The First Affiliated Hospital, and ²Department of Geriatrics, School of Medicine, The First Affiliated Hospital, Zhejiang University, Hangzhou, China. *To whom correspondence should be addressed: qiuyq@zju.edu.cn.

Keywords: hepatitis B virus, hepatocellular carcinoma, chronic liver disease, ribonucleotide reductase, serum ribonucleotide reductase subunit M2 biomarker

Abbreviations: CHB, chronic hepatitis B; LC, liver cirrhosis; HBC, hepatitis B cirrhosis; RR, ribonucleotide reductase; AASLD, American Association for the Study of Liver Diseases; HBsAg, hepatitis B surface antigen; HBsAb, hepatitis B surface antibody; HBeAg, hepatitis B e antigen; APRI, aspartate aminotransferase-to-platelet ratio index; MELD, Model for End-Stage Liver Disease; TNM, tumor node metastasis classification; TBIL, total bilirubin; HBeAb, hepatitis B e antibody; PEIU, Paul-Ehrlich-Institut units; S/CO, signal to cutoff ratio; HBcAb, hepatitis B c antibody; FIB4, fibrosis-4 score; Lg, Log₁₀

Laboratory Medicine 2023;54:626-632; <https://doi.org/10.1093/labmed/lmad013>

ABSTRACT

Background: Ribonucleotide reductase subunit M2 (RRM2) plays a key role in cell and hepatitis B virus (HBV) replication. Nevertheless, its clinical implications for managing liver diseases have been inadequately studied.

Methods: A total of 412 participants were enrolled, including 60 healthy control individuals, 55 patients with chronic hepatitis B (CHB), 173 patients with cirrhosis, and 124 patients with hepatocellular carcinoma (HCC). Serum RRM2 was measured via ELISA.

Results: The level of serum RRM2 in patients with CHB, cirrhosis, and HCC was higher than that in healthy controls ($P < .05$). A large difference in serum RRM2 was found between HBV-related and non-HBV-related patients in the cirrhosis group ($P < .001$), compared with the difference between HBV-related HCC and non-HBV-related HCC

($P = .86$). In the HBV-related cirrhosis group, the serum RRM2 level showed significant positive correlations with HBV DNA, hepatitis B surface antigen, hepatitis B e antigen, Child-Pugh scores, and MELD scores and played a strong role in diagnosing HBV-related cirrhosis in CHB, compared with fibrosis-4 score and aspartate aminotransferase-to-platelet ratio index.

Conclusions: Serum RRM2 is a reliable biomarker for accurate HBV-related cirrhosis diagnosis and evaluation. Also, serum RRM2 could reflect the expression state of HBV replication in patients with HBV-related cirrhosis.

Hepatitis B virus (HBV) infection is endemic worldwide and is one of the leading causes of viral hepatitis in Southeast Asia. According to the World Health Organization, approximately 2 billion people worldwide have been infected with HBV, and the number of people with chronic HBV infection is approximately 350 million.¹ In China and Southeast Asian countries, most patients become infected with HBV during the perinatal period. Due to the immature immune function of young children, they cannot clear the virus in a timely manner and they become chronically infected with HBV as adults, when the immune system becomes able to effectively fight against the infection. As a result, the viral infection is usually acute and self-limiting. In some patients, the disease progresses to chronic hepatitis B (CHB), liver cirrhosis (LC), and HCC due to long-term inflammation. Approximately 20% of patients with CHB develop hepatitis B cirrhosis (HBC), and approximately 3% develop cirrhosis yearly.^{2,3}

Ribonucleotide reductase (RR) is present in all types of living cells; as the only enzyme catalyzing the reduction of ribonucleotides to the corresponding deoxyribonucleotides, it is involved in metabolizing nucleotides. Human RR consists mainly of large (RRM1) and small subunits (RRM2). These subunits play a key role in cell proliferation by providing not only various precursor deoxyribonucleotides but also regulating the balance of the content of various dNTPs in DNA synthesis and repair.⁴

DNA synthesis and repair heavily depend on the balance of the dNTP pool, and an imbalance in dNTP levels and their relative amounts can lead to cell death or abnormal genetic metabolism. As a DNA polymerase

substrate, dNTP affects all aspects of the replication process, and reduced RR activity decreases intracellular dNTPs levels, thereby inhibiting DNA synthesis and repair, resulting in cell-cycle arrest.⁵ Therefore, RR plays an important role in controlling cell proliferation and maintaining genome stability. Previous study reports, such as Li et al,⁶ have stated that the activity of this enzyme depends on the level of RRM2 protein.

Recent study results, such as those reported by Liu et al,⁷ have shown that RR has a crucial role in HBV replication and proliferation in hepatocytes. Shao et al¹¹ have suggested that RRM2 is a potential target against HBV replication, and its inhibitors are potential novel potential drugs against HBV and HCC. Also, Ricardo-Lax et al⁸ have reported that HBV can activate the production of RRM2 through the DNA damage pathway.

Based on its close relationship with HBV replication and propagation, RR is feasible in the study of chronic liver diseases, especially CHB and HBC. Therefore, we made a relevant analysis of RR in the diagnosis and evaluation of chronic liver diseases and liver cancer, to provide a theoretical basis for its practical application in the clinical setting and future antiviral therapy.

Materials and Methods

Study Population

A total of 412 participants were enrolled in our study. These included 60 healthy control individuals, 55 patients with CHB, 173 patients with cirrhosis (of whom 90 had HBV-related cirrhosis), and 124 patients with liver cancer (of whom 98 had HBV-related cancer). All included subjects were from inpatient and outpatient settings in our hospital, The First Affiliated Hospital, Zhejiang University, Hangzhou, China, from March 2018 through March 2020. Patients with CHB, cirrhosis, or liver cancer were diagnosed according to the recent guidelines of the American Association for the Study of Liver Diseases (AASLD).

We excluded patients infected with viruses other than HBV and other liver diseases; those with lung cancer, pancreatic cancer, and ovarian cancer, and other malignant tumors except liver cancer; those with other comorbidities, including heart diseases, systematic inflammation, chronic kidney disease, etc; and those who had undergone radiofrequency ablation and surgical procedures before blood specimen collection.

The study was performed in accordance with the Code of Ethics of the World Medical Association (Declaration of Helsinki) and was based on the ethical standards of our institution. All study participants provided written informed consent. The study was approved by the Ethics Committee of our hospital.

Data Detection and Collection

Peripheral venous blood was drawn from fasting patients in the early morning, and the blood specimens were numbered based on the order in which patient specimens were collected. The supernatant was removed after centrifugation and stored in a -80°C freezer. Circulating RRM2 levels were detected by Human RRM2 ELISA Kits (Shanghai Run-BioTech). The specimens had 3 biological repetitions, and the kit instructions were strictly followed during all operations.

Other blood tests and imaging examinations were provided by the Laboratory Department and Imaging Department of the First Affiliated Hospital of Zhejiang University, including aspartate aminotransferase

(AST), <40 U/L; alanine aminotransferase (ALT), <40 U/L; alkaline phosphatase (ALP), $40\text{--}150$ U/L; gamma-glutamyl transferase (GGT), $11\text{--}50$ U/L; total bilirubin (TBIL), <21 $\mu\text{mol/L}$; alpha-fetoprotein (AFP), <20 ng/mL; and HBV-related tests (HBV DNA, hepatitis B surface antigen [HBsAg], hepatitis B surface antibody [HBsAb], hepatitis B e antigen [HBeAg], hepatitis B e antibody [HBeAb], and hepatitis B c antibody [HBcAb]). We calculated the relevant index as follows: APRI = $([100 \times \text{AST}] / \text{upper limit of normal AST}) / \text{platelets (PLT)} (\times 10^9 / \text{L})$ ⁹ fibrosis-4 (FIB4) = $(\text{age} \times \text{AST [U/L]} / (\text{PLT } [10^9 / \text{L}] \times \text{ALT}^{1/2} [\text{U/L}]))$ ¹⁰

Statistical Analysis

We processed the data and specimens using SPSS Statistics software, version 25 (IBM) and GraphPad Prism 7 (GraphPad Software). Measurement data were expressed as mean (SD) ($\bar{x} \pm s$). Data between 2 groups were analyzed by independent sample *t* testing, area under the curve (AUC) comparisons between groups were made by *z* testing. Analysis of variance (ANOVA) was used among multiple data groups, with $P < .05$ indicating statistical significance. Independent variables potentially affecting RRM2 were screened by regression analysis; curves were fitted to predict the correlation between RRM2 and other indicators (correlation coefficient *R*).

Results

Clinical Characteristics of Participants

Depending on the type of HBV infection and final diagnosis, we divided the enrolled participants into 6 groups: healthy control, CHB, HBV-related cirrhosis, non-HBV-related cirrhosis, HBV-related HCC, and non-HBV-related HCC. As shown in **TABLE 1**, each group comprised more men than women. The average age of people in the healthy control, CHB, cirrhosis, and HCC groups was 47.3, 46.7, 52.7, and 61.6 years, respectively, which was consistent with the progression of chronic liver disease.

As we expected, healthy controls had good biochemical parameters. In contrast, patients in other groups had higher liver function indicators such as ALT and AST. Patients with CHB had the highest circulating HBV DNA virus, serum HBsAg, and HBeAg levels among patients infected with HBV.

Serum RRM2 Level in All Groups

The serum level of RRM2 in patients with liver disease and healthy controls is shown in **FIGURE 1**. All patients had higher circulating RRM2 levels than healthy controls (mean [SD], $378.5 [79.8]$ U/L). In particular, RRM2 levels in patients with HBV-related cirrhosis and HCC were higher than that in patients with CHB. We further divided the cirrhosis and liver cancer groups into hepatitis B-related and non-hepatitis-B-related groups and observed that the HBV-related cirrhosis group had higher serum RRM2 levels than the non-HBV-related groups ($3827.3 [3158.3]$ U/L vs $761.5 [898.9]$ U/L; $P < .001$); there was no significant difference in serum RRM2 levels between HBV-related HCC and non-HBV-related HCC groups ($3326.6 [2885.1]$ U/L vs $3173.5 [4737.8]$ U/L; $P = .86$).

Serum RRM2 Values in Cirrhosis

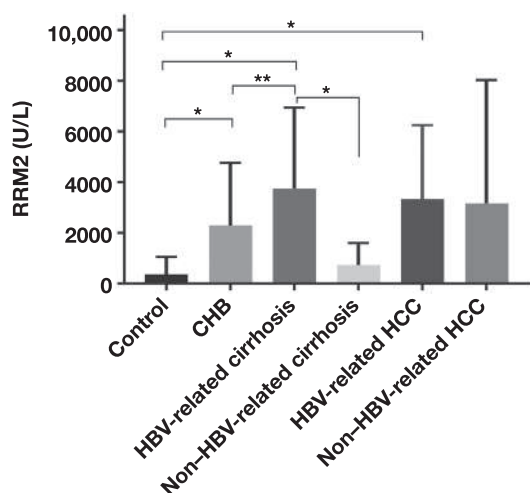
Because we found significantly higher serum RRM2 in the HBV-related cirrhosis group than that in the CHB group, we further analyzed the

TABLE 1. Characteristics of the Patients Enrolled in the Study

Variable	Control	CHB	HBV-related cirrhosis	Non-HBV-related cirrhosis	HBV-related HCC	Non-HBV-related HCC
Male/Female	32/28	37/18	68/22	50/33	84/14	18/8
Age (y), mean (SD)	47.3 (10.4)	46.7 (13.4)	50.0 (9.8)	55.6 (11.8)	60.9 (10.0)	61.6 (10.5)
ALT (IU/L), mean (SD)	23.9 (13.7)	278.3 (365.8)	75.0 (134.7)	72.1 (190.7)	82.5 (100.4)	72.7 (100.2)
AST (IU/L), mean (SD)	20.9 (7.2)	148.1 (168.2)	70.2 (107.8)	76.4 (124.0)	117.0 (216.3)	125.9 (241.3)
ALP (IU/L), mean (SD)	66.6 (22.0)	116.8 (101.1)	109.3 (91.4)	135.8 (113.7)	104.4 (77.5)	137.8 (107.6)
GGT (IU/L), mean (SD)	39.3 (25.5)	126.1 (125.7)	64.2 (81.1)	125.8 (137.4)	107.9 (138.4)	137.0 (176.5)
TBIL (μ mol/L), mean (SD)	11.9 (7.9)	68.1 (104.4)	69.9 (104.3)	85.3 (127.2)	34.8 (62.0)	42.3 (72.2)
AFP, mean (SD)	4.0 (1.9)	17.2 (24.6)	67.7 (306.0)	5.0 (8.0)	4768.1 (5008.1)	5426.0 (18331.5)
HBV DNA (Log_{10} IU/mL), mean (SD)	—	4.0 (2.3)	2.6 (2.8)	—	1.6 (2.1)	—
HBsAg (IU/mL) $\times 10^5$, mean (SD)	—	121.2 (169.7)	10.1 (16.5)	—	2.5 (5.0)	—
HBsAb (mIU/mL), mean (SD)	—	7.1 (32.3)	35.7 (108.4)	—	0.6 (1.3)	—
HBeAg (PEIU/mL), mean (SD)	—	100.2 (164.1)	17.8 (67.2)	—	21.0 (8.9)	—
HBeAb (S/CO), mean (SD)	—	12.9 (20.7)	3.4 (10.3)	—	3.3 (2.2)	—
HBcAb (S/CO), mean (SD)	—	8.9 (1.9)	7.9 (3.7)	—	8.4 (1.0)	—

AFP, alpha-fetoprotein; ALP, alkaline phosphatase; ALT, alanine aminotransferase; AST, aspartate aminotransferase; GGT, gamma-glutamyl transferase; HBcAb, hepatitis B c antibody; HBeAb, hepatitis B e antibody; HBeAg, hepatitis B e antigen; HbsAb, hepatitis B surface antibody; HBsAg, hepatitis B surface antigen; HBV, hepatitis B virus; HCC, hepatocellular carcinoma; PEIU, Paul-Ehrlich-Institut units; S/CO, signal-to-cutoff ratio; TBIL, total bilirubin.

FIGURE 1. Serum ribonucleotide reductase subunit M2 (RRM2) in chronic liver disease and liver cancer. Comparison of serum RRM2 in healthy control individuals, as well as patients with chronic hepatitis B (CHB), hepatitis B virus (HBV)-related cirrhosis, non-HBV-related cirrhosis, HBV-related hepatocellular carcinoma (HCC), and non-HBV-related HCC. * $P < .001$; ** $P < .01$.



value of RRM2 in the diagnosis and clinical staging of patients with liver cirrhosis. We compared the diagnostic performance of serum RRM2 with widely used serum markers of fibrosis, namely, FIB4 and aspartate aminotransferase-to-platelet ratio index (APRI). We found that at the cutoff value of 1715.6 U/L, serum RRM2 provided a sensitivity and specificity of 87.5% and 66.6%, respectively, for diagnosing HBV-related cirrhosis from CHB. FIB4 demonstrated sensitivity and specificity of 95.4% and 59.4%, respectively, at the cutoff value of 1.04. In contrast, APRI showed sensitivity and specificity of 87.4% and 21.9%, respectively, at the cutoff value of 0.52.

ROC analysis showed that serum RRM2 had a similar diagnostic value as FIB4 (AUC, 0.684 vs 0.737; $P = .45$) and had better AUC scores than APRI (AUC, 0.684 vs 0.462; $P < .01$). The detailed data are shown in **TABLE 2**. Also, when we used combined measurements of serum RRM2, APRI, and FIB4, we detected a higher AUC value (AUC = 0.791).

Serum RRM2 was also shown to be a potential indicator to assess the severity of HBV-related cirrhosis. Decompensated cirrhosis in patients in the HBV group had higher serum RRM2 levels than compensated cirrhosis in patients with HBV (4525.4 [3555.1] vs 2908.9 [2232.9] U/L; $P = .009$). In contrast, there was no significant difference between the compensated and decompensated groups of patients with non-HBV-related cirrhosis (818.9 [1038.8] vs 729.0 [807.5] U/L; $P = .93$) (**FIGURE 2A**). Using the Child-Pugh classification to verify the severity of cirrhosis in patients with that disease, we also acquired significant results, given that patients with Child-Pugh C who had HBV-related cirrhosis had a higher serum RRM2 level than that in patients with Child-Pugh A ($P < .001$) and Child-Pugh B ($P = .01$; **FIGURE 2B**).

A correlation between serum RRM2 and Child-Pugh and Model for End-Stage Liver Disease (MELD) scores was further examined. A significant positive correlation was found between RRM2 and Child-Pugh scores ($R = 0.37$; $P < .001$). MELD scores also showed a positive and significant correlation with RRM2 ($R = 0.40$; $P < .001$) (**FIGURE 2C**, **FIGURE 2D**).

Correlation between Serum RRM2 and HCC Stage and Biomarkers

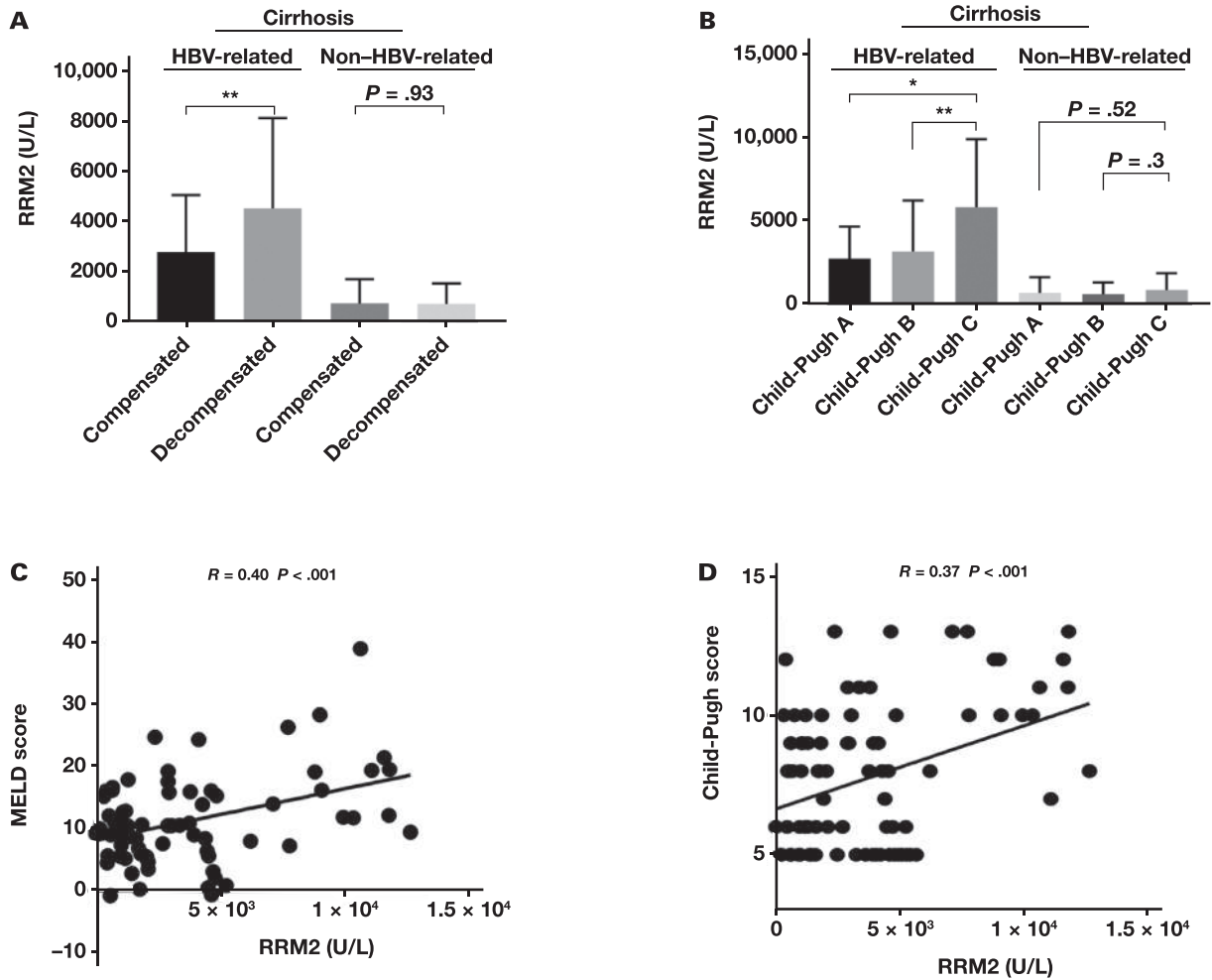
Participants in this study included 98 patients with HBV-associated HCC and 26 patients with non-HBV-associated HCC. Based on tumor node metastasis classification (TNM), among patients with HBV-related HCC, 44 patients had stage I disease, 33 patients had stage II/III, and 21 patients had stage IV. There was no significant difference in serum RRM2 among the aforementioned groups; the numbers of patients with

TABLE 2. Diagnostic Performance of RRM2, FIB4, and APRI, Separately and in Combination, in the Prediction of HBV-Related Cirrhosis

Analyte	AUC (%)	Sensitivity (%)	Specificity (%)	Cutoff	Youden index (%)	P value
RRM2	68.4	87.5	66.6	1715.6	54.2	.002
FIB4	73.7	95.4	59.4	1.0	36.0	<.001
APRI	46.2	87.4	21.9	0.5	21.4	.52
RRM2 + FIB4 + APRI	79.1	74.7	84.4	—	59.1	<.001

APRI, aspartate aminotransferase-to-platelet ratio index; FIB4, fibrosis-4 score; HBV, hepatitis B virus; RRM2, ribonucleotide reductase subunit M2.

FIGURE 2. Serum ribonucleotide reductase subunit M2 (RRM2) in cirrhosis. A, Serum RRM2 level in compensated and decompensated cirrhosis. B, Serum ribonucleotide reductase subunit M2 (RRM2) in cirrhosis. * $P < .001$; ** $P < .01$. Correlation analysis between RRM2 and MELD score (C) or Child-Pugh score (D).



stage I, II/III, and IV disease in the non-HBV-related group were 11, 9, and 6, respectively. The 1-way ANOVA results did not indicate a significant difference between the groups in patients in the HBV-related disease ($P = .42$) or non-HBV-related disease ($P = .72$) groups (Supplementary Figure 1).

A total of 57 patients with HCC underwent surgical resection or liver biopsy (9 in the non-HBV-related and 48 in the HBV-related groups). We obtained the immunohistochemical data of the tumors of these patients and made the correlation between these biomarkers with serum RRM2 levels. However, no obvious correlation was shown between serum RRM2 and immunohistochemical results (AFP and glypican-3). More details are shown in TABLE 3.

Linear Correlation between Serum RRM2 and HBV Markers

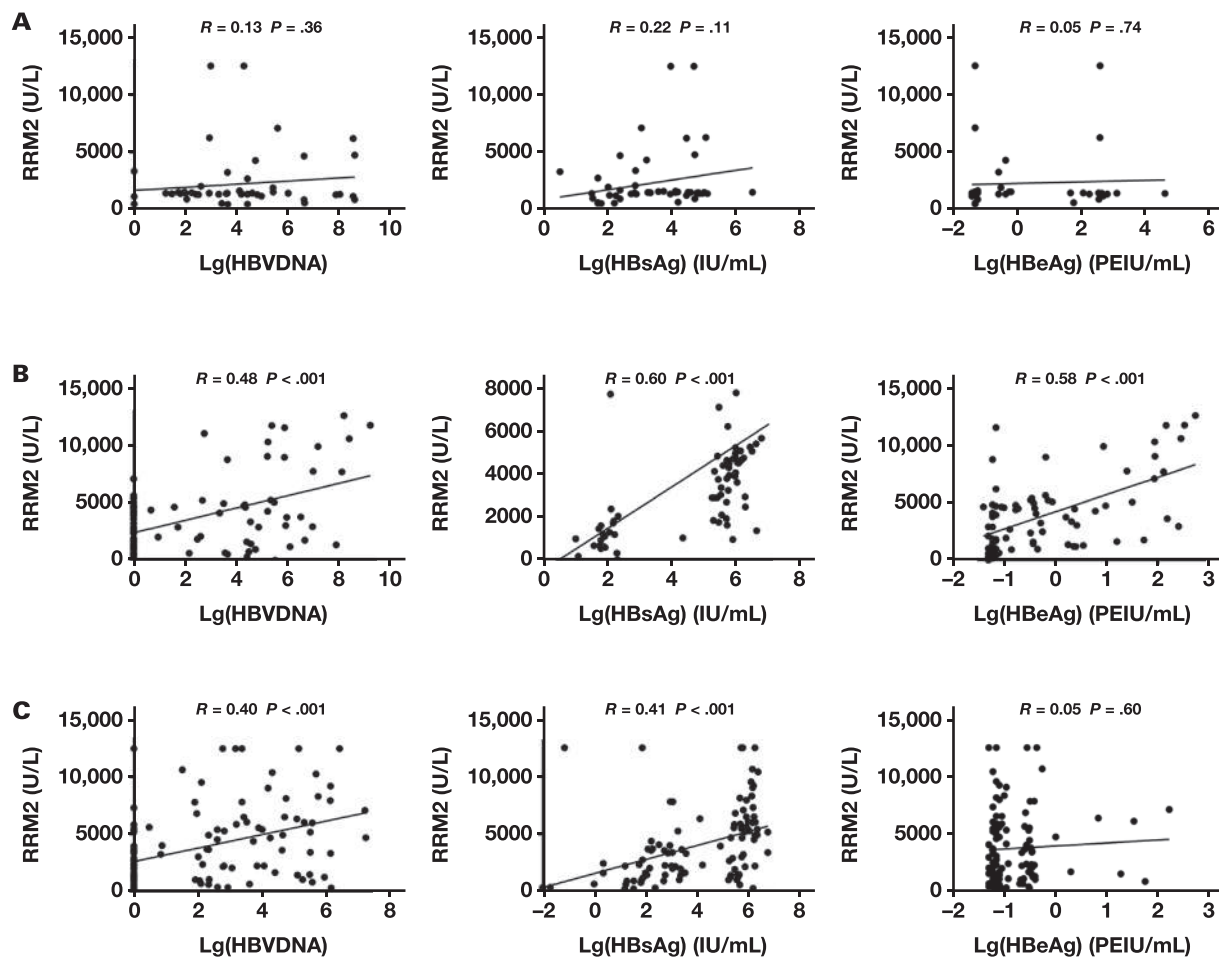
The results mentioned earlier herein demonstrated a strong association between serum RRM2 levels and HBV infection, especially in HBV-related cirrhosis. We used the Pearson correlation coefficient to analyze the linear correlation between RRM2 and HBV DNA, HBsAg, and HBeAg. There was no significant difference between serum RRM2 levels and HBV DNA, HBsAg, and HBeAg in the CHB group ($P > .05$; FIGURE 3A). The correlation coefficients between serum RRM2 level and HBV DNA, HBsAg, and HBeAg in patients with HBV-related cirrhosis were $R = 0.48$ ($P < .001$), $R = 0.60$ ($P < .001$), and $R = 0.58$ ($P < .001$), respectively (FIGURE 3B). In patients with HBV-related HCC,

TABLE 3. Correlation between RRM2 and Immunohistochemical Biomarkers in HCC

Variable	Result	HBV-related HCC			Non-HBV-related HCC		
		No.	RRM2	P value	No.	RRM2	P value
AFP	Negative	10	3104 (1797)	.88	5	3019 (4764)	—
	Positive	5	3368 (4568)		—	—	
GPC-3	Negative	4	2819 (3061)	.59	2	6350 (6150)	.35
	Positive	32	3821 (5079)		8	2394 (3999)	

AFP, alpha-fetoprotein; GPC-3, glypican-3; HBV, hepatitis B virus; HCC, hepatocellular carcinoma; RRM2, ribonucleotide reductase subunit M2.

FIGURE 3. Serum ribonucleotide reductase subunit M2 (RRM2) with hepatitis B virus (HBV). Linear relevance analysis between serum RRM2 and HBV-related indicators in chronic hepatitis B (A), HBV-related cirrhosis (B), and HBV-related hepatocellular carcinoma (C). HBeAg, hepatitis B e antigen; HBsAg, hepatitis B surface antigen; PEIU, Paul-Ehrlich-Institut units.



significant differences were found between circulating RRM2 and HBV DNA ($R = 0.40$; $P < .001$) and HBsAg ($R = 0.41$; $P < .001$) but not between RRM2 and HBeAg ($R = 0.05$; $P = .60$; **FIGURE 3C**).

We further performed a subgroup analysis in patients with HBV-related cirrhosis based on the level of ALT, AST, ALP, GGT, TBIL, and AFP. Patients with HBV-related cirrhosis with ALT, AST, TBIL, or AFP of twice the normal upper limit had higher RRM2 levels, compared with patients with those values in the normal ranges (**TABLE 4**). Also, better correlation performance was shown between RRM2 and HBV DNA, HBsAg, and HBeAg in patients with HBV-related cirrhosis whose ALT or ALP values were twice the normal upper limit (ALT-R value, HBV DNA:

0.58 vs 0.36; HBsAg: 0.71 vs 0.57; HBeAg: 0.59 vs 0.43; ALP-R value, HBV DNA: 0.82 vs 0.42; HBsAg: 0.72 vs 0.59; HBeAg: 0.76 vs 0.52).

Discussion

RR is an enzyme necessary for biological DNA synthesis and is one of the most highly conserved enzymes. It consists of a large subunit (RRM1) and a small subunit (RRM2), which are present at the site of substrate binding and metastable effectors and which control substrate specificity and enzyme activity. The contact inhibition region carried by RRM2 can control the substrate conversion function; hence, RRM2 has both

TABLE 4. Correlation between RRM2 and Biochemical Indicators in HBV-Related Cirrhosis

Analyte	Range	No.	RRM2	P value	R-Lg(HBV DNA)	R-Lg(HBsAg)	R-Lg(HBeAg)
ALT	NR	58	2980 (2208)	.008	0.36	0.57	0.43
	>2 ULN	17	5141 (4595)		0.58	0.71	0.59
AST	NR	51	2870 (272)	.001	0.33	0.72	0.34
	>2 ULN	24	5580 (933)		0.36	0.70	0.57
ALP	NR	67	3665 (349)	.52	0.42	0.59	0.52
	>2 ULN	13	4286 (1080)		0.82	0.72	0.76
GGT	NR	60	3366 (300)	.09	0.46	0.67	0.56
	>2 ULN	19	4705 (1041)		0.54	0.62	0.50
TBIL	NR	56	3088 (405)	.04	0.36	0.46	0.58
	>2 ULN	22	4644 (581)		0.51	0.60	0.54
AFP	NR	67	3305 (307)	.004	0.60	0.60	0.53
	>2 ULN	14	5981 (1304)		0.49	0.70	0.77

AFP, alpha-fetoprotein; ALP, alkaline phosphatase; ALT, alanine aminotransferase; AST, aspartate aminotransferase; GGT, gamma-glutamyl transferase; HBV, hepatitis B virus; NR, normal range; R-Lg(HBeAg), correlation between RRM2 level and the Log₁₀ of hepatitis B e antigen; R-Lg(HBsAg), correlation between RRM2 level and the Log₁₀ of hepatitis B surface antigen; R-Lg(HBV DNA), correlation between RRM2 level and the Log₁₀ of HBV DNA; RRM2, ribonucleotide reductase subunit M2; TBIL, total bilirubin; ULN, upper limit of normal.

catalytic and regulatory roles. The transcription of *RRM1* and *RRM2* is regulated by the cell cycle, and mRNA of *RRM1* and *RRM2* is not detected in G0/G1 phase cells; the mRNA expression of *RRM1* and *RRM2* reaches the maximum level in the S phase. *RRM1* has a half-life of 18–24 hours, and its level is almost constant in proliferating cells and relatively excessive throughout the cell cycle. In contrast, *RRM2* protein is specifically expressed in the S phase and synthesized in the late G1 or early S phase, with a shorter half-life of about 3–4 hours. It is rapidly degraded and then slowly accumulates in cells until late mitosis.¹¹ Therefore, the enzyme activity depends on the level of *RRM2* protein. Thus, in this study, the level of *RRM2* in the peripheral blood of patients was measured, to reflect the RR enzyme activity.

In our study, patients with CHB had significantly higher serum *RRM2* levels than healthy controls ($P < .001$). The same trend was observed in patients with cirrhosis, indicating that HBV can increase *RRM2* levels in hepatocytes, which is consistent with the findings of a previous study.⁸ In patients with cirrhosis, *RRM2* levels in the HBV-related group were obviously higher than those in healthy controls ($P < .001$) and CHB ($P < .01$); those levels in the non-HBV-related group were slightly higher than the levels in healthy controls ($P = .01$) but significantly lower compared with the levels in the CHB group ($P < .001$). The results of further correlation analysis showed the strong relevance between *RRM2* and HBV-related indicators (HBV DNA, HBsAg, and HBeAg) in the cirrhosis group. Our conclusion based on the aforementioned results is that cirrhosis and HBV infection could facilitate the serum *RRM2* level and had a synergistic effect on the rise of serum *RRM2*.

Because HBV does not carry RR genes, it cannot express RR enzyme and needs to rely on dNTPs in hepatocytes to complete the replication of its virions. HBV replication in primary rat hepatocytes has been reported to require HBV protein HBx to induce quiescent hepatocytes to exit the G0 phase and enter and arrest the G1 phase. Also, exiting the G0 and entering the G1 phase activates HBV polymerase and increases *RRM2* levels, enhancing HBV replication and providing a favorable cellular environment for HBV replication.¹²

These findings suggest that activation of *RRM2* production in hepatocytes by HBV was a potential cause of high serum *RRM2* levels in

patients with HBV. Results of the subgroup analysis revealed that patients with HBV-related cirrhosis with high ALT levels had higher *RRM2* levels and better correlations between *RRM2* and HBV-related indexes. These findings might partially be explained by the fact that in hepatocyte injury *RRM2* detected in the blood is more accurate and closer to the actual level of *RRM2* in hepatocytes and, as a result, more related to the secreted substances, such as HBV DNA, HBsAg, and HBeAg.

Previous study reports^{13–15} have stated that FIB4 may be more reliable than APRI for staging fibrosis in CHB and only moderately accurately and sensitively with both scoring systems, which is consistent with the findings from our study. We expand the literature by providing information regarding the accuracy of serum *RRM2* in diagnosing HBV-related cirrhosis and comparing it with currently widely used indicators. The ROC analysis revealed that serum *RRM2* achieved a similar diagnostic value to FIB4 and was better than APRI. Moreover, *RRM2* achieved the highest Youden index, which represented the best screening program. Circulating *RRM2* also acted as a good biomarker to assess the severity of liver cirrhosis. Compared with FIB4 and APRI, which comprise multiple indicators and require complex calculation formulas, *RRM2* is easy to apply and achieves similar clinical applications without a cumbersome calculation process.

Serum *RRM2* level was also high in patients with HBV-related HCC. Cancer cells rely on RR for dNTP biosynthesis; therefore, elevated RR expression is a feature of many types of cancer. The results of previous study^{16–18} have revealed *RRM2* overexpression in various malignancies, including oral, colorectal, and bladder cancers. Elford et al¹⁹ found a significant correlation between RR activity and tumor growth rate in a rat liver cancer model, with differences in RR enzyme activity of as high as 200-fold between fast-growing and slow-growing tumor cells. In our study findings, there was no significant trend in serum *RRM2* between HBV-associated cirrhosis and HBV-associated HCC or HBV-associated and non-HBV-associated HCC. These findings suggest that *RRM2* is not a biomarker of neoplastic transformation in chronic liver diseases.

There were some limitations to this experiment. First, the number of patients with various types of chronic liver diseases and liver cancers was quite small, and the study was somewhat biased; the results need to be further confirmed by larger samples and multicenter studies.

Second, there was a lack of pathological results; serum RRM2 may be unstable due to the influence of some unknown factors. Further testing of the pathological findings of the extent of liver fibrosis and intrahepatocellular RRM2 levels is needed to refine the conclusions.

Conclusions

RRM2 is a reliable biomarker for accurate diagnosis and evaluation of HBV-related cirrhosis. Moreover, the expression state of HBV replication in patients with cirrhosis and HBV can be indicated by serum RRM2.

Supplementary Data

Supplemental figures and tables can be found in the online version of this article at www.labmedicine.com.

Acknowledgments

The work was supported by the The First Affiliated Hospital of Zhejiang University, Hangzhou, China.

Conflict of Interest Disclosure

The authors have nothing to disclose.

REFERENCES

1. The Polaris Observatory Collaborators. Global prevalence, treatment, and prevention of hepatitis B virus infection in 2016: a modelling study. *Lancet Gastroenterol Hepatol*. 2018;3(6):383–403. doi: [10.1016/S2468-1253\(18\)30056-6](https://doi.org/10.1016/S2468-1253(18)30056-6)
2. Guan R, Lui HF. Treatment of hepatitis B in decompensated liver cirrhosis. *Int J Hepatol*. 2011;2011:918017. doi: [10.4061/2011/918017](https://doi.org/10.4061/2011/918017)
3. Hu KQ. A practical approach to management of chronic hepatitis B. *Int J Med Sci*. 2005;2(1):17–23. doi: [10.7150/ijms.2.17](https://doi.org/10.7150/ijms.2.17)
4. Guarino E, Salguero I, Kearsey SE. Cellular regulation of ribonucleotide reductase in eukaryotes. *Semin Cell Dev Biol*. 2014;30:97–103. doi: [10.1016/j.semcdb.2014.03.030](https://doi.org/10.1016/j.semcdb.2014.03.030)
5. Wijerathna SR, Ahmad MF, Xu H, et al. Targeting the large subunit of human ribonucleotide reductase for cancer chemotherapy. *Pharmaceuticals*. 2011;4(10):1328–1354. doi: [10.3390/ph4101328](https://doi.org/10.3390/ph4101328)
6. Li C, Zheng J, Chen S, et al. RRM2 promotes the progression of human glioblastoma. *J Cell Physiol*. 2018;233(10):6759–6767. doi: [10.1002/jcp.26529](https://doi.org/10.1002/jcp.26529)
7. Liu X, Xu Z, Hou C, et al. Inhibition of hepatitis B virus replication by targeting ribonucleotide reductase M2 protein. *Biochem Pharmacol*. 2016;103:118–128. doi: [10.1016/j.bcp.2016.01.003](https://doi.org/10.1016/j.bcp.2016.01.003)
8. Ricardo-Lax I, Ramanan V, Michailidis E, et al. Hepatitis B virus induces RNR-R2 expression via DNA damage response activation. *J Hepatol*. 2015;63(4):789–796. doi: [10.1016/j.jhep.2015.05.017](https://doi.org/10.1016/j.jhep.2015.05.017)
9. Wai C-T, Greenon JK, Fontana RJ, et al. A simple noninvasive index can predict both significant fibrosis and cirrhosis in patients with chronic hepatitis C. *Hepatology*. 2003;38(2):518–526. doi: [10.1053/jhep.2003.50346](https://doi.org/10.1053/jhep.2003.50346)
10. Sterling RK, Lissen E, Clumeck N, et al; APRICOT Clinical Investigators. Development of a simple noninvasive index to predict significant fibrosis in patients with HIV/HCV coinfection. *Hepatology*. 2006;43(6):1317–1325. doi: [10.1002/hep.21178](https://doi.org/10.1002/hep.21178)
11. Shao J, Liu X, Zhu L, Yen Y. Targeting ribonucleotide reductase for cancer therapy. *Expert Opin Ther Targets*. 2013;17(12):1423–1437. doi: [10.1517/14728222.2013.840293](https://doi.org/10.1517/14728222.2013.840293)
12. Cohen D, Adamovich Y, Reuven N, Shaul Y. Hepatitis B virus activates deoxynucleotide synthesis in nondividing hepatocytes by targeting the R2 gene. *Hepatology*. 2010;51(5):1538–1546. doi: [10.1002/hep.23519](https://doi.org/10.1002/hep.23519)
13. Kim BK, Kim DY, Park JY, et al. Validation of FIB-4 and comparison with other simple noninvasive indices for predicting liver fibrosis and cirrhosis in hepatitis B virus-infected patients. *Liver Int*. 2010;30(4):546–553. doi: [10.1111/j.1478-3231.2009.02192.x](https://doi.org/10.1111/j.1478-3231.2009.02192.x)
14. Mallet V, Dhalluin-Venier V, Roussin C, et al. The accuracy of the FIB-4 index for the diagnosis of mild fibrosis in chronic hepatitis B. *Aliment Pharmacol Ther*. 2009;29(4):409–415. doi: [10.1111/j.1365-2036.2008.03895.x](https://doi.org/10.1111/j.1365-2036.2008.03895.x)
15. Xiao G, Yang J, Yan L. Comparison of diagnostic accuracy of aspartate aminotransferase to platelet ratio index and fibrosis-4 index for detecting liver fibrosis in adult patients with chronic hepatitis B virus infection: a systemic review and meta-analysis. *Hepatology*. 2015;61(1):292–302. doi: [10.1002/hep.27382](https://doi.org/10.1002/hep.27382)
16. Morikawa T, Maeda D, Kume H, Homma Y, Fukayama M. Ribonucleotide reductase M2 subunit is a novel diagnostic marker and a potential therapeutic target in bladder cancer. *Histopathology*. 2010;57(6):885–892. doi: [10.1111/j.1365-2559.2010.03725.x](https://doi.org/10.1111/j.1365-2559.2010.03725.x)
17. Liu X, Zhang H, Lai L, et al. Ribonucleotide reductase small subunit M2 serves as a prognostic biomarker and predicts poor survival of colorectal cancers. *Clin Sci (Lond)*. 2013;124(9):567–578. doi: [10.1042/CS20120240](https://doi.org/10.1042/CS20120240)
18. Khor GH, Froemming GRA, Zain RB, Abraham MT, Thong KL. Screening of differential promoter hypermethylated genes in primary oral squamous cell carcinoma. *Asian Pac J Cancer Prev*. 2014;15(20):8957–8961. doi: [10.7314/apjcp.2014.15.20.8957](https://doi.org/10.7314/apjcp.2014.15.20.8957)
19. Elford HL, Freese M, Passamani E, Morris HP. Ribonucleotide reductase and cell proliferation: I. Variations of ribonucleotide reductase activity with tumor growth rate in a series of rat hepatomas. *J Biol Chem*. 1970;245(20):5228–5233.

Associations between apolipoprotein B/A1 ratio, lipoprotein(a), and the risk of metabolic-associated fatty liver diseases in a Korean population

Kyoung-Jin Park, MD, PhD¹ 

¹Department of Laboratory Medicine, Samsung Changwon Hospital, Sungkyunkwan University School of Medicine, Changwon, Republic of Korea. Corresponding author: Kyoung-Jin Park; unmar21@gmail.com.

Key words: metabolic-associated fatty liver disease (MAFLD); apolipoprotein B/A1 ratio; lipoprotein(a); Korean population

Abbreviations: MAFLD, metabolic-associated fatty liver disease; apo B/A1 apolipoprotein B/A1 ratio; NAFLD, nonalcoholic fatty liver disease; CVD, cardiovascular disease; BMI, body mass index; AST, aspartate aminotransferase; ALT, alanine aminotransferase; GGT, gamma-glutamyltransferase; HDL, high-density lipoprotein; LDL, low-density lipoprotein; HbA1c, hemoglobin A1c; hs-CRP, high-sensitivity C-reactive protein; HOMA-IR, homeostasis model assessment of insulin resistance; FIB-4, fibrosis-4; NFS, NAFLD fibrosis score; APRI, AST/platelet ratio index; APASL, Asian Pacific Association for the Study of the Liver

Laboratory Medicine 2023;54:633-637; <https://doi.org/10.1093/labmed/lmad021>

ABSTRACT

Objective: Metabolic-associated fatty liver disease (MAFLD) is new nomenclature for the fatty liver condition associated with metabolic dysfunction. This study aimed to investigate the association between apolipoprotein B/A1 (apo B/A1) ratio, lipoprotein(a), and MAFLD in a Korean population.

Methods: This study consisted of 14,419 subjects in the Korean population. Multivariate logistic regression was conducted to analyze the association between apo B/A1 ratio and MAFLD.

Results: The prevalence of MAFLD in the general Korean population was 34.5%. The apo B/A1 ratio (odds ratio: 3.913, $P = .019$) was independently associated with MAFLD. Lipoprotein(a) was significantly lower in patients with MAFLD with hepatic fibrosis ($P < .0001$).

Conclusion: Apolipoprotein B/A1 ratio and lipoprotein(a) have opposite associations with MAFLD. This study suggests that lipoprotein(a) should be used with caution as a biomarker for MAFLD, especially in patients with hepatic fibrosis.

Introduction

Nonalcoholic fatty liver disease (NAFLD) is one of the most common chronic liver diseases, with a global prevalence of 25%.¹ Metabolic abnormalities, including diabetes and dyslipidemia, are associated with NAFLD. Furthermore, NAFLD is significantly associated with an increased risk of cardiovascular disease (CVD) and CVD-related mortality.¹ Therefore, it is important to clarify the biomarkers for CVD in patients with NAFLD.

High apolipoprotein B/A1 ratio (apo B/A1), high lipoprotein(a), and NAFLD have been suggested as a risk factors for CVD.¹⁻³ The apo B/A1 is also associated with NAFLD, whereas the relationship between lipoprotein(a) and NAFLD remains controversial.⁴⁻⁷ Recent studies have reported that lipoprotein(a) in patients with NAFLD was lower than that in non-NAFLD patients, and the predictive value of lipoprotein(a) for CVD risk is impaired in patients with NAFLD.⁴⁻⁶

Recently, “metabolic-associated fatty liver disease (MAFLD)” has been proposed to replace “nonalcoholic fatty liver disease.”^{8,9} Metabolic-associated fatty liver disease is diagnosed based on hepatic steatosis detected by imaging, blood biomarkers, or histology in addition to the presence of overweight/obesity, type 2 diabetes, or evidence of metabolic dysregulation. It has been reported that the MAFLD criteria can better identify patients with metabolic dysfunction and high risk of disease progression, including CVD, than NAFLD criteria.¹⁰

Currently, few studies regarding the association between apolipoprotein and lipoprotein(a) and MAFLD have been performed. This study aimed to investigate the association between apolipoprotein B/A1 (apo B/A1) ratio, lipoprotein(a), and MAFLD based on new diagnostic criteria in a Korean population.

Materials and Methods

The study subjects were enrolled from the general Korean population that visited the author's institution for a routine health checkup. This cross-sectional study consisted of 14,419 adults who underwent abdominal ultrasonography among 51,496 subjects in the Korean population visiting a comprehensive health promotion center from January 2021 to December 2021. Clinical and biochemical data include age, gender, medical history, systolic blood pressure, diastolic blood pressure, body mass index (BMI), waist circumference, total protein, albumin, aspartate aminotransferase (AST), alanine aminotransferase (ALT), gamma-glutamyltransferase

TABLE 1. Clinical and laboratory data of Korean population with and without MAFLD^a

	Non-MAFLD			MAFLD			P value
	Male (n = 5447)	Female (n = 3994)	Total (n = 9441)	Male (n = 4216)	Female (n = 762)	Total (n = 4978)	
Age (y)	47 (46–47)	44 (44–44)	45 (45–46)	46 (45–46)	47 (46–48)	46 (46–46)	.0002
Sex (M/F)	5447/3994 (1.36)			4216/762 (5.53)			<.0001
Waist circumference (cm)	84.4 (84.2–84.6)	78.3 (78.1–78.6)	81.9 (81.7–82.1)	92.9 (92.7–93.3)	90.6 (89.6–91.7)	92.7 (92.4–93.0)	<.0001
Body mass index (/kg/m ²)	23.5 (23.4–23.6)	21.5 (21.4–21.6)	22.7 (22.7–22.8)	26.5 (26.3–26.6)	26.6 (26.3–27.0)	26.5 (26.4–26.6)	<.0001
Waist-hip ratio	0.88 (0.88–0.88)	0.87 (0.86–0.87)	0.87 (0.87–0.88)	0.92 (0.92–0.92)	0.92 (0.92–0.93)	0.92 (0.92–0.92)	<.0001
Total protein (g/dL)	7.3 (7.3–7.3)	7.3 (7.3–7.3)	7.3 (7.3–7.3)	7.4 (7.4–7.4)	7.4 (7.3–7.4)	7.4 (7.4–7.4)	<.0001
Albumin (g/dL)	4.9 (4.9–4.9)	4.8 (4.8–4.8)	4.9 (4.9–4.9)	5.0 (4.9–5.0)	4.8 (4.8–4.8)	4.9 (4.9–4.9)	<.0001
AST (IU/L)	21 (21–21)	18 (17–18)	20 (19–20)	15 (24–25)	21 (20–22)	24 (24–24)	<.0001
ALT (IU/L)	21 (21–21)	14 (13–14)	18 (17–18)	32 (32–33)	23 (22–24)	31 (30–31)	<.0001
GGT (IU/L)	26 (25–26)	14 (14–14)	20 (19–20)	41 (40–41)	23 (22–25)	37 (36–38)	<.0001
Total cholesterol (mg/dL)	199 (198–200)	195 (194–197)	197 (196–198)	205 (204–207)	202 (198–205)	205 (203–206)	<.0001
HDL (mg/dL)	57 (56–57)	68 (67–68)	61 (61–61)	49 (48–49)	53 (52–54)	50 (49–50)	<.0001
LDL (mg/dL)	130 (128–131)	120 (119–121)	126 (125–126)	135 (134–136)	130 (128–132)	134 (133–135)	<.0001
Triglyceride (mg/dL)	102 (100–103)	76 (75–77)	90 (89–91)	156 (153–159)	124 (118–130)	151 (148–153)	<.0001
Apolipoprotein B/A1 ratio	0.72 (0.71–0.73)	0.58 (0.58–0.59)	0.66 (0.65–0.66)	0.84 (0.83–0.85)	0.75 (0.74–0.77)	0.83 (0.82–0.83)	<.0001
Apolipoprotein A (mg/dL)	157 (156–157)	170 (170–172)	162 (162–163)	147 (146–148)	155 (152–157)	148 (147–149)	<.0001
Apolipoprotein B (mg/dL)	113 (112–114)	100 (99–101)	107 (107–108)	124 (123–125)	116 (114–118)	123 (122–124)	<.0001
Lipoprotein(a) (mg/dL)	9.72 (9.23–10.21)	10.27 (9.72–10.94)	9.93 (9.62–10.28)	7.32 (6.87–7.65)	10.54 (9.05–11.56)	7.68 (7.39–8.05)	<.0001
Fasting glucose (mg/dL)	95 (95–96)	92 (92–92)	94 (94–94)	100 (100–101)	99 (98–100)	100 (99–100)	<.0001
HbA1C (%)	5.6 (5.6–5.6)	5.5 (5.5–5.5)	5.5 (5.5–5.6)	5.8 (5.8–5.8)	5.8 (5.8–5.9)	5.8 (5.8–5.8)	<.0001
Insulin (mU/L)	5.04 (4.96–5.14)	5.39 (5.28–5.49)	5.19 (5.12–5.26)	8.89 (8.70–9.08)	11.09 (10.56–11.53)	9.18 (9.01–9.34)	<.0001
HOMA-IR	1.198 (1.178–1.222)	1.231 (1.202–1.261)	1.211 (1.194–1.231)	2.261 (2.213–2.303)	2.727 (2.624–2.916)	2.332 (2.277–2.377)	<.0001
hs-CRP (mg/L)	0.47 (0.46–0.48)	0.37 (0.36–0.39)	0.43 (0.42–0.44)	0.82 (0.79–0.84)	1.03 (0.95–1.15)	0.845 (0.82–0.88)	<.0001
FIB-4	0.860 (0.849–0.869)	0.806 (0.794–0.816)	0.834 (0.826–0.844)	0.770 (0.759–0.781)	0.713 (0.692–0.747)	0.763 (0.753–0.772)	<.0001
NFS	–2.826 (–2.866 to –2.792)	–2.925 (–2.979 to –2.884)	–2.87 (–2.898 to –2.84)	–2.600 (–2.640 to –2.560)	–2.585 (–2.693 to –2.446)	–2.599 (–2.637 to –2.564)	<.0001
APRI	0.285 (0.282–0.288)	0.227 (0.224–0.230)	0.261 (0.258–0.263)	0.319 (0.314–0.324)	0.247 (0.241–0.257)	0.309 (0.306–0.313)	<.0001

ALT, alanine aminotransferase; APRI, AST/platelet ratio index; AST, aspartate aminotransferase; FIB-4, fibrosis-4; GGT, gamma-glutamyltransferase; HbA1C, hemoglobin A1c; HDL, high-density lipoprotein; HOMA-IR, homeostasis model assessment–insulin resistance; hs-CRP, high-sensitivity C-reactive protein; LDL, low-density lipoprotein; MAFLD, metabolic-associated fatty liver disease; NFS, NAFLD fibrosis score.

^aContinuous data are expressed as median (95% CI).

(GGT), total cholesterol, high density lipoprotein (HDL)-cholesterol, low density lipoprotein (LDL)-cholesterol, lipoprotein(a), apolipoprotein A1, apolipoprotein B, triglyceride, fasting glucose, insulin, HbA1c, insulin, and high-sensitivity C-reactive protein (hs-CRP).

The BMI was calculated as body weight (kilograms) divided by height in meters squared (m²). Scores were calculated by formulas presented in previous studies as follows^{11–14}: homeostasis model assessment–insulin resistance (HOMA-IR) = (insulin × glucose)/405; fibrosis-4 (FIB-4) = age × AST/platelet × ALT^{1/2}; NAFLD fibrosis score (NFS) = –1.675 + 0.037 × age + 0.094 × BMI + 1.13 × fasting glucose intolerance/diabetes (Yes = 1, No = 0) + 0.99 × AST/ALT ratio – 0.013 × platelet – 0.66 × albumin; AST/platelet ratio index (APRI) = [(AST/upper limit of normal AST) × 100]/platelets.

Hepatic steatosis was assessed using abdominal ultrasonography by experienced physicians and MAFLD was diagnosed according to the Asian Pacific Association for the Study of the Liver (APASL) guidelines.^{8,9} The presence of hepatic fibrosis in patients with MAFLD

was assessed by using serum panels such as NFS >0.676, FIB-4 >2.67, and APRI >0.562.^{12–14} Hepatic fibrosis was defined as a score above the cutoff in more than 2 panels. This study was approved by the Institutional Review Board of Samsung Changwon Hospital.

Clinical data between MAFLD and non-MAFLD were compared using the χ^2 and Mann-Whitney tests, as appropriate. Multivariate logistic regression was conducted to analyze the independent association between apo B/A1 ratio, lipoprotein(a), and MAFLD. All statistical analyses were done by SPSS statistical software (version 18).

Results

The prevalence of MAFLD in the general Korean population was 34.5% (4978/14,419) and was higher in males (43.6%, 4216/9663) than in females (16.0% 762/4,756). There were significant differences in clinical and laboratory findings between MAFLD and non-MAFLD in both males and females (TABLE 1). Patients with MAFLD had higher BMI, waist

circumference, waist-hip ratio, total cholesterol, LDL-cholesterol, triglyceride, apo B, apo B/A1 ratio, fasting glucose, HbA1c, insulin, HOMA-IR, and hs-CRP ($P < .0001$ for all, **TABLE 1**). Compared to MAFLD patients without hepatic fibrosis, lipoprotein(a), apo B, and apo B/A1 ratio were significantly lower in MAFLD patients with hepatic fibrosis ($P < .0001$) (**FIGURE 1**). Lipoprotein(a) levels are inversely associated with the MAFLD ($P < .0001$) (**TABLE 1**, **FIGURE 1**).

Multivariate logistic regression analysis revealed that apo B/A1 ratio (odds ratio: 3.913, $P = .019$), HOMA-IR (odds ratio: 1.536, $P = .000$), and HbA1c (odds ratio: 1.619, $P = .000$) were independently associated with the MAFLD, whereas total cholesterol ($P = .103$), LDL-cholesterol ($P = .225$), and triglyceride ($P = .104$) were not associated with MAFLD (**TABLE 2**).

Discussion

This study demonstrates that apo B/A1 ratio and lipoprotein(a) levels had opposite associations with MAFLD. The apo B as the carrier of chylomicrons and LDL is a key atherogenic lipoprotein, whereas apo A1 is the major component of HDL particles. The apo B/A1 ratio has

been reported to be directly related to the risk for CVD and can be useful for cardiovascular risk stratification.^{2,3} Also, lipoprotein(a) as an LDL-like particle has been reported to be another independent biomarker for CVD.³ Therefore, high apo B/A1 and high lipoprotein(a) have been considered conventional cardiovascular risk factors. However, this study showed that lipoprotein(a) level was paradoxically reduced in subjects with MAFLD, especially with hepatic fibrosis. Considering that lipoprotein(a) is synthesized in the liver, serum lipoprotein(a) levels might decrease in hepatic fibrosis. Furthermore, the apo B/A1 ratio level in patients with hepatic fibrosis was lower than that in patients without fibrosis. This suggests that hepatic fibrosis might attenuate the clinical utility of apo B/A1 ratio in patients with MAFLD.

There are some studies regarding inverse associations between lipoprotein(a) and diabetes and metabolic syndrome.^{15,16} It could be inferred that lipoprotein(a) level decreases in patients with MAFLD because diabetes and metabolic syndrome are also risk factors for NAFLD and MAFLD. Few studies regarding the association between apolipoprotein and lipoprotein(a) and MAFLD have been performed.¹⁷ To the best of my knowledge, this is the first study regarding the association between apo B/A1 ratio, lipoprotein(a), and MAFLD in a Korean

FIGURE 1. Comparison of lipoprotein(a) (A), apolipoprotein B (B), apolipoprotein B/A1 ratio (C) among subgroups with or without metabolic-associated fatty liver disease (MAFLD) and hepatic fibrosis. * $P < .0001$.

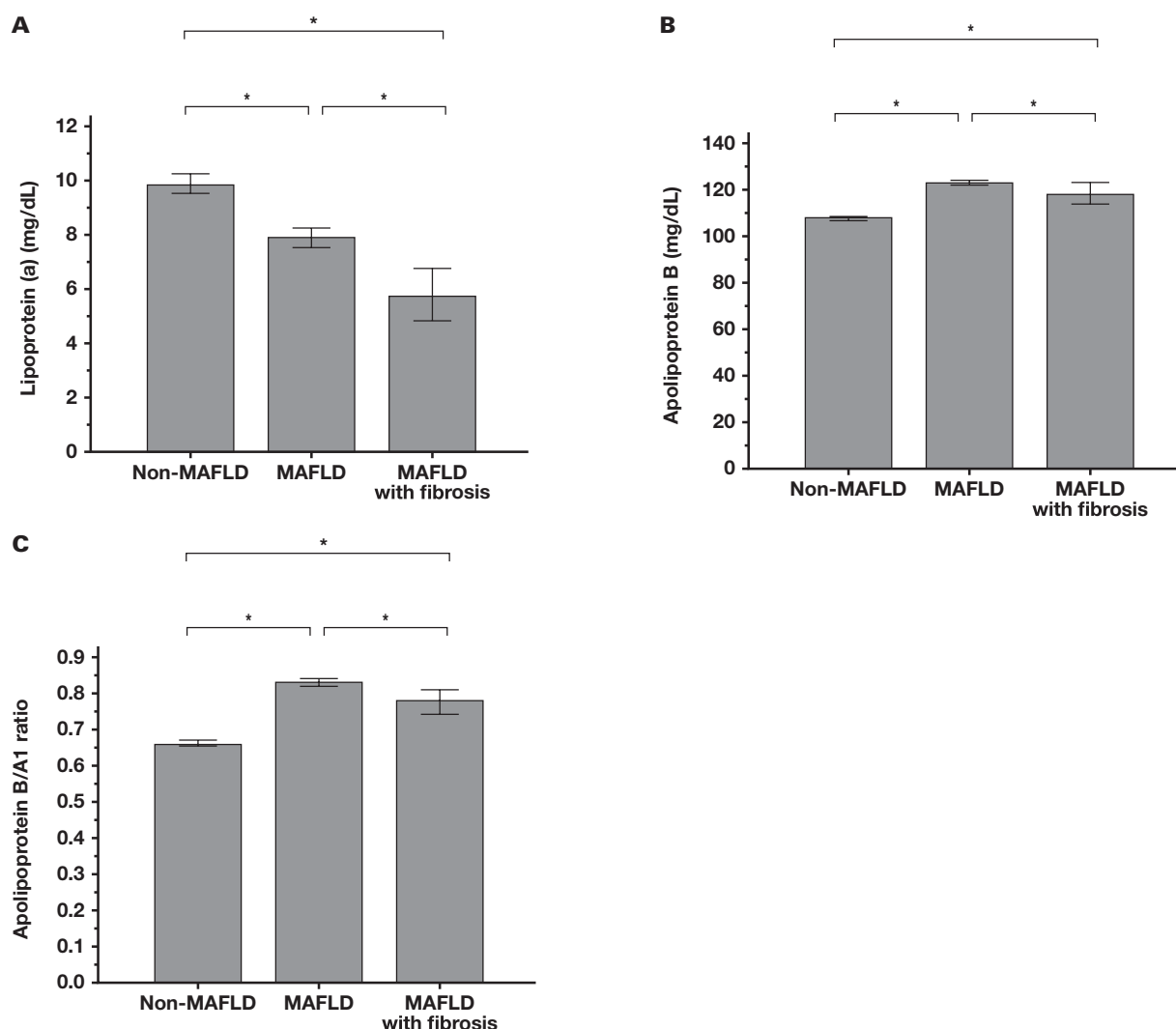


TABLE 2. Association with MAFLD by multiple logistic regression analysis

	Coefficients	Standard error	Walds	P value	Odds ratio	95% CI for odds ratio	
						Lower	Upper
Age	0.023	0.003	54.191	.000	1.023	1.017	1.03
Sex	−0.659	0.065	102.298	.000	0.517	0.455	0.588
Body mass index	0.269	0.018	227.096	.000	1.308	1.263	1.355
Waist circumference	0.047	0.006	54.762	.000	1.048	1.035	1.061
Cholesterol	−0.006	0.004	2.664	.103	0.994	0.987	1.001
LDL-cholesterol	−0.005	0.004	1.471	.225	0.995	0.987	1.003
HDL-cholesterol	−0.042	0.007	35.38	.000	0.959	0.945	0.972
Triglyceride	0.001	0.001	2.647	.104	1.001	1.000	1.002
Apolipoprotein A1	0.021	0.004	25.121	.000	1.021	1.013	1.029
Apolipoprotein B	0.015	0.005	7.271	.007	1.015	1.004	1.026
Apolipoprotein B/A1 ratio	1.364	0.583	5.486	.019	3.913	1.249	12.258
HOMA-IR	0.429	0.026	269.395	.000	1.536	1.459	1.617
HbA1C	0.482	0.043	125.802	.000	1.619	1.488	1.761
HS-CRP	0.027	0.011	6.052	.014	1.027	1.005	1.05

HbA1C, hemoglobin A1c; HDL, high-density lipoprotein; HOMA-IR, homeostasis model assessment-insulin resistance; hs-CRP, high-sensitivity C-reactive protein; LDL, low-density lipoprotein; MAFLD, metabolic-associated fatty liver disease.

population. This study could contribute to a better understanding of biomarker-driven therapeutics and clinical translation of the various therapeutics for fatty liver diseases.^{18,19}

Some limitations should be noted. First, fatty liver in this study was diagnosed by abdominal ultrasonography, which may be insensitive in case of mild steatosis and obesity. However, ultrasonography is the most common approach for fatty liver and the APASL guidelines also recommend use of imaging techniques as well as liver biopsy. Second, hepatic fibrosis was assessed by using noninvasive serum panels. Third, this was a cross-sectional study regarding the association between apo B/A1 ratio, lipoprotein(a), and MAFLD and does not prove the causality of them. Future prospective studies would be recommended to investigate a causal relationship between apo B/A1 ratio, lipoprotein(a), and MAFLD.

In conclusion, apo B/A1 ratio could be a useful biomarker for MAFLD, whereas lipoprotein(a) should be used with caution as a predictive biomarker for MAFLD in a Korean population. The apo B/A1 ratio was also less valuable as a predictive biomarker in MAFLD patients with hepatic fibrosis. Further clinical study would be warranted to investigate the relationship between lipoprotein(a) and CVD risk in MAFLD patients with hepatic fibrosis.

Acknowledgments

This work was supported by the Sungkyunkwan University School of Medicine, Samsung Changwon Hospital.

Conflict of Interest Disclosure

The author has nothing to disclose.

REFERENCES

- Powell EE, Wong VW, Rinella M. Non-alcoholic fatty liver disease. *Lancet*. 2021;397(10290):2212–2224. doi:10.1016/S0140-6736(20)32511-3.

- Andrikoula M, McDowell IF. The contribution of ApoB and ApoA1 measurements to cardiovascular risk assessment. *Diabetes Obes Metab*. 2008;10(4):271–278. doi:10.1111/j.1463-1326.2007.00714.x.
- Dahlen GH. Lp(a) lipoprotein in cardiovascular disease. *Atherosclerosis*. 1994;108(2):111–126. doi:10.1016/0021-9150(94)90106-6.
- Jung I, Kwon H, Park SE, et al. Serum lipoprotein(a) levels and insulin resistance have opposite effects on fatty liver disease. *Atherosclerosis*. 2020;308:1–5. doi:10.1016/j.atherosclerosis.2020.07.020.
- Nam JS, Jo S, Kang S, Ahn CW, Kim KR, Park JS. Association between lipoprotein(a) and nonalcoholic fatty liver disease among Korean adults. *Clin Chim Acta*. 2016;461:14–18. doi:10.1016/j.cca.2016.07.003.
- Wu T, Ye J, Shao C, et al. The ability of lipoprotein (a) level to predict early carotid atherosclerosis is impaired in patients with advanced liver fibrosis related to metabolic-associated fatty liver disease. *Clin Transl Gastroenterol*. 2022;13(7):e00504. doi:10.14309/ctg.0000000000000504.
- Brown WV, Moriarty PM, Remaley AT, Tsimikas S. JCL Roundtable: should we treat elevations in Lp(a)? *J Clin Lipidol*. 2016;10(2):215–224. doi:10.1016/j.jacl.2016.02.012.
- Eslam M, Sarin SK, Wong VW, et al. The Asian Pacific Association for the Study of the Liver clinical practice guidelines for the diagnosis and management of metabolic associated fatty liver disease. *Hepatol Int*. 2020;14(6):889–919. doi:10.1007/s12072-020-10094-2.
- Eslam M, Newsome PN, Sarin SK, et al. A new definition for metabolic dysfunction-associated fatty liver disease: an international expert consensus statement. *J Hepatol*. 2020;73(1):202–209. doi:10.1016/j.jhep.2020.03.039.
- Farahat TM, Ungan M, Vilaseca J, et al. The paradigm shift from NAFLD to MAFLD: a global primary care viewpoint. *Liver Int*. 2022;42(6):1259–1267. doi:10.1111/liv.15188.
- Matthews DR, Hosker JP, Rudenski AS, Naylor BA, Treacher DF, Turner RC. Homeostasis model assessment: insulin resistance and beta-cell function from fasting plasma glucose and insulin concentrations in man. *Diabetologia*. 1985;28(7):412–419. doi:10.1007/BF00280883.
- Sterling RK, Lissen E, Clumeck N, et al; APRICOT Clinical Investigators. Development of a simple noninvasive index to predict significant fibrosis in patients with HIV/HCV coinfection. *Hepatology*. 2006;43(6):1317–1325. doi:10.1002/hep.21178.
- Angulo P, Hui JM, Marchesini G, et al. The NAFLD fibrosis score: a noninvasive system that identifies liver fibrosis in patients with NAFLD. *Hepatology*. 2007;45(4):846–854. doi:10.1002/hep.21496.

14. Shaheen AA, Myers RP. Diagnostic accuracy of the aspartate aminotransferase-to-platelet ratio index for the prediction of hepatitis C-related fibrosis: a systematic review. *Hepatology*. 2007;46(3):912–921. doi:[10.1002/hep.21835](https://doi.org/10.1002/hep.21835).
15. Sung KC, Wild SH, Byrne CD. Lipoprotein (a), metabolic syndrome and coronary calcium score in a large occupational cohort. *Nutr Metab Cardiovasc Dis*. 2013;23(12):1239–1246. doi:[10.1016/j.numecd.2013.02.009](https://doi.org/10.1016/j.numecd.2013.02.009).
16. Koschinsky ML, Marcovina SM. The relationship between lipoprotein(a) and the complications of diabetes mellitus. *Acta Diabetol*. 2003;40(2):65–76. doi:[10.1007/s005920300007](https://doi.org/10.1007/s005920300007).
17. Zhao Y. Association between apolipoprotein B/A1 and the risk of metabolic dysfunction associated fatty liver disease according to different lipid profiles in a Chinese population: a cross-sectional study. *Clin Chim Acta*. 2022;534:138–145. doi:[10.1016/j.cca.2022.07.014](https://doi.org/10.1016/j.cca.2022.07.014).
18. Negi CK, Babica P, Bajard L, Bienertova-Vasku J, Tarantino G. Insights into the molecular targets and emerging pharmacotherapeutic interventions for nonalcoholic fatty liver disease. *Metabolism*. 2022;126:154925. doi:[10.1016/j.metabol.2021.154925](https://doi.org/10.1016/j.metabol.2021.154925).
19. Tarantino G, Balsano C, Santini SJ, et al. It is high time physicians thought of natural products for alleviating NAFLD: is there sufficient evidence to use them? *Int J Mol Sci*. 2021;22(24):13424. doi:[10.3390/ijms222413424](https://doi.org/10.3390/ijms222413424).

Clinical role of serum tumor markers SCC, NSE, CA 125, CA 19-9, and CYFRA 21-1 in patients with lung cancer

Aiwen Sun, BS¹

¹Beijing Chao-Yang Hospital, Capital Medical University, Beijing, China.
Corresponding author: Aiwen Sun; saw7000238704@163.com.

Key words: lung cancer; tumor markers; CYFRA 21-1; diagnosis

Abbreviations: BCDs, benign chest diseases; NSE, neuron-specific enolase; CA 125, cancer antigen 125; SCC, squamous cell carcinoma-related antigen; NSE, neuron-specific enolase; CA 19-9, cancer antigen 19-9; CYFRA 21-1, cytokeratin fragment 19; CT, computed tomography; ORs, odds ratios; ROC, receiver operating characteristic; AUC, area under the curve; SCLC, small cell lung cancer; NSCLC, non-small cell lung carcinoma

Laboratory Medicine 2023;54:638-645; <https://doi.org/10.1093/labmed/lmad020>

ABSTRACT

Objective: The aim of the study was to assess the diagnostic value of tumor markers in discriminating between lung cancer and benign chest diseases (BCDs).

Methods: There were 322 patients enrolled in this investigation including 180 cases of lung cancer and 142 cases of BCD. Serum neuron-specific enolase (NSE), cancer antigen 125, cancer antigen 19-9, squamous cell carcinoma-related antigen, and cytokeratin fragment 19 (CYFRA 21-1) were compared between different populations, cancer stages, and before and after treatment. Logistic regression and receiver operating characteristic curves were used to evaluate the diagnostic markers.

Results: Both NSE and CYFRA 21-1 were significantly associated with lung cancer. The CYFRA 21-1 showed the best performance, as well as its combinations, for lung cancer diagnosis. It also showed significant change 6 months after radical surgery in lung cancer patients.

Conclusion: The marker CYFRA 21-1 could be developed as an adjuvant marker for the early diagnosis of lung cancer and as a prognostic marker for lung cancer treatment.

Introduction

Lung cancer is the most common cancer and the leading cause of cancer death in China,¹ with a mortality of 610.2 per 100,000.² Early diagnosis

is critical for lung cancer patients to receive adequate and appropriate treatments in a timely manner to improve mortality.^{3,4} For lung cancer, the 5-year survival rate can reach 70% to 80% when the patients are diagnosed at early stages, but the rate is less than 15% when they are diagnosed at advanced stages.⁵ Based on the SEER Cancer Statistics Review 2016, with current approaches, only 16% of diagnosed lung cancer patients did not have metastases.⁶ This was partly due to poor detection because of the lack of history or symptoms of lung cancer. The primary screening methods for lung cancer include chest X-ray, computed tomography (CT), magnetic resonance imaging, and positron emission tomography. Although the low-dose CT widely used in lung cancer screening effectively reduces mortality, it has a considerable cost to the health system and the patient's body. Low-dose CT also has the problem of false positives.^{7,8} These issues would make noninvasive, convenient, and low-cost circulating screening markers highly valuable for the diagnosis of lung cancer and its progression assessment.

Currently, tumor markers such as neuron-specific enolase (NSE), cancer antigen 125 (CA 125), cancer antigen 19-9 (CA 19-9), squamous cell carcinoma-related antigen (SCC), and cytokeratin fragment 19 (CYFRA 21-1) are widely used for noninvasive cancer screening and monitoring of its progression.⁹⁻¹⁴ They have become increasingly accessible to patients, but their effectiveness is still unsatisfactory due to the heterogeneity of tumors and individuals. The clinical role of the serum tumor markers NSE, CA 125, CA 19-9, SCC, and CYFRA 21-1 in lung cancer remains unclear. In this study, changes in serum levels of tumor marker NSE, CA 125, CA 19-9, SCC, and CYFRA 21-1 were evaluated in patients with lung cancer to identify the most suitable markers for the diagnosis of lung cancer.

Materials and Methods

Ethical Approval

The study was carried out in accordance with the Declaration of Helsinki (as revised in 2013). This was a retrospective observational study covering a total of 322 patients successively admitted to Beijing Chao-Yang Hospital, and it was approved by the Ethics Committee of Beijing Chao-Yang Hospital.

Patients

The inclusion criteria were as follows: (1) patients diagnosed with lung cancer by pathological examination with a confirmed TNM staging; (2)

patients with complete data regarding serum levels of NSE, CA 125, CA 19-9, SCC, and CYFRA21-1 before treatment; and (3) patients with complete clinical data. Accordingly, 180 patients with lung cancer who met the criteria were enrolled. Also enrolled were 142 patients with benign chest diseases (BCD) as controls, for whom clinical data for tumor markers were available for this study. Data on clinicopathological characteristics, including sex, age, and TNM tumor staging information, were recorded for analysis.

Blood Sample Collection and Tumor Marker Measurement

Blood samples were obtained before patients received any therapy. The samples were centrifuged at 1000g for 15 min, followed by collection of serum. Electrochemiluminescence technology was used for immunoassay analysis per the manufacturer's instruction (Roche cobas e601 module) to measure the concentration of NSE, CA 125, CA 19-9, SCC, and CYFRA 21-1 in each sample. Levels above the following values was considered abnormal: NSE, 16.3 ng/mL; CA 125, 35 U/mL; CA 19-9, 39 U/mL; SCC, 1.5 ng/mL; and CYFRA 21-1, 3.3 ng/mL.

Statistical Analysis

Information is presented here as number (percentage) or median (interquartile range) for categorical characteristics. Univariate and multiple logistic regression models were used to identify correlation, in which odds ratios (ORs) with 95% CIs were calculated using SPSS (version 22.0 IBM). Diagnostic efficacy was evaluated using the receiver operating characteristic (ROC) curve. A two-tailed Wilcoxon paired test was used to compare biomarker levels before and after treatment.

Results

Clinicopathological Characteristics of the Study Population

The clinicopathological characteristics of all study participants, specifically age, tumor stage, and other chest diseases, are summarized in **TABLE 1**. There was no significant difference in age or sex between the lung cancer group and the benign chest disease (BCD) control group. The lung cancer patients were distributed relatively evenly across tumor stages, with 67 in stage I (37.2%), 53 in stage III (29.4%), 40 in stage IV (22.3%), and 20 in stage II (11.1%). The BCDs of patients in the control group included tuberculosis (2, 1.4%), chronic obstructive pulmonary disease (40, 28.2%), lung infection (22, 15.5%), pulmonary embolism (31, 21.8%), pulmonary fibrosis (13, 9.2%), and asthma (34, 23.9%).

Levels of NSE, CA 125, CA 19-9, SCC, and CYFRA 21-1 in Different Populations

Information on serum levels of NSE, CA 125, CA 19-9, SCC, and CYFRA 21-1 of the two study groups is listed in **TABLE 2**. Median levels of NSE and CYFRA 21-1 in the control group (12.47 ng/mL and 2.44 ng/mL) were significantly lower than those in the lung cancer group (14.94 ng/mL and 3.31 ng/mL) with $P < .001$. The rate of above-normal levels in the lung cancer group was much higher than in the control group for all 5 markers. In the lung cancer group, 51.7% of the participants showed a higher level of CYFRA 21-1, whereas 14.1% of participants with BCDs had a higher level of CYFRA 21-1.

We further evaluated the correlation between each marker and the lung cancer stages. The NSE, CA 125, and CYFRA 21-1 markers showed

TABLE 1. Clinicopathological characteristics

	Lung cancer group (n = 180)	Control group (n = 142)
Age, y		
Mean	61.79	62.66
Range	28–85	32–88
Sex		
Male	114	97
Female	66	45
Tumor stage, n (%)		
I	67 (37.2)	NA
II	20 (11.1)	NA
III	53 (29.4)	NA
IV	40 (22.3)	NA
Benign chest diseases, n (%)		
Tuberculosis	NA	2 (1.4)
Chronic obstructive pulmonary disease	NA	40 (28.2)
Lung infection	NA	22 (15.5)
Pulmonary embolism	NA	31 (21.8)
Pulmonary fibrosis	NA	13 (9.2)
Asthma	NA	34 (23.9)

NA, not applicable.

stepwise increases along with cancer progression (**TABLE 2**, median and range). Their levels during late stages (stages III and IV) were significantly higher than at early stages (stages I and II), as shown in **FIGURE 1**. Particularly for CYFRA 21-1, patients as early as stage II had significantly higher levels than those in the control group, which implies the possibility of an early marker.

These results indicate that NSE level and CYFRA 21-1 level are closely associated with lung cancer, and CYFRA 21-1 showed the divergence well in different stages of lung cancer.

Identification of Diagnostic Markers for Lung Cancer

To assess their value for diagnosis, univariate regression analyses were performed to identify biomarkers associated with the result (lung cancer or not). The markers NSE (OR = 1.119, $P < .001$), CA 19-9 (OR = 1.018, $P = .043$), and CYFRA 21-1 (OR = 2.007, $P < .001$) were found to be positive independent diagnostic risk factors, but SCC (OR = 1.040, $P = .405$) and CA 125 (OR = 1.004, $P = .104$) were not, as shown in **TABLE 3**. Additional multiple logistic regression analyses were performed, and the results showed NSE (OR = 1.070, $P = .022$) and CYFRA 21-1 (OR = 1.914, $P < .001$) to be true independent positive markers that were significantly correlated with lung cancer when the combination of the 3 factors was considered (**TABLE 3**).

Diagnostic Characteristics of Tumor Markers in Lung Cancer

The ROC curve was used for the assessment of the diagnostic performance of NSE, CA 19-9, CYFRA 21-1 and their combinations to discriminate patients with lung cancer patients from CBD patients (**FIGURE 2**). Results showed that the combination of CYFRA 21-1 and NSE had the best performance (area under the curve [AUC] = 0.748), followed by the single markers CYFRA 21-1 (AUC = 0.736), NSE

TABLE 2. Comparison of positive rates of SCC, NSE, CA 125, CA 19-9, and CYFRA 21-1 in the two groups

	Lung cancer group (n = 180)	Control group (n = 142)	P value
SCC (ng/mL) baseline			.345
Median (range)	0.51 (0.2–70)	0.59 (0.2–9.23)	
Normal (<1.5), n (%)	162 (90.0)	123 (86.6)	
Elevated (≥1.5), n (%)	18 (10.0)	19 (13.4)	
NSE (ng/mL) baseline			<.001
Median (range)	14.94 (8.15–311.6)	12.47 (7–35.69)	
Normal (<16.3), n (%)	113 (62.8)	122 (85.9)	
Elevated (≥16.3), n (%)	67 (37.2)	20 (14.1)	
CA 125 (U/mL) baseline			.353
Median (range)	12.49 (3.68–3064)	14.88 (2.84–327.4)	
Normal (<35), n (%)	134 (74.4)	112 (78.9)	
Elevated (≥35), n (%)	46 (25.6)	30 (21.1)	
CA 19-9 (U/mL) baseline			.076
Median (range)	12.29 (0.6–455.3)	9.7 (0.6–93.4)	
Normal (<39), n (%)	165 (91.7)	137 (96.5)	
Elevated (≥39), n (%)	15 (8.3)	5 (3.5)	
CYFRA 21-1 (ng/mL) baseline			<.001
Median (range)	3.31 (0.89–55.52)	2.44 (0.54–5.17)	
Normal (<3.3), n (%)	87 (48.3)	122 (85.9)	
Elevated (≥3.3), n (%)	93 (51.7)	20 (14.1)	

CA 19-9, cancer antigen 19-9; CA 125, cancer antigen 125; CYFRA 21-1, cytokeratin fragment 19; NSE, neuron-specific enolase; SCC, squamous cell carcinoma-related antigen.

(AUC = 0.659), and CA 19-9 (AUC = 0.599) (**FIGURE 2A–D**). The combination of CYFRA 21-1 and NSE has better AUC but has compromised specificity from 0.852 to 0.789 compared to the individual CYFRA 21-1 level. On the other hand, analysis of early diagnosis for lung cancer showed CYFRA 21-1 has the best performance (AUC = 0.612), followed by CA 19-9 (AUC = 0.585) and NSE (AUC = 0.562), as shown in **FIGURE 2E–G**. Although the performance of CYFRA 21-1 is not good enough to become an ideal early diagnostic marker, the specificity is as high as that of current lung cancer diagnosis, demonstrating that it could be a complement to the existing lung cancer early detection procedures to increase specificity. It is noteworthy that the combination of CYFRA 21-1 with NSE did not improve the performances at all for early diagnosis (AUC = 0.616) (**FIGURE 2H**).

Potential of CYFRA 21-1 as a Prognostic Marker for Lung Cancer

Because serum levels of some of the markers were significantly different across the tumor stages of lung cancer (**FIGURE 1**), although not qualified as early markers (**FIGURE 2B**), the question remained whether they could be prognostic markers for lung cancer. An in-house database of follow-up visits to the hospital was searched and it was found that 37 of the enrolled participants had been retested for the tumor markers in the 6-month follow-up visit after an operation following the first test. Paired comparisons of all 5 marker levels before and after surgery were performed (**FIGURE 3**). Results indicated that only CYFRA 21-1 had a significant decrease after tumor resection, whereas both CA 125 and CA 19-9 showed even higher levels after resection. This suggests the potential of CYFRA 21-1 as a prognostic marker for lung cancer treatment.

Discussion

The tumor marker CYFRA 21-1, a fragment of the protein cytokeratin 19 implicated in the transformation of epithelial cells to cancer cells, is released into circulation from inside cells when they undergo necrosis. Several studies have attempted to assess CYFRA 21-1 as a diagnostic biomarker of lung cancers.^{15,16} This is consistent with previous reports stating that CYFRA 21-1 is more specific than sensitive for the diagnosis¹⁷; even so, it is more sensitive than some other tumor antigen markers. The marker NSE, also known as enolase-2, is a multifunctional cytoplasmic enzyme, changes in which are related to several diseases, such as inflammation and cancers. Generally, NSE is expressed in some specific tissues but is elevated in serum when malignancy develops, especially lung cancers.¹⁸ Neuron-specific enolase usually works better individually than other tumor antigen markers,¹⁹ but its levels are also significantly higher in patients with benign lung diseases than in healthy controls.^{18,20} Similar to CYFRA 21-1, NSE has shown low sensitivity. However, Chen et al²⁰ reported that NSE is a biomarker with a high positive rate, but CYFRA 21-1 has a better sensitivity for stage I small cell lung cancer (SCLC). In this study, ROC revealed that both CYFRA 21-1 and NSE have relatively high specificity but poor sensitivity. All these could partly explain much, if not all, of why NSE can hardly be complementary to CYFRA 21-1 to improve the performance although both of them are independent factors. This situation is slightly different from some other reports in which NSE, CA 125, CA 19-9, or SCC could help improve the lung cancer diagnostic performance of CYFRA 21-1 when combined with it.^{21–23} Although many previous studies have presented significant correlations between cancers and CA 125, CA 19-9 or SCC levels, their role as diagnostic or prognostic biomarkers is still controversial. In this study, CA 19-9

FIGURE 1. Variations of tumor markers across lung cancer stages and the benign chest disease patients: SCC (A), NSE (B), CA 125 (C), CA 19-9 (D) and CYFRA 21-1 (E). Rank sum (Kruskal-Wallis) test was used for analysis. * $P < .05$, ** $P < .01$, vs control group.

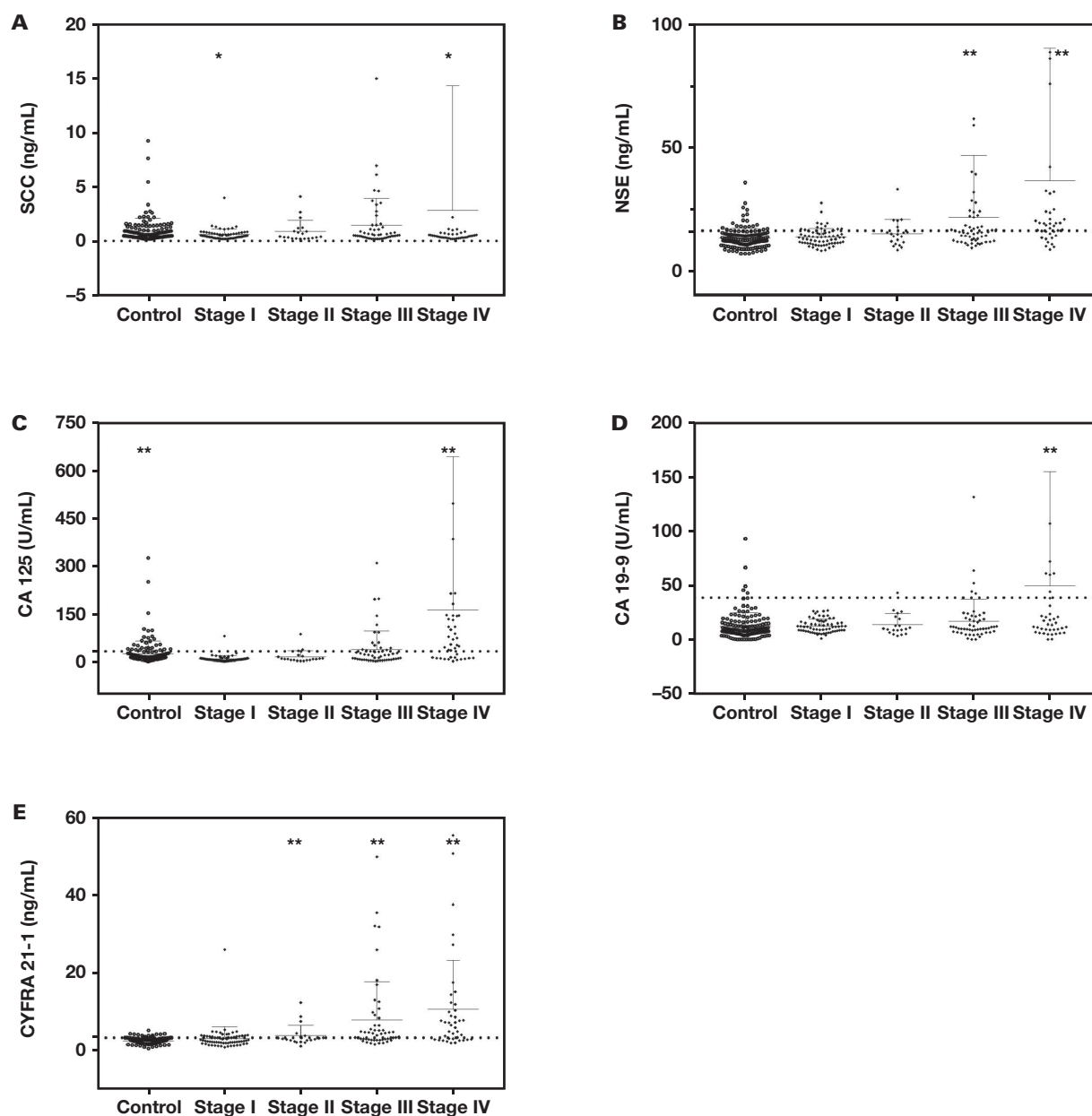


TABLE 3. Univariate and multiple logistic regression analyses to identify the individual risk factors for lung cancer

Various	Univariate logistic regression			Multiple logistic regression		
	OR	95% CI	P value	OR	95% CI	P value
SCC	1.040	0.948–1.141	.405	NA	NA	NA
NSE	1.119	1.060–1.182	<.001	1.070	1.010–1.134	.022
CA 125	1.004	0.999–1.009	.104	NA	NA	NA
CA 19-9	1.018	1.001–1.036	.043	1.004	0.987–1.022	.640
CYFRA 21-1	2.007	1.566–2.571	<.001	1.914	1.479–2.476	<.001

CA 19-9, cancer antigen 19-9; CA 125, cancer antigen 125; CYFRA 21-1, cytokeratin fragment 19; NA, not applicable; NSE, neuron-specific enolase; OR, odds ratio; SCC, squamous cell carcinoma-related antigen.

FIGURE 2. Receiver operating characteristic (ROC) analysis of identified lung cancer risk factors for diagnosis and early diagnosis. ROC of NSE (A, E), CA 19-9 (B, F), CYFRA 21-1 (C, G), and the combination of CA 19-9 and CYFRA 21-1 (D, H) for whole lung cancer patients (A-D) and early-stage lung cancer patients (E-H).

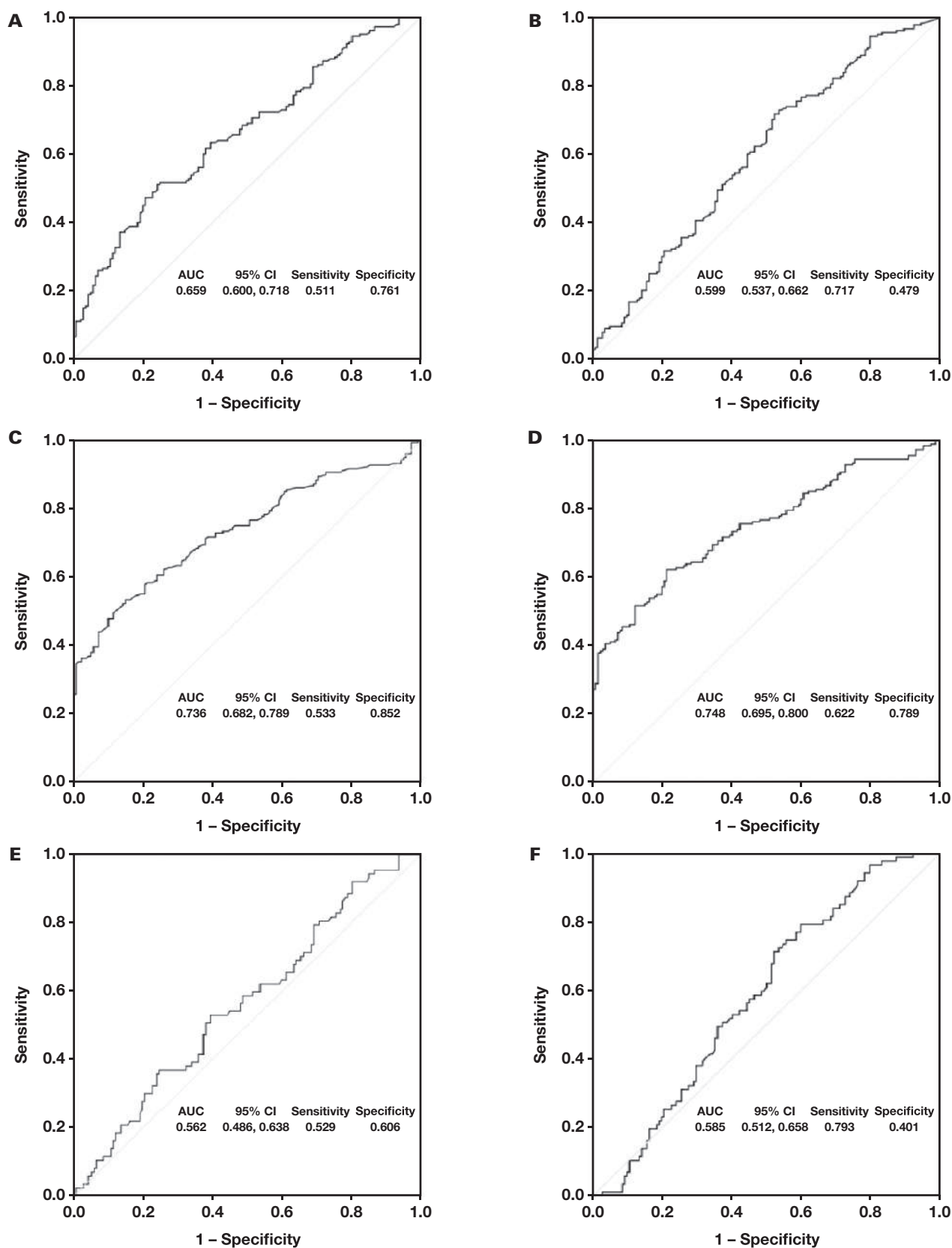
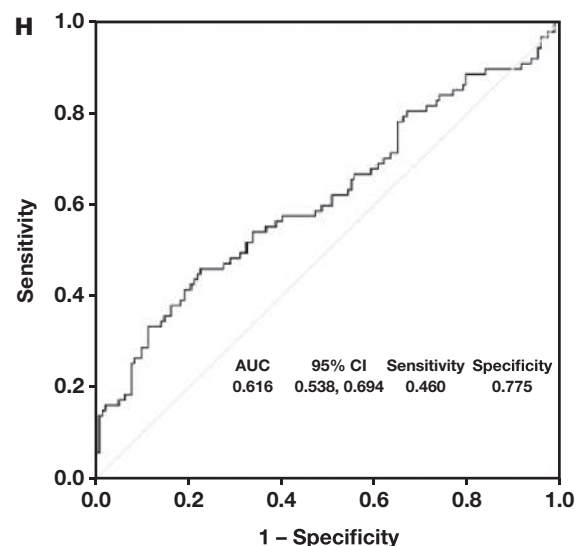
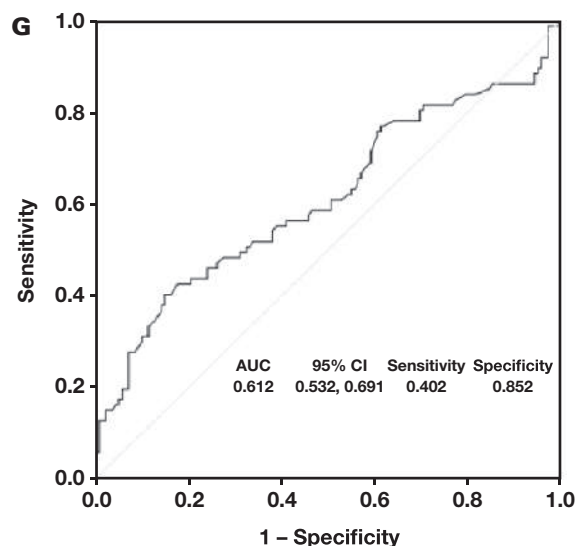


FIGURE 2. (cont)



presented limited significance as an independent risk factor in univariate regression. Heterogeneities in diseases, population, gender, geography, and other situations may explain the discrepancies. For instance, CA 19-9 might be more related to liver cancers and performed better when it was combined with radiological and imaging features of the cancer patients.²⁴ The marker CA 125 was found to be more specific for women with advanced-stage ovarian cancer, but it is also a marker for women with endometriosis.²⁵ Early studies support the diagnostic role of SCC in squamous types of cancers, but recent evidence has shown contrasting roles in non-SCLC (NSCLC), which implies a possible dual pathogenic role of SCC in different histologic types of NSCLC.²⁶ Therefore, a more detailed and rational grouping may explain the correlations of these biomarkers for specific patients.

Early diagnosis significantly improves the survival rates of lung cancer patients. In general, survival rates are 5 to 10 times higher for those diagnosed early than for those diagnosed late.²⁷ These results indicate that none of the markers except CYFRA 21-1 have much potential for the early diagnosis of lung cancer. This is not surprising and is consistent with the findings of previous reports, because solid tumors at such an early stage are so small that they are difficult to detect with noninvasive methods such as circulating biochemical alterations alone. Despite the poor performance in early diagnosis, we found CYFRA 21-1 to have relatively high specificity in the ROC analyses. This indicates that CYFRA 21-1 could be developed as an adjuvant diagnostic marker with existing detection methods such as CT to increase specificity and improve the situation of overdiagnosis.

The result of this study also showed CYFRA 21-1 was significantly associated with different stages of lung cancer, especially the late stages with a relatively high tumor burden, providing new information on the potential of CYFRA 21-1 to become a prognostic marker. Although many studies have been conducted on the role of biomarkers in diagnosis, few have assessed their role in cancer progression, so this result could shed light on such uses. Yu et al²⁸ found that CYFRA 21-1 was significantly higher in the patients with advanced lung cancers and associated with the overall survival in NSCLC, whereas Cabrera et al²⁹ reported that high levels of CYFRA 21-1 are related to distant metastasis. Recently, Chen et al³⁰ showed CYFRA 21-1 was significantly different

across lung cancer stages in particular NSCLC, and Yoshimura et al³¹ reported that the CYFRA 21-1 level measured 4 months after treatment is a valuable prognostic marker for NSCLC patients. In this work, a database was searched to collect clinical information on follow-ups of recruited patients, and it was found that the biomarker levels of 37 participants were measured 6 months after radical surgery. Similar to the above studies, the levels of CYFRA 21-1, but not the other markers of these patients, exhibited a decreased pattern. These observations agree with studies by others that CYFRA 21-1 is relevant to high tumor burden and poor survival of cancer patients.^{32,33} Also, CYFRA 21-1 was reported to predict therapeutic efficacy of chemotherapy³⁴ and immunotherapy.³⁵ Another study showed that a higher level of CYFRA 21-1 was correlated with more advanced stages and shorter overall survival in lung cancer²⁸ and was considered a prognostic marker in advanced NSCLC.³¹ Here, the results on CYFRA 21-1 further support this conclusion for early and advanced stages of Chinese lung cancer patients. However, the sample size in this study is very small. More clinical data on the long-term outcome using CYFRA 21-1 are required in future studies to establish a prognostic model.

Interestingly, rather than declining, CA 125 and CA 19-9 levels increased during the 6 months after tumor resection in 26 patients, although their CYFRA 21-1 level decreased. It is presumed that the levels were affected by inflammation caused by the surgery, because upregulation of CA 125 has also been reported to be associated with inflammation and congestion,^{36,37} and upregulated levels of CA 19-9 are common in pancreatitis and cholecystitis and co-occurred with upregulation of the inflammatory protein CRP.^{38,39}

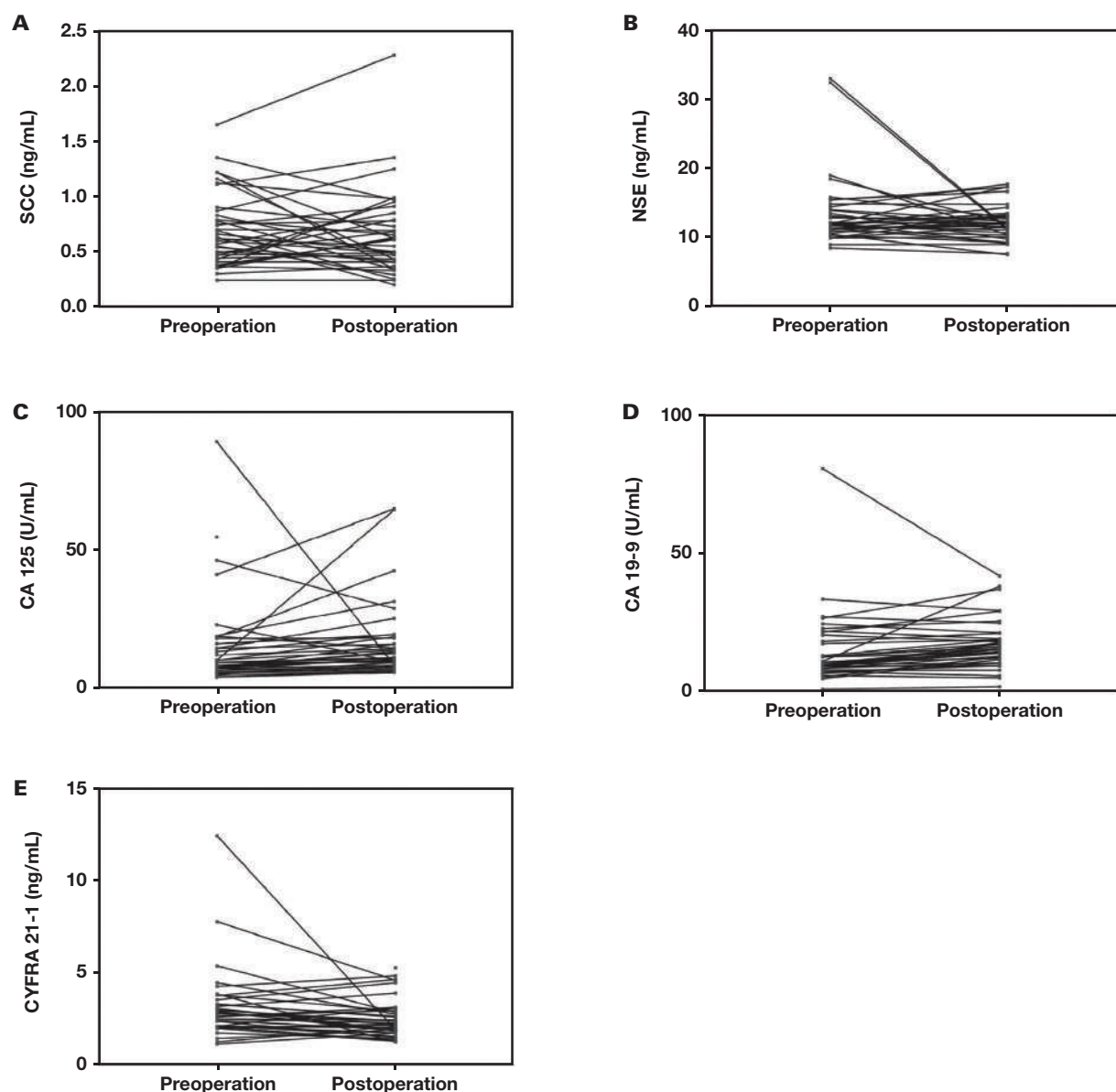
Conclusion

Based on the results of this study, it was concluded that CYFRA 21-1 could be developed as an adjuvant marker for the early diagnosis of lung cancer and as a prognostic marker for lung cancer treatment.

Limitations

This study had several limitations that should be recognized. First, the sample size was relatively small. This could have led to selection

FIGURE 3. Changes in serum levels of the five markers from preoperation to postoperation: SCC ($P > .05$) (A), NSE ($P > .05$) (B), CA 125 ($P = .003$) (C), CA 19-9 ($P = .001$) (D), and CYFRA 21-1 ($P = .015$) (E). CA 125 and CA 19-9 levels increased significantly when CYFRA 21-1 level decreased significantly.



bias, so a multiple-center study with a larger sample size is required to validate and assess the performance of CYFRA 21-1. Second, due to the retrospective nature of the study, there was a lack of follow-up visits of the enrolled patients to analyze long-term outcomes of cancer stages that would indicate progression, overall survival, and progression-free survival. Third, there was no analysis of the subtypes of lung cancer.

Acknowledgments

The author is thankful for the helpful contributions of all staff of the clinical laboratory.

Conflicts of Interest Disclosure

The author has nothing to disclose.

REFERENCES

1. Chen W, Zheng R, Zhang S, et al. Cancer incidence and mortality in China, 2013. *Cancer Lett.* 2017;401:63–71. doi:[10.1016/j.canlet.2017.04.024](https://doi.org/10.1016/j.canlet.2017.04.024).
2. Chen W, Zheng R, Baade PD, et al. Cancer statistics in China, 2015. *CA Cancer J Clin.* 2016;66(2):115–132. doi:[10.3322/caac.21338](https://doi.org/10.3322/caac.21338).
3. Rodriguez M, Ajona D, Seijo LM, et al. Molecular biomarkers in early stage lung cancer. *Transl Lung Cancer Res.* 2021;10(2):1165–1185. doi:[10.21037/tlcr-20-750](https://doi.org/10.21037/tlcr-20-750).
4. Jones GS, Baldwin DR. Recent advances in the management of lung cancer. *Clin Med.* 2018;18(suppl 2):s41–s46. doi:[10.7861/clinmedicine.18-2-s41](https://doi.org/10.7861/clinmedicine.18-2-s41).
5. Siegel R, Naishadham D, Jemal A. Cancer statistics, 2013. *CA Cancer J Clin.* 2013;63(1):11–30. doi:[10.3322/caac.21166](https://doi.org/10.3322/caac.21166).
6. Doll KM, Rademaker A, Sosa JA. Practical guide to surgical data sets: surveillance, epidemiology, and end results (SEER)

- database. *JAMA Surg.* 2018;153(6):588–589. doi:10.1001/jamasurg.2018.0501.
7. National Lung Screening Trial Research T; Aberle DR, Adams AM, Berg CD, et al. Reduced lung-cancer mortality with low-dose computed tomographic screening. *N Engl J Med.* 2011;365(5):395–409. doi:10.1056/NEJMoa1102873
8. Mulshine JL, D'Amico TA. Issues with implementing a high-quality lung cancer screening program. *CA Cancer J Clin.* 2014;64(5):352–363. doi:10.3322/caac.21239.
9. Liu L, Xie W, Xue P, Wei Z, Liang X, Chen N. Diagnostic accuracy and prognostic applications of CYFRA 21-1 in head and neck cancer: a systematic review and meta-analysis. *PLoS One.* 2019;14(5):e0216561. doi:10.1371/journal.pone.0216561.
10. Yang G, Xiao Z, Tang C, Deng Y, Huang H, He Z. Recent advances in biosensor for detection of lung cancer biomarkers. *Biosens Bioelectron.* 2019;141:111416. doi:10.1016/j.bios.2019.111416.
11. Coppola A, La Vaccara V, Farolfi T, et al. Role of CA 19.9 in the management of resectable pancreatic cancer: state of the art and future perspectives. *Biomedicine.* 2022;10(9):2091. doi:10.3390/biomedicine10092091.
12. Cedres S, Nunez I, Longo M, et al. Serum tumor markers CEA, CYFRA21-1, and CA-125 are associated with worse prognosis in advanced non-small-cell lung cancer (NSCLC). *Clin Lung Cancer.* 2011;12(3):172–179. doi:10.1016/j.clcc.2011.03.019.
13. Li M, Jiang F, Xue L, et al. Recent progress in biosensors for detection of tumor biomarkers. *Molecules.* 2022;27(21):7327. doi:10.3390/molecules27217327.
14. Zhang R, Siu MKY, Ngan HYS, Chan KKL. Molecular biomarkers for the early detection of ovarian cancer. *Int J Mol Sci.* 2022;23(19):12041. doi:10.3390/ijms231912041.
15. He X, Wang M. Application value of serum TK1 and PCDGF, CYFRA21-1, NSE, and CEA plus enhanced CT scan in the diagnosis of non-small cell lung cancer and chemotherapy monitoring. *J Oncol.* 2022;2022:8800787. doi:10.1155/2022/8800787.
16. Okamura K, Takayama K, Izumi M, Harada T, Furuyama K, Nakanishi Y. Diagnostic value of CEA and CYFRA 21-1 tumor markers in primary lung cancer. *Lung Cancer.* 2013;80(1):45–49. doi:10.1016/j.lungcan.2013.01.002.
17. Ciarlioni L, Ehrensberger SH, Imaizumi N, et al. Development and clinical validation of a blood test based on 29-gene expression for early detection of colorectal cancer. *Clin Cancer Res.* 2016;22(18):4604–4611. doi:10.1158/1078-0432.CCR-15-2057.
18. Xu CM, Luo YL, Li S, et al. Multifunctional neuron-specific enolase: its role in lung diseases. *Biosci Rep.* 2019;39(11):BSR20192732. doi:10.1042/BSR20192732.
19. Molina R, Auge JM, Filella X, et al. Pro-gastrin-releasing peptide (proGRP) in patients with benign and malignant diseases: comparison with CEA, SCC, CYFRA 21-1 and NSE in patients with lung cancer. *Anticancer Res.* 2005;25(3A):1773–1778.
20. Chen Z, Liu X, Shang X, Qi K, Zhang S. The diagnostic value of the combination of carcinoembryonic antigen, squamous cell carcinoma-related antigen, CYFRA 21-1, neuron-specific enolase, tissue polypeptide antigen, and progastrin-releasing peptide in small cell lung cancer discrimination. *Int J Biol Markers.* 2021;36(4):36–44. doi:10.1177/17246008211049446.
21. Chen ZQ, Huang LS, Zhu B. Assessment of seven clinical tumor markers in diagnosis of non-small-cell lung cancer. *Dis Markers.* 2018;2018:9845123. doi:10.1155/2018/9845123.
22. Wang W, Xu X, Tian B, et al. The diagnostic value of serum tumor markers CEA, CA19-9, CA125, CA15-3, and TPS in metastatic breast cancer. *Clin Chim Acta.* 2017;470:51–55. doi:10.1016/j.cca.2017.04.023.
23. Wang W, Liu M, Wang J, et al. Analysis of the discriminative methods for diagnosis of benign and malignant solitary pulmonary nodules based on serum markers. *Oncol Res Treat.* 2014;37(12):740–746. doi:10.1159/000369488.
24. Eschrich J, Kobus Z, Geisel D, et al. The diagnostic approach towards combined hepatocellular-cholangiocarcinoma-state of the art and future perspectives. *Cancers.* 2023;15(1):301. doi:10.3390/cancers15010301.
25. Brons PE, Nieuwenhuijzen-de Boer GM, Ramakers C, Willemsen S, Kengsakul M, van Beekhuizen HJ. Preoperative cancer antigen 125 level as predictor for complete cytoreduction in ovarian cancer: a prospective cohort study and systematic review. *Cancers.* 2022;14(23):5734. doi:10.3390/cancers14235734.
26. Zhu H. Squamous cell carcinoma antigen: clinical application and research status. *Diagnostics.* 2022;12(5):1065. doi:10.3390/diagnostics12051065.
27. Cho H, Mariotto AB, Schwartz LM, Luo J, Woloshin S. When do changes in cancer survival mean progress? The insight from population incidence and mortality. *J Natl Cancer Inst Monogr.* 2014;2014(49):187–197. doi:10.1093/jncimonographs/igu014.
28. Yu Z, Zhang G, Yang M, et al. Systematic review of CYFRA 21-1 as a prognostic indicator and its predictive correlation with clinicopathological features in non-small cell lung cancer: a meta-analysis. *Oncotarget.* 2017;8(3):4043–4050. doi:10.18632/oncotarget.14022.
29. Cabrera-Alarcon JL, Carrillo-Vico A, Santotoribio JD, et al. CYFRA 21-1 as a tool for distant metastasis detection in lung cancer. *Clin Lab.* 2011;57(11–12):1011–1014.
30. Li J, Chen Y, Wang X, Wang C, Xiao M. The value of combined detection of CEA, CYFRA21-1, SCC-Ag, and pro-GRP in the differential diagnosis of lung cancer. *Transl Cancer Res.* 2021;10(4):1900–1906. doi:10.21037/tcr-21-527.
31. Yoshimura A, Uchino J, Hasegawa K, et al. Carcinoembryonic antigen and CYFRA 21-1 responses as prognostic factors in advanced non-small cell lung cancer. *Transl Lung Cancer Res.* 2019;8(3):227–234. doi:10.21037/tlcr.2019.06.08.
32. Kanaji N, Kadota K, Tadokoro A, et al. Serum CYFRA 21-1 but not vimentin is associated with poor prognosis in advanced lung cancer patients. *Open Respir Med J.* 2019;13:31–37. doi:10.2174/1874306401913010031.
33. Kanaji N, Bandoh S, Ishii T, et al. Cytokeratins negatively regulate the invasive potential of lung cancer cell lines. *Oncol Rep.* 2011;26(4):763–768. doi:10.3892/or.2011.1357.
34. Sone K, Oguri T, Nakao M, et al. CYFRA 21-1 as a predictive marker for non-small cell lung cancer treated with pemetrexed-based chemotherapy. *Anticancer Res.* 2017;37(2):935–939. doi:10.21873/anticancer.11402.
35. Shirasu H, Ono A, Omae K, et al. CYFRA 21-1 predicts the efficacy of nivolumab in patients with advanced lung adenocarcinoma. *Tumour Biol.* 2018;40(2):1010428318760420. doi:10.1177/1010428318760420.
36. Kumric M, Kurir TT, Bozic J, et al. Carbohydrate antigen 125: a biomarker at the crossroads of congestion and inflammation in heart failure. *Card Fail Rev.* 2021;7:e19. doi:10.15420/cfr.2021.22.
37. Oliveira Junior WV, Turani SD, Marinho MAS, et al. CA-125 and CCL2 may indicate inflammation in peritoneal dialysis patients. *J Bras Nefrol.* 2021;43(4):502–509. doi:10.1590/2175-8239-JBN-2020-0255.
38. Zhang W, Wang Y, Dong X, et al. Elevated serum CA19-9 indicates severe liver inflammation and worse survival after curative resection in hepatitis B-related hepatocellular carcinoma. *Biosci Trends.* 2022;15(6):397–405.
39. Nurmi AM, Mustonen HK, Stenman UH, Seppanen HE, Haglund CH. Combining CRP and CA19-9 in a novel prognostic score in pancreatic ductal adenocarcinoma. *Sci Rep.* 2021;11(1):781. doi:10.1038/s41598-020-80778-0.

Semaphorin 3A levels in vascular and nonvascular phenotypes in systemic sclerosis

Mehmet Kayaalp, MD,¹ Abdulsamet Erden, MD,² Hakan Apaydin, MD,³ Serdar Can Güven, MD,³ Berkan Armağan, MD,³ Merve Çağlayan Kayaalp, MD,¹ Esma Andac Uzdogan, MD,⁴ Şeymanur Ala Enli, MD,¹ Ahmet Omma, MD,⁵ Orhan Kucuksahin, MD²

¹Department of Internal Medicine, Yıldırım Beyazıt University, Ankara, Turkey,

²Department of Internal Medicine, Division of Rheumatology, Ankara City Hospital, Yıldırım Beyazıt University, Ankara, Turkey, Departments of

³Rheumatology and ⁴Biochemistry, Ankara City Hospital, Ankara, Turkey,

⁵University of Health Sciences, Rheumatology, Ankara, Turkey.

Corresponding author: Hakan Apaydin; drhakanapaydin@gmail.com.

Key words: digital ulcer; pulmonary hypertension; semaphorin 3A; systemic sclerosis; vasculopathy

Abbreviations: Sema3A, semaphorin 3A; SSc, systemic sclerosis; DU, digital ulcer; SRC, scleroderma renal crisis; PAH, pulmonary arterial hypertension; ET-1, endothelin-1; NO, nitric oxide; VEGF, vascular endothelial growth factor; CRP, C-reactive protein; ESR, erythrocyte sedimentation rate; NP-1, neutrophilin 1; RA, rheumatoid arthritis; OA, osteoarthritis; VDAI, Valentini disease activity index; mRSS, modified Rodnan skin score

Laboratory Medicine 2023;54:646-651; <https://doi.org/10.1093/labmed/lmad019>

ABSTRACT

Objective: Semaphorin 3A (Sema3A) plays a regulatory role in immune responses. The aim of this study was to evaluate Sema3A levels in patients with systemic sclerosis (SSc), especially in major vascular involvements such as digital ulcer (DU), scleroderma renal crisis (SRC), pulmonary arterial hypertension (PAH), and to compare Sema3A level with SSc disease activity.

Methods: In SSc patients, patients with DU, SRC, or PAH were grouped as major vascular involvements and those without as nonvascular, and Sema3A levels were compared between the groups and with a healthy control group. The Sema3A levels and acute phase reactants in SSc patients, as well as their association with the Valentini disease activity index and modified Rodnan skin score, were evaluated.

Results: The Sema3A values (mean \pm SD) were 57.60 ± 19.81 ng/mL in the control group ($n = 31$), 44.32 ± 5.87 ng/mL in patients with major vascular involvement SSc ($n = 21$), and 49.96 ± 14.00 ng/mL in the nonvascular SSc group ($n = 35$). When all SSc patients were examined

as a single group, the mean Sema3A value was significantly lower than controls ($P = .016$). The SSc with major vascular involvement group had significantly lower Sema3A levels than SSc with nonmajor vascular involvement group ($P = .04$). No correlation was found between Sema3A, acute phase reactants, and disease activity scores. Also, no relationship was observed between Sema3A levels and diffuse (48.36 ± 11.47 ng/mL) or limited (47.43 ± 12.38 ng/mL) SSc types ($P = .775$).

Conclusion: Our study suggests that Sema3A may play a significant role in the pathogenesis of vasculopathy and can be used as a biomarker in SSc patients with vascular complications such as DU and PAH.

Introduction

Systemic sclerosis (SSc) is a connective tissue disorder with an unclear etiology characterized by vasculopathy, autoimmunity, and fibrosis of skin and internal organs.¹ Major vascular involvements comprise digital ulcers (DU) and pulmonary arterial hypertension (PAH), which may lead to significant morbidity and even mortality.¹⁻⁵ Frequent periods of vasospasm and subsequent fibrointimal proliferation result in tissue hypoxemia/ischemia and damage. Endothelial dysfunction, a major underlying pathologic factor of vasculopathy, arises from increased levels of endothelin-1 (ET-1), a potent vasoconstrictor, in skin, lungs, and the sera, and decreased levels of nitric oxide (NO), which is a potent vasodilator. Vascular endothelial growth factor (VEGF) further contributes to the pathologic process via defective angiogenesis and profibrotic effects.⁶

Acute-phase reactants such as C-reactive protein (CRP) and erythrocyte sedimentation rate (ESR) levels can be within normal range in patients with SSc, and the search for biomarkers predicting prominent vasculopathy (DU, renal crisis, PAH) is in progress.⁷ Accordingly, predictive values for ET-1 and VEGF have been investigated.⁸ Likewise, the role of another biomarker of DU and PAH, semaphorin 3A (Sema3A), is also a matter of interest.

Semaphorins are molecules that are thought to mediate various biological processes such as axonal growth, inflammation, apoptosis, angiogenesis and bone remodeling.⁹ Sema3A is a member of the semaphorin family affecting the nervous system, tumor growth, autoimmunity, and

rheumatic diseases via its receptor neutrophilin 1 (NP1).¹⁰ Sema3A is assumed to be involved in competitive inhibition against VEGF via NP1.¹¹ Reduced levels of Sema3A in the sera and the synovial fluid of rheumatoid arthritis (RA) patients in comparison with osteoarthritis (OA) patients has been demonstrated.¹² Furthermore, injection of Sema3A reduced disease activity and joint damage in mice with RA.¹³ Similarly, it has been observed that serum Sema3A levels are lower in lupus patients when compared to healthy controls.¹⁴ Injection of Sema3A reduced the level of proteinuria in mice with lupus nephritis.¹⁵ In familial Mediterranean fever patients, Sema3A levels during an attack were observed to be lower than healthy subjects.¹⁶ In SSc patients, Rimar et al¹⁷ reported levels of Sema3A were reduced in comparison with healthy controls but were similar to those of lupus patients. In contrast, Romano et al¹⁸ observed similar Sema3A levels in SSc patients and healthy subjects, yet in SSc patients with a history of DU, levels of Sema3A receptor NP1 were lower than in patients without DU. Because reduced levels of Sema3A have been demonstrated in various vasculopathic conditions such as diabetic retinopathy, lupus, and SSc (particularly in patients with DUs), it is intriguing to consider whether Sema3A can distinguish major vascular involvements in SSc.

In this study, we aimed to evaluate Sema3A levels in SSc patients with and without major vascular involvement and to better elucidate the contribution of Sema3A to the etiopathogenesis.

Materials and Methods

Study Design

This study was conducted with Yıldırım Beyazıt University Faculty of Medicine Clinical Research Ethics Committee approval (IRB No. E21-21) and was therefore carried out in accordance with ethical standards set forth in the 1964 Declaration of Helsinki and its latter amendments.

Study Subjects

Between March 1 and June 1, 2021, consecutive SSc patients at Yıldırım Beyazıt University Faculty of Medicine and Ankara City Hospital Rheumatology Clinic meeting 2013 American College of Rheumatology/European League Against Rheumatism SSc classification criteria¹⁹ between ages 18 and 70 were enrolled. Patients under the age of 18, or those with peripheral arterial disease, pregnancy, or malignancy were excluded from the study. A control group was formed from healthy subjects with similar age and gender characteristics, without any disease or drug use. Written consent was obtained from all participants. Data regarding demographics, clinical characteristics, laboratory and imaging findings, and pulmonary function test results were obtained from hospital records and are recorded. Valentini disease activity index (VDAI) score and modified Rodnan skin score (mRSS) were calculated.

The patient cases were defined as diffuse and limited scleroderma according to skin involvement. Diffuse cutaneous systemic sclerosis is the form of the disease that extends from the distal of the extremities to the proximal and the trunk and shows the hardening of the skin in a relatively short time, such as months or years. Limited systemic sclerosis is slower progression to the proximal parts of the upper extremities.

The mRSS is a semiquantitative method for evaluation of skin thickness through palpation. Seventeen skin areas (on the face, anterior chest, abdomen and upper arm, forearm, hand, fingers, thigh, leg, foot bilaterally) are scored using a semiquantitative scale of 0 to 3 (0,

normal skin; 1, mild thickness; 2, moderate thickness; 3, severe thickness with inability to pinch the skin into a fold) up to a maximum score of 51.²⁰ The VDAI was used to measure disease activity. It comprises 10 variables: presence of sclerodema, digital necrosis, arthritis, mRSS greater than 14, lung carbon monoxide diffusing capacity lower than 80%, ESR greater than 30 mm/h, hypocomplementemia (low C3 and/or C4), and patient-reported worsening of cardiopulmonary, and skin and vascular symptoms in the past month. The total score ranges from 0 to 10.²¹ The North American working group defines DU as a lesion with a visually noticeable depth and loss of continuity of the epithelial lining, which may be peeling or covered with a crust or necrotic tissue.²² Pulmonary arterial hypertension is defined as mean pulmonary artery pressure >20 mmHg, pulmonary wedge pressure <15 mmHg, and pulmonary vascular resistance ≥ 3 Wood's units.²³ Among SSc patients, patients with PAH, DU, and SSc renal crisis were grouped as patients with major vascular involvement.

Laboratory Investigations

Venous participant samples were centrifuged at 1000g at 4°C for 10 minutes. Separated serum samples were stored at -80°C until biochemical workup. Before analyses, frozen serum samples were thawed at room temperature and vortexed to homogenization. The Sema3A levels were measured by a commercial enzyme-linked immunosorbent assay kit (Human Semaphorin 3A ELISA, Elabscience) in accordance with the manufacturer's manual (with intra-assay and interassay coefficients of variation, 3.77% and 4.2%, respectively).

Statistical Analysis

Statistical analysis of the data was conducted with SPSS 24.0 (IBM) package program. Normality of variables was evaluated with Shapiro-Wilk test and visually by plots and histograms. Continuous variables were presented as mean \pm SD and compared between groups by Student *t*-test or one-way analysis of variance test, according to number of groups compared. Categorical variables are presented as number and percentage and compared between groups by χ^2 test or by Fisher exact test in case the 1 or more cell count is less than 5. All *P* values <.05 were considered statistically significant.

Results

A total of 56 SSc patients (21 with major vascular involvement) and 31 healthy controls were enrolled. Demographics, comorbidities, and SSc manifestations are presented in **TABLE 1**. No differences regarding age and sex were observed between SSc patients and healthy controls. The age in SSc group was 51.78 ± 11.33 (mean \pm SD) years, with Raynaud's phenomenon being the most common symptom (100%) followed by sclerodactyly (82.1%), gastroesophageal reflux (62.5%), dyspnea (46%), and arthritis (33.9%). When the antibody profiles of patients with diffuse and limited scleroderma were evaluated, anti-SCL-70 positivity was higher in diffuse SSc (18 [64.2]) than in limited SSc (7 [21.8]) (*P* < .001) (**TABLE 2**).

Mean Sema3A levels were significantly lower in SSc patients than healthy subjects (47.85 ± 11.88 vs 57.60 ± 19.8 ng/mL, *P* = .016). In SSc patients with major vascular involvements, Sema3A levels were lower than in both healthy subjects and SSc patients without major vascular involvements (**TABLE 3**). In SSc patients without major vascular involvements, Sema3A levels were not significantly different from

TABLE 1. Demographics and Clinical Characteristics of Patients With Systemic Sclerosis and Control Group

	All SSc patients (n = 56)	Control group (n = 31)		P value
Age (y), mean (SD)	51.78 (11.33)	47.45 (12.24)		.101 ^a
Sex, female, n (%)	53 (94.6)	29 (93.5)		.834 ^a
	All SSc patients (n = 56)	SSc patients		P value
	All SSc patients (n = 56)	Major vascular involvement (n = 21)	Nonmajor vascular (n = 35)	P value
Sex, female, n (%)	53 (94.6)	19 (90.5)	34 (97.1)	.549 ^a
Age (y), mean (SD)	51.78 (11.33)	48.40 (13.4)	53.7 (9.5)	
Smoking, n (%)				
Nonsmoker	37 (66.1)	14 (66.7)	23 (65.7)	.916 ^a
Smoker	7 (12.5)	3 (14.3)	4 (11.4)	
Ex-smoker	12 (21.4)	4 (19)	8 (22.9)	
Age at diagnosis (y), mean (SD)	41.96 (12.71)	37.71 (11.83)	44.51 (12.7)	.052 ^a
Clinical findings, n (%)				
Raynaud's phenomenon	56 (100)	21 (100)	35 (100)	
Calcinosis	3 (5.4)	2 (9.5)	1 (2.9)	.549 ^b
Sclerodactyly	46 (82.1)	19 (90.5)	27 (77.1)	.29 ^a
Telangiectasia	17 (30.4)	9 (42.4)	8 (22.9)	.202 ^a
Arthritis	19 (33.9)	6 (28.6)	13 (37.1)	.716 ^a
GERD	35 (62.5)	14 (66.7)	21 (60)	.831 ^a
Dysphagia	19 (33.9)	9 (42.9)	10 (28.6)	.423 ^a
Dyspnea	26 (46.4)	9 (42.9)	17 (48.6)	.890 ^a
Cough	19 (33.9)	9 (42.9)	10 (28.6)	.423 ^a
Digital ulcer	21 (37.5)	21 (100)	0 (0)	<.001 ^b
Lung involvement	20 (35.7)	10 (47.6)	10 (28.6)	.249 ^a
PAH	1 (1.8)	1 (4.8)	0 (0)	.375 ^b
Current medications, n (%)				
Acetylsalicylic acid	41 (73.2)	16 (76.2)	25 (71.4)	
Calcium channel blockers	27 (48.2)	11 (52.4)	16 (45.7)	
Corticosteroid	21 (37.5)	10 (47.6)	11 (31.4)	
Hydroxychloroquine	32 (57.1)	12 (57.1)	20 (57.1)	
Methotrexate	7 (12.5)	4 (19)	3 (8.6)	
Bosentan	0	0	0	
Phosphodiesterase V inhibitors	6 (10.7)	4 (19)	2 (5.7)	
Pentoxifylline	11 (19.6)	4 (19)	7 (20)	
Proton pump inhibitors	11 (19.6)	5 (23.8)	6 (17.1)	
Mycophenolate mofetil	5 (8.9)	4 (19)	1 (2.9)	
Azathioprine	11 (19.6)	5 (23.8)	6 (17.1)	
Colchicine	10 (17.9)	5 (23.8)	5 (14.3)	
ACE inhibitors or ARB	16 (28.6)	6 (28.6)	10 (28.6)	
Nonsteroidal anti-inflammatory drugs	4 (7.1)	1 (4.8)	3 (8.6)	
Rituximab	1 (1.8)	1 (4.8)	0 (0)	
Cyclophosphamide	2 (3.6)	0	2 (5.7)	

ACE, angiotensin-converting enzyme inhibitors; ARB, angiotensin II receptor blockers; GERD, gastroesophageal reflux disease; PAH, pulmonary arterial hypertension; SSc, systemic sclerosis.

^aPearson χ^2 test.

^bFisher exact test.

healthy subjects (49.96 ± 14 vs 57.6 ± 19 , 81 ng/mL, $P = .07$). The Sema3A levels were also similar when SSc patients were grouped as limited and diffuse (TABLE 3).

When SSc patients were subgrouped according to VDAI (3 as cutoff) and mRSS scores (14 as cutoff), no significant differences were observed in CRP, ESR, fibrinogen, and Sema3A levels (TABLE 4).

Discussion

Our results demonstrated significantly reduced levels of Sema3A in SSc patients compared with healthy subjects. Furthermore, Sema3A levels were significantly lower in SSc patients with major vasculopathic manifestations (DU, SRC, and PAH) than SSc patients without. Sema3A levels were not significantly different between patients without major vascular involvement and healthy subjects. When SSc patients were grouped according to mRSS and VDAI, Sema3A levels were similar.

The semaphorin family comprises nearly 20 extracellular signal proteins, playing roles in various biological processes, including in-

flammation, apoptosis, fibrosis, angiogenesis, and bone remodeling. In class 8, 1 and 2 semaphorins exist in nonvertebrates, whereas 3 to 7 exist in vertebrates and 8 in viruses. In class 1, 4 to 6 act as transmembrane proteins, 2, 3, and 5 are secreted, and 7 bound to glycosylphosphatidylinositol. Semaphorins are found in immune pathways and tumor pathogenesis in addition to neurons, where they were first discovered. Semaphorin 3A and VEGF competitively bind to NP-1 receptor. Additionally, Sema3A downregulates CD100 and upregulates CD72 in B lymphocytes. In CD19, CD25 B regulatory lymphocytes, expression of interleukin 10, transforming growth factor β , and Sema3A were increased. Semaphorin 3A also inhibits the Ras/mitogen-activated protein kinase (MAPK) pathway in T cells.²⁴ Semaphorin 3A is effective in the collapse of the actin cytoskeleton in endothelial cells.²⁵ It was determined that Sema3A increased hepatocellular carcinoma progression in cells by increasing the expression of the gelsolin-like actin-capping protein, galectin-3, enolase 2, and epithelial cell adhesion molecule. Semaphorin 6D exerts distinct biological activities on endothelial cells in different regions of the cardiac tube.²⁶ Satue et al²⁷ found the Sema E gene was overexpressed in metastatic lung cancer cells.

Semaphorin 3A has been demonstrated to be involved in the pathogenesis of various rheumatic conditions. In RA, Sema3A levels were reduced both in the sera and the synovial fluid in comparison to OA and healthy controls and had a negative correlation with disease activity parameters.¹² In patients with lupus and antiphospholipid syndrome, Sema3A levels were lower than in controls and further reduced in existence of a thrombotic event or obstetric comorbidity.²⁸ In another study on lupus patients, Sema3A levels were lower in lupus patients with nephritis than in patients without.²⁹ Semaphorin 3A injections altered

TABLE 2. Antibody Positivity Percentages in Patients With Limited and Diffuse Cutaneous Scleroderma

	lcSSc, n (%)	dcSSc, n (%)	P^a
Anti-centromere	13 (40.6)	6 (21.4)	.083
Anti-Scl-70	7 (21.8)	18 (64.2)	<.001

dcSSc, diffuse cutaneous scleroderma; lcSSc, limited cutaneous scleroderma.

^aPearson χ^2 test.

TABLE 3. Comparisons of Semaphorin 3A Levels Between Different Involvement of SSc Patients and Control Group^a

	SSc patients		Control group	P value			
Semaphorin 3A (ng/mL), mean (SD)	47.85 (11.88)		57.60 (19.81)	.016 ^b			
	Major vascular involvement SSc	Nonmajor vascular SSc	Control group	P value	P ₁	P ₂	P ₃
Semaphorin 3A (ng/mL), mean (SD)	44.32 (5.87)	49.96 (14.00)	57.6 (19.81)	.008 ^c	.04	.001	.07
	Diffuse cutaneous SSc	Limited cutaneous SSc	P value				
Semaphorin 3A (ng/mL), mean (SD)	48.36 (11.47)	47.43 (12.38)	.775 ^c				

SSc, systemic sclerosis.

^aP₁: major vascular involvement SSc vs nonmajor vascular SSc; P₂: major vascular involvement SSc vs control group; P₃: nonmajor vascular SSc vs control group.

^bStudent t-test.

^cAnalysis of variance.

TABLE 4. Evaluation of Disease Activity With Semaphorin 3A and Acute-Phase Reactants According to Valentini Disease Activity Score and Modified Rodnan Skin Score

	Valentinidisease activity score <3	Valentinidisease activity score >3	P value ^a
Semaphorin 3A (ng/mL), mean (SD)	47.92 (12.57)	47.85 (12.57)	.916
CRP, mean (SD)	2.24 (3.79)	8.22 (12.55)	.169
ESR (mm/h), mean (SD)	13.62 (8.12)	23.6 (20.30)	.159
Fibrinogen (g/L), mean (SD)	3.11 (0.96)	2.86 (0.81)	.627
	Modified Rodnan skin score <14	Modified Rodnan skin score >14	
Semaphorin 3A (ng/mL), mean (SD)	47.57 (13.55)	47.73 (10.01)	.96
CRP (mg/L), mean (SD)	2.93 (5.91)	3.31 (7.10)	.829
ESR (g/L), mean (SD)	15.10 (9.21)	16.00 (14.45)	.784
Fibrinogen, mean (SD)	3.06 (1.09)	2.93 (5.91)	.915

CRP, C-reactive protein; ESR, erythrocyte sedimentation rate.

^aStudent t-test.

neovascularization in mice with diabetic retinopathy VEGF.³⁰ In our study, we observed further reduced levels of Sema3A in SSc patients with major vascular involvement, regardless of VDAI and mRSS scores, in accordance with the potential protective role of Sema3A in vasculopathic processes.

Pulmonary arterial hypertension is one of the most devastating vasculopathic complications of SSc, with significant functional deterioration and increased mortality. Decreased NO and prostacyclin expression and increased ET-1 production lead to endothelial damage and dysfunction.³¹ In the pathogenesis of DU, VEGF, endostatin, ET 1, asymmetric dimethyl-L-arginine, platelet activating factor acetyl hydrolase, galectin-1, and angiopoietin-like protein 3 are assumed to play a role.^{32,33} It has been reported that Sema3E levels were higher in SSc patients than in patients with Raynaud's phenomenon, with early capillaroscopic changes and with DUs.³⁴ In another study, increased VEGF and decreased NP-1 levels were observed in SSc patients.³⁴ Rimar et al¹⁷ reported decreased levels of Sema3A in SSc and demonstrated a negative correlation with anti-Scl-70 positivity. On the other hand, Romano et al¹⁸ observed similar Sema3A levels in SSc patients and healthy subjects, yet in SSc patients with history of DU, levels of Sema3A receptor NP-1 were lower than in patients without DU. In our study, DU was present in all SSc patients in the vasculopathic group and the Sema3A levels were significantly lower than in the nonvasculopathic group, which imply that decreased Sema3A levels can be attributed to its increased consumption in a prominent vasculopathic process.

There were several limitations to our study in addition to its single-center and cross-sectional nature. The number of patients with PAH and renal crisis was limited. The participant composition of this study was female (94.65% and 93.5% in the SSc and control groups, respectively). Systemic sclerosis is a rare disease and the female-to-male ratio ranges from 3: 1 to 8: 1,¹ similar to our study. The female-dominated sample did not cause bias due to the nature of the disease. Furthermore, most of the patients were under appropriate treatment. Although patients under treatment were included in the study due to the cross-sectional nature of the study, no statistically significant difference was found between drug use in the vascular and nonvascular groups. Further studies of a prospective nature involving treatment-naïve patients will better demonstrate the true role of Sema3A in SSc and related vasculopathy.

Conclusion

Our results suggest a relation between vasculopathy and Sema3A levels in SSc and imply that Sema3A may be a biomarker for distinguishing patients with potential to manifest major vascular involvement. Larger and prospective studies would further elucidate the potential use of Sema3A in SSc patients as a biomarker.

Conflict of Interest Disclosure


The authors have nothing to disclose.

REFERENCES

- Varga J. *Clinical Manifestations and Diagnosis of Systemic Sclerosis (Scleroderma) In Adults*. Waltham, MA: UpToDate. 2020. <https://www.medilib.ir/uptodate/show/7539>.
- Ingegnoli F, Ughi N, Mihai C. Update on the epidemiology, risk factors, and disease outcomes of systemic sclerosis. *Best Pract Res Clin Rheumatol*. 2018;32(2):223–240. doi:10.1016/j.berh.2018.08.005.
- Varga J. *Risk Factors for and Possible Causes of Systemic Sclerosis (Scleroderma)*. Waltham, MA: UpToDate; 2005. <https://www.medilib.ir/uptodate/show/7557>.
- Hughes M, Herrick AL. Digital ulcers in systemic sclerosis. *Rheumatology*. 2017;56(1):14–25.
- Hopkins W, Rubin LJ. Treatment of pulmonary arterial hypertension (group 1) in adults: pulmonary hypertension-specific therapy. *UpToDate*. Retrieved October 20, 2021. <https://www.medilib.ir/uptodate/show/8250>.
- Kayser C, Fritzler MJ. Autoantibodies in systemic sclerosis: unanswered questions. *Front Immunol*. 2015;6:167. doi:10.3389/fimmu.2015.00167.
- Muangchan C, Harding S, Khimdas S, Bonner A, Baron M, Pope J. Association of C-reactive protein with high disease activity in systemic sclerosis: results from the Canadian Scleroderma Research Group. *Arthritis Care Res*. 2012;64(9):1405–1414. doi:10.1002/acr.21716.
- Silva I, Teixeira A, Oliveira J, Almeida I, Almeida R, Vasconcelos C. Predictive value of vascular disease biomarkers for digital ulcers in systemic sclerosis patients. *Clin Exp Rheumatol*. 2015;33(4 suppl 91):S127–S130.
- Garcia S. Role of semaphorins in immunopathologies and rheumatic diseases. *Int J Mol Sci*. 2019;20(2):374. doi:10.3390/ijms20020374.
- Staton CA. Class 3 semaphorins and their receptors in physiological and pathological angiogenesis. *Biochem Soc Trans*. 2011;39(6):1565–1570. doi:10.1042/BST20110654.
- Gu C, Giraudo E. The role of semaphorins and their receptors in vascular development and cancer. *Exp Cell Res*. 2013;319(9):1306–1316.
- Takagawa S, Nakamura F, Kumagai K, et al. Decreased semaphorin3A expression correlates with disease activity and histological features of rheumatoid arthritis. *BMC Musculoskelet Disord*. 2013;14(1):1–11.
- Catalano A. The neuroimmune semaphorin-3A reduces inflammation and progression of experimental autoimmune arthritis. *J Immunol*. 2010;185(10):6373–6383. doi:10.4049/jimmunol.0903527.
- Vadasz Z, Toubi E. Semaphorin 3A—a marker for disease activity and a potential putative disease-modifying treatment in systemic lupus erythematosus. *Lupus*. 2012;21(12):1266–1270. doi:10.1177/0961203312456753.
- Bejar J, Kessler O, Sabag AD, et al. Semaphorin3A: a potential therapeutic tool for lupus nephritis. *Front Immunol*. 2018;9:634. doi:10.3389/fimmu.2018.00634.
- Rimar D, Rosner I, Slobodin G, et al. Semaphorin3A, a potential immune regulator in familial Mediterranean fever. *Clin Exp Rheumatol*. 2016;34(suppl 102):52–55.
- Rimar D, Nov Y, Rosner I, et al. Semaphorin 3A: an immunoregulator in systemic sclerosis. *Rheumatol Int*. 2015;35(10):1625–1630. doi:10.1007/s00296-015-3269-2.
- Romano E, Chora I, Manetti M, et al. Decreased expression of neuropilin-1 as a novel key factor contributing to peripheral microvasculopathy and defective angiogenesis in systemic sclerosis. *Ann Rheum Dis*. 2016;75(8):1541–1549. doi:10.1136/annrheumdis-2015-207483.
- Van Den Hoogen F, Khanna D, Fransen J, et al. 2013 classification criteria for systemic sclerosis: an American College of Rheumatology/ European League against Rheumatism collaborative initiative. *Arthritis Rheum*. 2013;65(11):2737–2747. doi:10.1002/art.38098.
- Medsger T, Silman A, Steen V, et al. A disease severity scale for systemic sclerosis: development and testing. *J Rheumatol*. 1999;26(10):2159–2167.
- Della Rossa A, Valentini G, Bombardieri S, et al. European multicentre study to define disease activity criteria for systemic sclerosis: I. Clinical and epidemiological features of 290 patients from 19 centres. *Ann Rheum Dis*. 2001;60(6):585–591. doi:10.1136/ard.60.6.585.

22. Baron M, Chung L, Gyger G, et al. Consensus opinion of a North American Working Group regarding the classification of digital ulcers in systemic sclerosis. *Clin Rheumatol*. 2014;33(2):207–214. doi:[10.1007/s10067-013-2460-7](https://doi.org/10.1007/s10067-013-2460-7).
23. Simonneau G, Montani D, Celermajer DS, et al. Haemodynamic definitions and updated clinical classification of pulmonary hypertension. *Eur Respir J*. 2019;53(1):1801913. doi:[10.1183/13993003.01913-2018](https://doi.org/10.1183/13993003.01913-2018).
24. Catalano A, Caprari P, Moretti S, Faronato M, Tamagnone L, Procopio A. Semaphorin-3A is expressed by tumor cells and alters T-cell signal transduction and function. *Blood*. 2006;107(8):3321–3329. doi:[10.1182/blood-2005-06-2445](https://doi.org/10.1182/blood-2005-06-2445).
25. Guttman-Raviv N, Shraga-Heled N, Varshavsky A, Guimaraes-Sternberg C, Kessler O, Neufeld G. Semaphorin-3A and semaphorin-3F work together to repel endothelial cells and to inhibit their survival by induction of apoptosis. *J Biol Chem*. 2007;282(36):26294–26305. doi:[10.1074/jbc.M609711200](https://doi.org/10.1074/jbc.M609711200).
26. Toyofuku T, Kikutani H. Semaphorin signaling during cardiac development. *Adv Exp Med Biol*. 2007;600:109–117. doi:[10.1007/978-0-387-70956-7_9](https://doi.org/10.1007/978-0-387-70956-7_9).
27. Martín-Satué M, Blanco J. Identification of semaphorin E gene expression in metastatic human lung adenocarcinoma cells by mRNA differential display. *J Surg Oncol*. 1999;72:18–23. doi:[10.1002/\(sici\)1096-9098\(199909\)72:1<18::aid-jso5>3.0.co;2-p](https://doi.org/10.1002/(sici)1096-9098(199909)72:1<18::aid-jso5>3.0.co;2-p).
28. Kart Bayram GS, Erden A, Bayram D, et al. Semaphorin 3A levels in lupus with and without secondary antiphospholipid antibody syndrome and renal involvement. *Lab Med*. 2022;53(3):285–289. doi:[10.1093/labmed/lmab096](https://doi.org/10.1093/labmed/lmab096).
29. Doron R, Merav L, Nasrin E, et al. Low urine secretion of semaphorin3a in lupus patients with proteinuria. *Inflammation*. 2022;45(2):603–609. doi:[10.1007/s10753-021-01570-4](https://doi.org/10.1007/s10753-021-01570-4).
30. Binet F, Beaulieu N, Beauchemin K, et al. Semaphorin3A-trap accelerates vascular regeneration in ischemic retinopathy and reduces retinal edema. *Investig Ophthalmol Vis Sci*. 2019;60(9):1648.
31. Matucci-Cerinic M, Kahaleh B, Wigley FM. Evidence that systemic sclerosis is a vascular disease. *Arthritis Rheum*. 2013;65(8):1953–1962.
32. Yanaba K, Asano Y, Tada Y, Sugaya M, Kadono T, Sato S. Clinical significance of circulating platelet-activating factor acetylhydrolase levels in systemic sclerosis. *Arch Dermatol Res*. 2012;304(3):203–208. doi:[10.1007/s00403-011-1196-y](https://doi.org/10.1007/s00403-011-1196-y).
33. Ichimura Y, Asano Y, Akamata K, et al. Serum angiopoietin-like protein 3 levels: possible correlation with progressive skin sclerosis, digital ulcers and pulmonary vascular involvement in patients with systemic sclerosis. *Acta Derm Venereol*. 2014;94(2):157–162.
34. Chora I, Romano E, Manetti M, et al. Evidence for a derangement of the microvascular system in patients with a very early diagnosis of systemic sclerosis. *J Rheumatol*. 2017;44(8):1190–1197. doi:[10.3899/jrheum.160791](https://doi.org/10.3899/jrheum.160791).

Comparison of the optimized direct spectrophotometric serum prolidase enzyme activity assay method with the currently used spectrophotometric assay methods and liver fibrosis indexes to distinguish the early stages of liver fibrosis in patients with chronic hepatitis B infection

Huseyin Kayadibi, MD,^{1,2}  İbrahim Hakkı Köker, MD,³ Zuhal Gucin, MD,⁴ Hakan Şentürk, MD,³ Sakine Candan Merzifonlu, MD,⁵ Ali Tüzün İnce, MD³

¹Department of Medical Biochemistry, Eskisehir Osmangazi University School of Medicine, Eskisehir, Turkey, ²Department of Medical Biochemistry, Hitit University School of Medicine, Corum, Turkey, Departments of ³Gastroenterology and ⁴Pathology, Bezmialem University School of Medicine, Istanbul, Turkey, ⁵Biochemistry Laboratory, Corum Chest Diseases Hospital, Corum, Turkey. Corresponding author: Huseyin Kayadibi; mdkayadibi@yahoo.com

Key words: APRI; early stage; FIB-4; HBV; liver fibrosis; optimized prolidase assay

Abbreviations: SPEA, serum prolidase enzyme activity; CHB, chronic hepatitis B; ALT, alanine aminotransferase; AST, aspartate aminotransferase; AAR, AST-to-ALT ratio; API, age platelet index; APRI, AST-to-platelet ratio index; CDS, cirrhosis discriminate score; FIB-4, fibrosis index based on four factors; GUCI, Goteborg University Cirrhosis Index; HCl, hydrochloric acid; TCA, trichloroacetic acid; GAA, glacial acetic acid; OPA, orthophosphoric acid; CV, coefficients of variation; CLSI, Clinical and Laboratory Standards Institute; INR, international normalization ratio; ROC, receiver operating characteristic; AUROC, areas under the curve; GSH, reduced glutathione

Laboratory Medicine 2023;54:652-658; <https://doi.org/10.1093/labmed/lmad025>

ABSTRACT

Objective: The aim of this study was to optimize the currently used direct spectrophotometric serum prolidase enzyme activity (SPEA) assay method and compare its diagnostic accuracy with current precipitation and direct spectrophotometric assay methods, AST-to-ALT ratio, age platelet index, AST-to-platelet ratio index, cirrhosis discriminate score, Doha score, FIB-4, FibroQ, fibrosis index, Goteborg University Cirrhosis Index, King's score, and Pohl score for distinguishing Ishak F0 from F1–F3 in patients with chronic hepatitis B (CHB) infection.

Methods: Liver biopsy results from 112 patients were included in this study.

Results: The SPEA values were 529 (292–794) U/L, 671 (486–927) U/L, and 1077 (867–1399) U/L with the precipitation, current, and optimized direct spectrophotometric assay methods, respectively. According to multivariate logistic regression analysis optimized direct spectrophotometric SPEA was the only statistically significant parameter to predict the early stages of liver fibrosis.

Conclusions: Optimized direct spectrophotometric SPEA assay method could be used to distinguish early stages of liver fibrosis in patients with CHB infection instead of the currently used spectrophotometric SPEA assay methods and other evaluated liver fibrosis indexes.

Distinguishing the early stages of liver fibrosis is critical for the management of patients with chronic hepatitis B (CHB) infection.^{1,2} To determine the stage of liver fibrosis, liver biopsy is the gold standard diagnostic tool used today. However, it is invasive, prone to many complications, and inconsistent results may be encountered due to sampling error or within-between observer variabilities.^{3–5} For these reasons, there is a great need for a simple, noninvasive, cost-effective, and easily accessible biochemical test such as serum prolidase enzyme activity (SPEA).

Prolidase enzyme (EC 3.4.13.9) is a manganese-dependent cytosolic exopeptidase that is involved in the degradation of iminodipeptides with proline and/or hydroxyproline at the C-terminus in the final step of collagen breakdown.^{6,7} Spectrophotometric SPEA assay methods used today are the precipitation and direct assays. The direct spectrophotometric SPEA assay method is more practical and less time-consuming than the precipitation assay.^{8,9} However, higher accuracy in a direct spectrophotometric SPEA assay method is needed, as different results are obtained with the currently used spectrophotometric SPEA assay methods carried out for determination of fibrosis stages in different kinds of diseases, as the prolidase enzyme has been shown to be important in the pathophysiology of different kinds of disorders.^{10–14}

In this study, we aimed to optimize the currently used spectrophotometric SPEA assay method and compare its diagnostic accuracy with the precipitation and currently used direct spectrophotometric SPEA assay methods and other noninvasive liver fibrosis indexes such as aspartate aminotransferase (AST)-to-alanine aminotransferase (ALT) ratio (AAR), age platelet index (API), AST-to-platelet ratio index (APRI), cirrhosis discriminant score (CDS), Doha score, fibrosis index based on four factors (FIB-4), FibroQ, fibrosis index, Goteborg University Cirrhosis Index (GUCI), King's score, and Pohl score for the differentiation of early stages of liver fibrosis (F0 vs F1–F3) in liver biopsy performed patients with CHB infection.

Materials and Methods

Patient Selection

After gaining the approval of the local ethics committee of Hitit University (2016–18) and informed consent from all participants, patients with CHB infection who had a liver biopsy 1 to 3 day after having blood drawn were included in this study; 14 stage 0 and 10 stage 1 liver fibrosis patients' SPEA were analyzed from blood samples drawn within 6 months after liver biopsy. Patients <18 years of age, taking antiviral treatment, with co-infection with hepatitis C, D, or HIV, autoimmune hepatitis, or cholangitis were excluded from the study.

Materials

Human recombinant prolidase, trizma base, $\text{MnCl}_2 \cdot 4\text{H}_2\text{O}$, reduced glutathione (GSH), Triton X-100, gly-pro, proline, hydrochloric acid (HCl), trichloroacetic acid (TCA), glacial acetic acid (GAA), orthophosphoric acid (OPA) and ninhydrin were used for spectrophotometric SPEA assay methods. All chemicals were of analytical grade. Absorbances were measured at 515 nm using a UV/Vis spectrophotometer (Biochrom Libra S60).

Procedures of the Precipitation and Direct Spectrophotometric SPEA Assay Methods

In the precipitation spectrophotometric SPEA assay method, the serum sample was diluted and activated with 50 mM pH 7.8 Tris-HCl buffer containing 1 mM MnCl_2 and then incubated at 37°C for 180 minutes (original method is 24 hours). Activated serum was mixed with 50 mM of pH 7.8 Tris-HCl buffer containing 94 mM glycine-L-proline and 1 mM MnCl_2 for the enzyme-substrate incubation at 37°C for 30 minutes. At the end of this incubation, 0.45 M TCA was added immediately and samples were centrifuged. For the ninhydrin reaction, supernatant, GAA, and ninhydrin reagent (25 g/L ninhydrin was prepared with 600 mL GAA and 400 mL of 6 M orthophosphoric acid mixture) were pipetted, vortexed, and incubated at 90°C for 10 minutes. At the end of the incubation, absorbances were read against the reagent blank in spectrophotometer at the 515 nm wavelength.

In the currently used direct spectrophotometric SPEA assay method, the serum sample was diluted and activated with 50 mM pH 7.0 Tris-HCl buffer containing 50 mM MnCl_2 and 1 mM GSH, and incubated at 37°C for 30 minutes. Enzyme-substrate incubation was performed for 5 minutes at 37°C with 50 mM pH 7.8 Tris-HCl buffer containing 144 mM glycine-L-proline, 50 mM MnCl_2 , and 1 mM GSH. To inhibit the SPEA by pH change, GAA was added immediately. For the ninhydrin reaction, 50 mM pH 7.8 Tris-HCl buffer and ninhydrin reagent (30 g/L ninhydrin was prepared with 0.5 M orthophosphoric acid) were pipetted, vortexed, and incubated at 90°C for 20 minutes. At the end of the incubation,

samples were immediately kept in ice water, and absorbances were read against the sample blank in which the substrate was not added in the spectrophotometer at the 515 nm wavelength.

Optimization of the Direct Spectrophotometric SPEA Assay Method

Enzyme-substrate incubation, activation, and proline assay steps of the currently used direct spectrophotometric SPEA assay method have been optimized as follows, and method validation was performed.

Enzyme-Substrate Incubation Step

Optimum enzyme-substrate incubation time and temperature were determined by incubation of the gly-pro substrate with the presence or absence of human recombinant prolidase at 37°C, 45°C, 50°C, and 55°C for 5, 10, 15, 20, 25, 30, 40, 50, and 60 minutes after activation with 1 mM GSH and 50 mM $\text{MnCl}_2 \cdot 4\text{H}_2\text{O}$ at 37°C for 30 minutes.

Activation Step

This step was optimized using different concentrations of $\text{MnCl}_2 \cdot 4\text{H}_2\text{O}$, GSH and Triton X-100 as activators at 45°C for 0, 5, 10, 15, 20, 25, 30, 40, 50, 60, 90, 120, 150, and 180 minutes of incubation. For incubation temperature, 45°C was selected based on the maximum SPEA that was determined at this temperature in the enzyme-substrate incubation step.

Proline Assay Step

For the optimization of proline-ninhydrin condensation step, the following experiments were done. First, it was decided whether the samples should be cooled at room temperature or in ice water after the incubation of 12.5 mg/dL of proline standard with ninhydrin reagent (25 g/L ninhydrin, 0.6 L GAA, and 0.4 L 6 M OPA) at 80°C by considering whether pH 7.8 Tris-HCl buffer was necessary or not. Second, optimum ninhydrin reagent was determined by comparing the coefficients of variation (CV) percentage and maximum delta absorbance values obtained with the following 4 different ninhydrin reagents for 12.5 mg/dL of proline standard repeated 20 times in 60 minutes of incubation at 80°C: reagent A: 12.5 g ninhydrin was dissolved in 1 L GAA; reagent B: 25 g ninhydrin was dissolved in 1 L 0.5 M OPA; reagent C: 25 g ninhydrin was dissolved in 0.6 L GAA and 0.4 L 6 M OPA; reagent D: 20 g ninhydrin was dissolved in 0.6 L GAA and 0.4 L distilled water. Third, optimum ninhydrin concentration was determined by taking into account the lowest CV percentage and maximum delta absorbance results obtained with the use of following ninhydrin reagents in 40, 45, 50, 60, 70, and 80 minutes of incubation for 12.5 mg/dL and 24 mg/dL of proline standards at 80°C: reagent E: 10 g ninhydrin was dissolved in 0.6 L GAA and 0.4 L distilled water; reagent F: 15 g ninhydrin was dissolved in 0.6 L GAA and 0.4 L distilled water; reagent G: 20 g ninhydrin was dissolved in 0.6 L GAA and 0.4 L distilled water; reagent H: 25 g ninhydrin was dissolved in 0.6 L GAA and 0.4 L distilled water. Fourth, optimum reading interval was determined according to the stability time of proline-ninhydrin condensation in ice water. For this purpose, a series of 12.5 mg/dL of proline standards were incubated at 80°C for 45 minutes and cooled for 5, 10, 20, 30, 40, 50, 60, 70, 80, and 90 minutes in ice water.

Method Validation

Intra- and inter-day precisions and linearity were performed according to the protocols of the Clinical and Laboratory Standards Institute (CLSI).

Intra- and Inter-Assay Precision.—The intra- and inter-assay precision studies were done based on CLSI EP05-A3 and CLSI EP15-A3 protocols, respectively.^{15,16} Both of these precision studies were performed using low and high SPEA levels of pooled human sera separately. Intra-assay precision was determined by analyzing a total of 40 samples, 20 in the morning and 20 in the afternoon, at low and high SPEA levels, respectively, of pooled human sera within a day. The inter-assay precision was determined based on a total of 20 measurement results by analyzing 4 replicates per day over a total of 5 consecutive days for low and high SPEA levels of pooled human sera separately.

Linearity.—Linearity was determined according to the CLSI EP06-A protocol.¹⁷ In this experiment, human serum pool with a high SPEA level (4492 U/L) was diluted with human serum pool with a low SPEA level (150 U/L) according to the procedure that was determined in CLSI EP06-A protocol using 8 different sample combinations. Each dilution was measured 3 times in a single run, and linearity was evaluated by linear regression analysis. The observed values were plotted against the expected values wherein $R^2 > 0.99$ was considered as linear and acceptable.

Other Biochemistry Tests

The AST, ALT, albumin, total bilirubin, direct bilirubin, international normalization ratio (INR), and complete blood count analysis were done with commercially available kits. The AAR, API, APRI, CDS, Doha Score, FIB-4, FibroQ, fibrosis index, GUCI, King's Score and Pohl Score were calculated as follows:

AAR = AST/ALT; API = [Age in years: <30 = 0; 30–39 = 1; 40–49 = 2; 50–59 = 3; 60–69 = 4; ≥70 = 5. Platelet ($\times 10^9/L$): ≥225 = 0; 200–224 = 1; 175–199 = 2; 150–174 = 3; 125–149 = 4; <125 = 5]; APRI = $100 \times (\text{AST}/\text{AST upper limit of normal})/\text{Platelet} (\times 10^9/L)$; CDS = $[\text{Platelet} (\times 10^9/L) + (\text{ALT}/\text{AST}) + \text{INR} \cdot \text{Platelet} (\times 10^9/L)]$; ≥340 = 0; 280–339 = 1; 220–279 = 2; 160–219 = 3; 100–159 = 4; 40–99 = 5; <40 = 6. ALT/AST: ≥1.7 = 0; 1.2–1.7 = 1; 0.6–1.19 = 2; <0.6 = 3. INR: ≤1.1 = 0; 1.1–1.4 = 1; >1.4 = 2]; Doha score = $8.5 - [0.2 \times \text{albumin (g/dL)}] + (0.01 \times \text{AST}) - [0.02 \times \text{Platelet} (\times 10^9/L)]$; FIB-4 = $\text{Age} \times \text{AST}/\text{Platelet} (\times 10^9/L) \times \text{ALT}^{1/2}$; FibroQ = $10 \times \text{Age} \times \text{AST} \times \text{INR}/\text{Platelet} (\times 10^9/L) \times \text{ALT}$; Fibrosis index = $8 - (0.01 \times \text{Platelet} (\times 10^9/L)) - \text{albumin (g/dL)}$; GUCI = $100 \times \text{AST} \times \text{INR}/\text{Platelet} (\times 10^9/L)$; King's score = $\text{Age} \times \text{AST} \times \text{INR}/\text{Platelet} (\times 10^9/L)$; Pohl score = Positive if AAR ≥1 and Platelet ($\times 10^9/L$) <150.

Liver Biopsy

Liver biopsy was used as the gold standard diagnostic tool to compare the diagnostic accuracy of the spectrophotometric SPEA assay methods. Liver fibrosis stages were determined according to the Ishak staging system.¹⁸ A single senior pathologist (Z.G.) interpreted all liver biopsy specimens independent of the SPEA results.

Statistical Analysis

Hitit University licensed IBM SPSS 23 package program was used for statistical analysis of the results. According to the Kolmogorov–Smirnov analysis, continuous variables were presented as mean ± SD or median (25th–75th quartile), as appropriate. Kruskal–Wallis analysis of variance (ANOVA) or one-way ANOVA with Bonferroni correction and nonparametric related samples Friedman two-way ANOVA by ranks test were done for the comparison of groups. Spearman correlation analysis was used to determine the associations between fibrosis stages and biochemistry tests. The diagnostic powers of spectrophotometric SPEA assay methods and commonly used fibrosis indexes were determined by

performing receiver operating characteristic (ROC) analysis for the differentiation of F0 and F1 to F3 fibrosis stages. For the prediction of early stage liver fibrosis, logistic regression analyses were used. A $P < .05$ was considered statistically significant.

Results

Patients Characteristics

According to the Ishak fibrosis score, the numbers of patients with F0, F1, F2, and F3 fibrosis were 42, 43, 21, and 6, respectively. The SPEA values were 529 (292–794) U/L, 671 (486–927) U/L, and 1077 (867–1399) U/L with the precipitation, currently used direct and optimized direct assay methods, respectively. Demographics, laboratory test values, and SPEA results of the spectrophotometric assay methods based on fibrosis stages are presented in **TABLE 1**.

Associations between the early stages (F0–F3) of liver fibrosis and optimized direct SPEA, currently used direct SPEA, precipitation SPEA, age, albumin, ALT, AST, direct bilirubin, total bilirubin, INR, platelets, AAR, API, CDS, Doha score, FIB-4, FibroQ, fibrosis index, GUCI, King's score, and Pohl score are shown in **TABLE 2**.

Optimized Direct Spectrophotometric SPEA Assay Method

Enzyme-Substrate Incubation Step

The highest enzyme activity was determined at 5 minutes of incubation at 37°C, 45°C, 50°C, and 55°C incubation temperatures; the highest enzyme activity was obtained at 45°C.

Activation Step

In 0, 5, 10, 15, 20, 25, 30, 40, 50, 60, 90, 120, 150, and 180 minutes of activation incubations at 45°C, the highest enzyme activity was achieved at 150, 120, 30, and 25 minutes, consecutively, without a statistically significant difference ($P = .440$). To not increase the total analysis time for the SPEA assay method, 30 minutes incubation time was preferred. After deciding the optimum activation time, optimum concentrations of $\text{MnCl}_2 \cdot 4\text{H}_2\text{O}$, GSH, and Triton X-100 as an activator were determined by 25 mM, 38 mM, 51 mM, 63 mM, 76 mM, and 101 mM of $\text{MnCl}_2 \cdot 4\text{H}_2\text{O}$; 1 mM and 2 mM of GSH; and 0.1% Triton X-100 combinations. The highest enzyme activity was obtained with the combination of 63 mM $\text{MnCl}_2 \cdot 4\text{H}_2\text{O}$ and 1 mM GSH as activators.

Proline Assay Step

The maximum delta absorbance value was obtained with the addition of pH 7.8 Tris-HCl buffer by cooling the samples in ice water. In the comparison of the delta absorbance values obtained with ninhydrin reagents A, B, C, and D, the lowest CV percentage and maximum delta absorbance value were obtained with reagent D. In comparison of the delta absorbance values obtained with ninhydrin reagents E, F, G, and H, maximum delta absorbance value with the lowest CV% was obtained with reagent F. As a result, for the proline assay, it was decided to incubate the samples for 45 minutes at 80°C with ninhydrin reagent containing 15 g/L ninhydrin, 0.6 L GAA, and 0.4 L distilled water. Optimum reading interval was up to 90 minutes for samples kept in ice water because there were no statistically significant differences among the absorbance values, according to the nonparametric related samples Friedman two-way analysis of variance by ranks test ($P = .943$).

TABLE 1. Demographics and laboratory test results according to the liver fibrosis stages

Variables	Stage 0 (n = 42)	Stage 1 (n = 43)	Stage 2 (n = 21)	Stage 3 (n = 6)	P
Age, y	41 ± 12	43 ± 11	45 ± 11	50 ± 16	.320
Sex, F/M	19/23	18/25	10/11	0/6	.182
Optimized direct SPEA, U/L	922 (795–1126) ^a	1034 (919–1332) ^b	1384 (1100–1766)	1790 (1403–2548)	<.001
Currently used direct SPEA, U/L	634 (480–880)	685 (529–807)	909 (516–986)	733 (469–932)	.502
Precipitation SPEA, U/L	389 (255–678)	557 (294–802)	658 (407–1294)	767 (594–965)	.049
Albumin, g/L	44 ± 3.2 ^c	43 ± 2.4	42 ± 4.5	40 ± 2.0	.008
ALT, U/L	32 (19–56)	39 (18–69)	58 (33–89)	83 (64–541) ^d	.004
AST, U/L	24 (18–29) ^e	25 (18–48)	41 (26–72)	46 (36–224)	.002
Direct bilirubin, mg/dL	0.22 (0.17–0.30)	0.22 (0.19–0.33)	0.27 (0.22–0.37)	0.43 (0.20–0.65)	.054
Total bilirubin, mg/dL	0.58 (0.39–0.80)	0.59 (0.44–0.83)	0.69 (0.62–0.89)	1.14 (0.75–1.49) ^f	.020
INR	1.04 ± 0.07 ^g	1.07 ± 0.09	1.11 ± 0.11	1.16 ± 0.09	.001
Platelets, ×10 ⁹ /L	232 ± 62 ^h	214 ± 44	207 ± 53	154 ± 42	.009
AAR	0.80 (0.58–1.00)	0.76 (0.53–1.01)	0.75 (0.55–0.93)	0.49 (0.42–0.65)	.102
API	2 (2–4) ⁱ	3 (2–4)	4 (2.5–5)	6 (3–8)	.024
APRI	0.29 (0.24–0.41) ^j	0.32 (0.25–0.72) ^k	0.52 (0.38–0.93)	0.92 (0.56–5.65)	<.001
CDS	4.54 (4.03–5.38)	4.99 (4.07–5.99)	5.11 (4.40–6.36)	6.67 (5.75–7.53) ^l	.009
Doha score	3.17 (2.60–4.00) ^m	3.84 (2.92–4.77)	3.97 (3.14–5.03)	5.21 (4.28–7.71)	.005
FIB-4	0.79 (0.63–1.02) ⁿ	0.94 (0.63–1.29)	0.97 (0.82–1.84)	2.24 (1.10–3.38)	.006
FibroQ	1.48 (1.12–1.91)	1.59 (1.17–2.38)	1.57 (1.13–2.81)	2.09 (1.15–3.17)	.561
Fibrosis index	1.27 (0.86–1.70)	1.59 (1.14–1.95)	1.69 (1.09–2.28)	2.45 (1.86–2.99) ^o	.002
GUCI	10 (8.5–15) ^p	12 (8.9–26)	19 (14–39)	35 (22–226) ^r	<.001
King's score	4.24 (3.56–6.22) ^s	5.77 (3.10–8.93)	8.59 (5.91–16.9)	18.7 (12.6–106) ^t	<.001
Pohl score (+/–)	1/41	0/43	0/21	0/6	

ALT, alanine aminotransferase; AST, aspartate aminotransferase; INR, international normalization ratio; AAR, AST-to-ALT ratio; API, age platelet index; APRI, AST-to-platelet ratio index; CDS, cirrhosis discriminate score; GUCI, Goteborg University Cirrhosis Index; SPEA, serum prolidase enzyme activity.

^aP = .001 vs stage 2, P = .001 vs stage 3.

^bP = .026 vs stage 3.

^cP = .034 vs stage 2.

^dP = .014 vs stage 0, P = .05 vs stage 1.

^eP = .016 vs stage 2, P = .019 vs stage 3.

^fP = .045 vs stage 0, P = .044 vs stage 1.

^gP = .015 vs stage 2, P = .009 vs stage 3.

^hP = .007 vs stage 3.

ⁱP = .05 vs stage 3.

^jP = .008 vs stage 2, P = .005 vs stage 3.

^kP = .038 vs stage 3.

^lP = .006 vs stage 0, P = .044 vs stage 1.

^mP = .007 vs stage 3.

ⁿP = .020 vs stage 3.

^oP = .004 vs stage 0, P = .05 vs stage 1.

^pP = .004 vs stage 2, P = .003 vs stage 3.

^qP = .031 vs stage 1.

^rP = .002 vs stage 2, P = .002 vs stage 3.

^sP = .034 vs stage 1.

Method Validation

Intra- and Inter-Assay Precision.—The intra-assay CV levels were 7.4% and 6.2%, whereas inter-assay CV levels were 9.2% and 7.7% for low and high SPEA levels of pooled human sera, respectively.

Linearity.—The correlation coefficient of the SPEA calibration curve was found to be 0.992 ($P < .001$). The SPEA was linear between 150 and 4492 U/L.

Diagnostic Accuracy of the Spectrophotometric SPEA Assay Methods and Biochemical Tests

According to the ROC analysis to distinguish the F0 from F1 to F3 fibrosis stages, areas under the curve (AUROC) with 95% CI for the precipitation, currently used, and optimized direct spectrophotometric SPEA assay methods were 0.638 (0.519–0.757), 0.585 (0.461–0.708),

and 0.775 (0.669–0.880) ($P = .014$, $P = .187$, and $P < .001$), respectively. AUROC values for other parameters are presented in **FIGURE 1**. The AUROC of optimized direct spectrophotometric SPEA was higher than the other evaluated 11 liver fibrosis indexes in our study cohort. In addition, optimized direct spectrophotometric SPEA was the only statistically significant parameter according to the multivariate logistic regression analysis among the statistically significant parameters in univariate logistic regression analysis for the prediction of early stage liver fibrosis (**TABLE 3**).

Discussion

To the best of our knowledge, this is the first study in which direct spectrophotometric SPEA assay method was optimized. The diagnostic accuracy of currently used spectrophotometric SPEA assay methods and

TABLE 2. Associations between the early stages (F0–F3) of liver fibrosis and evaluated parameters

Variables	Early stages of liver fibrosis
Optimized direct SPEA, U/L	$r = 0.462, P < .001$
Currently used direct SPEA, U/L	$r = 0.131, P = .167$
Precipitation SPEA, U/L	$r = 0.263, P = .005$
Age, y	$r = 0.114, P = .231$
Albumin, g/L	$r = -0.290, P = .002$
ALT, U/L	$r = 0.307, P = .001$
AST, U/L	$r = 0.329, P < .001$
Direct bilirubin, mg/dL	$r = 0.228, P = .017$
Total bilirubin, mg/dL	$r = 0.219, P = .021$
INR	$r = 0.363, P < .001$
Platelets, $\times 10^9/L$	$r = -0.268, P = .005$
AAR	$r = -0.155, P = .105$
API	$r = 0.270, P = .004$
APRI	$r = 0.377, P < .001$
CDS	$r = 0.260, P = .006$
Doha score	$r = 0.310, P = .001$
FIB-4	$r = 0.321, P = .001$
FibroQ	$r = 0.130, P = .176$
Fibrosis index	$r = 0.328, P = .001$
GUCI	$r = 0.400, P < .001$
King's score	$r = 0.414, P < .001$
Pohl score (+/–)	$r = -0.111, P = .250$

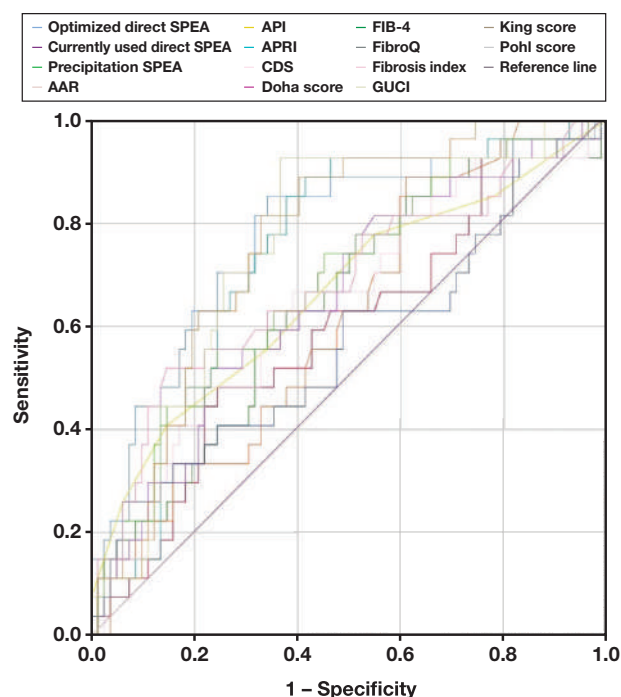
ALT, alanine aminotransferase; AST, aspartate aminotransferase; INR, international normalization ratio; AAR, AST-to-ALT ratio; API, age platelet index; APRI, AST-to-platelet ratio index; CDS, cirrhosis discriminate score; GUCI, Goteborg University Cirrhosis Index; SPEA, serum prolidase enzyme activity.

some liver fibrosis indexes, AAR, API, APRI, CDS, Doha score, FIB-4, FibroQ, fibrosis index, GUCI, King's score and Pohl score, were also evaluated to distinguish the F0 and F1 to F3 liver fibrosis stages in patients with CHB infection. According to this study, an optimized direct spectrophotometric SPEA assay method could be preferred over the currently used methods, as well as some fibrosis indexes for the evaluation of early liver fibrosis stages in patients with CHB infection.

Hepatitis B is a worldwide viral infection, causing acute and chronic liver diseases. According to WHO, 296 million people were living with CHB infection in 2019, and approximately 820,000 of these patients died, generally from cirrhosis and hepatocellular carcinoma-related complications.¹⁹ Starting medical therapy for CHB infection as soon as possible prevents or delays cirrhosis, complications, hepatocellular carcinoma, and transition to the decompensated phase and increases survival.^{1,2} Liver biopsy is currently the gold standard diagnostic tool for staging the liver fibrosis, but it is invasive and carries many risks and complications.^{3–5} Therefore, the search for noninvasive methods like SPEA to diagnose the early stages of liver fibrosis is critical.

There are 2 spectrophotometric SPEA assay methods used today. One of them requires TCA precipitation whereas the other does not.^{8,9} Of these, the direct assay method is cost-effective, more practical, and less time-consuming than the precipitation method. However, the analytical steps of the direct method should be optimized in terms of activators such as $MnCl_2 \cdot 4H_2O$ and GSH concentrations, incubation times and in-

FIGURE 1. Areas under the curve (AUROC) of serum prolidase enzyme activities and liver fibrosis indexes to distinguish the F0 from F1–F3 liver fibrosis stages. ALT, alanine aminotransferase; AST, aspartate aminotransferase; INR, international normalized ratio. AAR, AST-to-ALT ratio; API, age platelet index; APRI, AST-to-platelet ratio index; CDS, cirrhosis discriminate score; GUCI, Goteborg University Cirrhosis Index; SPEA, serum prolidase enzyme activity.



	AUROC (95 CI%)	P
Optimized direct SPEA	0.775 (0.670–0.880)	<.001
Currently used direct SPEA	0.592 (0.469–0.716)	.152
Precipitation SPEA	0.641 (0.521–0.761)	.028
AAR	0.614 (0.499–0.728)	.077
API	0.663 (0.537–0.789)	.011
APRI	0.745 (0.644–0.846)	<.001
CDS	0.642 (0.521–0.763)	.028
Doha score	0.659 (0.540–0.777)	.014
FIB-4	0.685 (0.570–0.801)	.004
FibroQ	0.565 (0.432–0.698)	.312
Fibrosis index	0.682 (0.557–0.807)	.005
GUCI	0.755 (0.653–0.856)	<.001
King score	0.762 (0.669–0.856)	<.001
Pohl score (+/–)	0.506 (0.381–0.631)	.925

cubation temperatures for activation, enzyme-substrate incubation, and proline-ninhydrin condensation steps, as these factors are not evaluated in the currently used direct SPEA assay method. Therefore, in this study, optimum activation, enzyme-substrate, and proline-ninhydrin condensation incubation conditions were determined for the direct spectrophotometric SPEA assay method based on the higher enzyme activity to improve the diagnostic power of SPEA in a collagen metabolism-related disorder like fibrosis in patients with CHB infection. On the other hand, Triton X-100 is used in the precipitation spectrophotometric SPEA assay method,⁸ but it should be noted that the use of Triton X-100 is forbidden in the European Union since January 2021 due to its effect as a hormone disrupter. Therefore, the precipitation spectrophotometric SPEA assay method has become less practical and will not be appropriate for future studies. Because Triton X-100 is not used in direct spectrophotometric SPEA assay methods, optimized direct spectrophotometric SPEA assay method would be the method of choice in the future for spectrophotometric SPEA analysis.

TABLE 3. Variables associated with the prediction of early stage liver fibrosis by univariate and multivariate logistic regression analyses

Variables	Univariate analysis			Multivariate analysis		
	OR (95% CI)	Wald	P	OR (95% CI)	Wald	P
Optimized direct SPEA, U/L	1.002 (1.001–1.004)	15.5	<.001	1.002 (1.001–1.004)	9.23	.002
Precipitation SPEA, U/L	1.001 (1.000–1.002)	5.70	.017	1.001 (1.000–1.002)	1.71	.191
Albumin, g/L	0.113 (0.026–0.492)	8.45	.004	0.231 (0.022–2.446)	1.48	.223
ALT, U/L	1.004 (1.000–1.007)	3.95	.047	0.991 (0.965–1.017)	0.48	.489
Direct Bilirubin, mg/dL	9.106 (0.974–85.15)	3.75	.053	2.760 (0.147–51.70)	0.46	.497
Total bilirubin, mg/dL	3.782 (1.191–12.01)	5.09	.024	1.708 (0.183–15.98)	0.22	.639
INR	3359 (22.38–504,235)	10.1	.001	133.2 (0.007–2,689,836)	0.94	.333
Platelets, $\times 10^9/L$	0.990 (0.982–0.999)	4.77	.029	1.017 (0.920–1.124)	0.11	.744
AAR	0.215 (0.041–1.119)	3.34	.068	0.006 (0.000–5.306)	2.19	.139
API	1.421 (1.116–1.810)	8.12	.004	1.344 (0.546–3.307)	0.42	.520
APRI	1.323 (1.001–1.747)	3.88	.049	0.029 (0.000–116.1)	0.70	.402
CDS	1.487 (1.033–2.141)	4.56	.033	0.268 (0.040–1.822)	1.81	.178
Doha score	1.444 (1.075–1.939)	5.97	.015	5.829 (0.046–736.4)	0.51	.475
FIB-4	1.682 (1.075–2.633)	5.18	.023	0.262 (0.001–87.52)	0.21	.651
FibroQ	1.420 (0.939–2.148)	2.76	.097	1.553 (0.076–31.86)	0.08	.775
Fibrosis index	2.786 (1.411–5.501)	8.72	.003	0.189 (0.000–4.251)	0.11	.744
GUCI	1.007 (1.000–1.014)	4.02	.045	1.087 (0.891–1.326)	0.67	.412
King's score	1.019 (1.001–1.037)	4.51	.034	1.039 (0.800–1.350)	0.08	.774

ALT, alanine aminotransferase; AST, aspartate aminotransferase; INR, international normalization ratio; AAR, AST-to-ALT ratio; API, age platelet index; APRI, AST-to-platelet ratio index; CDS, cirrhosis discriminate score; GUCI, Goteborg University Cirrhosis Index; SPEA, serum prolidase enzyme activity.

Apart from activator, incubation time, and temperature, spontaneous hydrolysis of gly-pro is a problem that should be addressed in spectrophotometric SPEA assay methods. To increase accuracy, spontaneous hydrolysis of gly-pro should be minimized. In this study, whether the spontaneous formation of glycine and proline from gly-pro substrate could be stopped with 5, 10, 15, and 20 minutes of incubation in ice water or not was also investigated. In this experiment, mean SPEA of the samples that were not kept in ice water and kept in ice water for 5 minutes were the same ($P = 1.000$), but mean SPEA of the samples that were kept in ice water for 10, 15, and 20 minutes were statistically significantly lower ($P = .008$). Therefore, it was shown, in ice water, that enzyme-substrate incubation time should be as short as possible to achieve minimum spontaneous hydrolysis of gly-pro substrate as well as the maximum SPEA.

Sample blank was added for each sample to eliminate the interference that may derive from ornithine, citrulline, cysteine, lysine, and hydroxylysine at the ninhydrine condensation step.²⁰

In the study by Myara et al,⁸ as in our study, it was concluded that SPEA increased in patients with liver fibrosis. They did not find a statistically significant association between fibrosis stages and SPEA, but there were statistically significant correlations between the fibrosis stages and both precipitation and optimized direct spectrophotometric SPEA assay method results in our study. This may be explained by the optimization of the currently used direct spectrophotometric SPEA assay method as well as the inclusion of patients with early stage liver fibrosis (F0–F3) in our study. Myara and colleagues considered that SPEA may increase only in the early stage of liver fibrosis and may decrease in advanced liver fibrosis due to slower collagen turnover in the advanced liver fibrosis stages as a result of the high level of collagen deposition. In our study, both the precipitation and optimized direct spectrophotometric SPEA assay method results increased at least until stage 3, but the

currently used direct spectrophotometric SPEA assay method results increased until stage 2 liver fibrosis. It is not known whether the precipitation and optimized direct spectrophotometric SPEA assay method results increase or decrease in patients with cirrhosis, but according to this study, it can be predicted that results of the currently used direct spectrophotometric SPEA assay method will decrease.

Myara et al⁸ found that SPEA was not statistically significantly correlated with ALT, AST, alkaline phosphatase, γ -glutamyltransferase, total bilirubin, or albumin, but in our study, optimized direct spectrophotometric SPEA assay method results statistically significantly correlated with AST, ALT, albumin, and platelets, whereas precipitation spectrophotometric SPEA assay method results statistically significantly correlated only with AST. According to the ROC and logistic regression analyses, SPEA measured by the optimized direct spectrophotometric assay had the highest diagnostic accuracy among the evaluated parameters. We therefore considered that especially the optimized direct spectrophotometric SPEA assay method could be used to distinguish the early stages of liver fibrosis.

Duygu et al²¹ concluded that SPEA measured with the currently used direct spectrophotometric assay method increased in patients with CHB infection and inactive hepatitis B infection compared with the control group, and SPEA may be used as a biomarker in CHB infection, as in our study. They did not find an association between SPEA and Knodell fibrosis score. In our study, there was no statistically significant association between fibrosis stages and currently used direct spectrophotometric SPEA assay method results, as in their study. Both of these results show that currently used direct spectrophotometric SPEA assay method may not have enough diagnostic accuracy especially to distinguish the liver fibrosis stages, and it should be optimized as was done in our study.

Nazligul et al²² observed a statistically significant correlation between precipitation spectrophotometric SPEA results and fibrosis score in patients with CHB and chronic viral hepatitis C (n=29 and n=25, respectively). They found that SPEA was statistically significantly higher in patients with chronic viral hepatitis than controls. According to their analysis, there was no statistically significant difference for SPEA, ALT, and fibrosis scores in terms of the chronic viral hepatitis etiology. They concluded that SPEA may be used for predicting stage of liver fibrosis in patients with viral hepatitis.

One study limitation is that the blood samples were not drawn within 3 days of the liver biopsy in 14 stage 0 and 10 stage 1 liver fibrosis patients for the SPEA assays. However, no interference was expected due to the time interval between liver biopsy and blood draw for SPEA results, because patients were not taking antiviral treatment, did not have co-infection with hepatitis C, D, or HIV, autoimmune hepatitis, or cholangitis and had F0 and F1 stage liver fibrosis, and <6 histological activity index. In addition, most of these blood samples were drawn within 2 months after liver biopsy.

In conclusion, optimized direct spectrophotometric SPEA assay method could be preferred instead of the currently used spectrophotometric SPEA assay methods to distinguish the early stages of liver fibrosis (F0 vs F1–F3) in patients with CHB infection. In this optimized direct spectrophotometric SPEA assay method, after 30 minutes of activation with pH 7.0 Tris-HCl buffer containing 63 mM MnCl₂·4H₂O and 1 mM GSH at 45°C, enzyme-substrate incubation was performed for 5 minutes at 45°C with pH 7.8 Tris-HCl buffer containing 94 mM of glycine-L-proline substrate. At the end of this incubation, GAA was added immediately to inhibit the SPEA by pH change. For the ninhydrin reaction, ninhydrin reagent (600 mL of GAA, 400 mL of distilled water, and 15 g/L ninhydrin) and pH 7.8 Tris-HCl buffer are pipetted, vortexed, and then incubated at 80°C for 45 minutes. At the end of the incubation, samples were immediately kept in ice water for 5 minutes and absorbances were read against the reagent blank in spectrophotometer at 515 nm wavelength within 90 minutes.

Funding

This study was supported by Hitit University. Project numbers are TIP19002-16.002 and TIP19002-19.001.

Conflict of Interest Disclosure

The authors have nothing to disclose.

REFERENCES

1. Terrault NA, Lok ASF, McMahon BJ, et al. Update on prevention, diagnosis, and treatment of chronic hepatitis B: AASLD 2018 hepatitis B guidance. *Hepatology*. 2018;67(4):1560–1599.
2. European Association for Study of Liver and Asociacion Latinoamericana para el Estudio del Higado. EASL-ALEH clinical practice guidelines: non-invasive tests for evaluation of liver disease severity and prognosis. *J Hepatol*. 2015;63(1):237–264.
3. Seeff LB, Everson GT, Morgan TR, et al; HALT-C Trial Group. Complication rate of percutaneous liver biopsies among persons with advanced chronic liver disease in the HALT-C trial. *Clin Gastroenterol Hepatol*. 2010;8(10):877–883. doi:10.1016/j.cgh.2010.03.025.
4. Regev A, Berho M, Jeffers LJ, et al. Sampling error and intraobserver variation in liver biopsy in patients with chronic HCV infection. *Am J Gastroenterol*. 2002;97(10):2614–2618. doi:10.1111/j.1572-0241.2002.06038.x.
5. Castera L, Pinzani M. Biopsy and non-invasive methods for the diagnosis of liver fibrosis: does it take two to tango? *Gut*. 2010;59(7):861–866. doi:10.1136/gut.2010.214650.
6. Wilk P, Wątor E, Weiss MS. Prolidase- a protein with many faces. *Biochimie*. 2021;183:3–12. doi:10.1016/j.biochi.2020.09.017.
7. Aganga IE, Lanaghan ZM, Balasubramaniam M, et al. Prolidase: a review from discovery to its role in health and disease. *Front Mol Biosci*. 2021;8:723003.
8. Myara I, Myara A, Mangeot M, et al. Plasma prolidase activity: a possible index of collagen catabolism in chronic liver disease. *Clin Chem*. 1984;30(2):211–215.
9. Ozcan O, Gultepe M, Ipcioglu OM, et al. Optimization of the photometric enzyme activity assay for evaluating real activity of prolidase. *Turk J Biochem*. 2007;32(1):12–16.
10. Kurien D'Souza A, Miller D, Matsumoto H, et al. Prolidase deficiency and the biochemical assays used in its diagnosis. *Anal Biochem*. 2006;349(2):165–175. doi:10.1016/j.ab.2005.10.018.
11. Krishna G, Sivakumar PT, Dahale AB, et al. Increased prolidase activity in Alzheimer's dementia: a case-control study. *Asian J Psychiatr*. 2020;53:102242. doi:10.1016/j.ajp.2020.102242
12. Sawicka MM, Sawicki K, Łysoń T, et al. Proline metabolism in malignant gliomas: a systematic literature review. *Cancers*. 2022;14(8):2030. doi:10.3390/cancers14082030
13. Pellegrinelli V, Cuenca SR, Rouault C, et al. Dysregulation of macrophage PEPD in obesity determines adipose tissue fibro-inflammation and insulin resistance. *Nat Metab*. 2022;4(4):476–494.
14. Say M, Tella E, Boccara O, et al; on behalf of the Angio-Dermatology Group of the French Society of Dermatology, the Research Group of the French Society of Pediatric Dermatology. Leg ulcers in childhood: a multicenter study in France. *Ann Dermatol Venerol*. 2022;149(1):51–55. doi:10.1016/j.annder.2021.05.004.
15. Clinical Laboratory Standards Institute (CLSI). *Evaluation of Precision of Quantitative Measurement Procedures; Approved Guideline*. 3rd ed. Clinical and Laboratory Standards Institute; 2018 document EP05-A3E.
16. Clinical Laboratory Standards Institute (CLSI). *User Verification of Precision and Estimation of Bias; Approved Guideline*. 3rd ed. Clinical and Laboratory Standards Institute; 2014 document EP15-A3.
17. Clinical Laboratory Standards Institute (CLSI). *Evaluation of the Linearity of Quantitative Measurement Procedures: A Statistical Approach; Approved Guideline*. Clinical and Laboratory Standards Institute; 2003 document EP06-A.
18. Ishak K, Baptista A, Bianchi L, et al. Histological grading and staging of chronic hepatitis. *J Hepatol*. 1995;22(6):696–699. doi:10.1016/0168-8278(95)80226-6.
19. <https://www.who.int/news-room/fact-sheets/detail/hepatitis-b>
20. Chinard FP. Photometric estimation of proline and ornithine. *J Biol Chem*. 1952;199(1):91–95.
21. Duygu F, Aksoy N, Cicek AC, Butun I, Unlu S. Does prolidase indicate worsening of hepatitis B infection? *J Clin Lab Anal*. 2013;27(5):398–401. doi:10.1002/jcla.21617.
22. Nazligul Y, Aslan M, Taskin A, et al. Serum prolidase activity may be an index of liver fibrosis in chronic viral hepatitis. *East J Med*. 2015;20(3):125–130.

Correction to: A meta-analysis of the accuracy of Xpert MTB/RIF in diagnosing intestinal tuberculosis

This is a correction to: Yuan-Lin Ding, BSMed, and others, A meta-analysis of the accuracy of Xpert MTB/RIF in diagnosing intestinal tuberculosis, *Laboratory Medicine*, 2023; lmad072, <https://doi.org/10.1093/labmed/lmad072>.

In the originally published version of this manuscript, the corresponding author's surname was incorrectly represented. The correct name is Xu-Guang Guo, where the last name is Guo.

This error has been corrected online.

Is very high platelet count always associated with essential thrombocythemia? An unusual presentation in a child

Elif Habibe Aktekin, MD^{1,*}, Nalan Yazıcı^{1,*}, İlknur Kozanoğlu^{2,*}, Ayşe Erbay^{1,*}

¹Department of Pediatrics Division of Pediatric Hematology-Oncology, and ²Department of Physiology and the Apheresis Unit Adult Bone Marrow Transplant Centre, Baskent University, Adana, Turkey Corresponding author: Elif Habibe Aktekin; elifaktekin@yahoo.com

Key words: JAK mutation; extreme thrombocytosis; essential thrombocythemia; chronic myeloid leukemia; childhood.

Abbreviations: CML, chronic myeloid leukemia; ET, essential thrombocythemia; IS, international scale; MDS, myelodysplastic syndrome; MPN, myeloproliferative neoplasm

Laboratory Medicine 2023;54:e170-e176; <https://doi.org/10.1093/labmed/lmad053>

ABSTRACT

Myeloproliferative neoplasms are rare in childhood. They are categorized as Philadelphia chromosome-positive and Philadelphia chromosome-negative. Chronic myeloid leukemia (CML) is the most common myeloproliferative disease in which the Philadelphia chromosome is detected as a result of BCR-ABL rearrangements. In others, the most common genetic abnormality is JAK2V617F mutation. The coexistence of these 2 abnormalities in CML is unexpected, and rare cases have recently been reported in adults. We present a child who had a very high platelet count in which we found this coexistence. The clinical presentation, laboratory findings, management, and prognosis of this coexistence is challenging in such a rare condition.

Patient History

An 11-year-old female patient was admitted to our center with severe headache and intermittent vomiting that started 2 weeks before. Platelet count was found to be very high in a test 3 days before in a local hospital where she went with these complaints. It is known that patient's platelet count was $298 \times 10^9/L$ 1 year before. The patient had no history of disease or drug use. There is also no family history with a diagnosis of thrombosis and thrombocytosis. Her grandmother and aunt were un-

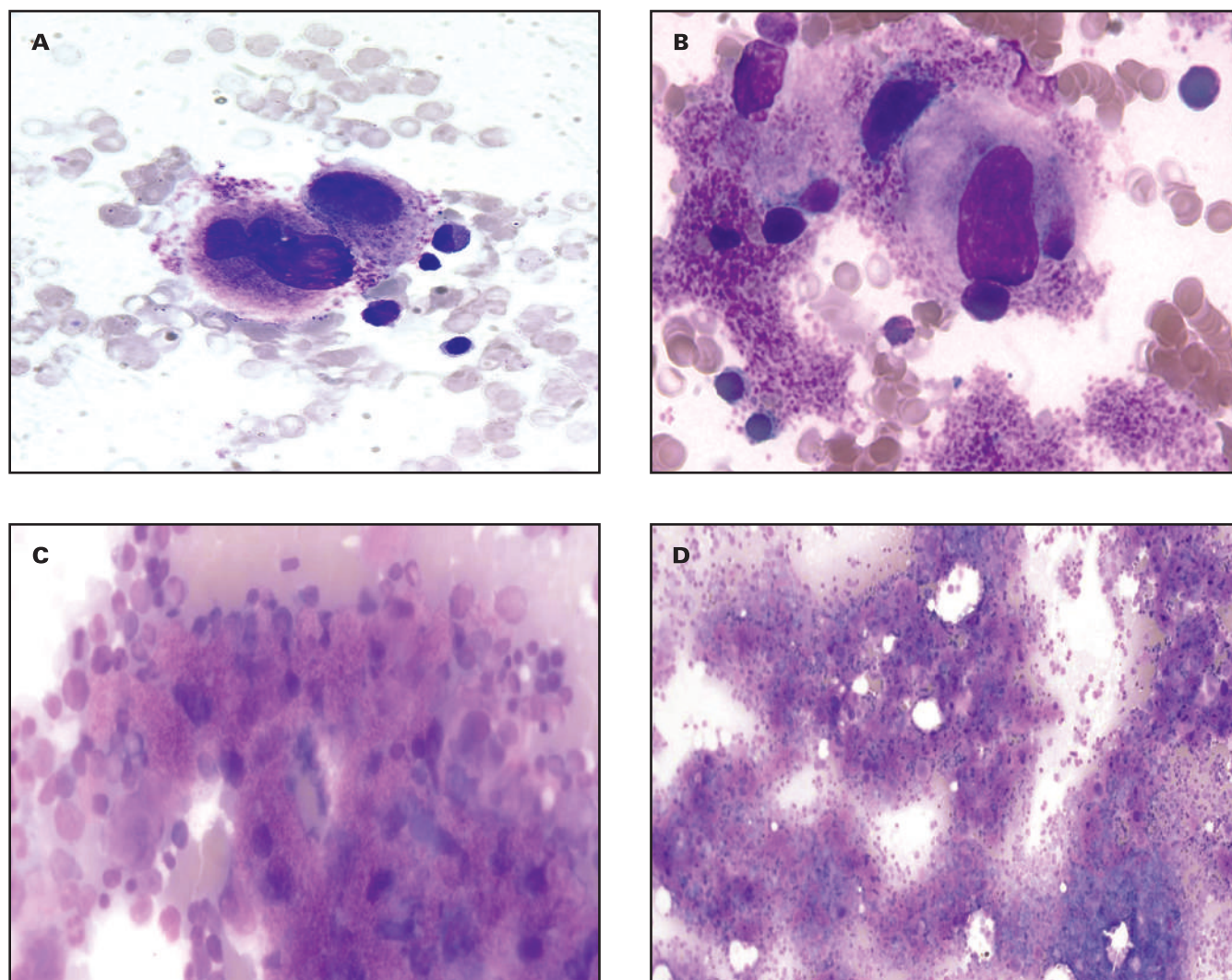
der follow-up due to brain tumor. There was no hepatosplenomegaly or lymphadenopathy, and her neurological examination was normal. For treatment, acetylsalicylic acid and hydroxyurea were given.

In our evaluation, complete blood count revealed the following: hemoglobin 12.7 g/dL, red cell blood count $500 \times 10^{10}/L$, leukocyte count $13.5 \times 10^9/L$, and platelet count $>3000 \times 10^9/L$. For leukocyte subgroups, neutrophil count was $7.8 \times 10^9/L$ and basophil count was $0.8 \times 10^9/L$. Peripheral smear showed myeloid precursors, basophilia, and thrombocytosis. Liver and kidney function tests and other biochemical parameters were in the normal range. The sedimentation rate was 76 mm/h and platelet function tests (PFA-100) were too high to be measured. There was no pathological finding in magnetic resonance imaging of the central nervous system. Abdominal ultrasonography (USG) evaluation was also normal.

Bone marrow aspiration was performed on the patient. Direct microscopic examination revealed an increase in myeloid precursors and an increased number of atypical megakaryocytes (FIGURE 1). No atypical cells were detected in the flowcytometric analysis of the bone marrow, and 2.1% progenitor cells were found. Bone marrow cytogenetic analysis revealed the karyotype as $46XX,t(9;22)(q34,q11.2)[7]/92,XXXX,t(9;22)(q34,q11.2)[3]$. The BCR-ABL and JAK2 V617F mutations were studied. The quantitative value of $t(9;22)$ -p210 was 0.60134292 positive, the ABL copy number was 125,845, the BCR-ABL copy number was 75,676, and the international scale (IS) value was 30.65727162. The JAK2 V617F mutation was identified at a low variant allele frequency of 2% to 5%.

Given these results, the patient was diagnosed with CML presenting with extreme thrombocytosis. As an emergent approach, intravenous hydration was given to the patient with 0.45% saline and 5% dextrose at a dose of 3000 mL/m²/d. Thrombopheresis was performed daily for 4 days. Acetylsalicylic acid was discontinued due to the risk of acquired von Willebrand disease because of excessive platelet count and the impaired platelet function test. Low-molecular-weight heparin was given at a dose of 200 U/kg/d. Because the JAK2 V617F mutation was identified at a low variant allele frequency (2%-5%), it was decided that ruxolitinib treatment would not be beneficial. Anagrelide 1.5 mg/d, hydroxyurea 20 mg/kg/d and imatinib mesylate 300 mg/m²/d were combined as initial therapy. Hydroxyurea was discontinued and the other medications were continued in the outpatient setting. In weekly control examinations after discharge, the platelet counts were $388 \times 10^9/L$, $290 \times 10^9/L$, and $180 \times 10^9/L$. Given these platelet counts and patient's well-being, low-molecular-weight heparin was discontinued first and then the anagrelide dose was halved. Platelet counts during

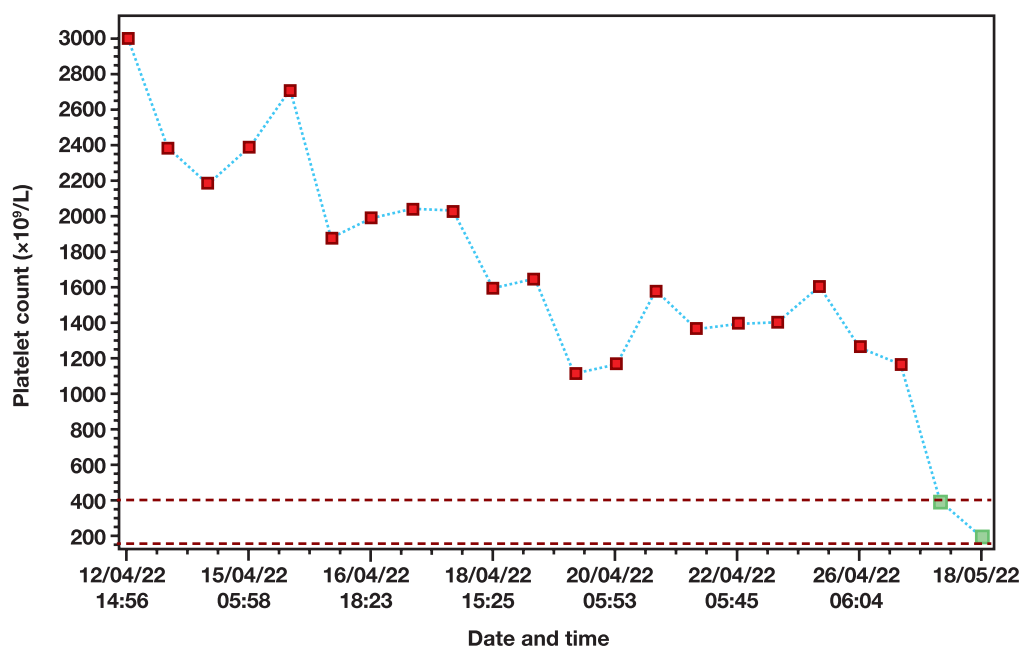
FIGURE 1. A and B: Atypical (dwarf) megakaryocytes with magnification $\times 100$, C: Atypical (dwarf) megakaryocytes with magnification $\times 40$, D: Atypical (dwarf) megakaryocytes with magnification $\times 10$.



1 month are shown in **FIGURE 2**. A control bone marrow aspiration was performed 40 days after initial diagnosis with a $263 \times 10^9/L$ platelet count. Morphology was normal on direct microscopic examination. The quantitative value of t(9;22)-p210 was positive at the rate of 0.05253886, the ABL copy number was 35,764, the BCR-ABL copy number was 1879, and the IS value was 3.803873263. A significant decrease in BCR-ABL copy numbers was obtained compared with the initial diagnosis. The JAK2 V617F mutation was also negative. Anagrelide was discontinued and treatment with imatinib mesylate was continued. In the follow-up, the platelet counts remained within the normal range. Bone marrow aspiration was reassessed 8 months after first admission with normal morphological findings. The quantitative value of t(9;22)-p210 was 0.00107803, the ABL copy number was 147,491, the BCR-ABL copy number was 159, and the IS value was 0.098071794. Eventually, the patient had a major molecular response to imatinib mesylate. At the time of this report, patient was still under follow-up for 8 months after diagnosis, and her BCR-ABL copy numbers had decreased regularly, platelet counts were within normal limits, and she is being followed up with imatinib mesylate treatment without problems.

Clinical and Laboratory Information

Although chronic myeloid leukemia (CML) is known as an adult disease, it is also seen in childhood, with an estimated incidence of 2.5 cases per million per year.¹ Detection of the Philadelphia chromosome, which is defined by the presence of BCR-ABL gene rearrangements, is essential for the diagnosis of CML. Common laboratory findings are leukocytosis, increased basophil count, thrombocytosis, and mild anemia in which myeloid precursors can be detected in a peripheral blood smear.² Chronic myeloid leukemia cases presenting with isolated excessive thrombocytosis are rarely encountered.^{3,4} Other myeloproliferative disorders such as essential thrombocythemia (ET) and polycythemia vera are rare in children, and the JAK2 V617F mutation is positive in some of these patients.^{5,6} In the diagnostic criteria of these myeloid disorders, it is stated that BCR-ABL must be negative and for CML, there should be no abnormalities other than BCR-ABL.⁷ However, in the last decade, JAK mutations with BCR-ABL and various other rare genetic disorders have been identified in adult CML. A literature review of adult CML cases with BCR-ABL and JAK2 V617F mutation is shown in **TABLE 1**.⁸⁻³⁷

FIGURE 2. Platelet counts during 1 month.

Discussion

Myeloproliferative neoplasms are clonal disorders of hematopoietic stem cells. Essential thrombocythemia is a disease associated with isolated thrombocytosis and associated bleeding or thrombosis complications. The annual incidence of ET, which is very rare in children, is approximately 1 child in 10,000,000.³⁸ Although JAK2 V617F mutation is detected in approximately 55% of adult ET patients, the genetic profile of pediatric cases has not yet been clarified due to the small number of patients. One of the certain diagnostic criteria for ET is that BCR-ABL rearrangements should not be detected.³⁹ Problems related to bleeding and thrombosis are taken into consideration in treatment strategies and follow-up for ET patients. Although acetylsalicylic acid is generally the first choice, hydroxyurea and anagrelide can be added to drug combinations according to symptoms and platelet count.⁴⁰ Because it is known that very high platelet counts can lead to acquired von Willebrand disease, acetylsalicylic acid should be used carefully. We discontinued acetylsalicylic acid because our patient's platelet count was too high to be measured at the first application, and we applied low-molecular-weight heparin in terms of thrombosis risk. In addition, thrombopheresis was performed daily for 4 days to reduce the very high platelet count rapidly until the effectiveness of the drugs was revealed. There are some studies in which therapeutic thrombopheresis is effective in reducing thrombotic problems that may be caused by thrombocytosis in adult patients with myeloproliferative disorders.^{41,42} Similarly, there are some data about the efficacy and safety of hydroxyurea and anagrelide combined with imatinib mesylate in reducing platelet count in adults in chronic or accelerated phases of CML.⁴³⁻⁴⁵ We also administered hydroxyurea and anagrelide together with imatinib mesylate for a short time. We did not encounter any side effects and observed that these medications were effective in reducing the platelet count.

It has not been clarified how BCR-ABL coexists with JAK mutation in CML. There are different opinions, such as a single clone car-

rying both abnormalities together or 2 different clones having these abnormalities separately.³⁶ The definitive effect on the prognosis of this association, which has been recently defined in adult cases, is not yet known. There are case reports that JAK mutation may remain positive while BCR-ABL becomes negative with imatinib mesylate treatment and that second-generation tyrosine kinase inhibitors might be more effective in these patients due to the development of resistance to imatinib mesylate. In addition, it is emphasized that cases with persistent JAK mutation positivity should be followed up for development of polycythemia vera or myelofibrosis.¹⁴ We also found JAK2 V617F mutation with BCR-ABL at the initial diagnosis of our patient. However, we did not add ruxolitinib to her treatment because the JAK2 V617F mutation was identified at a low variant allele frequency of 2% to 5%. The control JAK2 V617F status of bone marrow 40 days after the initial diagnosis was found to be negative, and the BCR-ABL rearrangement ratio was significantly reduced. Presumably, in childhood CML cases with JAK2 V617F mutation accompanying at first diagnosis and without splenomegaly, response to imatinib mesylate treatment can be better, and this mutation may become negative in the follow-up, unlike adults. Also, additional cytogenetic abnormalities with BCR-ABL can be detected in 5% to 10% of adult cases.⁴⁶ It has also been reported that these are rare conditions in children and their effects on prognosis are uncertain.⁴⁷ The karyotype analysis of our patient's bone marrow was 46XX,t(9;22)(q34,q11.2)[7]/92,XXXX,t(9;22)(q34,q11.2)[3]. The patient will be followed closely for the development of resistance to the first-generation tyrosine kinase inhibitor and need for stem cell transplantation.

Whereas JAK2, CALR, and MPL mutations are considered driver events, mutations in other genes, particularly TET2, ASXL1, and DNMT3A, are found in over half of patients with myeloproliferative disorders.⁴⁸ In some pediatric case reports, cases with these mutations without BCR-ABL, which had similar laboratory and physical examination findings to CML, have been described as atypical CML.^{49,50} However, according to latest classification of the World Health Organization

TABLE 1. Literature review of adult chronic myeloid leukemia cases with BCR-ABL and JAK2 V617F

References	Age (years)/sex	JAK2 V617F status	Treatment	Outcomes
Kramer et al ⁸	50/ M	Simultaneous	Imatinib	BCR-ABL negative/ JAK2 positive
Campiotti et al ⁹	69/ M	Simultaneous	Imatinib	BCR-ABL and JAK2 decreased
Lewandowski et al ¹⁰	80/ M	Simultaneous	Imatinib, hydroxyurea	BCR-ABL decreased/ JAK2 positive
	58/ M	Simultaneous	Imatinib	BCR-ABL decreased/ JAK2 positive
	80/ F	Simultaneous	Hydroxyurea	BCR-ABL increased/ JAK2 positive
Pagnano et al ¹¹	73/ M	Simultaneous	Imatinib, hydroxyurea	BCR-ABL decreased/ JAK2 positive
Hassan et al ¹²	60/ M	Simultaneous	Hydroxyurea, imatinib	Death
Hussein et al ¹³	55/ M	Simultaneous	Imatinib	BCR-ABL decreased/ JAK2 positive
Xu et al ¹⁴	21/ F	Simultaneous	Imatinib	BCR-ABL decreased/ JAK2 positive
Mirza et al ¹⁵	73/ F	Simultaneous	Hydroxyurea, imatinib	NA
Inami et al ¹⁶	43/ M	Simultaneous	Interferon, hydroxyurea, imatinib	BCR-ABL decreased/ JAK2 positive
Bornhauser et al ¹⁷	66/ M	Simultaneous	Imatinib, hydroxyurea	BCR-ABL increased/ JAK2 positive
Cambier et al ¹⁸	64/ M	Simultaneous	Imatinib	BCR-ABL decreased/ JAK2 positive
Scott et al ¹⁹	NA/M	Simultaneous	Imatinib	NA
Park et al ²⁰	36/ M	Simultaneous	Hydroxyurea	BCR-ABL increased/ NA
	58/ M	Simultaneous	Hydroxyurea, dasatinib	BCR-ABL increased/ NA
De Conchon et al ²¹	52/ F	Simultaneous	Hydroxyurea, imatinib	BCR-ABL and JAK2 decreased
Pardini et al ²²	67/ M	Simultaneous	Imatinib, hydroxyurea	BCR-ABL decreased/ JAK2 positive
Kim et al ²³	49/ M	Simultaneous	Imatinib, dasatinib	BCR-ABL and JAK2 decreased
	64/ M	Simultaneous	Imatinib, nilotinib	BCR-ABL decreased/ JAK2 positive
Hussein et al ²⁴	45/ M	Simultaneous	Imatinib	BCR-ABL and JAK2 decreased
	32/ M	CML after MPN	Anagrelide, hydroxyurea, imatinib	BCR-ABL and JAK2 decreased
Veronese et al ²⁵	82/ F	Simultaneous	Imatinib, hydroxyurea, salicylic acid	BCR-ABL decreased/ JAK2 positive
	62/ M	Simultaneous	Imatinib, salicylic acid	BCR-ABL decreased/ JAK2 positive
Caocci et al ²⁶	70/ M	Simultaneous	Interferon, imatinib	BCR-ABL decreased/ JAK2 positive
Pastore et al ²⁷	42/ F	Simultaneous	Imatinib	BCR-ABL decreased/ JAK2 positive
Lee et al ²⁸	53/ M	MPN after CML	Interferon, imatinib, anagrelide, hydroxyurea	BCR-ABL decreased/ JAK2 positive
	60/ F	MPN after CML	Imatinib, nilotinib, anagrelide	BCR-ABL decreased/ JAK2 positive
Maerki et al ²⁹	77/ M	Simultaneous	Bortezomib, anti-CML therapy	NA
Shi et al ³⁰	65/ M	Simultaneous	Hydroxyurea, Imatinib, Dasatinib	BCR-ABL decreased/ JAK2 positive
Gattenlohner et al ³¹	67/ M	Simultaneous	Imatinib	BCR-ABL decreased/ JAK2 positive
Inokuchi et al ³²	43/ M	Simultaneous	Interferon, hydroxyurea, imatinib, dasatinib	BCR-ABL decreased/ JAK2 negative
Ursuleac et al ³³	61/ M	CML after MPN	Hydroxyurea, imatinib	BCR-ABL decreased/ JAK2 positive
Pingali et al ³⁴	39/ M	CML after MPN	Imatinib, dasatinib, nilotinib	BCR-ABL decreased/ JAK2 positive
Warsi et al ³⁵	68/ M	Simultaneous	Imatinib, hydroxyurea, salicylic acid	BCR-ABL negative/ NA
Frikha et al ³⁶	60/ M	Simultaneous	Imatinib	NA
	39/ F	Simultaneous	Imatinib	BCR-ABL increased/ NA
Ali et al ³⁷	57/ M	Simultaneous	Hydroxyurea, dasatinib	BCR-ABL decreased/ JAK2 negative

CML, chronic myeloid leukemia; F, female; M, male; MPN, myeloproliferative neoplasm; NA, not available

in 2022, the term “myelodysplastic syndrome (MDS)/ myeloproliferative neoplasm (MPN) with neutrophilia” replaces the term atypical CML.⁴⁸ When the literature was reviewed in terms of other mutations detected with BCR-ABL, simultaneous ASXL1 mutations were detected in 3 pediatric cases. Because it was a period before the use of tyrosine kinase inhibitors **TABLE 2**, all of them underwent stem cell transplantation, and 2 of them died.⁵¹

In conclusion, although the most common etiologies of thrombocytosis include reactive causes, such as secondary iron deficiency anemia, infections, surgery etc. in childhood, extremely high

platelet count and absence of splenomegaly on physical examination do not suggest CML initially for children. There are some concerns that patients with CML who have unusual physical examinations and laboratory findings may rapidly progress to the accelerated phase; therefore, this is an important point to take into account. Moreover, the presence of additional genetic abnormalities with BCR-ABL require careful monitoring in terms of drug resistance or the development of other myeloproliferative diseases over time. Multicenter studies and further research are needed to better define these rare diseases in childhood.

TABLE 2. Pediatric chronic myeloid leukemia cases with other rare mutations

Patient no.	Age (year)	Sex	Splenomegaly	Leukocyte/L	Hemoglobin (g/dl)	Platelet/L	Blood smear finding	BCR/ABL status	Other mutation(s)	Treatment	HSCT	Outcome
1	14	F	NA	NA	NA	NA	NA	positive	ASXL1	Hydroxyurea Interferon	+	Alive
2	13	F	NA	NA	NA	NA	NA	positive	ASXL1	Hydroxyurea Interferon	+	Dead
3	13	F	NA	NA	NA	NA	NA	positive	ASXL1	Hydroxyurea Interferon	+	Dead

F, female; HSCT, hematopoietic stem cell transplantation; NA, not available

Acknowledgments

The authors would like to thank Nazım Emrah Koçer from the Department of Pathology, Baskent University for providing images patient's bone marrow samples.

E.H.A. made a definitive diagnosis and wrote the paper. N.Y. made a definitive diagnosis and wrote the paper. İ.K. performed genetic and molecular analysis. A.E. made a definitive diagnosis.

Written informed consent was obtained from the patient's parents.

Conflict of Interest Disclosure

The authors have nothing to disclose.

Data Availability

The data that support the findings of this study are available from the corresponding author upon reasonable request.

REFERENCES

- Howlader N, Noone AM, Krapcho M, et al. *SEER Cancer Statistics Review, 1975-2017*. Bethesda, MD: National Cancer Institute; 2020. November 2019 SEER data submission. <https://seercancer.gov/1975-2017/>,
- Smith SM, Hijjiya N, Sakamoto KM. Chronic myelogenous leukemia in childhood. *Curr Oncol Rep*. 2021;23(4):40. doi:10.1007/s11912-021-01025-x
- Huho AN, Issaq N, Iacobas I, et al. A rare case of pediatric chronic myelogenous leukemia presenting with severe thrombocytosis without leukocytosis. *Pediatr Dev Pathol*. 2018;21(1):100-104. doi:10.1177/1093526617698601
- Boklan JL, Walsh AM, de la Maza MC, Su LL, Nizzi FA, Schafernak KT. Pediatric chronic myeloid leukemia presenting with extreme thrombocytosis simulating essential thrombocythemia. *J Pediatr Hematol Oncol*. 2018;40(6):456-457. doi:10.1097/MPH.0000000000001154
- Turkina A, Wang J, Mathews V, et al. TARGET: a survey of real-world management of chronic myeloid leukaemia across 33 countries. *Br J Haematol*. 2020;190(6):869-876. doi:10.1111/bjh.16599
- Yassin MA, Taher A, Mathews V, et al. MERGE: a multinational, multicenter observational registry for myeloproliferative neoplasms in Asia, including Middle East, Turkey and Algeria. *Cancer Med*. 2020;9(13):4512-4526. doi:10.1002/cam4.3004
- Arber DA, Orazi A, Hasserjian R, et al. The 2016 revision to the World Health Organization classification of myeloid neoplasms and acute leukemia. *Blood*. 2016;127(20):2391-2405. doi:10.1182/blood-2016-03-643544
- Kramer A, Reiter A, Kruth J, et al. JAK2-V617F mutation in a patient with Philadelphia-chromosome-positive chronic myeloid leukemia. *Lancet Oncol*. 2007;8(7):658-660. doi:10.1016/S1470-2045(07)70206-1
- Campiotti L, Appio L, Solbiati F, Ageno W, Venco A. JAK2-V617F mutation and Philadelphia positive chronic myeloid leukemia. *Leuk Res*. 2009;33(11):e212-e213. doi:10.1016/j.leukres.2009.06.011
- Lewandowski K, Gniot M, Wojtaszewska M, et al. Coexistence of JAK2 or CALR mutation is a rare but clinically important event in chronic myeloid leukemia patients treated with tyrosine kinase inhibitors. *Int J Lab Hematol*. 2018;40(3):366-371. doi:10.1111/ijlh.12798
- Pagnano KBB, Delamain MT, Magnus MM, et al. Concomitant essential thrombocythemia with JAK2 V617F mutation in a patient with chronic myeloid leukemia with major molecular response with imatinib and long-term follow-up. *Oncol Lett*. 2016;12(1):485-487. doi:10.3892/ol.2016.4631

12. Hassan A, Dogara LG, Babadoko AA, Awwalu S, Mamman AI. Coexistence of JAK2 and BCR-ABL mutation in patient with myeloproliferative neoplasm. *Niger Med J*. 2015;56(1):74-76. doi:10.4103/0300-1652.149177
13. Hussein K, Bock O, Seegers A, et al. Myelofibrosis evolving during imatinib treatment of a chronic myeloproliferative disease with coexisting BCR-ABL translocation and JAK2V617F mutation. *Blood*. 2007;109(9):4106-4107. doi:10.1182/blood-2006-12-061135
14. Xu W, Chen B, Tong X. Chronic myeloid leukemia patient with co-occurrence of BCR-ABL junction and JAK2 V617F mutation. *Int J Hematol*. 2014;99(1):87-90. doi:10.1007/s12185-013-1480-z
15. Mirza I, Frantz C, Clarke G, Voth AJ, Turner R. Transformation of polycythemia vera to chronic myelogenous leukemia. *Arch Pathol Lab Med*. 2007;131(11):1719-1724. doi:10.5858/2007-131-1719-TOPVTC
16. Inami M, Inokuchi K, Okabe M, et al. Polycythemia associated with the JAK2V617F mutation emerged during treatment of chronic myelogenous leukemia. *Leukemia*. 2007;21(5):1103-1104. doi:10.1038/sj.leu.2404591
17. Bornhauser M, Mohr B, Oelschlaegel U, et al. Concurrent JAK2(V617F) mutation and BCR-ABL translocation within committed myeloid progenitors in myelofibrosis. *Leukemia*. 2007;21(8):1824-1826. doi:10.1038/sj.leu.2404730
18. Cambier N, Renneville A, Cazaentre T, et al. JAK2V617F-positive polycythemia vera and Philadelphia chromosome-positive chronic myeloid leukemia: one patient with two distinct myeloproliferative disorders. *Leukemia*. 2008;22(7):1454-1455. doi:10.1038/sj.leu.2405088
19. Scott LM, Campbell PJ, Baxter EJ, et al. The V617F JAK2 mutation is uncommon in cancers and in myeloid malignancies other than classic myeloproliferative disorders. *Blood*. 2005;106(8):2920-2921. doi:10.1182/blood-2005-05-2087
20. Park SH, Chi H-S, Cho Y-U, et al. Two cases of myeloproliferative neoplasm with a concurrent JAK2 (V617F) mutation and BCR/ABL translocation without chronic myelogenous leukemia phenotype acquisition during hydroxyurea treatment. *Ann Lab Med*. 2013;33(3):229-232. doi:10.3343/alm.2013.33.3.229
21. De Conchon MRM, Costa JL, Novaes MMY, Dorlhiac-Llacer PE, de Alencar Fischer Chamone D, Bendit I. Simultaneous detection of JAK2 V617F mutation and Bcr-Abl translocation in a patient with chronic myelogenous leukemia. *Int J Hematol*. 2008;88(2):243-245. doi:10.1007/s12185-008-0131-2
22. Pardini S, Fozza C, Contini S, et al. A case of coexistence between JAK2V617F and BCR/ABL. *Eur J Haematol*. 2008;81(1):75-76. doi:10.1111/j.1600-0609.2008.01063.x
23. Kim Y-K, Shin M-G, Kim H-R, et al. Simultaneous occurrence of the JAK2V617F mutation and BCR-ABL gene rearrangement in patients with chronic myeloproliferative disorders. *Leuk Res*. 2008;32(6):993-995. doi:10.1016/j.leukres.2007.10.018
24. Hussein K, Bock O, Theophile K, et al. Chronic myeloproliferative diseases with concurrent BCR-ABL junction and JAK2V617F mutation. *Leukemia*. 2008;22(5):1059-1062. doi:10.1038/sj.leu.2404993
25. Veronese L, Tchirkov A, Richard-Pebrel C, et al. A thrombocytosis occurring in Philadelphia positive CML in molecular response to imatinib can reveal an underlying JAK2V617F myeloproliferative neoplasm. *Leuk Res*. 2010;34(4):e94-e96. doi:10.1016/j.leukres.2009.09.025
26. Caocci G, Atzeni S, Orru N, et al. Response to imatinib in a patient with chronic myeloid leukemia simultaneously expressing p190BCR-ABL oncoprotein and JAK2V617F mutation. *Leuk Res*. 2010;34(1):e27-e29. doi:10.1016/j.leukres.2009.08.009
27. Pastore F, Schneider S, Christ O, Hiddemann W, Spiekermann K. Impressive thrombocytosis evolving in a patient with a BCR-ABL positive CML in major molecular response during dasatinib treatment unmasks an additional JAK2V617F. *Exp Hematol Oncol*. 2013;2(1):24. doi:10.1186/2162-3619-2-24
28. Lee YJ, Moon JH, Shin HC, et al. Two CML patients who subsequently developed features of essential thrombocythemia with JAK2-V617F mutation while in complete cytogenetic remission after treatment with imatinib mesylate. *Int J Hematol*. 2013;97(6):804-807. doi:10.1007/s12185-013-1326-8
29. Maerki J, Katava G, Siegel D, Silberberg J, Bhattacharyya PK. Unusual case of simultaneous presentation of plasma cell myeloma, chronic myelogenous leukemia, and a Jak 2 positive myeloproliferative disorder. *Case Rep Hematol*. 2014;2014:738428. doi:10.1155/2014/738428
30. Shi X-B, Jiang J-F, Jin F-X, Cheng W. Coexistence of breakpoint cluster region-Abelson 1 rearrangement and janus kinase 2 V617F mutation in chronic myeloid leukemia: a case report. *World J Clin Cases*. 2019;7(9):1087-1092. doi:10.12998/wjcc.v7.i9.1087
31. Gattenlohner S, Volker HU, Etschmann B, Einsele H, Müller-Hermelink H-K. BCR-ABL positive chronic myeloid leukemia with concurrent JAK2(V617F) positive myelodysplastic syndrome/ myeloproliferative neoplasm (RARS-T). *Am J Hematol*. 2009;84(5):306-307. doi:10.1002/ajh.21296
32. Inokuchi K, Yamaguchi H, Tamai H, et al. Disappearance of both the BCR/ABL1 fusion gene and the JAK2V617F mutation with dasatinib therapy in a patient with imatinib-resistant chronic myelogenous leukemia. *J Clin Exp Hematol*. 2012;52(2):145-147.
33. Ursuleac I, Colita A, Adam T, Jardan C, Ilea A, Coriu D. The concomitant occurrence of JAK2V617F mutation and BCR/ABL transcript with phenotypic expression- an overlapping myeloproliferative disorder or two distinct diseases? Case report. *J Med Life*. 2013;6(1):34-37.
34. Pingali SR, Mathiason MA, Lovrich SD, Go RS. Emergence of chronic myelogenous leukemia from a background of myeloproliferative disorder: JAK2V617F as a potential risk factor for BCR-ABL translocation. *Clin Lymphoma Myeloma*. 2009;9(5):E25-E29. doi:10.3816/CLM.2009.n.080
35. Warsi A, Alamoudi S, Alsuraiah AK, et al. A 68-year-old man with a cytogenetic diagnosis of chronic myeloid leukemia and bone marrow findings of Philadelphia chromosome translocation between the long arm of chromosomes 9 and 22, leading to the BCR-ABL1 fusion gene and V617F mutation in the JAK2 gene. *Am J Case Rep*. 2023;24:e938488. doi:10.12659/AJCR.938488
36. Frikha R, Turki F, Kassar O, Elloumi M, Kamoun H. Co-existence of BCR-ABL and JAK2V617F mutation in resistant chronic myeloid leukemia in the imatinib era: is there a correlation? *J Oncol Pharm Pract*. 2021;27(7):1784-1789. doi:10.1177/1078155221991646
37. Ali EAH, Al-Akiki S, Yassin MA. A case report of BCR-ABL-JAK2-positive chronic myeloid leukemia with complete hematological and major molecular response to dasatinib. *Case Rep Oncol*. 2021;14(1):690-694. doi:10.1159/000514632
38. Teofilii L, Giona F, Martini M, et al. Markers of myeloproliferative diseases in childhood polycythemia vera and essential thrombocythemia. *J Clin Oncol*. 2007;25(9):1048-1053. doi:10.1200/JCO.2006.08.6884
39. Barbui T, Thiele J, Gisslinger H, Finazzi G, Vannucchi AM, Tefferi A. The 2016 revision of WHO classification of myeloproliferative neoplasms: clinical and molecular advances. *Blood Rev*. 2016;30(6):453-459. doi:10.1016/j.blre.2016.06.001
40. Ameen M, Siddiqui K, Khan S, Saleh M, Al-Jefri A, Al-Musa A. Essential thrombocythemia in children: a retrospective study. *J Hematol*. 2021;10(3):106-113. doi:10.14740/jh822
41. Nguyen TH, Bach KQ, Vu HQ, Nguyen NQ, Duong TD, Wheeler J. Therapeutic thrombocytapheresis in myeloproliferative neoplasms: a single-institution experience. *J Clin Apher*. 2021;36(1):101-108. doi:10.1002/jca.21847
42. Boddu P, Falchi L, Hosing C, Newberry K, Bose P, Verstovsek S. The role of thrombocytapheresis in the contemporary management of hyperthrombocytosis in myeloproliferative neoplasms: a case-based review. *Leuk Res*. 2017;58:14-22. doi:10.1016/j.leukres.2017.03.008
43. Voskaridou E, Terpos E, Komninaka V, Eftyhiadis E, Mantzourani M, Loukopoulou D. Chronic myeloid leukaemia with marked thrombocytosis in a patient with thalassaemia major: complete haematological remission under the combination of hydroxyurea and

anagrelide. *Br J Haematol*. 2002;116(1):155-157. doi:[10.1046/j.1365-2141.2002.03241.x](https://doi.org/10.1046/j.1365-2141.2002.03241.x)

44. Silver RT. Anagrelide is effective in treating patients with hydroxyurea-resistant thrombocytosis in patients with chronic leukemia. *Leukemia*. 2005;19(1):39-43. doi:[10.1038/sj.leu.2403556](https://doi.org/10.1038/sj.leu.2403556)
45. Fruchtmann SM, Pettitt RM, Gilbert HS, Fiddler G, Lyne A; Anagrelide Study Group. Anagrelide: analysis of long-term efficacy, safety and leukemogenic potential in myeloproliferative disorders. *Leuk Res*. 2005;29(5):481-491. doi:[10.1016/j.leukres.2004.10.002](https://doi.org/10.1016/j.leukres.2004.10.002)
46. Fabarius A, Leitner A, Hochhaus A, et al., Schweizerische Arbeitsgemeinschaft für Klinische Krebsforschung (SAKK) and the German CML Study Group. Impact of additional cytogenetic aberrations at diagnosis on prognosis of CML: long-term observation of 1151 patients from the randomised CML study IV. *Blood*. 2011;118(26):6760-6768. doi:[10.1182/blood-2011-08-373902](https://doi.org/10.1182/blood-2011-08-373902)
47. Millot F, Dupraz C, Guilhot J, et al. Additional cytogenetic abnormalities and variant t(9;22) at the diagnosis of childhood chronic myeloid leukemia: the experience of the International Registry for Chronic Myeloid Leukemia in Children and Adolescents. *Cancer*. 2017;123(18):3609-3616. doi:[10.1002/cncr.30767](https://doi.org/10.1002/cncr.30767)
48. Khoury JD, Solary E, Abla O, et al. The 5th edition of the World Health Organization classification of haematolymphoid tumors: myeloid and histiocytic/dendritic neoplasms. *Leukemia*. 2022;36(7):1703-1719. doi:[10.1038/s41375-022-01613-1](https://doi.org/10.1038/s41375-022-01613-1)
49. Freedman JL, Desai AV, Bailey LC, et al. Atypical chronic myeloid leukemia in two pediatric patients. *Pediatr Blood Cancer*. 2016;63(1):156-159. doi:[10.1002/pbc.25694](https://doi.org/10.1002/pbc.25694)
50. Choi YJ, Baek HJ, Kim BR, et al. A pediatric case of atypical chronic myeloid leukemia with CSF3R mutation not responding to ruxolitinib, but rescued by allogeneic transplantation. *Clin Pediatr Hematol Oncol*. 2021;28(1):93-97.
51. Ernst T, Busch M, Rinke J, et al. Frequent ASXL1 mutations in children and young adults with chronic myeloid leukemia. *Leukemia*. 2018;32(9):2046-2049. doi:[10.1038/s41375-018-0157-2](https://doi.org/10.1038/s41375-018-0157-2)

Plasmablastic transformation of chronic lymphocytic leukemia: a review of literature and report on 2 cases

Anurag Khanna, MBBS¹, Bradley R. Drumheller, MD¹, George Deeb, MD¹, Ethan Wade Tolbert, MD², Saja Asakrah, MD, PhD^{1,✉}

¹Emory University School of Medicine, Department of Pathology and Laboratory Medicine, Atlanta, GA, US, ²NHCI Georgia Cancer Specialist, Atlanta, GA, US
Corresponding author: Saja Asakrah; saja.asakrah@emory.edu

Key words: plasmablastic transformation; chronic lymphocytic leukemia; clonality relatedness; EBV infected lymphoma cells; mutational analysis.

Abbreviations: CLL/SLL, chronic lymphocytic leukemia/small lymphocytic lymphoma; PBL, plasmablastic lymphoma; DLBCL, diffuse large B-cell lymphoma; EBV, Epstein-Barr virus; Ig, immunoglobulin; R-CHOP, rituximab, doxorubicin, dexamethasone, vincristine, and cyclophosphamide; DA-R-Velcade EPOCH, dose adjusted rituximab, bortezomib (velcade), etoposide, prednisone, vincristine, cyclophosphamide, and doxorubicin; FISH, fluorescence in situ hybridization; HHV-8, human herpes virus 8

Laboratory Medicine 2023;54:e177-e185; <https://doi.org/10.1093/labmed/lmad060>

ABSTRACT

Chronic lymphocytic leukemia/small lymphocytic lymphoma (CLL/SLL) is the most common leukemia in adults in Western countries. Transformation of CLL/SLL to plasmablastic lymphoma (PBL) is exceedingly rare and often has an extremely poor response to treatment. A thorough molecular workup may help in determining clonality-relatedness and prognosis. We describe two cases of CLL/SLL that transformed into PBL, with an extensive molecular workup in one case, and a review of the literature.

Introduction

Chronic lymphocytic leukemia/small lymphocytic lymphoma (CLL/SLL) is a neoplasm composed of small mature B-cells. It is the most common leukemia among adults in Western countries, with an annual incidence rate of about 5 cases per 100,000 population.¹ The disease usually follows an indolent course with many factors (patient demographics, clinical stage, and molecular markers) affecting the prognosis.

A subset of patients with CLL/SLL transforms into a more aggressive lymphoma (Richter transformation), with a reported incidence of 2% to 8%.² Diffuse large B-cell lymphoma (DLBCL) accounts for 95% to 99% of the transformation cases whereas classic Hodgkin lymphoma

and less common lymphoma subtypes comprise the remainder.³ Diffuse large B-cell lymphoma may be clonally related or unrelated to CLL/SLL. Establishing the clonal relationship is important because clonally related cases have a worse prognosis and are treated more aggressively. Clonally unrelated DLBCL has a prognosis similar to de novo DLBCL.⁴

Transformation of CLL/SLL to plasmablastic lymphoma (PBL) is exceedingly rare, with few cases reported in the literature.^{5–17} Here, we review all reported cases that had a preexisting CLL/SLL in addition to 2 cases we encountered in our practice. We discuss defining morphological and phenotypic features, diagnostic challenges, determining relatedness to the initial CLL/SLL, association with Epstein-Barr virus (EBV) infection, treatment, and outcome. Also, we discuss a detailed mutational and genetic analysis that was performed on 1 of our cases.

Methods

The pertinent samples available for pathologic assessment included bone marrow aspirate and core biopsy, pleural fluid, and axillary lymph node tissue. All the samples were processed and stained using standard procedures. Immunohistochemical stains, flow cytometry, and molecular testing¹⁸ were performed using standard techniques. Please see the supplementary material for details on procedures, antibodies, primers, and probes used.

Case 1

An elderly patient with chronic kidney disease and monoclonal gammopathy was examined to rule out plasma cell neoplasm. A bone marrow biopsy was performed. The marrow aspirate showed trilineage hematopoiesis and frequent mature-appearing, mainly small lymphoid cells with scant cytoplasm, condensed nuclear chromatin, and inconspicuous nucleoli as well as few plasma cells. The bone marrow core biopsy (40% cellular) showed multiple lymphoid aggregates of small lymphoid cells (**FIGURE 1A**). Immunohistochemical staining revealed aggregates of CD19-positive B cells (25% of total) expressing CD23 (**FIGURE 1B**) and immunoglobulin (Ig)M (dim) and interstitially present, CD138-positive, plasma cells (5% of total) expressing IgM. Cyclin D1 was negative in both.

Flow cytometric analysis revealed a monotypic B-cell population (29%) which was small in size and positive for CD5, CD19, CD20, CD22, CD200, CD5, HLA-DR, and CD45 with kappa light chain restriction (**FIGURE 2A**). CD38 was negative. In addition, a population of plasma cells comprising 2% of the total sample was also identified which was

FIGURE 1. Bone marrow core biopsy -case1 (A-B): (A) H&E section shows multiple interstitial lymphoid aggregates are present (focally paratrabecular). The vast majority of the lymphocytes are small and mature-looking. (B) B-cells are estimated as about 25% of cells in sections, and positive for CD23. Pleural fluid- case-1 (C-D): (C) W-G stained smear demonstrates numerous large lymphoid cells with mono/multi nuclei, prominent nucleoli and moderate amount of cytoplasm with vacuoles. (D) The neoplastic cells are positive for IgM, and negative for ALK1 and HHV-8 immunostains (not shown). Lymph node biopsy-case-2 (E-F): (E) mostly shows small monomorphic mature lymphocytes. (F) Immunohistochemical stains on the lymph node biopsy reveal the cells to be positive for CD23 as well as other stains that are not shown including CD5, CD20, and PAX5. Pleural fluid-case-2 (G-H): (G) Monotonous proliferation of plasmablast-like cells. (H) These cells were positive for MUM1. H&E: hematoxylin and eosin, WG-Wright-Giemsa stain.

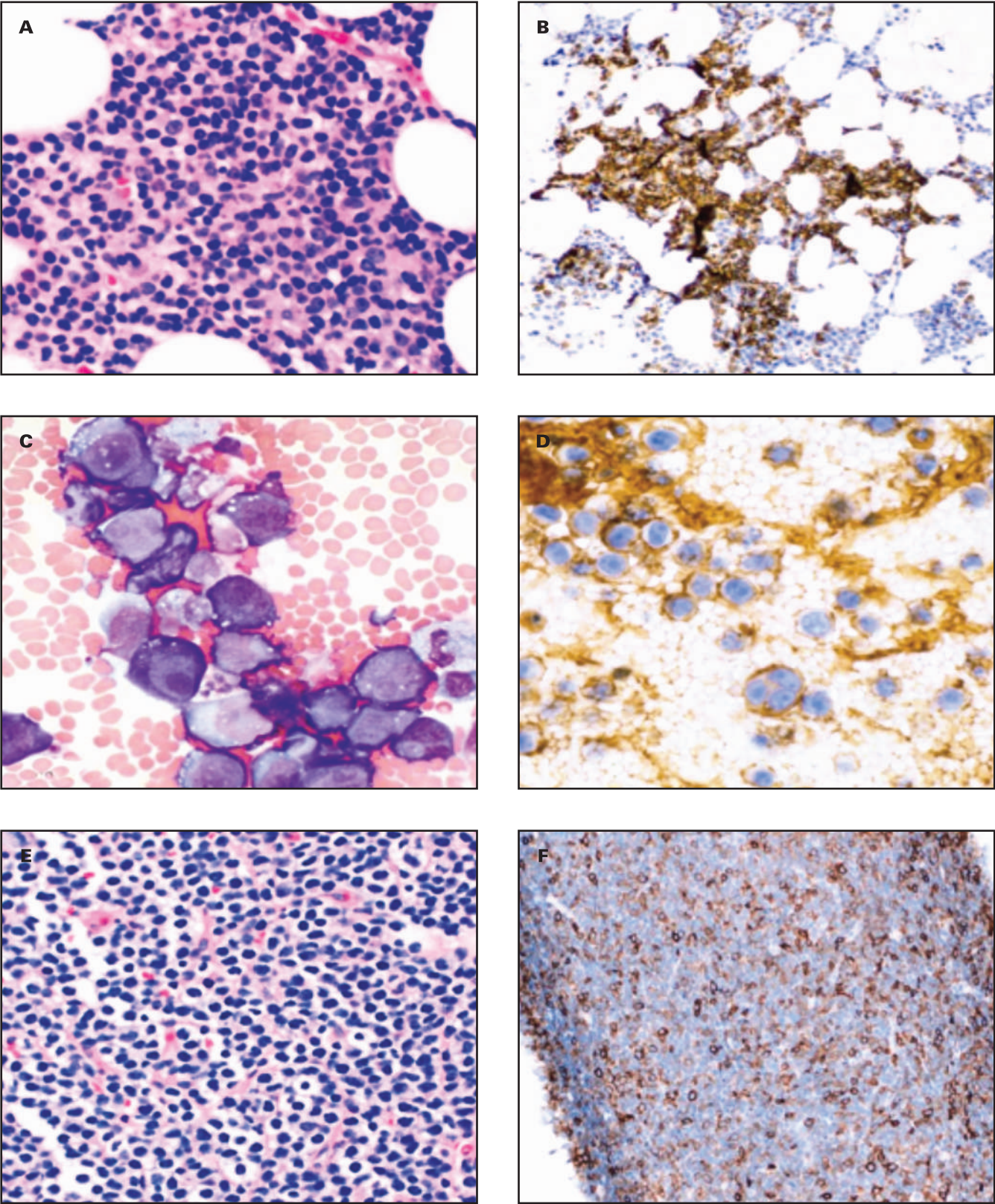
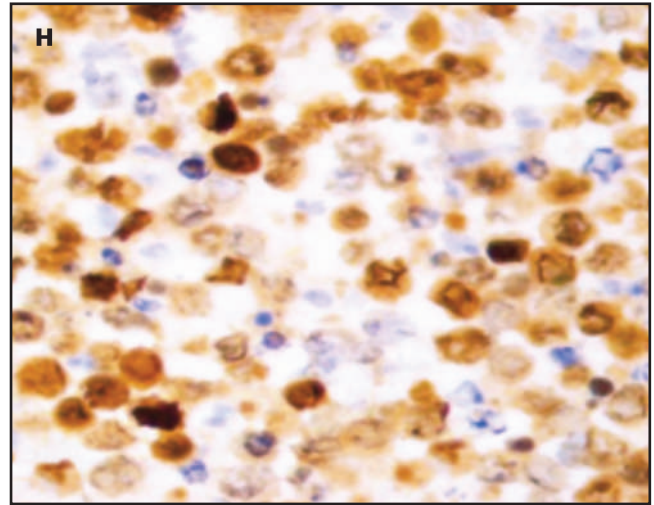
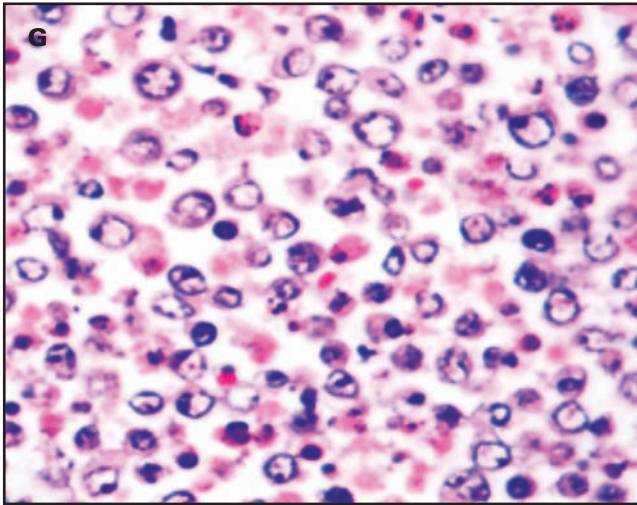


Figure 1. Continued



positive for CD38, CD138, CD19, CD27, CD81, CD200, and CD45 (dim) with kappa light chain restriction (**FIGURE 2A**). Cytogenetic studies showed a normal karyotype, 46, XX (30). A fluorescence in situ hybridization (FISH) panel for CLL revealed monosomy 6 in 44% of the cells (**FIGURE 3A**), whereas a FISH panel for plasma cell myeloma did not reveal any abnormalities. The phenotype is characteristic of CLL/SLL. A differential diagnosis of B-cell lymphoma with plasmacytic differentiation including CLL/SLL, marginal zone lymphoma, and lymphoplasmacytic lymphoma versus coexisting mature B-cell lymphoma with IgM plasma cell dyscrasia/IgM monoclonal gammopathy of undetermined significance were considered. The phenotypic and cytological characteristics are more supportive of CLL/SLL. At that time, the patient was asymptomatic with mild anemia, and therefore a “wait and watch” approach was adopted.

One month later, the patient presented with a large right-sided pleural effusion. A positron emission tomography scan revealed numerous fluorodeoxyglucose-avid lymph nodes within the neck, axillae, right hilar region, retroperitoneum, and bilateral inguinal region. Microscopic examination of the pleural fluid revealed numerous large plasmablast-like cells with single or multiple nuclei, prominent nucleoli, and cytoplasmic vacuoles (**FIGURE 1C** and **D**). Flow cytometric analysis revealed 2 populations: a monotypic plasmacytic population (26% of the total events) with large cell size, positive for CD38, CD138, CD45(dim) with cytoplasmic kappa light chain restriction and negative for CD19, CD20, CD22, CD11c, CD5, CD10 and CD200 (**FIGURE 2B**), and a monotypic small cell size B-cell population (2% of the total events), which was positive for CD19, CD20, CD22, CD5, CD200, HLA-DR, CD45 (bright), CD26 (dim) with a cytoplasmic kappa light chain restriction and negative for CD38 (**FIGURE 2B**). Additionally, the plasmablast-like cells were positive for IgM (**FIGURE 1D**) and negative for ALK-1 and human herpes virus 8 (HHV-8) by immunohistochemistry and negative for EBER by in situ hybridization. A FISH test for 6q23 was performed on the pleural fluid cell block and showed monosomy 6 in 39% of cells (**FIGURE 3B**).

Whole exome and transcriptome sequencing using the DuoSeq platform¹⁹ revealed that both the plasmablast-like cells and the cells from CLL/SLL had *TP53* E258K, *TP53* T155S, and *KMT2D* R4964C mutations. Additionally, both also had t(2;3). The plasmablast-like cells showed

MYC-IGH fusion t(8;14), and t(1;6), which were not seen in the cells of CLL/SLL. The *MYD88* mutation was not identified in either CLL or plasmablastic neoplastic cells (complete findings in **TABLE 1**)

The patient was treated with an anti-CD38 (daratumumab)-based regimen with an initially remarkable clinical response. However, the response was not sustained, and the patient’s disease progressed. The therapy was changed to rituximab, doxorubicin, dexamethasone, vincristine, and cyclophosphamide (R-CHOP). The patient’s disease became refractory to therapy and unfortunately, she died.

Case 2

The second case involved an elderly patient with a history of left-breast invasive ductal carcinoma and CLL/SLL. The patient’s breast carcinoma and CLL/SLL were diagnosed simultaneously in an axillary lymph node biopsy.

The lymph node biopsy findings were consistent with CLL/SLL with no evidence of transformation (mature small lymphocytes, positive for CD5, CD20 [dim], CD23, and PAX5 (**FIGURE 1E** and **F**) and negative for CD10, CD30, CD15, BCL-6, cyclin D1, with a low Ki67. A subsequent bone marrow biopsy revealed up to 90% involvement by similar B-cell lymphoma. The flow cytometric analysis performed on the same sample revealed a kappa-restricted mature B-cell population positive for CD19, CD20, CD22, HLA-DR, and CD5 (dim) (**FIGURE 2C**). The patient was prescribed bendamustine. Rituxan was also prescribed but was held after the first cycle.

Five years after the initial diagnosis, the patient developed right pleural effusion with monotonous proliferation of plasmablast-like mononuclear cells positive for MUM1 (**FIGURE 1G** and **H**) and CD30, CD45, c-MYC (partial), and CD3 (partial) with kappa light chain restriction (by in situ hybridization). The cells were diffusely positive for EBER (ISH) and negative for CD20, CD79a, PAX5, CD138, CD56, Cyclin D1, HHV-8, ALK-1, pan-keratin AE1-3, GATA-3.

Flow cytometric analysis revealed a distinct kappa-restricted population of plasmacytic cells positive for CD38 (bright), CD56 (bright), CD138 (dim), CD22 (dim) and CD81 and negative/dim for CD45 (**FIGURE 2D**). *IGH/IGK* (immunoglobulin heavy and light chain) gene rearrangement polymerase chain reaction studies on the pleural fluid

FIGURE 2. Representative dot-plots of 10-color flow cytometry analysis (antibody-fluorochrome combination is listed along the axes of the plots): (A) Case1 CLL/SLL: Monotypic B-cell population (green population), small cell size, 29% of total analyzed cells): Positive for CD19, CD5, CD200, CD45, and exhibits kappa immunoglobulin light chain restriction. Plasma cell population (Blue population) positive for CD19, CD200 (bright), and surface kappa light chain. T/NK-cells painted cyan. (B) Case1 PBL: Monotypic plasmablast-like population (blue) 26% of total analyzed events): Positive for CD38, and showing cytoplasmic kappa light chain restriction. Monotypic B-cells 2% (green) showing kappa light chain restriction (C) Case2 CLL/SLL: Monotypic B-cell population (blue) 80% positive for CD19, CD5(dim), CD20, CD200 (bright), and exhibits kappa immunoglobulin light chain restriction. (D) Case 2 PBL: A distinct plasmablast-like population (blue), positive for CD38, CD138 (dim), CD56 (bright), and kappa restriction.

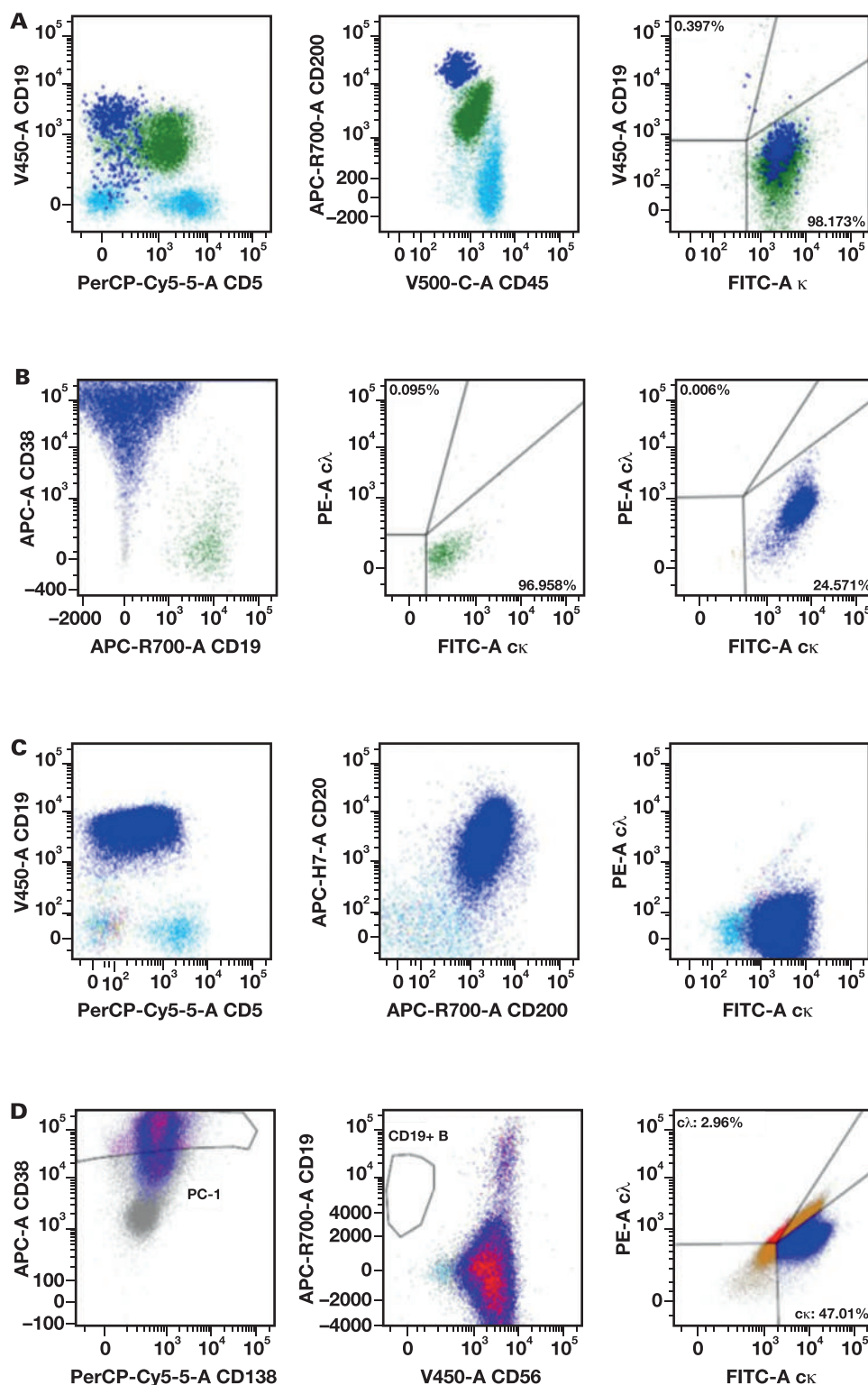


FIGURE 3. (A) Case 1 CLL/SLL: A FISH panel for CLL revealed monosomy 6 in 44% of the cells. (B) Case 1 PBL: FISH test for 6q23 performed on the pleural fluid cell block section showed monosomy 6 in 39% of cells.

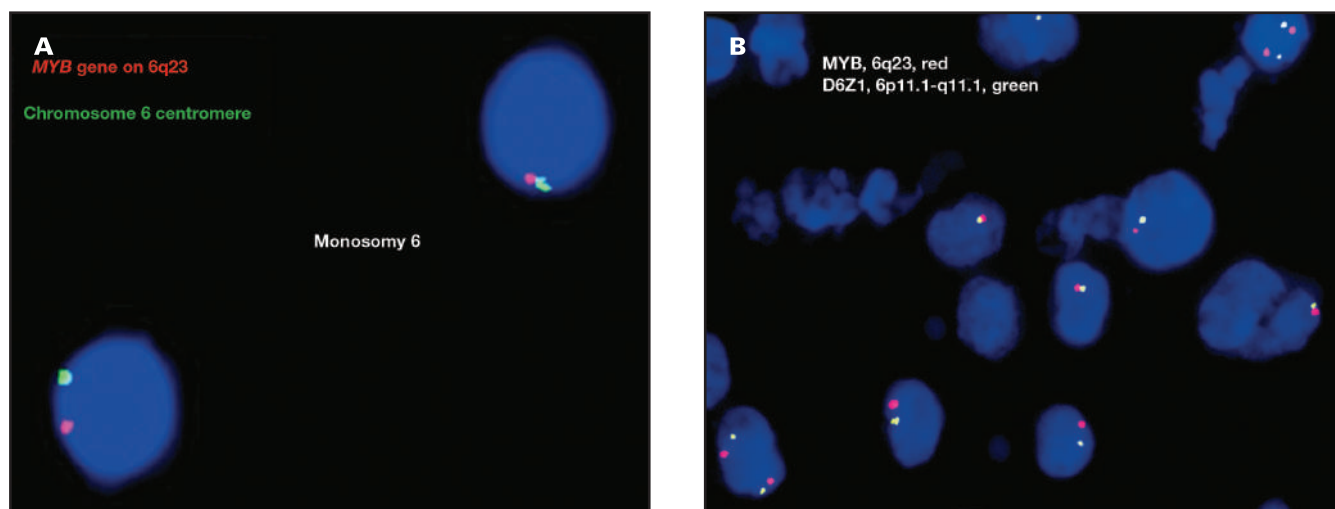


FIGURE 4. Case 2 B-cell IGH/IGK gene rearrangement PCR studies on the initial right axillary lymph node sample (A) and the pleural fluid sample (B) show similar peaks (150 bp and 200 bp) of kappa light chain, indicating clonal relatedness.

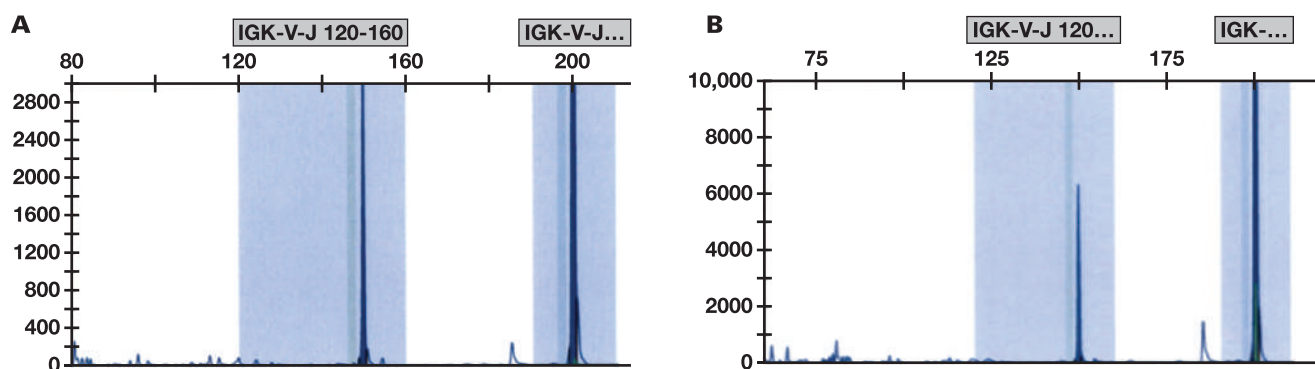


TABLE 1. Molecular and cytogenetic testing results for case 1

Variants identified by WES and Translocations/fusions	Chronic lymphocytic leukemia	Plasmablastic lymphoma
<i>TP53</i> E258K	Present	Present
<i>TP53</i> T155S	Present	Present
<i>KMT2D</i> R4964C	Present	Present
<i>MYC</i> - <i>IGH</i> fusion, t(8;14)(q24;q32)	Absent	present
<i>RCC</i> ; <i>IRF4</i> , t(1;6)(p35;p25)	Absent	present
<i>ANKMY1</i> ; Unknown t(2;3)(q37;p21)	Present	present
<i>FBXL5</i> ; Unknown T(4;13)(p15;q14)	Absent	present

sample and the initial right axillary lymph node biopsy showed similar peaks in both samples, indicating clonal relatedness (FIGURE 4). The patient received DA-R-Velcade EPOCH (dose adjusted rituximab, bortezomib [velcade], etoposide, prednisone, vincristine, cyclophosphamide, and doxorubicin). The patient's clinical condition unfortunately worsened, and a computed tomography scan confirmed refractory disease.

Discussion

There are multiple recognized large B-cell lymphomas that are characterized by plasmablastic differentiation that require a specific immunohistochemistry panel and diligent clinical correlation for definitive identification.²⁰ Some of these lymphomas are often associated with immunosuppression, such as primary effusion lymphoma and PBL, whereas others are characterized by certain genetic aberrations, such as

TABLE 2. Reported cases of plasmablastic lymphoma in the setting of CLL

Paper	Year	No. of cases	EBV/HIV/ HHV-8	IGH gene rearrangements	Mutations	Translocations/chromosomal abnormalities	Clonal status	Treatment	Outcome
Our cases	2022	2	EBV-negative in case 1 and positive in case 2; HIV-N/A for case 1 and negative for case 2; HHV-8: negative in both	Case 1: not done; Case2: identical in CLL and PBL	Case1: Both PBL and CLL/SLL had <i>TP53</i> <i>E258K</i> , <i>TP53</i> <i>T155S</i> , and <i>KMT2D</i> <i>R4964C</i> mutations; Case 2: not done	Case 1: Both CLL and PBL had t (2;3). The PBL also had <i>MYC-IGH</i> fusion t (8;14), and t (1;6), which were not seen in the cells of the CLL/SLL. Case 2: Not done	Clonally related in both cases	Case 1: daratumumab and R-CHOP; Case 2: R-CHOP (1 cycle), and DA-R-Velcade EPOCH	Both patients died
Gasljevic et al ⁵	2020	1	EBV-negative; HIV-N/A; HHV-8-N/A	CLL-/IGHV gene rearrangements seen; PBL-N/A	N/A	CLL-trisomies 12, 3 and 18; PBL-trisomies 12, 3 and 18	Clonally related	None	Patient died
Marvin et al ⁶	2020	1	Anti-EBV IgG positive but EBV ISH negative in PBL; HIV-N/A; HHV-8-N/A	Identical in both CLL and PBL	N/A	N/A	Clonally related	Modified COP regimen etoposide and daratumumab added from cycle 2	Patient died
Hatzimichael et al ⁷	2017	1	EBV-positive; HIV-negative; HHV-8-N/A	N/A	N/A	N/A	Unknown	Bortezomib and dexamethasone	Patient died
Ronchi et al ⁸	2017	1	EBV-negative; HIV-negative; HHV-8-negative	Identical in both CLL and PBL	N/A	N/A	Clonally related	6 cycles of the Hyper-C-PAD (cyclophosphamide, vincristine, adriablastin, bortezomib, and dexamethasone) regimen	Patient died
Chan et al ⁹	2017	2	EBV-negative; HIV-N/A; HHV-8-negative	Identical in both CLL and PBL	N/A	N/A	Clonally related	Salvage chemotherapy	Both patients died
Evans et al ¹⁰	2015	1	N/A	Identical in both CLL and PBL	CLL- <i>TP53</i> mutation: <i>p.Gly245Ser</i> (heterozygous) and <i>p.Val197Glu</i> (heterozygous); PBL- <i>TP53</i> mutation (<i>p.Gly245Ser</i> (hemizygous))	None detected	Clonally related	Radiation therapy to jaw	Patient died
Pan et al ¹¹	2013	2	EBV-negative; HIV-negative; HHV-8-negative	Identical in both CLL and PBL	N/A	Case1: CLL -ve for <i>MYC</i> rearrangement, PBL +ve for <i>MYC</i> (8q24) rearrangement Case2: both CLL and PBL were +ve for t(8;14) with <i>MYC</i> rearrangement	Clonally related	Case 1- no information; Case2-localized radiation and chemotherapy	Case 1: Patient died; Case 2: Patient was in stable condition
Martinez et al ¹²	2013	3	EBV-2 cases were negative and 1 case (only in PBL of case 2) was positive; HIV-negative; HHV-8-negative	Case 1: identical in both CLL and PBL; Case 2: N/A; Case 3: N/A	N/A	Cases 1 and 2: deletion of 13q14.3 in CLL and PBL of both cases 1 and 2 and deletion of 11q22 in CLL and PBL of case 1; Case 3: N/A	Case 1 and 2: clonally related; Case 3: unknown	Case1: 2 cycles of R-CHOP; Case 2: 6 cycles of R-CHOP; Case 3: 1 cycle of VAD and 3 cycles of CHOP	All patients died
Holderness et al ¹³	2013	1	EBV-N/A; HIV-negative; HHV-8-negative	N/A	N/A	N/A	Unknown	R-CHOP bortezomib, ifosfamide, etoposide, carboplatin, mesna, radiotherapy brentuximab	Patient died
Foo et al ¹⁴	2010	1	EBV-positive in PBL; HIV-N/A; HHV-8-N/A	Not identical	N/A	N/A	Clonally unrelated	5 cycles of R-CHOP and localized radiation to the naso-pharynx	Patient died

TABLE 2. Continued

Paper	Year	No. of cases	EBV/HIV/ HHV-8	IGH gene rearrangements	Mutations	Translocations/chromosomal abnormalities	Clonal status	Treatment	Outcome
Ramalingam et al ¹⁵	2008	1	EBV-negative; HIV-negative; HHV-8-positive	N/A	N/A	The primary clone (likely to be CLL): t(9;11) with breakpoints at 9p22 and 11q23 and a deletion del(16) with a breakpoint at 16q22. The second sub-clone (likely to be PBL): complex chromosomal abnormalities in addition to t(9;11) and del(16) including t(1;17), del(5), t(1;12) and additional del(12) resulting from t(12;14). Loss of chromosomes 4, 14, 17, and 18 and gain of chromosome 7	Likely clonally related	Steroids, radiation, CHOP, hyper-CVAD and intrathecal cytarabine	Patient died
Robak et al ¹⁶	2001	1	EBV-negative; HIV-negative; HHV-8-N/A	Not identical	N/A	N/A	Clonally unrelated	1 cycle of VAD, 3 cycles of CHOP	Patient died
Pines et al ¹⁷	1984	1	N/A	N/A	N/A	N/A	Clonally relatedness was inconclusive. Identical surface Ig (IgM kappa) noted on both PBL and CLL	Radiation therapy	Patient died

Negative: negative by serology and/or IHC staining. Positive: positive by serology and/or IHC staining. N/A: not available; VAD: Vincristine, Adriamycin, Dexanathasone; CVAD: Cyclophosphamide, Vincristine, Adriamycin, Dexanathasone.

ALK-positive DLBCL. In rare situations, lower-grade lymphomas¹² or plasma cell myeloma²¹ may show plasmablastic transformation as the disease progresses. Plasmablastic transformation of CLL/SLL is exceedingly rare with very few reported cases^{5–17} (see TABLE 2).

In addition to what has been reported elsewhere, we present 2 CLL/SLL cases that subsequently transformed into PBL. Both cases presented with pleural effusion with numerous neoplastic cells morphologically and phenotypically consistent with plasmablasts. The lack of ALK-1 and HHV-8 staining by immunohistochemistry rule out ALK-1-positive DLBCL and HHV-8-associated lymphoproliferative disorders, respectively.

Demonstrating shared genetic aberrations, molecular mutations, and *IGH/IGK* clones between the CLL and PBL lymphoma cells are the best diagnostic methods to confirm the plasmablastic transformation of CLL. Only a few cases of CLL/SLL and PBL with proven clonality relatedness have been reported (see TABLE 2). In a few cases, a common clonal origin was demonstrated between the plasmablastic cells and the CLL/SLL cells by *IGH* gene rearrangement molecular studies.^{6,8–12} Gasljevic et al⁵ used the presence of trisomies 12, 3, and 8 in both the original CLL and the transformed cells as proof of clonal relatedness. Ramalingam et al¹⁵ and Pines et al¹⁷ assumed clonal relatedness based on heavy and light chain restriction, but this could not rule out de novo PBL. In a large subset of the reported cases, cytogenetic and molecular studies were either not done^{7,13,17} or did not display clonal relatedness.^{14,16} Clonality relatedness with the initial CLL/SLL is demonstrated in both of our cases. Similar mutations, genetic aberrations, and light chain restriction in the CLL cells and the plasmablastic cells were observed in the first case. Both CLL and PBL lymphomas showed monosomy 6, by FISH, and similar *TP53* and *KMT2D* mutations (see TABLE 1). Similar clonal peaks on *IGH/IGK* gene rearrangement studies on both the CLL cells and plasmablastic cells are observed in the second case. In both cases, these genetic findings support the diagnosis of a plasmablastic transformation of the patient's known CLL/SLL.

Unique to this report, a comprehensive mutational analysis was performed in case 1, which not only showed the common *TP53* and *KMT2D* mutations between the CLL and PBL clones but also showed additional *MYC* and *IRF4* rearrangement exclusively in the transformed PBL lymphoma (TABLE 1). It is well known that *TP53* gene disruptions confer poor prognosis and treatment resistance in B-cell lymphomas, including CLL.^{22,23} Chronic lymphocytic leukemia clones with *TP53* mutation show expansion and fitness advantage under therapeutic selection.²⁴

Mutations in *KMT2D* have been implicated in multiple B-cell malignancies with high frequencies in follicular lymphoma and DLBCL; however, it has been rarely reported in CLL, particularly in Western study cohorts.^{25–27} The *KMT2D* mutation is more frequent in Chinese patients with CLL and is an independent risk factor for disease progression and earlier treatment.²⁸ The *IRF4* gene is located in chromosome 6p25-p23 in humans and encodes the *IRF4* transcription factor that is abundantly expressed in macrophages, dendritic cells, B cells, plasma cells, and activated T cells. It regulates the differentiation and development of B cells. *IRF4* gene rearrangement is found in a well-recognized large B-cell lymphoma entity by the World Health Organization with distinct morphologic and clinical features. It is rarely reported in low-grade B-cell lymphomas.²⁹ We found a single study that reported t (1;6) resulting in *IRF4* rearrangement in 8 CLL cases.³⁰ In this study, t (1;6) was found exclusively in unmutated CLL and was frequently associated with an advanced clinical

stage and transformation to DLBCL. The role of *MYC* translocations in CLL is well studied.^{31–33} *MYC* translocations in CLL are associated with increased polymphocytes, complex cytogenetic abnormalities, and a poor prognosis. In addition, *MYC* gene rearrangement is not uncommonly seen in de novo and transformed PBL.^{12,20} All these genetic changes could explain the aggressive clinical course and poor response to therapy in our case. However, their role in the plasmablastic transformation of CLL is not known and requires further investigation.

Epstein-Barr virus-driven PBL is often associated with dysfunctional immune response and HIV infection and presents as a de novo disease.³⁴ It is rarely reported in transformed PBL.^{6,12} Only 1 of our PBL cases and 1 of the reported transformed PBL cases¹² (see **TABLE 2**) showed EBV positivity with a proven clonal relatedness to the initial CLL. Recent studies show EBV infecting a subset of chronic lymphocytic leukemia cells, particularly observed under immunosuppressive medication and often associated with a more clinically aggressive course and Richter's transformation, which may represent a novel type of immunodeficiency-related lymphoma.³⁵ Case 2 was negative for HIV; however, the patient received a platin-based regimen for a nonhematology malignancy, which might have caused immune dysregulation and subsequent EBV-driven plasmablastic transformation. There was no HIV testing for case 1 and the patient did not receive any chemotherapy before the transformation.

Treatment for a transformation to PBL requires an aggressive and multimodal (radiation and chemotherapy) approach.^{6–17} Both myeloma and lymphoma-based regimens were attempted in the limited number of reported cases with no improvement in outcome. Previously reported cases have used cyclophosphamide, vincristine, dexamethasone, etoposide, bortezomib, rituximab, prednisone, and doxorubicin in different combinations and doses^{6–8,12–16} (see **TABLE 2**). One case report reported the use of daratumumab as well.⁶ In all the previously reported cases, the patients died despite aggressive treatment.^{5–17} In our cases, the first case was initially treated with daratumumab with an initial good response but was changed to doxorubicin, Rituxan, dexamethasone, vincristine, and cyclophosphamide after relapse. The second case was treated with 1 cycle of R-CHOP which was changed to DA-R-Velcade-EPOCH. Unfortunately, both patients' diseases had an overall poor response to therapy, and follow-up ended with refractory disease.

Conclusion

In conclusion, we have described 2 cases of CLL that transformed into clonally related PBL. The clonal relation, in the first case, was proved by the presence of similar mutations and light chain restriction in the CLL and PBL cells. In the second case, clonality was proven by the presence of clonal rearrangements with similar peaks in IGH/IGK studies on both the CLL cells and plasmablastic cells. For the first case, a thorough molecular workup revealed the presence of *TP53* and *KMT2D* mutations in both the CLL and PBL and the acquisition of new translocations, t(1;6) and t(8;14), by the PBL cells. These genetic abnormalities may play a critical role in the disease's progression and transformation. Immunosuppression before transformation (case 2) may also have a role in disease progression and transformation.

Acknowledgments

We would like to acknowledge the Society for Hematopathology and Data-Driven Bioscience (Duoseq platform), Durham, North Carolina,

for performing the molecular and cytogenetic tests for case 1. We are very grateful for their help.

Per Emory institutional review board (IRB) guidelines this study is considered non-human subject research thus an IRB approval is not required and therefore not obtained.

AK combined the clinical, pathological, and molecular findings and the results of the literature review into the first draft of the manuscript, created images, and created the figures and tables. BRD created images for the figures, helped in the interpretation of the molecular findings, and provided edits to the manuscript, images, and tables. GD performed the pathological examination and workup, provided the final diagnosis for case 2, helped in the interpretation of the flow cytometric findings of case 1, and provided edits to the manuscript, images, and tables. EWT provided the clinical information and updates for 1 of the presented cases. SA performed the pathological examination and workup, provided the final diagnosis for case 1, edited and added information to the manuscript, images, and tables, and created images for case 1.

Funding

No funding was received for this study.

Conflict of Interest Disclosure

The authors have nothing to disclose.

REFERENCES

1. Campo E, Ghia P, Montserrat E, et al. Chronic lymphocytic leukemia/small lymphocytic lymphoma. In: Swerdlow S, Campo E, Harris N, et al., eds. *WHO Classification of Tumours of Haematopoietic and Lymphoid Tissues*. IARC WHO Classification of Tum; 2017:216–221.
2. Tsimberidou A-M, O'Brien S, Khouri I, et al. Clinical outcomes and prognostic factors in patients with Richter's syndrome treated with chemotherapy or chemoimmunotherapy with or without stem-cell transplantation. *J Clin Oncol*. 2006;24(15):2343–2351. doi:10.1200/JCO.2005.05.0187
3. Chabot-Richards D, Zhang Q-Y, Foucar K. B-cell chronic lymphocytic leukemia/small lymphocytic lymphoma, monoclonal B-cell lymphocytosis, and B-cell polymphocytic leukemia. In: Jaffe ES, Arber DA, Campo E, Harris NL, Quintanilla-Fend L, eds. *Hematopathology*. Elsevier Health Sciences; 2016:261–284.
4. Rossi D, Spina V, Deambrogi C, et al. The genetics of Richter syndrome reveals disease heterogeneity and predicts survival after transformation. *Blood*. 2011;117(12):3391–3401.
5. Gasljevic G, Grat M, Kloboves Prevodnik V, et al. Chronic lymphocytic leukemia with divergent Richter's transformation into a clonally related classical Hodgkin's and plasmablastic lymphoma: a case report. *Case Rep Oncol*. 2020;13(1):120–129. doi:10.1159/000505683. PubMed PMID: 32231533; PubMed Central PMCID: PMC7098336.
6. Marvyn K, Tjonnfjord EB, Bréland UM, Tjonnfjord GE. Transformation to plasmablastic lymphoma in CLL upon ibrutinib treatment. *BMJ Case Rep*. 2020;13(9):e235816. doi:10.1136/bcr-2020-235816. PubMed PMID: 32994268; PubMed Central PMCID: PMC7526319.
7. Hatzimichael E, Papathanasiou K, Zerdes I, Flindris S, Papoudou-Bai A, Kapsali E. Plasmablastic lymphoma with coexistence of chronic lymphocytic leukemia in an immunocompetent patient: a case report and mini-review. *Case Rep Hematol*. 2017;2017:2861596. doi:10.1155/2017/2861596. PubMed PMID: 29387498; PubMed Central PMCID: PMC5735622.
8. Ronchi A, Marra L, Frigeri F, Botti G, Franco R, De Chiara A. Richter syndrome with plasmablastic lymphoma at primary diagnosis: a case

- report with a review of the literature. *Appl Immunohistochem Mol Morphol*. 2017;25(6):e40-ee5.
9. Chan KL, Blombery P, Jones K, et al. Plasmablastic Richter transformation as a resistance mechanism for chronic lymphocytic leukaemia treated with BCR signaling inhibitors. *Br J Haematol*. 2017;177(2):324-328. doi:10.1111/bjh.14062
 10. Evans AG, Rothberg PG, Burack WR, et al. Evolution to plasmablastic lymphoma evades CD19-directed chimeric antigen receptor T cells. *Br J Haematol*. 2015;171(2):205-209. doi:10.1111/bjh.13562
 11. Pan Z, Xie Q, Repertinger S, Richendollar BG, Chan WC, Huang Q. Plasmablastic transformation of low-grade CD5+ B-cell lymphoproliferative disorder with MYC gene rearrangements. *Hum Pathol*. 2013;44(10):2139-2148. doi:10.1016/j.humpath.2013.04.008
 12. Martinez D, Valera A, Perez NS, et al. Plasmablastic transformation of low-grade B-cell lymphomas: report on 6 cases. *Am J Surg Pathol*. 2013;37(2):272-281. doi:10.1097/PAS.0b013e31826cb1d1. PubMed PMID: 23282972.
 13. Holderness BM, Malhotra S, Levy NB, Danilov AV. Brentuximab vedotin demonstrates activity in a patient with plasmablastic lymphoma arising from a background of chronic lymphocytic leukemia. *J Clin Oncol*. 2013;31(12):e197-e199. doi:10.1200/jco.2012.46.9593
 14. Foo W-C, Huang Q, Sebastian S, Hutchinson CB, Burchette J, Wang E. Concurrent classical Hodgkin lymphoma and plasmablastic lymphoma in a patient with chronic lymphocytic leukemia/small lymphocytic lymphoma treated with fludarabine: a dimorphic presentation of iatrogenic immunodeficiency-associated lymphoproliferative disorder with evidence suggestive of multiclonal transformability of B cells by Epstein-Barr virus. *Hum Pathol*. 2010;41(12):1802-1808. doi:10.1016/j.humpath.2010.04.019
 15. Ramalingam P, Nayak-Kapoor A, Reid-Nicholson M, Jones-Crawford J, Ustun C. Plasmablastic lymphoma with small lymphocytic lymphoma: clinicopathologic features, and review of the literature. *Leuk Lymphoma*. 2008;49(10):1999-2002. doi:10.1080/10428190802251795
 16. Robak T, Urbanska-Rys H, Strzelecka B, et al. Plasmablastic lymphoma in a patient with chronic lymphocytic leukemia heavily pretreated with cladribine (2-CdA): an unusual variant of Richter's syndrome. *Eur J Haematol*. 2001;67(5-6):322-327. doi:10.1034/j.1600-0609.2001.00592.x. PubMed PMID: 11872081.
 17. Pines A, Ben-Bassat I, Selzer G, Ramot B. Transformation of chronic lymphocytic leukemia to plasmacytoma. *Cancer*. 1984;54(9):1904-1907.
 18. Michaux L, Wlodarska I, Rack K, et al. Translocation t(1;6) (p35.3;p25.2): a new recurrent aberration in "unmutated" B-CLL. *Leukemia*. 2005;19(1):77-82. doi:10.1038/sj.leu.2403543
 19. Rozzi C, O'Neill S, Hsi ED, et al. Development and validation of Duoseq as a novel diagnostic and companion assay for lymphoma and other cancers. In: Friedberg JW, ed. *American Society of Clinical Oncology*. Rochester, NY: University of Rochester; 2022.
 20. Montes-Moreno S, Montalban C, Piris MA. Large B-cell lymphomas with plasmablastic differentiation: a biological and therapeutic challenge. *Leuk Lymphoma*. 2012;53(2):185-194. doi:10.3109/10428194.2011.608447. PubMed PMID: 21812534.
 21. McKenna R, Kyle R, Kuehl W, Harris N, Coupland R, Fend F. Plasma cell neoplasms. In: Swerdlow S, Campo E, Harris N, et al., eds. *WHO Classification of Tumours of Haematopoietic and Lymphoid Tissues*. IARC WHO Classification of Tum; 2017:241-258.
 22. Ferrero S, Rossi D, Rinaldi A, et al. KMT2D mutations and TP53 disruptions are poor prognostic biomarkers in mantle cell lymphoma receiving high-dose therapy: a FIL study. *Haematologica*. 2020;105(6):1604-1612. doi:10.3324/haematol.2018.214056. PubMed PMID: 31537689; PubMed Central PMCID: PMC7271566.
 23. Rushton CK, Arthur SE, Alcaide M, et al. Genetic and evolutionary patterns of treatment resistance in relapsed B-cell lymphoma. *Blood Adv*. 2020;4(13):2886-2898. doi:10.1182/bloodadvances.2020001696. PubMed PMID: 32589730; PubMed Central PMCID: PMC7362366.
 24. Landau DA, Tausch E, Taylor-Weiner AN, et al. Mutations driving CLL and their evolution in progression and relapse. *Nature*. 2015;526(7574):525-530. doi:10.1038/nature15395
 25. Ortega-Molina A, Boss IW, Canela A, et al. The histone lysine methyltransferase KMT2D sustains a gene expression program that represses B cell lymphoma development. *Nat Med*. 2015;21(10):1199-1208. doi:10.1038/nm.3943. PubMed PMID: 26366710; PubMed Central PMCID: PMC4676270.
 26. Bogusz AM, Bagg A. Genetic aberrations in small B-cell lymphomas and leukemias: molecular pathology, clinical relevance and therapeutic targets. *Leuk Lymphoma*. 2016;57(9):1991-2013. doi:10.3109/10428194.2016.1173212. PubMed PMID: 27121112.
 27. Johansson P, Klein-Hitpass L, Grabellus F, et al. Recurrent mutations in NF- κ B pathway components, KMT2D, and NOTCH1/2 in ocular adnexal MALT-type marginal zone lymphomas. *Oncotarget*. 2016;7(38):62627-62639. doi:10.18632/oncotarget.11548. PubMed PMID: 27566587; PubMed Central PMCID: PMC5308752.
 28. Yi S, Yan Y, Jin M, et al. High incidence of MYD88 and KMT2D mutations in Chinese with chronic lymphocytic leukemia. *Leukemia*. 2021;35(8):2412-2415. doi:10.1038/s41375-021-01124-5
 29. Zhou L, Gu B, Shen X, et al. B cell lymphoma with IRF4 rearrangement: a clinicopathological study of 13 cases. *Pathol Int*. 2021;71(3):183-190. doi:10.1111/pin.13067
 30. Huh YO, Lin KI, Vega F, et al. MYC translocation in chronic lymphocytic leukaemia is associated with increased polyclonal lymphocytes and a poor prognosis. *Br J Haematol*. 2008;142(1):36-44. doi:10.1111/j.1365-2141.2008.07152.x. PubMed PMID: 18477041.
 31. Put N, Van Roosbroeck K, Konings P, et al. Chronic lymphocytic leukemia and polyclonal lymphocytic leukemia with MYC translocations: a subgroup with an aggressive disease course. *Ann Hematol*. 2012;91(6):863-873. doi:10.1007/s00277-011-1393-y
 32. Li Y, Hu S, Wang SA, et al. The clinical significance of 8q24/MYC rearrangement in chronic lymphocytic leukemia. *Mod Pathol*. 2016;29(5):444-451. doi:10.1038/modpathol.2016.35
 33. Dolcetti R, Carbone A. Epstein-Barr virus infection and chronic lymphocytic leukemia: a possible progression factor? *Infect Agents Cancer*. 2010;5(1):22. doi:10.1186/1750-9378-5-22
 34. Langerak AW, Groenen PJ, Brüggemann M, et al. EuroClonality/BIOMED-2 guidelines for interpretation and reporting of Ig/TCR clonality testing in suspected lymphoproliferation. *Leukemia*. 2012;26(10):2159-2171. doi:10.1038/leu.2012.246
 35. Fernández-Álvarez R, Sancho J-M, Ribera J-M. Plasmablastic lymphoma. *Med Clin (Engl Ed)*. 2016;147(9):399-404. doi:10.1016/j.medcle.2016.11.027

A novel internal training program using Kern's 6-step approach to curriculum development for medical laboratory scientists training to be international quality assurance/quality control coordinators

Anne Leach, BS, MT(ASCP)^{*,1}, Josephine Shim, MBA, MT(ASCP)^{*,1}, Kristin Murphy, MS, MLS(ASCP)^{CM1}, Mandana Godard, MBA, MS, MT(ASCP)¹, Felix Ortiz, MPH, MT(ASCP)¹, Mark Swartz, MBA, MT(ASCP)¹, Lori J. Sokoll, PhD¹

¹Clinical Chemistry Division, Department of Pathology, Johns Hopkins University School of Medicine, Baltimore, MD, US Corresponding author: Lori J. Sokoll; lsokoll@jhmi.edu; *These authors contributed equally.

Key words: curriculum development; training program; quality assurance

Abbreviations: pSMILE, Patient Safety Monitoring in International Laboratories; NIH, National Institutes of Health; DAIDS, Division of AIDS; MLSs, medical laboratory scientists; QA/QC, quality assurance/quality control; EQA, external quality assessment; GCLP, good clinical laboratory practice; SOPs, standard operating procedures; IT, information technology; ISO, International Organization for Standardization

Laboratory Medicine 2023;54:e186-e196; <https://doi.org/10.1093/labmed/lmad068>

ABSTRACT

Objective: Patient Safety Monitoring in International Laboratories (pSMILE) is a resource ensuring quality testing in clinical laboratories performing National Institutes of Health-funded HIV research requiring specific staff training. We demonstrate the development of an online asynchronous training model using Kern's 6-step approach to support pSMILE functions.

Methods: An existing curriculum was revamped to incorporate Kern's approach. Metrics for success were described in rubrics with feedback guiding improvements and updates.

Results: Curriculum updates took more than a year. Direct observations of skills informed curriculum changes. Module self-evaluations were reviewed to assess performance and the overall curriculum. The content, curriculum, and training documentation were deemed compliant with International Organization for Standardization (ISO) 9001:2015.

Conclusion: Asynchronous training for highly skilled and self-directed staff is a novel way to deploy training while maintaining productivity of existing staff. Feedback and evaluation allowed for curriculum

updates including previously underdeveloped topics. Kern's approach ensured that the needs of the sponsor, management, laboratories, and learners were met.

Introduction

Patient Safety Monitoring in International Laboratories (pSMILE) is a contract resource between the National Institutes of Health (NIH) Division of AIDS (DAIDS) and Johns Hopkins University with a mission to provide laboratory quality assurance support, guidance, and training to international clinical laboratories performing NIH-funded research originally focused on HIV but now including other infectious diseases. The 10 technical team members of pSMILE are medical laboratory scientists (MLSs) with an average of 20 years of clinical laboratory experience in diverse settings and disciplines. Staff members are credentialed laboratorians, holding MLS certifications from the American Society for Clinical Pathology and American Medical Technologists. They possess a wide range of experience from large university hospital laboratories and commercial laboratories as well as international research and clinical laboratories. Team members also possess a wide range of knowledge and experience gained from working in nearly every department, including chemistry, hematology, immunology, microbiology, and flow cytometry.¹ The international quality assurance/quality control (QA/QC) coordinators are expected to use their professional knowledge of clinical laboratory principles, theories, practices, and methodologies to review and recommend quality improvement, assurance and control programs in international laboratories. This includes extensive work coordinating and monitoring external quality assessment (EQA), also referred to as proficiency testing, activities.

Although our work encompasses the knowledge and experience gained from working in clinical laboratories, it is unique, requiring specific and detailed training. Each employee works with approximately 20 international laboratories on a variety of issues related to compliance with DAIDS good clinical laboratory practice (GCLP).² We have developed standard operating procedures (SOPs) for all of the types of laboratory

assistance that we provide. All new employees need to be thoroughly trained in pSMILE procedures as well as taught how to interact and navigate the collaboration between the laboratories, NIH, and clinical trials networks and investigators that perform the research studies. Additionally, many of our core function processes are automated, driven by 3 databases designed and created by the pSMILE information technology (IT) team. These automated processes are complex and require extensive training to ensure that the deliverables of the contract are fulfilled in compliance with our contractual requirements, GCLP standards and our ISO 9001:2015 certification. Completion of the entire training curriculum for new pSMILE employees takes approximately 12 months and includes an online asynchronous training program combined with 1-on-1 mentorship training with current staff members.

This online asynchronous training program was designed for new pSMILE employees in 2007.³ Over the years, portions of the curriculum were updated to align with changes to the pSMILE project scope and direction. With an evolution in workflow and documentation of processes, the pSMILE training team undertook a complete redesign of the curriculum in 2013 using the Six-Step Approach to Curriculum Development for Medical Education by David Kern.^{4,5} The delivery method was also moved from the Moodle open-source software (moodle.org) platform to Blackboard (Blackboard.com) in 2017. The program was thoroughly reviewed and updated again in 2020 to ensure that the modules remained current and relevant. In 2021, the curriculum was once again modified to address a staffing shortage that necessitated more expeditious training, with a reduction in training time from 9 months to 4 months. See **FIGURE 1** for timeline summary. Herein we describe our experience with the creation of an online asynchronous training model to ensure evidence-based education that produces International QA/QC Coordinators who are competent and prepared to assist international laboratories.

Kern's approach identifies 6 progressive steps to evaluate the curriculum's applicability, appropriateness, and feasibility. Applicability can be defined as the determination that the curriculum meets the goals and objectives of the training program. Appropriateness refers to the notion that the instructional procedures work well for both the targeted learners and the curriculum content. Feasibility can include both budgetary and logistical considerations. It is the process of determining that what may appear to be a great curriculum in theory can actually be practically achieved.

The steps to curriculum development as described by Kern are meant to create a cyclical process in which the steps influence each other, although they are presented in sequential order.^{4,5} The 6 steps are as follows: (1) problem identification and general needs assessment, (2) targeted needs assessment, (3) goals and objectives, (4) educational strategies, (5) implementation, and (6) evaluation and feedback. Each of the 6 steps leads the developer through a series of questions designed to help guide the creation or redesign of the curriculum. The steps are described below along with pSMILE's assessment of each of the successive steps (also see **FIGURE 2**). The format and the additional questions in each step were completed according to the Kern model.

Step 1: Problem Identification and General Needs Assessment

In step 1 of Kern's approach, the educator identifies the problem that necessitates a new (or modified) curriculum and compares the current educational approach with the ideal approach. This allows the identification of limitations in the existing curriculum and the proposal of improvement that will address the needed end product of the curriculum.

Problem Identification

The pSMILE staff must be adequately and appropriately trained to ensure the health and safety of research study participants, the integrity of study data, and the safety of the international staff performing laboratory testing. Although the staff are experienced MLSSs, the job of an international QA/QC coordinator is complex and requires training to ensure that staff meet contractual and regulatory requirements, in addition to possessing the technical skills to perform the job.

Limitations in Curriculum Prior to Redesign

pSMILE international QA/QC coordinators were previously trained using an asynchronous training curriculum developed in 2006 using the Moodle delivery platform.⁶ As of 2013, the curriculum had not been updated, although many internal pSMILE procedures had changed. In addition, the pSMILE contract had just been renewed for 7 more years. The new pSMILE

FIGURE 1. Timeline summarizing the evolution of the pSMILE training curriculum.

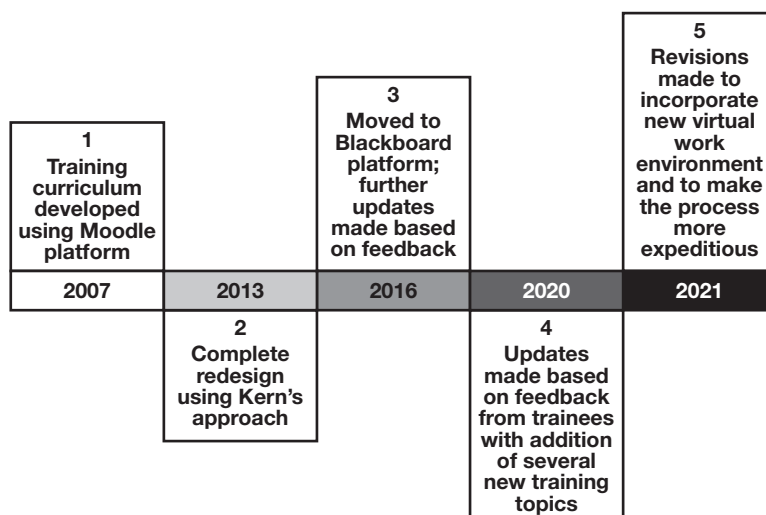
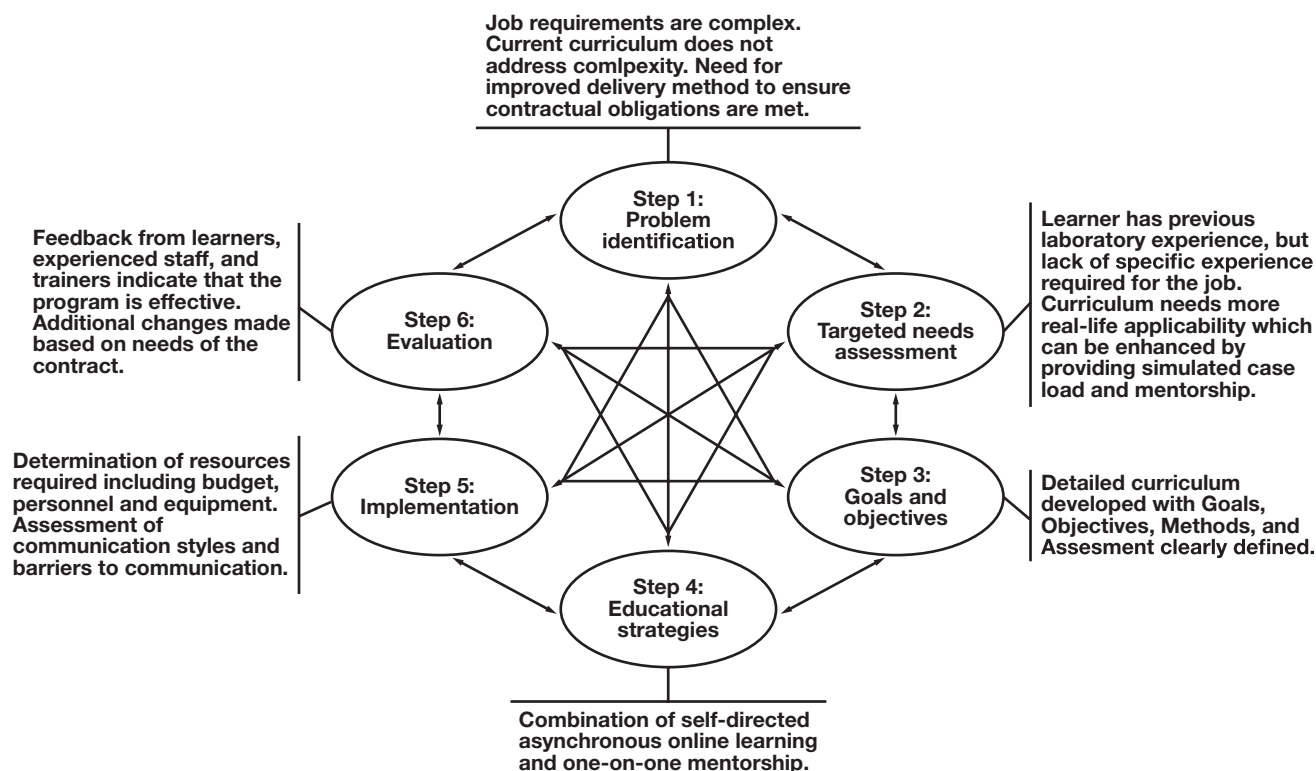


FIGURE 2. Steps for curriculum development as assessed by pSMILE. Thomas, Patricia A., MD, David E. Kern, MD, MPH, Mark T. Hughes, MD, MA, Sean A. Tackett, MD, MPH, and Belinda Y. Chen, MD, eds. *Curriculum Development for Medical Education: A Six-Step Approach*. pp. 9, Figure 1.1 . © 2022 Johns Hopkins University Press. Figure reprinted with permission of Johns Hopkins University Press.



contract contained many changes in approach, scope, and requirements that needed to be incorporated into an updated curriculum.

Following completion of the Moodle online training modules, new pSMILE staff members were paired with experienced coordinators for 1 to 2 weeks. New employees were rotated through the staff to give them exposure to unique styles and approaches to solving problems and to a wide variety of projects and tasks. Although the mentorship rotations were effective, they lacked a standardized, validated assessment tool to ensure the learners acquired the desired knowledge from the rotation.

Approaches to Improve Curriculum

By evaluating what had been the existing approach and comparing it with an ideal approach, Kern guides us to analyze the gaps between current practice and what we seek to achieve. By delineating between the responsibilities of the sponsor, the contracted organization, and the contract team itself, we were able to identify external resources to assist with the comprehensive training. We were also able to focus our efforts on the finer details of pSMILE coordinator task training and identify ways to improve over the current training model.

Sponsor

- Provides training to all new pSMILE employees on GCLP- and NIH-specific procedures for completion of contract deliverables

Institution

- Provides institutional/department-based mandatory training

- Provides access to basic computer skills training (MS Outlook, MS Excel, MS Word, SharePoint, MS PowerPoint)

pSMILE

- Provides in-depth, hands-on training in all pSMILE processes and procedures
- Provides simulated training working with mock scenarios to build familiarity and comfort level with pSMILE processes and procedures
- Provides up to 2 weeks of 1-on-1 mentorship with each of the experienced pSMILE coordinators, which has clear objectives, requirements for covered topics, and an assessment tool to ensure that the mentorship rotation is effective.

Step 2: Targeted Needs Assessment

A curriculum for the training of new pSMILE coordinators already existed. The program had been highly successful and was used to train 8 coordinators. However, areas for improvement in the program were identified through the feedback of learners and trainers, leading us to identify this as a targeted environment that could benefit from curriculum redesign. In step 2, Kern suggests that the educators focus on the needs of the targeted learners. To determine the needs of the targeted learners, the following methods were used: (1) review of the curriculum with the education/training committee to determine applicability and effectiveness, (2) careful review of the contract to ensure that the training program met the requirements of the new contract, and (3)

informal discussions with experienced pSMILE staff, many of whom completed the curriculum, to obtain suggestions for improvement.

Targeted Learners

The targeted learners for this curriculum are new employees of the pSMILE project. The learners are experienced MLSs with extensive backgrounds in all areas of the clinical laboratory. They typically have some background in QA, QC, laboratory audits, and proficiency testing. They may or may not have international experience, which also affects how well they comprehend the nature of the work and how quickly they assimilate certain aspects of the curriculum.

Needs Assessment

Informal feedback from learners and trainers using the Moodle curriculum modules was previously used to make changes and updates to the training modules. However, the need to completely redesign the curriculum was determined based on the response by learners and trainers alike that the modules felt somewhat disjointed and at times lacked continuity. The training committee surveyed recent graduates of the program and the project manager and determined that a simulated work environment would provide the best sense of continuity to the modules.

Survey of Recent Graduates, Trainers and Management

Kern's model for curriculum development relies heavily on the feedback of all recent participants in the training program to inform improvements. Prior to the initial redesign of the curriculum in 2013, The 3 most recent graduates of the training curriculum were surveyed to determine their feedback on the current program's strengths and weaknesses. At the time, there had been very little turnover in staff, so the number of recent graduates was small. To further validate the need for change, current and former trainers were also interviewed informally to determine feedback on the program's effectiveness and difficulties in delivering it.

All felt that the modules were valuable but lacked depth and connection to the actual work at pSMILE. They also felt that the modules stood disconnected from one another, making it difficult to understand how the pieces of the curriculum fit together to make up a typical pSMILE coordinator's caseload. All recent graduates felt that using a simulated caseload of international laboratories would help add relevance to each module.

The pSMILE management acknowledged gaps in the existing Moodle training, such as handling investigation reports required when a laboratory has unsatisfactory performance on a proficiency testing event. Management agreed that the use of a simulated caseload would improve the training program.

Since the initial redesign, an additional 5 coordinators were trained on the new curriculum. Their feedback allowed for the continued improvement of the program, a key to the Kern model, which is not meant to be static but rather an ongoing, fluid process of improvement. Trainee feedback was reviewed by the training team at the completion of each module. When trainee responses identified problems in training organization or content every effort was made to address the issue in real time.

Step 3: Goals and Objectives

Goals

The goal of the training curriculum is to develop pSMILE international QA/QC coordinators who are competent to perform all tasks required to

provide laboratory QA support, training, and guidance to NIH-funded international HIV research laboratories.

Objectives

The module-specific objectives were written to address specific tasks required for job performance. The detailed steps for each of these tasks are outlined in the pSMILE internal SOPs. Trainees are expected to meet the objectives in adherence to the pSMILE Internal SOPs. Detailed curriculum objectives are provided in **TABLE 1**, which contains a summary of each training module of the newly developed curriculum.

Step 4: Educational Strategies

Kern's step 4 identifies and selects educational strategies that will allow the curriculum to attain the goals identified in step 3.

The educational strategy developed uses a combination of online asynchronous training modules originally delivered via the Moodle online platform. Once the curriculum was revised, the individual training topics were loaded onto the Blackboard platform. Additional training is provided by 1-on-1 mentoring with experienced coordinators. The online training modules are designed to simulate the work environment of an international QA/QC coordinator by providing the learners with a caseload of simulated international laboratories. The pSMILE skills must be built onto the learners' prior knowledge, and the Moodle modules allow for a constructivist method of building this expertise. The use of simulation reinforces the construction of new knowledge and incorporates experiential learning by allowing the learner to experience the typical workflow of the pSMILE job.

After completing the online training modules, the learner works side by side with an experienced coordinator on a 7-week rotation. During the mentorship rotation, the learning is at first observational learning. The trainee learns by observing their mentor and is then given a chance to reinforce that learning by reproducing the mentor's work. By the end of the rotation, the trainee should be completing all the work with the mentor standing by to observe and correct any mistakes, allowing for experiential learning. By spending 1 week with each coordinator, the learner is exposed to a variety of work styles and experiences the daily workflow of the pSMILE project firsthand.

Content

The curriculum content was designed to provide pSMILE international QA/QC coordinators with the specific skills needed to perform all job duties. Completion of the training program serves as the evidence of initial competency of newly hired staff.

Methods

Blackboard asynchronous training modules are followed by 1-on-1 mentorship by experienced pSMILE coordinators. Time for completion of this portion of the training is approximately 6 months. The content outline (**TABLE 1**) is very similar to the original curriculum. The full curriculum contains 17 topics. Following the successful completion of the first 10 training topics, new coordinators will be assigned their first set of site laboratories. Topics 1 through 10 include orientation and an overview of the project followed by detailed training on the daily operations and job duties of the coordinators. Topics 11 through 17 provide additional specialized supplemental skills, such as validation and travel procedures, which can be completed after the coordinators begin working with their

TABLE 1. pSMILE training curriculum for international QA/QC coordinators

Module number: name (approx. time to complete)	Summary of learning objectives	Summary of measurement of proficiency
1: Introduction (1 week)	<ul style="list-style-type: none"> Select and access the appropriate tools to begin the training program Schedule and complete required JHU-specific training modules Describe the applicable components of the work environment Review and prepare for the requirements for working remote or virtual 	<ul style="list-style-type: none"> Complete and pass all quizzes for institution -specific modules (with a minimum of 80% score) and required DAIDS IT security training Print out and begin completing items on the pSMILE training checklist Demonstrate ability to work off site productively from laptop through using the current method for connecting to the pSMILE server
2: International Involvement and Diversity (1 week)	<ul style="list-style-type: none"> Explain the role of the pSMILE contract within the DAIDS International HIV studies Demonstrate knowledge and understanding of the pSMILE contract, workflow, network/NIH partners and international involvement Demonstrate awareness and knowledge of pSMILE's mission, vision, and core values 	<ul style="list-style-type: none"> Discuss the role of pSMILE and the pSMILE contract Discuss pSMILE's mission, vision, and core values Discuss the assigned diversity activities
3: Protocols, PALs and Preparing Site Folders (1 week)	<ul style="list-style-type: none"> Correctly follow approved methods of pSMILE data collection, storage, and development Identify the laboratory safety testing used in NIH supported studies Correctly follow approved methods to set up a new laboratory on the pSMILE internal server 	<ul style="list-style-type: none"> Correctly prepare a laboratory site folder complete with subfolders following pSMILE internal SOPs Review assigned SOPs and network protocols Complete a spreadsheet that relates information from network protocols to the information in the corresponding site PALs
4: GCLP & QM (1 week)	<ul style="list-style-type: none"> Navigate DAIDS GCLP guidelines Detect DAIDS GCLP failures 	<ul style="list-style-type: none"> Complete and pass the required DAIDS GCLP online course Discuss current DAIDS GCLP Guidelines and other QM resources Discuss the pSMILE quality policy and QM system
5: Site Assessment and Action Plans (1 week)	<ul style="list-style-type: none"> Interpret DAIDS requirements from an annual Laboratory Assessment report Develop APs using available resources and review the process of working with a site to resolve AP items Discuss best practices for communication with site laboratories via email 	<ul style="list-style-type: none"> Review assigned audits and related APs Prepare a complete AP from an assigned Laboratory Assessment report Prepare an Audit/AP email using pSMILE template
6: EQA Theory (2 weeks)	<ul style="list-style-type: none"> Explain purpose and identify significant items and attachments in the EQA Summary, Schedule, and EQA Monthly Report List major EQA providers, log into and navigate major provider websites using own accounts Identify qualitative and quantitative peer group information from different providers' Participant Summary Reports Use HIV package inserts to determine correct information on assay and results 	<ul style="list-style-type: none"> Demonstrate comprehension of the critical sections of each EQA document type as outlined in the topic 6 Assignments section by independently successfully completing 80% of the tasks Use HIV test package inserts to correctly identify test generation, reporting requirements and testing method
7: AutoSMILE (8 weeks) *This includes working with each coordinator for 1 to 2 weeks after completion of topic 8	<ul style="list-style-type: none"> Navigate the AutoSMILE home page Enter and review EQA results Create EQA reviews, schedules and monthly EQA and AP emails Correctly file analytes according to method 	<ul style="list-style-type: none"> Review and complete assigned EQA Reviews providing appropriate comments and/or suggested actions with 90% accuracy Generate a monthly EQA email including appropriate attachments Successfully complete a 1- or 2-week rotation with each pSMILE coordinator
8: Investigation Reports (1 week)	<ul style="list-style-type: none"> Describe the investigation process from initiation to completion Analyze the data presented for completeness, accuracy and correct conclusion Recommend additions or corrections to the IR as needed Review the process of investigating EQA failures using the electronic IR 	<ul style="list-style-type: none"> Review and complete assigned IRs, providing appropriate comments and/or suggested actions, with 80% accuracy
9: pSMILE Website (3 days)	<ul style="list-style-type: none"> Manually upload and download documents to site folders Upload documents by accessing the pSMILE mass upload functions Correctly manage requests for site access, documents and resources Locate and obtain site information from the oversight master list 	<ul style="list-style-type: none"> Correctly upload and download documents to the pSMILE website Successfully upload EQA documents both manually and using the mass upload function Search "Resource" section to access requested documents and successfully download identified documents
10: Preparation for Working with Site Laboratories (1 week)	<ul style="list-style-type: none"> Review ISO 9001 standards and certification process Demonstrate an awareness of pSMILE's Quality Key Indicators, core functions, quality objectives, and QMS Take notes during the pSMILE staff meeting Complete the process of reviewing all required SOPs. 	<ul style="list-style-type: none"> Demonstrate an awareness of ISO 9001 standards and certification process Complete reading and signing off on assigned SOPs Successfully take minutes at pSMILE staff meetings for one week Review all the available information on assigned site laboratories

Table 1. Continued

Following the successful completion of the first 10 training topics, new coordinators will be assigned their first set of site laboratories. They will begin working with those laboratories following the completion of topic 10. They should continue working through training topics 11-17, as time allows, with the goal of completing the entire training program by the end of the first 12 months at pSMILE.		
11: Validation (2 weeks)	<ul style="list-style-type: none"> Identify and describe the required elements of qualitative and quantitative validations Explain the concept of total allowable error (TEa) and use the pSMILE TEa table appropriately Describe the requirements for, and evaluation of, precision, accuracy, linearity, measurement and reportable ranges, and reference range verification Demonstrate proficiency with the pSMILE validation tools 	<ul style="list-style-type: none"> Correctly analyze precision, accuracy, and linearity data using pSMILE validation tools Identify causes of failed validation results and suggest methods for troubleshooting Review a completed validation plan and summary Evaluate a site validation summary and develop a response using the pSMILE validation email and review templates
12: QC (2 weeks)	<ul style="list-style-type: none"> Explain the concept of internal QC and interpret QC charts and data Outline the internal QC differences between quantitative and qualitative methods Describe the usefulness of sensitive QC ranges and how to acquire them Identify causes of QC failures and how to address them 	<ul style="list-style-type: none"> Locate pSMILE QC tools available in the Resources section of the psmile.org website Correctly identify a bias, shift and trend in both quality control and EQA records Accurately calculate SD and coefficient of variation of raw data provided Provide solutions to given QC failure examples
13: Correlation Testing (1 week)	<ul style="list-style-type: none"> Describe the pSMILE approach to correlation testing and how it can be implemented to meet GCLP guidelines Direct site laboratories to appropriate resources for developing correlation testing policy and SOPs Assist sites with correlation testing action items listed in site audits and APs 	<ul style="list-style-type: none"> Review all assigned materials and discuss application with members of the training team Complete correlation exercises with 80% accuracy Respond to correlation action items on assigned APs with minimum 80% accuracy
14: Parallel Testing and Reagent Lot Verification (1 week)	<ul style="list-style-type: none"> Outline acceptable methods of parallel testing and communicate this information to laboratories participating in DAIDS clinical trials Assist pSMILE site laboratories with the development of appropriate parallel testing programs for new lot numbers of testing reagents and control materials 	<ul style="list-style-type: none"> Review written materials including SOPs related to reagent lot verification and parallel testing Apply knowledge of reagent lot verification and parallel testing to resolution of action items from selected APs
15: pSMILE EQA Audit (2 weeks)	<ul style="list-style-type: none"> Develop a working knowledge of the pSMILE EQA audit process Review the process for ordering EQA surveys Complete an EQA audit for assigned site 	<ul style="list-style-type: none"> Locate pSMILE EQA Audit templates Correctly complete all 4 parts of EQA audit for assigned site
16: pSMILE Travel (3 days)	<ul style="list-style-type: none"> Explain the roles and responsibilities of the pSMILE coordinator while traveling Follow travel policies and procedures while traveling for the contract, from DAIDS travel request to submitting request for reimbursement Promote security awareness through studying relevant SOPs. Access the necessary tools in order to submit a travel request, prepare a coverage plan, complete trip reimbursement, and write a trip report. 	<ul style="list-style-type: none"> Review all travel related SOPs Demonstrate ability to retrieve pSMILE travel references, tools, and resources located on the internal server Review documents generated for a completed site visit
17: Training Completion (2 days)	<ul style="list-style-type: none"> Complete all training checklists for topics 1-16 Complete the pSMILE Training Completion Form 	<ul style="list-style-type: none"> N/A

AP, action plan; DAIDS, Division of AIDS; EQA, external quality assessment; GCLP, good clinical laboratory practice IT, information technology; IR, investigation report; NIH, National Institutes of Health; pSMILE, Patient Safety Monitoring in International Laboratories; QC, quality control; QM, quality management; QMS, QM system; SOPs, standard operating procedures; PALs, protocol analyte lists; ISO, International Organization for Standardization.

laboratories. The goal is to complete the entire training program, including the supplemental topics, by the end of the first 12 months at pSMILE.

The primary changes to the curriculum involved the use of a simulated work environment that includes providing the learner with a simulated laboratory. The learner is given a background story so that they can understand the laboratory's culture, language, and any barriers to communication. All modules revolve around the same simulated laboratory so that the learner can build that information into improved understanding of the laboratory. Additionally, improved evaluation tools help to guide the ongoing real-time improvement of the curriculum.

Step 5: Implementation

In Kern's step 5, the necessary resources to implement the curriculum are identified and an implementation strategy is initiated. Implementation of this curriculum was made possible by the support of the pSMILE project manager, the university, and the sponsor. Proper training of personnel is key to the success of the pSMILE project. Adequate time, resources, equipment, and facilities are provided by the project in support of this curriculum.

Resources

Personnel

Two training coordinators who are certified and experienced MLSs and have extensive international QA/QC experience on the pSMILE project

are dedicated to the training team. Both coordinators have a strong desire to teach and have a caring and supportive attitude. When they have an active trainee, approximately 20% of their workday is devoted to teaching. Salary support is provided by the pSMILE contract. The remaining pSMILE staff (who serve as mentors to the learners) provide additional training support during the mentorship phase.

Facilities, Equipment, Materials

When first implemented, the training took place in an office location with provision of all necessary computer equipment, software, and office supplies. The project staff has since moved to telecommuting and remote work. All training activities are now conducted via virtual tools, with computer equipment and software provided for off-site work.

Funding

Budget for all the materials and equipment listed above is provided by the NIH contract that supports the pSMILE project. Additional funding for materials and personnel support is provided by the institution.

Communication

Communication between educators and learners occurs verbally, by phone teleconference, by email, and through the feedback mechanisms included in each module. The learner attends the daily pSMILE staff meeting. Updates are provided to the staff on the progress of training as applicable. The learner then meets with the training coordinators to discuss the day's activities, goals, and objectives and answer any questions. The learner works independently on the Blackboard modules.

Operations

The training coordinators are responsible for preparation of the Blackboard modules and providing all supporting documents needed to complete each module. They are responsible for directing the daily activities of the learner to ensure that the training progresses efficiently. The trainers also collect all evaluation data and make any necessary curriculum revisions.

Barriers

Primary barriers to the implementation of this curriculum are the demands of the pSMILE project that would necessitate the training coordinators pausing their training duties to handle emergent duties related to the contract. In addition, there are times that the learner may have to be redirected in their training schedule to meet immediate contract demands. These barriers can be overcome by flexibility on the part of the trainee and the trainers.

Additional barriers are occasionally encountered when a mentorship fails due to personnel or personality conflicts. Training coordinators must be vigilant and monitor the mentor-mentee relationship to ensure that personality differences do not affect the learning.

Introducing the Curriculum

The introduction of the original asynchronous Moodle-based curriculum occurred in 2007. Small and subtle changes to the curriculum occurred continuously to adapt to needs and changes of the project. The redesigned curriculum developed using the Kern model was introduced in 2017 when 2 new staff members were hired. The new curriculum was piloted and reevaluated after the pilot period to determine effectiveness.

Step 6: Evaluation

The sixth and final step in the Kern approach to curriculum development is evaluation and feedback. In this step, both the curriculum and its effectiveness and the individual learners are assessed. The evaluation can be both formative (occurring throughout the training process) and summative (occurring at the conclusion of training).

The evaluation of the pSMILE curriculum occurred over a period of several years. This curriculum is typically used by only 1 learner at a time, and over the last 15 years, there have been only 13 coordinators trained using this program. This makes evaluation slow and somewhat unreliable. In the early years of the curriculum, formal evaluation was conducted in the form of a questionnaire at the end of each module. The questionnaire consisted of very general "customer satisfaction" questions. Learner evaluation was conducted by grading written assignments; however, the grading was done by different instructors and an answer key was not used. This led to inconsistent grading of assignments and potential instrument bias and interrater unreliability. Informal evaluation also occurred during the mentorship phase using informal feedback given to the learners by the mentors. As the evaluation methods previously used lacked validity, a revamp of the evaluation at the end of each module was added in 2020.

For the redesigned curriculum, we proposed to improve the evaluation and feedback process. The learner self-evaluations at the end of each module now contain questions that are more targeted to the objectives and competencies of each module. The evaluation also includes questions that address the curriculum components. Additionally, the evaluation of the learners based on written assignments is graded with the use of a standardized answer key and a grading rubric. This not only standardizes the grading of each assignment, providing interrater reliability, but it helps to eliminate instrument bias. The data collected is also used to guide feedback to the learners. The use of the rubric allows for the collection of valid data that will either give evidence of the effectiveness of the training or will guide the improvement of the curriculum. During the mentorship phase, mentors are given an evaluation form that directs and guides the evaluation of their trainees, rather than leaving the feedback to random comments.

Evaluation Questions and Measurement Methods

An example of a module course evaluation form is shown in **FIGURE 3** and the mentorship evaluation rubric is provided in **TABLE 2**. Measurement of the evaluation of learners is conducted by a combination of direct observation of skills, self-evaluation, and evaluation by a mentor. The direct observation of skills takes place at the end of each module. The training coordinator will give direct feedback to the learner. Scores on the direct observation are used to inform changes to the curriculum.

Analysis of Training Evaluation

The training coordinators collect feedback on the effectiveness of each training module. Trainees are not permitted to move to the next module without completing the postmodule evaluation. The training coordinators also compile cumulative feedback following completion of the entire curriculum.

The training coordinators analyze feedback from the post module self-evaluations and the grading of written assignments is compared to determine whether there is a weakness in the curriculum or a need for the learner to repeat any sections to ensure competency. Feedback from the mentorship evaluation is also compared with the cumulative module evaluations to determine whether improvements to the curriculum are necessary.

FIGURE 3. Example of training module evaluation form. EQA, external quality assessment; pSMILE, Patient Safety Monitoring in International Laboratories

<p>pSMILE Coordinator Training Evaluation Blackboard Training Curriculum</p> <p>Module #6 EQA Theory</p> <p>Please complete this evaluation for the training course. Your experience in learning the content of the module is highly valued. Please respond honestly. All responses will contribute to changes in the course.</p> <p>After completing Module #6 EQA Theory:</p>		<p>Please evaluate the effectiveness of the instruction to meet the objectives outlined at the beginning of the module:</p>
<p>1. I understand the purpose of the EQA Schedule and can identify the purpose of each row and column.</p> <p>Agree _____ Somewhat Agree _____ Somewhat Disagree _____ Disagree _____ Comments:</p>	<p>1. The amount of time allowed for this module was appropriate.</p> <p>Agree _____ Somewhat Agree _____ Somewhat Disagree _____ Disagree _____ Comments:</p>	
<p>2. I can identify the major EQA providers and navigate their websites to obtain information that I need for EQA review.</p> <p>Agree _____ Somewhat Agree _____ Somewhat Disagree _____ Disagree _____ Comments:</p>	<p>2. The module adequately explained the requirements to complete each of the objectives.</p> <p>Agree _____ Somewhat Agree _____ Somewhat Disagree _____ Disagree _____ Comments:</p>	
<p>3. I understand the EQA summary and can explain the purpose, including the significance of color coding and the purpose of each row and column.</p> <p>Agree _____ Somewhat Agree _____ Somewhat Disagree _____ Disagree _____ Comments:</p>	<p>3. The instructor provided opportunities for face-to-face interactions.</p> <p>Agree _____ Somewhat Agree _____ Somewhat Disagree _____ Disagree _____ Comments:</p>	
<p>4. I am able to make updates to an EQA summary based on the information gathered from the EQA review.</p> <p>Agree _____ Somewhat Agree _____ Somewhat Disagree _____ Disagree _____ Comments:</p>	<p>4. The instructor's feedback was appropriate.</p> <p>Agree _____ Somewhat Agree _____ Somewhat Disagree _____ Disagree _____ Comments:</p>	
<p>5. I understand the purpose of the monthly EQA email following the approved pSMILE format, including all required attachments.</p> <p>Agree _____ Somewhat Agree _____ Somewhat Disagree _____ Disagree _____ Comments:</p>	<p>Thank you for taking the time to fill in this evaluation</p>	

TABLE 2. Excerpt from pSMILE coordinator training: mentorship evaluation rubric

Criteria for evaluation of coordinator trainee		Does not demonstrate criteria	Adequate demonstration of criteria, but needs improvement	Excellent demonstration of criteria
		1	3	5
1	EQA review	Does not complete EQA review independently following the pSMILE internal SOP. Incorrectly identifies shifts, trends, bias. Incorrectly identifies need for an investigation.	Completes the EQA review independently with few errors or corrections necessary by the mentor.	Completes the EQA review independently, in compliance with pSMILE internal SOPs with no errors or corrections necessary.
2	EQA summary	Does not update EQA summary correctly based on review (e.g., Uses incorrect color-coding, comments are incorrect, missing date reviewed, etc.)	Correctly updates EQA summary based on review. Occasional errors or corrections necessary by the mentor.	Correctly updates EQA summary based on review. No errors or corrections necessary by the mentor.
3	Investigation reports	Does not demonstrate understanding of the investigation process and workflow. Unable to assess whether an investigation is acceptable. Unable to assist laboratory with investigation steps.	Demonstrates understanding of the investigation process and workflow. Able to assess whether an investigation is acceptable with assistance from the mentor. Able to assist laboratory with investigation steps with assistance from the mentor.	Demonstrates understanding of the investigation process and workflow. Able to assess whether an investigation is acceptable without assistance from the mentor. Able to assist laboratory with investigation steps without assistance from the mentor.
4	Email correspondence	Uses incorrect email contact list for laboratory. Does not follow pSMILE template for email format. Does not include appropriate attachments to EQA email.	Requires occasional assistance from mentor to perform the following: uses correct email contact list for laboratory; follows pSMILE template for email format; includes appropriate attachments to EQA email.	Performs the following independently: uses correct email contact list for laboratory; follows pSMILE template for email format; includes appropriate attachments to EQA email.
5	pSMILE web-site	Unable to navigate through website. Unable to upload, download or update documents on website.	With occasional assistance is able to navigate website, upload, download, and update documents on website.	Independently is able to navigate website, upload, download, and update documents on website.
6	Laboratory site assessment	Does not demonstrate understanding of GCLP audit report. Unable to distinguish audit findings.	With minimal assistance from mentor, demonstrates understanding of GCLP audit report. Distinguishes audit findings.	Independently reviews and understands GCLP audit report. Distinguishes audit findings.
7	Action plans	Does not develop an action plan from GCLP audit report using the approved template and SOP. Unable to describe audit findings and provide appropriate suggested actions.	Develops an action plan from a GCLP audit report using the approved template and SOP with minimal assistance. Describes audit findings and provides appropriate suggested actions most of the time. Occasionally deviates from the approved format.	Develops an action plan from a GCLP audit report using the approved template and SOP without assistance. Describes audit findings and provides appropriate suggested actions. Does not deviate from the approved format.

AP, action plan; EQA, external quality assessment; pSMILE, Patient Safety Monitoring in International Laboratories; SOP, standard operating procedure.

Reporting of Results

Collated evaluation results, including the mentorship evaluation, are presented to the project manager. This information is used to determine whether the learner is ready to graduate to full work responsibilities. Evaluation results are also discussed between the training committee and the project manager in an effort to continue ongoing improvement to the curriculum. The effectiveness of the curriculum is further shown by the successful addition of the new coordinators to the pSMILE workflow. Following their first year of employment, all new staff members received annual review ratings at or above expectations.

Discussion

The transition from Moodle to Blackboard was a lengthy process involving selection of a new training platform, learning how to use Blackboard effectively, and determining how to best optimize training materials for the selected platform. A small committee of trainers collaborated on reorganization of existing training materials with the goal of updating them to accommodate changes in pSMILE procedures as well as making training information and assignments more relevant. Blackboard training updates included a requirement for new coordinators to complete an evaluation at the end of each training section. Information obtained during review of these evaluations as well as direct discussion with trainees was invaluable in making meaningful revisions to training materials on an ongoing basis.

Lessons Learned and Future Challenges

Laboratory support for international laboratories participating in NIH HIV, tuberculosis, and other infectious disease clinical trials is not static. The work of pSMILE coordinators is constantly evolving to meet changing requirements generated by new protocols, testing methods, and shifting site laboratory responsibilities. Although these changes are incorporated into the flow of work for pSMILE coordinators on an ongoing basis, the process of updating the training program is often slower, leading to the situation in 2020 where a complete revamp of the training program was required. Revising the training program is time consuming if updates are allowed to accumulate. One of the major challenges is making revisions in real time, avoiding making a large number of modifications prior to preparing the training program for a new learner. This process has already been initiated as shown in [TABLE 3](#) (Examples of Real Time Updates to the Training Program). The table identifies issues with the training program that needed to be addressed and how the training team responded.

Another area of the training program that could be better supported is the time allocated for new learners to shadow and work with experienced pSMILE coordinators. Two identifiable factors make this area of training challenging for the trainer. First, the lack of in-person contact with the learner and reliance on a now totally virtual platform for communication, and second, the ability to meet the demands of regular work requirements while training at the same time. The workload for coordinators is often difficult to predict, making it challenging to

TABLE 3. Examples of real time updates to the training program

Source of change	Issue	Discussion
Learner-generated feedback	Training material failed to successfully explain pSMILE's working relationships with collaborating organizations.	Learners did not fully understand the complex relationships between pSMILE, NIH, and collaborating networks. Failure to grasp these interactions caused confusion and frustration that affected progress on other training topics. The training team developed visual resources to better explain the relationships between organizations and pSMILE. In addition, more time was allotted in feedback sessions with the training team to ensure that trainees fully understood the most important interactions. Additional considerations: There may be a need for members of the training team to work 1-on-1 with the learner while covering this topic.
	Reorganization of training topics to improve the logical flow of training activities.	Learners made meaningful suggestions that assisted pSMILE trainers with improving the flow of training materials and assignments. One example involved moving the topic on creating APs to follow DAIDS GCLP. This made sense as the AP section is highly dependent on GCLP knowledge. Previously it would have taken many weeks before learners had the opportunity to begin the AP topic.
Initiated by the pSMILE training team	Adapting the training program to accommodate the ability to work virtually and transitioning to a total virtual platform.	The ability to work effectively using a virtual platform gained increased importance over time, especially in response to the COVID-19 pandemic and the decision for pSMILE to move to a totally virtual workplace. The training team moved topics on working virtually from the end of the training program to the beginning. Extensive IT support was initiated for new learners to ensure they had access to equipment and resources needed to effectively work on assigned training modules.
	Implementing changes to the HIV EQA section to improve clarity.	HIV EQA is currently particularly challenging due to the many test methods and generations of each test available. Accurate knowledge of this testing area is critically important to ensure that appropriate EQA is ordered and that results are correctly submitted and evaluated. This section was revised to include different scenarios requiring trainee coordinators to select the appropriate HIV EQA. Additional exercises were provided when necessary to ensure optimal comprehension of HIV testing requirements.
Changes to pSMILE's internal processes	Updating training program to incorporate the introduction of the online IR	IR review is an important part of the work performed by pSMILE coordinators. Site laboratories are required to complete an IR when they receive a score of less than 100% on any protocol analyte. During the process of making updates to the training program significant changes were made to incorporate changing this process from a manual process to an online process.

AP, action plan; DAIDS, Division of AIDS; EQA, external quality assessment; GCLP, good clinical laboratory practice IT, information technology; IR, investigation report; pSMILE, Patient Safety Monitoring in International Laboratories.

create an optimal training environment where there is time to answer questions, provide guidance, and review work for the trainee coordinator. Future measures that could be introduced to improve the experience for both educator and learner include providing coordinators with opportunities to develop training skills, such as webinars and in-person continuing education programs, if available, and using backup coordinators to help with day-to-day work if more time is needed for the trainer to provide effective training.

The pSMILE training program is long and often stressful for trainee coordinators. New employees are invariably well qualified and highly motivated, but it can still be confusing and difficult to put all the pieces together prior to beginning the process of working with site laboratories. Trainers should be able to provide encouragement as well as help with connecting the dots and explaining how pSMILE interacts with laboratories, networks, and other organizations. The ability of trainers to provide motivation and reassurance will aid the development of a training environment conducive to producing effective, confident, and knowledgeable pSMILE coordinators with the ability to use their skills to support the work of international clinical laboratories.

Conclusion

The use of asynchronous training for highly skilled and self-directed staff is a novel way to deploy training without hampering the productivity of existing staff. For this model to be successful, it is important to ensure that the curriculum is well developed and continually updated for relevance. Using feedback and evaluation of trainees allowed us to update our curriculum to include topics that

had previously been lacking or underdeveloped. We were also able to improve the mentorship rotations, which is key to the success of the program. The fact that we have updated the curriculum continuously since the initial 2013 redesign demonstrates one of the key points of the Kern 6-step method, which is meant to be fluid, interactive, and interchangeable. The 6 steps are not intended to be purely sequential, but rather are designed to lead the curriculum developer to return again and again to previous steps to ensure continuous improvement. The use of Kern's 6-step approach in this manner ensured that the curriculum met the needs of the contract, the sponsor, the project manager, and the learners, thereby validating its appropriateness, applicability, and feasibility.

Acknowledgments

The authors thank Daniella Livnat, Division of AIDS, National Institute of Allergy and Infectious Diseases, NIH, for her leadership and support of the pSMILE program and for critical review of the manuscript. We also thank the entire pSMILE project team members, both current and former, who contributed to this project. We would especially like to recognize Peggy Coulter, who developed the original training curriculum that provided the framework for this project.

Funding

This work was supported in whole or in part with federal funds from the National Institute of Allergy and Infectious Diseases, National Institutes of Health, Department of Health and Human Services, under Contract No. 75N93020C00001.

REFERENCES

1. Patient safety monitoring in international laboratories. *MLO*. 2021;53(2):40-44.
2. NIH Division of AIDS (DAIDS) Clinical Research Policies and Standard Procedures, Requirements for DAIDS Funded and/or Sponsored Laboratories in Clinical Trials. MAN-A-OD-001.01 -DAIDS Good Clinical Laboratory Practice (GCLP) Standards, version 4.1. Effective 16 August 2021. <https://www.niaid.nih.gov/sites/default/files/gclpstandards.pdf>
3. Geng S, Law KMY, Niu B. Investigating self-directed learning and technology readiness in blending learning environment. *Int J Educ Technol High Educ*. 2019;16(1):17. <https://doi.org/10.1186/s41239-019-0147-0>
4. Kern DE, Thomas PA, Hughes MT. *Curriculum Development for Medical Education: A Six-Step Approach*. 2nd ed. Baltimore, MD: Johns Hopkins University Press; 2009.
5. Chen BY, Kern DE, Kearns RM, Thomas PA, Hughes MT, Tackett S. From modules to MOOCs: application of the six-step approach to online curriculum development for medical education. *Acad Med*. 2019;94(5):678-685. <https://doi.org/10.1097/ACM.0000000000002580>
6. McNeill MA, Arthur LS, Breyer YA, Huber E, Parker AJ. Theory into practice: designing Moodle training for change management. *Asian Soc Sci*. 2012;8(14):58-64.

The exclusion of anti-D alloantibody in a suspected anti-G antibody in a pregnant 28-year-old Odiya Indian woman

Kella Nivedita, MBBS, MD; Somnath Mukherjee, MBBS, MD[✉]; Satya Prakash, MBBS, MD; Ansuman Sahu, MBBS, MD; Debasish Mishra, MBBS, MD^{1,✉}

¹Department of Transfusion Medicine, All India Institute of Medical Sciences, Bhubaneswar, India Corresponding author: dr.debasish01@gmail.com

Keywords: anti-G, Rh immunoglobulin, differential absorption and elution, antibody screening, antibody identification, blood-group discrepancy

Abbreviations: HDFN, hemolytic disease of the fetus and newborn; DTT, dithiothreitol; DAT, direct antiglobulin test

Laboratory Medicine 2023;54:e197-e200; <https://doi.org/10.1093/labmed/lmad067>

ABSTRACT

The Rh-D negative pregnancy is commonly associated with alloimmunization against D-antigen. It can be prevented by anti-D prophylaxis in pregnant patients with negative results on antibody screening. Hence, it is essential to exclude alloantibody-D in the presence of multiple alloantibodies. Anti-G antibody is formed after exposure to G antigen in neonate RBCs. Blood-group discrepancy was noted in reverse grouping, and antibody-screening results were positive in our case individual, a 28-year old Odiya Indian woman. We performed antibody identification on serum specimens from this patient, which revealed the pattern of anti-D + anti-C antibody specificity. Blood-group discrepancy was solved using rr (ce/ce)-phenotype pooled cells for reverse grouping. We identified anti-G antibodies by themselves without anti-D and anti-C after performing sequential adsorption of serum with r'r' (Ce/Ce) and R2R2 (DcE/DcE) group-O RBCs in the mother, who had rr phenotype and primigravida designation. After completing antibody screening at the first antenatal check-up, we recommended prophylactic anti-D for the mother in any future pregnancies she may have.

The G antigen belongs to the Rh blood-group system; the amino acid serine on the RBCs secures its phenotyping as G-antigen. Allen and Tippett¹ first documented the existence of the G antigen in 1958 in most D-positive and all C-positive RBCs. The amino acid substitution from

serine to proline at position 103 on the RhD-RhCE proteins results in a G-negative phenotype.² Anti-G exists as the combined reactive pattern of anti-C and anti-D on antibody-identification testing. It was first noticed in a patient with the rr phenotype who received a transfusion of D-antigen-positive RBCs.¹

Anti-G-antibody identification is vital in patients testing Rh-negative in pregnancy who lack the C and D antigens needed to provide RhIg prophylaxis, after excluding the presence of anti-D.¹⁻⁴ Hemolytic disease of the fetus and newborn (HDFN) caused by anti-G is mild to moderate in severity and rarely intrauterine; exchange transfusion is required in rare instances. In our case individual, we found anti-G by itself, without anti-D and anti-C. Anti-G may be IgM, IgG, or a combination of IgM + IgG, causing a discrepancy in the reverse grouping. Hence, we advised that anti-D prophylaxis be administered to prevent alloimmunization against Rh D antigen and HDFN in the fetus in any future pregnancies.

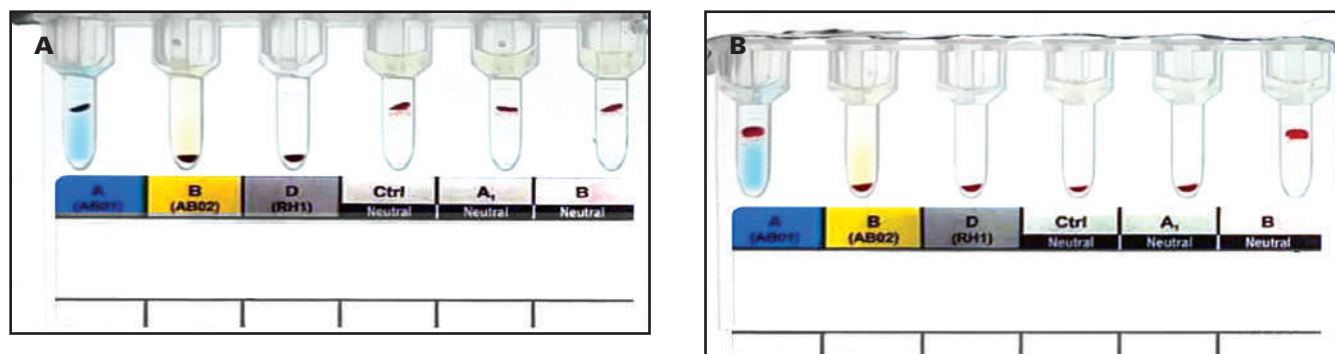
Case Report

A 28-year-old Odiya Indian Woman with the primigravida designation, who was at 38 weeks gestation and had an Hb measurement of 11.9 g/dL, was admitted to the labor room for delivery. She had no previous history of trauma or invasive procedures such as cordocentesis, amniocentesis, abortion, or transfusion. She had been given a prophylactic transfusion of Rh immunoglobulin at 20 weeks gestation in another hospital.

Blood grouping was performed with column agglutination technology (Tulip Diagnostics Pvt. LTD). There was no forward blood-group discrepancy; discrepancy in reverse grouping was noted with pooled A, B, and O cells (**FIGURE 1A**). The discrepancy was solved using rr-phenotype pooled cells (**FIGURE 1B**). The patient had an RBC phenotype of rr (D-C-c+E-e+). The antibody-screening result was positive (**FIGURE 2A**), and an anti-D and anti-C pattern was observed in the antibody-identification panel (**FIGURE 2B**).

Primarily, we suspected anti-D and anti-C antibodies. We performed sequential serial adsorption of patient serum with r'r' (dCe/dCe) and R2R2 (DcE/DcE) group-O RBCs in 2 separate test tubes at 37°C for 1 hour to exclude the possible presence of anti-G antibody. Adsorption of patient serum was performed with r'r' RBCs 3 times. Then the adsorbed

FIGURE 1. A, Blood group showing discrepancy in mother. B, Resolution of Blood Group Discrepancy.



serum was tested with r'r' and R2R2 RBC suspension. We observed no reaction with r'r' RBCs, reflecting the complete adsorption of anti-G or anti-G+C. There was also no reaction with R2R2 RBC suspension; thus, anti-D was ruled out (**FIGURE 3**).

Similarly, we tested the adsorbed serum of R2R2 RBCs 3 times against R2R2 and r'r' RBC suspension. Here, also, no reaction with R2R2 RBC suspension indicates complete adsorption of anti-G or anti-G+D. Anti-C was excluded because there was no r'r' RBC suspension reaction with adsorbed serum (**FIGURE 3**). Acid elution was performed via the Gamma Elu-Kit II (Immucor Inc.). We tested eluate of the first adsorbed serum specimens of r'r' and R2R2 RBCs against antibody-screening-reagent RBCs. The presence of the reaction pattern of anti-D+C with antibody-screening-reagent RBCs implies the existence of anti-G antibodies (**FIGURE 3**).

The titre of the serum from the mother with r'r' RBCs was 64. We noted IgM and IgG specificities of the antibody after DTT (dithiothreitol, 0.01 M) treatment of the serum from the mother. The results from the direct antiglobulin test (DAT) of the baby were 3+ and with IgG specificity. The blood group of the baby, a boy, was O-positive. Further, cold acid elution of the RBCs of the neonate was performed; the eluate showed a pattern of anti-D and anti-C. The baby had pathological jaundice, with total serum bilirubin of 7.3 mg/dL at 6 hours after birth and was treated with a double dose of phototherapy for 24 hours. The total serum bilirubin was 14.1 mg/dL at 72 hours after birth and 14.8 mg/dL at 96 hours after birth; at that point, mother and baby were discharged from the hospital.

Discussion

D antigen is the most immunogenic Rh antigen; it produces anti-D antibodies in Rh D-negative pregnancy. To provide anti-D prophylaxis, one must exclude anti-D in the presence of anti-G antibodies. Anti-G causes discrepancy in reverse grouping. Additional reverse-grouping reactions are mainly due to unexpected antibodies in patient serum. These antibodies can be found via antibody screening and identification testing. After identifying antibody specificity, antigen-negative pooled cells of identified specificity are used to solve discrepancies in the reverse grouping. DTT treatment determines the nature of the antibody (ie, IgG or IgM). DTT disrupts the sulfide bonds of IgM antibodies and diagnoses underlying IgG antibodies. In our case individual, anti-G is of IgG and IgM type.

In a study by Palfi et al,⁵ in 27 women with alloimmunization, the combination of antibodies was anti-G + anti-C (14.8%), anti-D + anti-G (25.9%), anti-D + anti-C (11.1%), and anti-D + anti-C + anti-G (48.1%). Of 27 specimens, 24 (88.9%) of anti-G specimens existed in a mixture with anti-D and/or anti-C.⁵ Anti-G is present in approximately 30% of cases with combined anti-D + anti-C reactivity in serological testing.⁶ The basis of anti-G formation is that blood donors testing D-negative are not compulsively screened for antigens other than D antigens. It is rare to find incompatibility between RBC donor cells with a recipient who tests positive for C, E, or G antigen and negative for anti-D antigen. So, there is always a risk of anti-D alloimmunization when transfused to females of childbearing potential testing D-negative or patients with the rr phenotype testing D-negative who have received multiple D positive transfusions.⁷

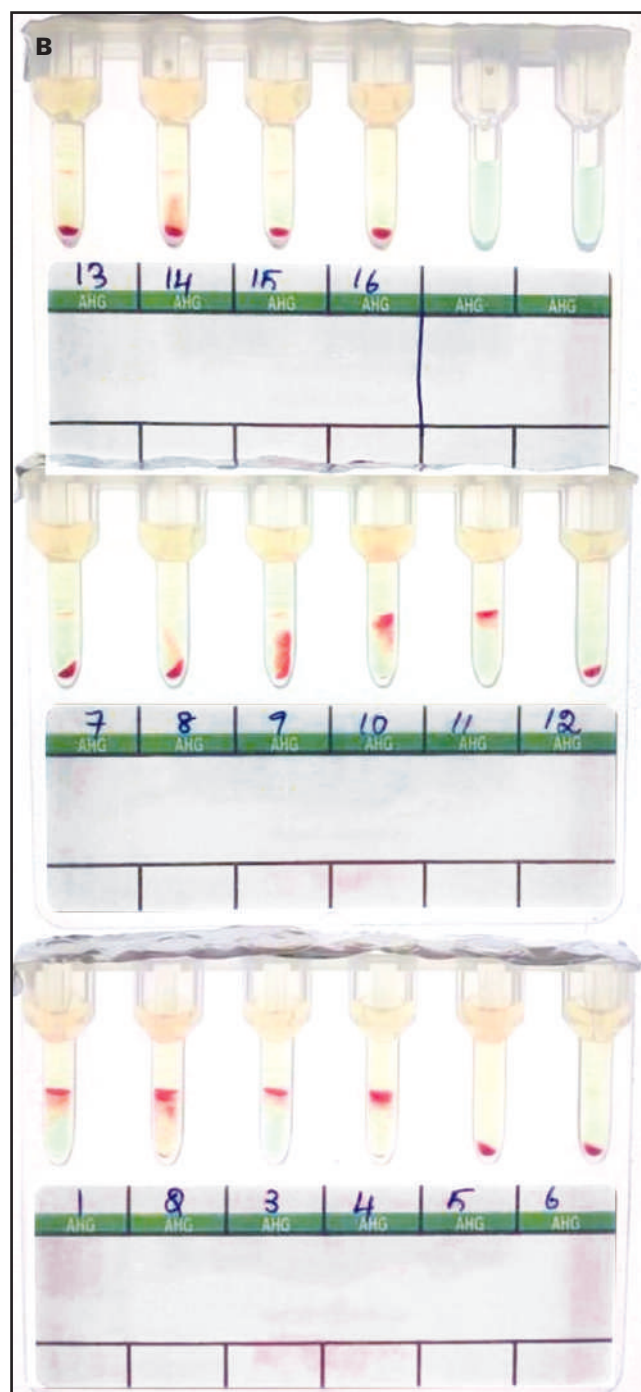
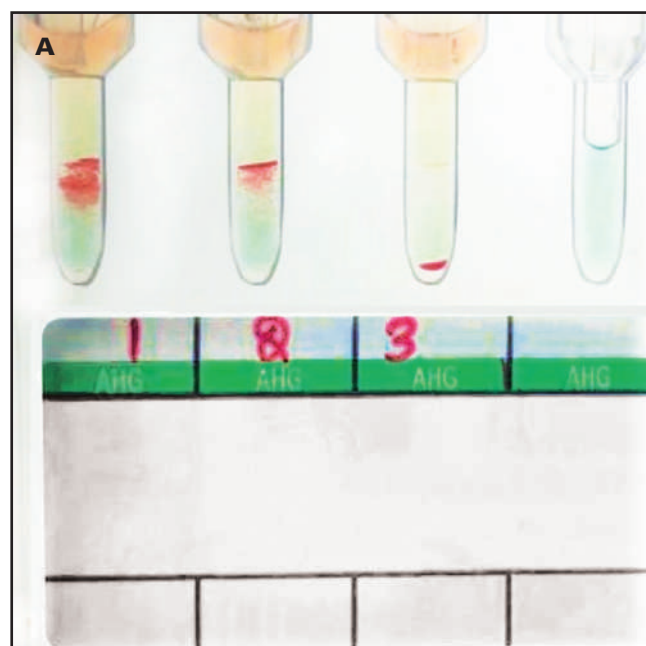
Differential adsorption and elution techniques are generally used to differentiate anti-G, anti-C, and anti-D due to feasibility.^{8,9} Rare rGr reagent cells can be used to detect anti-G in patients.¹⁰ Due to the unavailability of rGr reagent cells to identify anti-G, we performed an absorption elution study. R2R2 (DcE/ DcE) and r'r' (Ce/ce) RBCs should also be used for titration of anti-D and anti-C per the recommendation of Jernman et al.¹⁰ However, the inadequate amount of specimen material from the mother did not allow us to titrate with R2R2-phenotype RBCs.

Anti-G in the causation of HDFN mainly has been reported to be of mild intensity¹¹; occasionally, it is reported to be of moderate to severe intensity and may require intrauterine transfusion or exchange transfusion.^{7,10} RBCs for exchange transfusion should be D-, C-, and G-antigen negative. Due to the nonavailability of rGr reagent cells, we performed titration using rr RBC suspension. The condition of the patient was managed using phototherapy and did not require an exchange transfusion. In our case, the results from DAT of the baby were positive, and elution showed a pattern of anti-C. Differentiation of anti-D, anti-C, and anti-G by themselves, in combination with the eluate from the baby, was not performed due to the unavailability of a sufficient specimen. We counseled clinicians and the relatives of the mother and baby to monitor the presence of anti-D alloimmunization in any future pregnancies.

Conclusion

To determine whether anti-G antibody by itself or a combination of anti-G and/or anti-D antibody is present, anti-C, sequential

FIGURE 2. A, Antibody Screening. B, Antibody Identification.



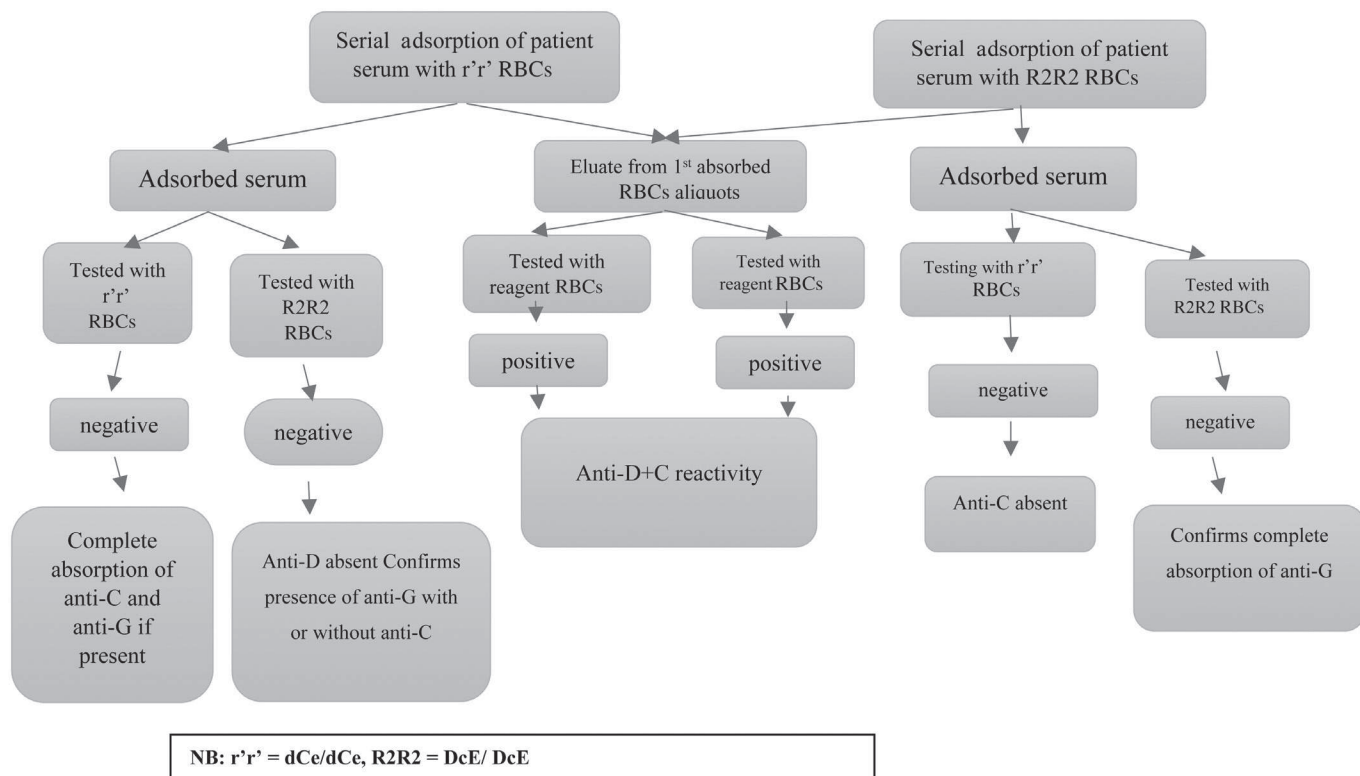
adsorption, and elution techniques are required. The presence of anti-D and anti-C can be masked by anti-G. The confirmation of the presence of anti-D is vital to prevent anti-D alloimmunization in pregnancy. It is necessary to identify anti-D in such circumstances so that timely RhIg prophylaxis can be administered to pregnant female patients who test Rh-D-negative. Hence, it is essential to find out whether anti-G is present by itself or in combination with another antibody or antibodies. In the case we discuss herein, the

mother should have been transfused with rr packed RBCs when indicated.

Acknowledgements

Dr Mukherjee is supported by grant no. 0000-0002-2272-5569; Dr Prakash by grant no. 0000-0001-6814-8106; Dr Sahu by grant no. 0000-0001-7901-3434; and Dr Mishra by grant no. 0000-0002-9977-5409.

FIGURE 3. Flowchart of serial adsorption and elution to identify anti-G antibody.



REFERENCES

- Allen FH Jr, Tippett PA. A new Rh blood type which reveals the Rh antigen G. *Vox Sang*. 1958;3(5):321-330. <https://doi.org/10.1111/j.1423-0410.1958.tb04013.x>
- Faas BHW, Beckers EAM, Simsek S, et al. Involvement of Ser103 of the Rh polypeptides in G epitope formation. *Transfusion*. 1996;36(6):506-511. <https://doi.org/10.1046/j.1537-2995.1996.36696269508.x>
- Qureshi H, Massey E, Kirwan D, et al; British Society for Haematology. BCSH guideline for the use of anti-D immunoglobulin for the prevention of haemolytic disease of the fetus and newborn. *Transfus Med*. 2014;24(1):8-20. <https://doi.org/10.1111/tme.12091>
- Makroo RN, Kaul A, Bhatia A, Agrawal S, Singh C, Karna P. Anti-G antibody in alloimmunized pregnant women: report of two cases. *Asian J Transfus Sci*. 2015;9(2):210-212. <https://doi.org/10.4103/0973-6247.162724>
- Palfi M, Gunnarsson C. The frequency of anti-C + anti-G in the absence of anti-D in alloimmunized pregnancies. *Transfus Med*. 2001;11(3):207-210. <https://doi.org/10.1046/j.1365-3148.2001.00306.x>
- Hadley AG, Poole GD, Poole J, Anderson NA, Robson M. Haemolytic disease of the newborn due to anti-G. *Vox Sang*. 1996;71(2):108-112. <https://doi.org/10.1046/j.1423-0410.1996.7120108.x>
- Chen J, Liu F. A case of mild HDFN caused by anti-C, anti-D, and anti-G: diagnostic strategy and clinical significance of distinguishing anti-G from anti-D and anti-C. *Transfus Apher Sci*. 2020;59(1):102602. <https://doi.org/10.1016/j.transci.2019.06.027>
- Das S, Shastry S, Murugesan M, B PB [sic], Shastry S. What is it really? Anti-G or Anti-D plus Anti-C: clinical significance in antenatal mothers. *Indian J Hematol Blood Transfus*. 2017;33(2):259-263. <https://doi.org/10.1007/s12288-016-0729-0>
- Huber AR, Leonard GT, Driggers RW, Learn SB, Gilstad CW. Case report: moderate hemolytic disease of the newborn due to anti-G. *Immunohematology*. 2006;22(4):166-170.
- Jernman R, Stefanovic V, Korhonen A, et al. Case report: severe hemolytic disease of the fetus and newborn due to anti-C+G. *Immunohematology*. 2015;31(3):123-127.
- Cash K, Brown T, Strupp A, Uehlinger J. Anti-G in a pregnant patient. *Transfusion*. 1999;39(5):531-533. <https://doi.org/10.1046/j.1537-2995.1999.39050531.x>

Evusheld, a SARS-CoV-2 spike protein–directed attachment inhibitor, appears in serum protein electrophoresis and immunofixation: a case study

Sumit K. Shah, MD¹, and Hoda A. Hagrass, MD, PhD¹

¹Department of Pathology, University of Arkansas for Medical Sciences, Little Rock, AR, US Corresponding author: Hoda Hagrass; Hhagrass@uams.edu, hudahagrass@gmail.com

Key words: multiple myeloma; interferences; monoclonal therapy antibodies; immunofixation; electrophoresis.

Abbreviations: SPE, serum protein electrophoresis; IFE, immunofixation; MM, multiple myeloma; TmAbs, therapeutic monoclonal antibodies; Ig, immunoglobulin

Laboratory Medicine 2023;54:e201–e203; <https://doi.org/10.1093/labmed/lmad085>

ABSTRACT

Serum protein electrophoresis (SPE) and immunofixation (IFE) assays are commonly used to diagnose and monitor patients with multiple myeloma (MM).

Identifying analytical interferences in SPE and IFE caused by therapeutic monoclonal antibodies (tmAbs) can be challenging. Here we report the case of a 72-year-old male with a long history of relapsed immunoglobulin (Ig)G kappa MM. A follow-up SPE showed the original peak plus 2 additional cathode peaks. Immunofixation was ordered as a reflex test to investigate the new peaks that showed initial patient monoclonal IgG kappa in addition to 2 restricted bands of the IgG kappa type. Therapeutic monoclonal antibody interference was suspected and the patient's chart was reviewed. The patient was not on any antimyeloma monoclonal antibody therapy. However, preexposure prophylaxis therapeutic monoclonal antibodies tixagevimab plus cilgavimab (Evusheld) for severe acute SARS-CoV-2 was administered approximately 45 minutes before sample collection, which led to the identifiable spikes and correlated bands. After 2 days, the IgG kappa bands disappeared, confirming this therapy's effect on SPE and IFE. Therefore, clinical pathologists should be aware of when providers prescribe new monoclonal antibody therapy and become familiar with the position of commonly prescribed (tmAbs) therapies at their institutions.

Clinical History

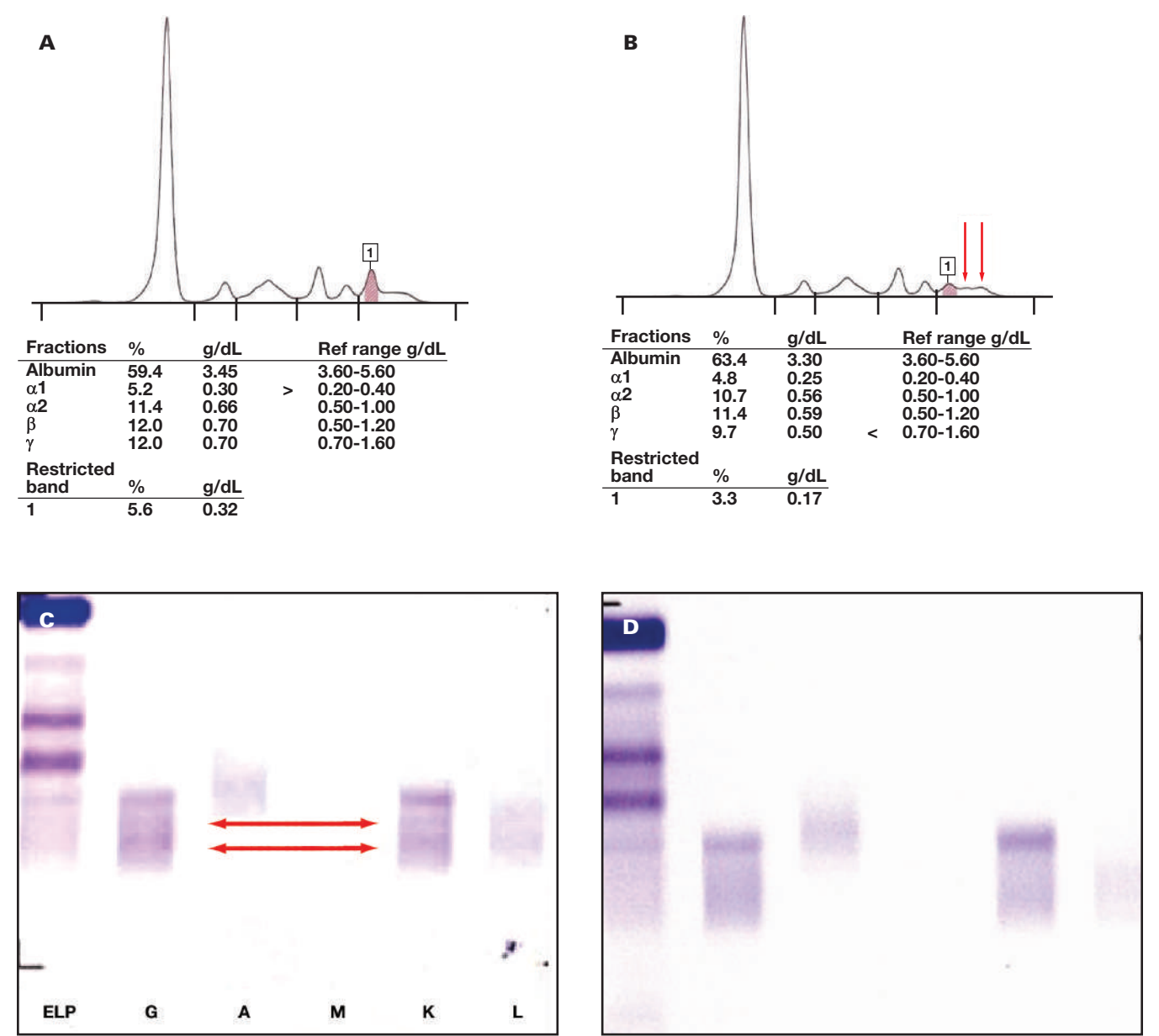
A 73-year-old male was followed for a medical history of relapsed immunoglobulin (Ig)G kappa multiple myeloma (MM) who was being managed and maintained on chemotherapy and immunosuppressants. He was diagnosed with MM in August 2013 and was initially treated with Velcade, Revlimid, and dexamethasone (VRD). He presented again in March 2016 with a biochemical relapse. At that point, he was prescribed the VDT-PACE regime (bortezomib, dexamethasone, thalidomide, cisplatin, doxorubicin, cyclophosphamide, and etoposide) and stem-cell collection for autologous stem-cell transplant in May 2016. However, the patient did not undergo an autologous stem-cell transplant as he had achieved clinical remission. He continued the VRD regimen with dose adjustments due to neuropathy as an adverse treatment effect. He maintained a zero M-protein by protein electrophoresis and immunofixation until August 2019, when he had an indolent relapse, and the M-protein level was 0.1 g/dL. The M-protein level fluctuated and rose to 0.4 g/dL in September 2019 (**FIGURE 1A**) and 0.2 g/dL in November 2019. He was switched to daratumumab/Pomalyst in early 2020 with minimal improvement in idle relapse status.

Clinical and Laboratory Data

The patient underwent an autologous stem-cell transplant in 2021 and has been on carfilzomib, lenalidomide, and dexamethasone (KRD) maintenance therapy since then. His M-protein level was 0.3 in the middle of 2021. This patient recently received a combination of SARS-CoV-2 spike protein-directed attachment inhibitor monoclonal antibody. The pathologist found 2 unusual peaks in the serum protein electrophoresis (SPE) approximately 45 minutes postadministration (**FIGURE 1B**) and ordered immunofixation (IFE), which showed 2 additional restricted bands along with the patient's original M-protein (**FIGURE 1C**).

On further investigation and after chart review, we discovered that the interference was due to Evusheld, which is a combination of tixagevimab with cilgavimab used for preexposure prophylaxis against SARS-CoV-2 infection (COVID-19) for immunocompromised populations. The peaks and the restricted bands disappeared in the subsequent specimen collection (**FIGURE 1D**) (after 2 days). This interference has been found in several other patients when the specimens were collected within 90 minutes of drug administration.

FIGURE 1. Serum protein electrophoresis (SPE) and immunofixation (IFE). **A:** SPE showing the original M-protein position. **B:** SPE showing the original M-protein plus the 2 additional peaks from therapy interference. **C:** IFE showing the original M-protein position plus the 2 additional bands from therapy interference. **D:** IFE showing the original M-protein position only after 2 days.



Discussion

Electrophoretic techniques such as SPE and IFE are commonly used for diagnosis and assess therapeutic responses in patients with MM. Although therapeutic monoclonal antibodies (tmAbs) have been in use for several decades, a relatively recent clinical trial involving siltuximab for the treatment of MM was the first instance when interference with SPE and IFE results was recognized.¹ Identifying analytical interference in SPE and IFE results introduced by exposure to tmAbs can be challenging. Humanized IgG1 κ monoclonal antibodies such as siltuximab, daratumumab, and elotuzumab can all produce a spike in concentrations up to 1 g/L.¹ For example, daratumumab, a frequently used monoclonal antibody that targets CD38 causing analytical inference, is now a well-documented phenomenon.^{2,3}

Global vaccinations against the SARS-CoV-2 infections have been used to control the pandemic. However, certain immunocompromised patients may not be able to mount an appropriate immune response to the vaccines and require additional prophylactic measures.⁴ Therapeutic monoclonal antibodies can provide rapid immunoprophylaxis against certain infections irrespective of the immune system status.⁵ However, they can produce interference in SEP and IFE results in patients with plasma cell neoplasms.⁶ To the best of our knowledge, the case we presented is the first ever documentation of analytic interference of tixagevimab with cilgavimab administered for preexposure prophylaxis for COVID-19.

The tixagevimab/cilgavimab combination has been used to prevent COVID-19 infection in immunocompromised populations.

Both are recombinant human IgG monoclonal antibodies that prevent the SARS-CoV-2 virus from entering the cells and causing infection. They simultaneously bind to the receptor-binding domain of the spike protein on the virus. This prevents the interaction of the virus with the angiotensin-converting enzyme 2 receptor, inhibiting it from attaching to the cells and getting activated.⁶ A recent study examined the analytical interference of the tixagevimab/cilgavimab combination using serum samples from patients with hypogammaglobulinemia and normal globulin levels. The serum samples were spiked with tixagevimab and/or cilgavimab at 1 times and 10 times Cmax (maximum drug serum concentration after administration). Saline was used as a negative control. Serum drug concentrations were measured using standard manufacturer protocols for the SPIFE 3000 analyzer (Helena Laboratories). They reported no increase in serum immunoglobulin levels.³ We use a different system, the Capillarys 3 TERA electrophoresis system (Sebia), which may have a lower limit of detection. This was proved when we verified with our capillary instrument that we could measure any peaks down to 0.05 g/dL.

Other parameters could also explain the discrepancy between the 2 assays, such as low M-protein concentrations, hypogammaglobulinemia background, and M-protein central gamma migration.⁷

The growing list and expanding use of tmAbs poses a problem for clinical pathologists and oncologists with interpreting SPE and IFE results for patients with plasma cell neoplasms. The tmAb artifact can be detected in patients taking this kind of therapy, which affects the interpretation of SPE/IFE results and subsequently can affect the monitoring of the patients with plasma cell neoplasms. Therefore, clinical pathologists should be aware of the position of commonly prescribed tmAbs at their institutions. Also, oncologists should be aware of the potential false-positive results. Immunofixation is more sensitive than SPE to distinguish tmAb from M-protein. Care must be taken to follow the patients on monoclonal antibody therapy with IFE and SPE, and not SPE alone.

Conclusion

It is impossible to avoid interference from tmAbs on electrophoretic assays. Laboratory personnel should be conscious of this phenomenon, as misinterpretation can lead to significant clinical consequences. A note from the pharmacist each time a plasma cell neoplasm patient receives tmAb treatment may also help raise awareness and identify artifactual M-protein spikes. At the same time, continuous communication between the pathologists and the clinical team may help create awareness of this phenomenon and prevent adverse clinical outcomes for patients.

REFERENCES

1. McCudden CR, Jacobs JFM, Keren D, Caillon H, Dejoie T, Andersen K. Recognition and management of common, rare, and novel serum protein electrophoresis and immunofixation interferences. *Clin Biochem.* 2018;51(1):72-79. <https://doi.org/10.1016/j.clinbiochem.2017.08.013>
2. Aydin O, Aykas F. Therapeutic monoclonal antibody interference in monoclonal gammopathy monitoring: a denosumab experience. *Lab Med.* 2023;54(3):e95-e97. <https://doi.org/10.1093/labmed/lmac129>
3. Baloda V, McCreary EK, Gosicki BK, Shurin MR, Wheeler SE. Tixagevimab plus cilgavimab does not affect the interpretation of electrophoretic and free light chain assays. *Am J Clin Pathol.* 2023;159(1):10-13. <https://doi.org/10.1093/ajcp/aqac137>
4. Pires SM, Wyper GMA, Wengler A, et al. Burden of disease of COVID-19: strengthening the collaboration for national studies. *Front Public Health.* 2022;10:907012. <https://doi.org/10.3389/fpubh.2022.907012>
5. Levin MJ, Ustianowski A, De Wit S, et al, PROVENT Study Group. Intramuscular AZD7442 (tixagevimab-cilgavimab) for prevention of Covid-19. *N Engl J Med.* 2022;386(23):2188-2200. <https://doi.org/10.1056/NEJMoa2116620>
6. Martin JC. tixagevimab-cilgavimab: COVID-19 pre-exposure prophylaxis. *Clin J Oncol Nurs.* 2022;26(5):479-482. <https://doi.org/10.1188/22.CJON.479-482>
7. Jacobs JFM, Turner KA, Graziani MS, et al. An international multi-center serum protein electrophoresis accuracy and M-protein isotyping study. Part II: limit of detection and follow-up of patients with small M-proteins. *Clin Chem Lab Med.* 2020;58(4):547-559. <https://doi.org/10.1515/cclm-2019-1105>

Utilization of an immunochromatographic lateral flow assay for rapid detection of carbapenemase production in gram negative bacilli

Emily Sullivan, MS¹, Maria D. Macias Jimenez, MS², Nicholas M. Moore, PhD^{1,2,3,✉}

¹Department of Medical Laboratory Science, Rush University, Chicago, IL, US, ²Department of Pathology, and ³Division of Infectious Diseases, Department of Internal Medicine, Rush University Medical Center, Chicago, IL, US Corresponding author: Nicholas M. Moore; nicholas_moore@rush.edu

Key words: antimicrobial resistance; carbapenemase; gram negative bacilli, rapid diagnostics.

Abbreviations: LFA, lateral flow assay; GNB, gram negative bacilli; AST, antimicrobial susceptibility testing; mCIM, modified carbapenem inactivation method; CLSI, Clinical and Laboratory Standards Institute; PPA, positive percent agreement; NPA, negative percent agreement; PCR, polymerase chain reaction; eCIM, EDTA-carbapenem inactivation method; MIC, minimal inhibitory concentration

Laboratory Medicine 2023;54:e204-e206; <https://doi.org/10.1093/labmed/lmad090>

ABSTRACT

Background: Rapid detection of carbapenemase production in gram negative bacilli has important treatment considerations.

Objective: We evaluated a lateral flow assay (LFA) for carbapenemase production compared with molecular detection of 5 (*bla*_{KPC}, *bla*_{NDM}, *bla*_{VIM}, *bla*_{IMP}, and *bla*_{OXA-48}) carbapenemase genes.

Methods: A total of 218 carbapenem nonsusceptible strains, including species of Enterobacterales, *Pseudomonas aeruginosa* isolated from clinical cultures were tested using the Cepheid Xpert Carba-R assay and the NG Biotech Carba-5 lateral flow immunoassay.

Results: Overall agreement with LFA was 98.2% with accuracy for each target >99% compared with polymerase chain reaction. Results were available within 15 minutes compared with 1 hour for molecular detection.

Conclusion: The use of accurate, rapid diagnostics complements antimicrobial stewardship programs.

Introduction

Antimicrobial resistance is an ever-growing threat to the global public health. Carbapenemase-producing Enterobacterales are 1 of the most critically concerning antimicrobial-resistant pathogens. In 2019, antibiotic-resistant bacteria and fungi caused more than 2.8 million infections and 35,000 deaths within the United States alone.¹ Two additional urgent threats include carbapenem-resistant *Acinetobacter* species and carbapenem-resistant *Pseudomonas aeruginosa*.¹ Although there are multiple mechanisms of carbapenem resistance, resistance due to enzymatic hydrolysis is of particular concern. Organisms that encode carbapenemases, coupled with other antimicrobial resistance (AMR) genes, can express an extremely drug-resistant phenotype making these infections difficult to treat.^{2,3} Five of the most common carbapenemase enzymes identified in clinical isolates are *bla*_{KPC}, *bla*_{NDM}, *bla*_{VIM}, *bla*_{IMP}, and *bla*_{OXA-48}.

Accurate testing methods are crucial to identify gram-negative bacilli (GNB)-expressing carbapenemases. This is usually done through a combination of cultured-based methods coupled with phenotypic antimicrobial susceptibility testing (AST), which is then confirmed with a molecular assay or additional phenotypic testing, for example, the modified carbapenem inactivation method (mCIM). There are, however, some practical issues with some of these testing methods. Culture methods are usually cost-effective but have slow turnaround times and are less sensitive. Molecular methods usually have faster turnaround times along with high sensitivity and specificity but are more expensive and may require more training and expertise to perform.⁴

In this study, we sought to evaluate the performance and diagnostic accuracy of the NG-Test Carba 5 (NG Biotech), an immunochromatographic lateral flow assay for the rapid detection and differentiation of 5 carbapenemases directly from isolated colonies grown in culture.

Methods

We evaluated diagnostic accuracy and analytic performance using well-characterized isolates that had been identified in clinical cultures from Rush University Medical Center in Chicago, IL. Clinical culture sources included bloodstream, urine, respiratory, and wound/tissue specimens. We did not include surveillance isolates. Isolates were tested fresh or passaged twice from frozen stocks on to trypticase soy agar with 5% sheep blood (Remel) and incubated overnight at 37°C in ambient air.

Routine AST was performed using the NM56 panel on the MicroScan WalkAway (Beckman Coulter). Representative colonies from cultures containing a carbapenem nonsusceptible organism based on clinical breakpoints established by the Clinical and Laboratory Standards Institute (CLSI) (meropenem and imipenem imipenem minimal inhibitory concentration (MIC) ≥ 2 $\mu\text{g/mL}$; ertapenem MIC ≥ 1 $\mu\text{g/mL}$ for Enterobacterales, and meropenem and imipenem MIC ≥ 4 $\mu\text{g/mL}$ for *P. aeruginosa* and *Acinetobacter* spp.) were selected and tested for phenotypic production of a carbapenemase in accordance with the NG-Test Carba 5 assay package insert.⁵ Briefly, 150 μL of extraction buffer was dispensed into microtubes provided with the kit. Three representative colonies were re-suspended by vortexing the suspension for 5 to 10 seconds. Then 100 μL of the sample mixture was added to the sample well on the test cassette and incubated for 15 minutes at room temperature. Results were interpreted only if the valid internal control line appeared. We constructed 2×2 data tables to determine the positive percent agreement (PPA) and negative percent agreement (NPA) for each carbapenemase target using the Xpert Carba-R assay (Cepheid) as the comparator.⁶ Measures of agreement using the kappa statistic were determined based on the method of Landis.⁷ Analyses were performed using Prism 9 (GraphPad).

Results

In this single center study, we tested 218 GNB isolates using the NG-Test Carba 5 assay. The majority of isolates (85%) were Enterobacterales, mostly *Klebsiella pneumoniae* ($n = 84$) and *Escherichia coli* ($n = 59$), along with 35 nonfermenting GNB. There were 132 carbapenemase-producing organisms and 86 carbapenem-resistant, non-carbapenemase-producing isolates in total. Two isolates, 1 *E. coli* and 1 *K. pneumoniae*, expressed multiple carbapenemases.

There were 128 carbapenemases detected using the LFA, with the majority being identified as *bla*_{KPC}. Overall, the PPA and NPA was 97.0% (95% CI 92.4%-99.2%) and 100% (95% CI 95.8%-100%), respectively. Analytic performance of the device stratified by each carbapenemase is shown in TABLE 1. The PPA for each target was above 92% for all targets except for *bla*_{IMP}, which had a PPA of 82.3% (a single false positive). This false-positive isolate was positive for *bla*_{IMP} using a different polymerase chain reaction assay (data not shown). We attribute the reduced performance to the number of isolates included that were positive for *bla*_{IMP} by molecular testing. Notably, the test showed excellent NPA (100% for all targets) when compared against the Xpert Carba-R assay. Overall agreement of the NG-Test Carba-5 assay was 98.2% (95% CI 95.3%-99.5%), and the LFA had an almost perfect level of agreement ($\kappa = 0.962$, 95% CI .925-0.999) when compared with results obtained by molecular testing.

There was a single isolate that yielded an invalid result (internal control line not present) with the LFA on initial testing. This was a very mucoid isolate of *K. pneumoniae* that on repeat testing yielded a valid internal control and target test results. We hypothesize that the colony consistency was the cause of the initial invalid result and that insufficient biomass was gathered on the loop to resuspend in the extraction buffer reagent.

There were 4 samples that yielded discordant test results between the NG-Test Carba-5 and the Xpert Carba-R assay. In all instances, a carbapenemase gene was detected using the Xpert assay but the lateral flow assay was reported as negative for all targets. Internal controls on each cassette were valid on testing.

We also compared the direct test cost and setup demands. The list price for 1 NG-Test Carba 5 kit is \$473, with a direct cost per test of \$23.65. The list price for 1 kit of the Xpert Carba-R is \$590, with a direct cost per test of \$59. These prices do not include other fixed or variable costs for performing testing, such as the price of a GeneXpert system or personnel costs. Estimated hands-on time for setting up a sample for the NG-Test Carba 5 and the Xpert Carba-R were the same at approximately 2 minutes per sample. Time to detection on the GeneXpert is 48 minutes from assay initialization, whereas the results with the LFA device were available within 15 minutes of adding the sample to the test cassette. To the best of our knowledge, this is the fastest phenotypic test for carbapenemase detection and differentiation available.

Discussion

Carbapenem resistance in GNB represents a growing problem for health care facilities and the public health. New combination beta-lactam/beta-lactamase inhibitor agents are only effective against certain classes of carbapenemases.³ Therefore, accurate detection and identification of carbapenemase production in GNB is critical for patient management.

There is no single approach for carbapenemase detection in GNB recovered from clinical cultures. One commonly used phenotypic approach that confirms carbapenemase production is the mCIM⁸ and the EDTA-carbapenem inactivation method (eCIM),⁹ which differentiates metallo-beta-lactamases from serine carbapenemases. Both the mCIM and eCIM can be performed with relative ease in most clinical microbiology laboratories and both are recommended by the CLSI for carbapenemase detection/confirmation.¹⁰ These assays have performed well in studies examining their performance compared to rapid molecular diagnostics or culture plus sequencing for Enterobacterales and *Pseudomonas aeruginosa*.^{11,12} Despite the relative ease in which the mCIM and eCIM can be performed, the main limitation of these methods is the additional overnight incubation requirement. The mCIM has not been endorsed by the

TABLE 1. Performance of the NG-Test Carba 5 assay stratified by carbapenemase

Carbapenemase gene	TP	FP	FN	TN	Positive percent agreement	95% CI	Negative percent agreement	95% CI	Kappa statistic	95% CI
<i>bla</i> _{IMP}	5	0	1	212	83.3	35.9, 99.6	100.0	98.3, 100.0	0.907	0.725, 1.000
<i>bla</i> _{KPC}	70	0	1	147	98.6	92.4, 99.9	100.0	97.5-100.0	0.990	0.969, 1.000
<i>bla</i> _{NDM}	26	0	1	191	96.3	81.0, 99.9	100.0	98.1-100.0	0.967	0.922, 1.000
<i>bla</i> _{OXA-48}	17	0	0	201	100.0	80.5, 100.0	100.0	98.2, 100.0	1.000	1.000, 1.000
<i>bla</i> _{VIM}	12	0	1	205	92.3	64.0, 99.8	100.0	98.2, 100.0	0.958	0.875, 1.000
Overall	128	0	4	86	97.0	92.4, 99.2	100.0	95.8, 100.0	0.962	0.925, 0.999

FN, false negative; FP, false positive; TN, true negative; TP, true positive

CLSI for *Acinetobacter* species due to reduced sensitivity and specificity that has been described.¹³ Furthermore, these phenotypic tests do not specify which carbapenemase is expressed. Another rapid phenotypic test is the Rapidec Carba NP. This test performs well and is easier to setup than the traditional Carba NP but also fails to specify the carbapenemase detected.¹⁴ Results are available for this test within 2 hours.

With multiple enzymes capable of yielding a resistant phenotype and with targeted antimicrobial therapy options available, identifying the carbapenemase present in a carbapenem-resistant isolate is essential to guide antimicrobial therapy decisions. Molecular testing options are available that can differentiate among the most common carbapenemase enzymes that may be produced. These assays display good analytic performance¹⁵ but require analyzers, molecular expertise to implement, and are more expensive than phenotypic alternatives.

The NG-Test Carba 5 assay is a lateral flow immunochromatographic assay that can detect and differentiate between 5 of the most common carbapenemases frequently identified in clinical isolates. Our results of the performance of the NG-Test Carba 5 are similar to those of Jenkins and colleagues¹⁶ in their multicenter evaluation of the assay. Other lateral flow assays have shown similar performance, although 1 assay, the RESIST-4, does not test for the presence of *bla*_{IMP}.¹⁷ As we and others have shown, the NG-Test Carba 5 is simple and rapid to perform, making it the fastest test currently available for detection and differentiation of clinically relevant carbapenemases.

In settings of low prevalence, or where molecular equipment or expertise is limited, this assay could fill a critical niche in the detection and differentiation of clinically relevant carbapenemases from specimens. Moreover, this test can be used to help guide antimicrobial therapy decisions while awaiting formal AST results with combination beta-lactam/beta-lactamase inhibitor (βL/βLI) if such testing is not routinely performed in the local microbiology laboratory.

Our study does have limitations. First, this was a single center study. Another limitation is the diversity of carbapenemases present in our isolates. In this study, the majority of carbapenemases produced by isolates was *bla*_{KPC}, and only a limited number of isolates were positive for *bla*_{IMP}. Therefore, the results may not be widely generalizable in areas where *bla*_{KPC} is not the predominant carbapenemase. Finally, we did not perform sequencing analyses of isolates to determine whether false negatives with NG-test Carba 5 were due to certain subtypes or mutations that might affect antibody binding. Additional studies investigating LFA negative/PCR positive carbapenemase discrepant results are needed.

In conclusion, the NG Carba-5 assay is a rapid lateral flow device that is both easy to perform and interpret and displays excellent performance in detecting carbapenemases in GNB isolates recovered in culture. Use of this test in settings without molecular capabilities would be prudent given the increasing prevalence and risk for worse outcomes due to improper treatment.

Acknowledgments

The authors thank the technical staff in Rush Medical Laboratories that performed the initial clinical culture testing.

REFERENCES

- Centers for Disease Control and Prevention. 2019. *Antibiotic Resistance Threats in the United States, 2019*. Services Atlanta, GA: US

Department of Health and Human Services: CDC. www.cdc.gov/DrugResistance/Biggest-Threats.html.

- Rodriguez-Bano J, Gutierrez-Gutierrez B, Machuca I, Pascual A. Treatment of infections caused by extended-spectrum-beta-lactamase-, AmpC-, and carbapenemase-producing Enterobacteriaceae. *Clin Microbiol Rev*. 2018;31(2):e00079-e00017. doi:10.1128/CMR.00079-17
- Tamma PD, Aitken SL, Bonomo RA, Mathers AJ, van Duin D, Clancy CJ. Infectious Diseases Society of America 2022 guidance on the treatment of extended-spectrum beta-lactamase producing Enterobacterales (ESBL-E), carbapenem-resistant Enterobacterales (CRE), and *Pseudomonas aeruginosa* with difficult-to-treat resistance (DTR-P. aeruginosa). *Clin Infect Dis*. 2022;75(2):187-212. doi:10.1093/cid/ciac268
- Viau R, Frank KM, Jacobs MR, et al. Intestinal carriage of carbapenemase-producing organisms: current status of surveillance methods. *Clin Microbiol Rev*. 2016;29(1):1-27. doi:10.1128/CMR.00108-14
- NG Biotech. 2019. *NG-Test Carba 5 package insert*. France: Guipry.
- Traczewski MM, Carretto E, Canton R, Moore NM, Carba RST. Multicenter evaluation of the Xpert Carba-R assay for detection of carbapenemase genes in gram-negative isolates. *J Clin Microbiol*. 2018;56(8):e00272-18. doi: 10.1128/JCM.00272-18.
- Landis JR, Koch GG. The measurement of observer agreement for categorical data. *Biometrics*. 1977;33(1):159-174.
- Pierce VM, Simner PJ, Lonsway DR, et al. Modified carbapenem inactivation method for phenotypic detection of carbapenemase production among Enterobacteriaceae. *J Clin Microbiol*. 2017;55(8):2321-2333. doi:10.1128/JCM.00193-17
- Sfeir MM, Hayden JA, Fauntleroy KA, et al. EDTA-modified carbapenem inactivation method: a phenotypic method for detecting metallo-beta-lactamase-producing Enterobacteriaceae. *J Clin Microbiol*. 2019;57(5):e01757-e01718. doi:10.1128/JCM.01757-18
- CLSI. 2022. *Performance Standards for Antimicrobial Susceptibility Testing*. 32nd ed. Wayne, PA: CLSI Supplement M100. Clinical and Laboratory Standards Institute.
- Tsai YM, Wang S, Chiu HC, Kao CY, Wen LL. Combination of modified carbapenem inactivation method (mCIM) and EDTA-CIM (eCIM) for phenotypic detection of carbapenemase-producing Enterobacteriaceae. *BMC Microbiol*. 2020;20(1):315. doi:10.1186/s12866-020-02010-3
- Gill CM, Lasko MJ, Asempa TE, Nicolau DP. Evaluation of the EDTA-modified carbapenem inactivation method for detecting metallo-beta-lactamase-producing pseudomonas aeruginosa. *J Clin Microbiol*. 2020;58(6):e02015-e02019. doi: 10.1128/JCM.02015-19.
- Simner PJ, Johnson JK, Brasso WB, et al. Multicenter evaluation of the modified carbapenem inactivation method and the Carba NP for detection of carbapenemase-producing *Pseudomonas aeruginosa* and *Acinetobacter baumannii*. *J Clin Microbiol*. 2018;56(1):e01369-e01317. doi: 10.1128/JCM.01369-17.
- Poirer L, Nordmann P. Rapidec Carba NP test for rapid detection of carbapenemase producers. *J Clin Microbiol*. 2015;53(9):3003-3008. doi:10.1128/JCM.00977-15
- Yoo IY, Shin DP, Heo W, Ha SI, Cha YJ, Park YJ. Comparison of BD MAX check-points CPO assay with Cepheid Xpert Carba-R assay for the detection of carbapenemase-producing Enterobacteriaceae directly from rectal swabs. *Diagn Microbiol Infect Dis*. 2022;103(3):115716. doi:10.1016/j.diagmicrobio.2022.115716
- Jenkins S, Ledeboer NA, Westblade LF, et al. Evaluation of NG-test Carba 5 for rapid phenotypic detection and differentiation of five common carbapenemase families: results of a multicenter clinical evaluation. *J Clin Microbiol*. 2020;58(7):e00344-e00320. doi:10.1128/JCM.00344-20
- Rosner S, Kamalanabhaiah S, Kusters U, Kolbert M, Pfennigwerth N, Mack D. Evaluation of a novel immunochromatographic lateral flow assay for rapid detection of OXA-48, NDM, KPC and VIM carbapenemases in multidrug-resistant Enterobacteriaceae. *J Med Microbiol*. 2019;68(3):379-381. doi:10.1099/jmm.0.000925

Impact of COVID-19 pandemic on accredited programs and graduates who sat for the American Society for Clinical Pathology–Board of Certification Examination: program directors' perspective

Dana Duzan, MLS(ASCP)^{CM1}, Karen Fong, M.Ed.¹, Vicki S. Freeman, PhD, MASCP, MLS(ASCP)^{CM}, SCCM, FAACC^{1,2}, Nancy Goodyear, PhD, MLS(ASCP)^{CM1,3}, Teresa S. Nadder, PhD, MLS(ASCP)^{CM1,4}, Amy Spiczka, MS, HTL(ASCP)^{CM}, SCT^{CM}, MBCM, CPHQ¹, Teresa Taff, MA, MLS(ASCP), SM(ASCP)^{CM1,5}, Patricia Tanabe, MPA, MASCP, MLS(ASCP)^{CM1}

¹American Society for Clinical Pathology Board of Certification, Chicago, IL, US
²University of Texas Medical Branch Department of Clinical Laboratory Sciences, Galveston, TX, US
³University of Massachusetts Lowell Department of Biomedical and Nutritional Sciences, Lowell, MA, USA
⁴Virginia Commonwealth University Department of Medical Laboratory Sciences, Richmond, VA, US
⁵Mercy Hospital St. Louis School of Clinical Laboratory Science, Aurora, MO, US
 Corresponding author: Karen Fong; karen.fong@ascp.org

Key words: programs; pandemics; impact; COVID-19; graduates; BOC.

Abbreviations: BOC, Board of Certification; PD, program director; ASCP, American Society for Clinical Pathology; NAACLS, National Accrediting Agency for Clinical Laboratory Science; ABHES, and Accrediting Bureau of Health Education Schools; CAAHEP, Commission on Accreditation of Allied Health Education Programs; MLT, Medical Laboratory Technician; MLS, Medical Laboratory Scientist; COVID-19 pandemic

Laboratory Medicine 2023;54:e207–e214; <https://doi.org/10.1093/labmed/lmad082>

ABSTRACT

Objective: Health professions education programs were severely affected by the COVID-19 pandemic at clinical and didactic training levels. The purpose for this American Society for Clinical Pathology–Board of Certification (BOC) study was to determine the impact of the COVID-19 pandemic on the graduates who sat for BOC certification in their respective professional disciplines from the perspective of program directors (PDs). A separate article will be published on the graduates' perspective.

Methods: A survey was sent to all PDs from the National Accrediting Agency for Clinical Laboratory Science, Accrediting Bureau of Health Education Schools, and Commission on Accreditation of Allied Health Education Programs, accredited programs whose graduates are certified by the BOC, to determine the impact of COVID-19 on healthcare graduates and education programs during the pandemic.

Results: A total of 201 PDs responded. All programs consistently reported that the pandemic had a negative impact on their students' BOC pass rate and scores. When asked what educational formats were used, all groups used virtual live lectures and recorded lectures. University programs were found to use more online student laboratories and simulation laboratory sessions than the hospital programs, affecting the psychomotor skills of their students.

Conclusion: The results indicated that the effects from the COVID-19 pandemic were related to the inherent differences between hospital and university programs. This study revealed that the pandemic affected university programs more than hospital programs.

Introduction

Health professions education programs were severely affected by the COVID-19 pandemic at clinical and didactic training levels. Beginning in March 2020, United States hospitals witnessed a massive increase in the number of patients needing specialized care and diagnostic laboratory testing, especially for COVID-19. The pandemic resulted in exhaustion of personnel, equipment, and financial resources in most medical facilities. The increased spread of COVID-19 also had major effects on the education systems, as these medical facilities were used as training sites for most health professional students, and social distancing restrictions affected didactic training.

Several studies have looked at how the pandemic affected the education of healthcare professionals.^{1–3} At the beginning of the pandemic, health professional programs moved quickly to online or other distance-learning solutions to lessen the spread of the virus.² A metanarrative found many programs that rapidly shifted to remote education tried to imitate the in-person classroom through video-conferencing (called emergency remote education or ERE).³ As the pandemic progressed, programs became more innovative, especially in the use of digital tools.⁴ This led to

increased workload for faculty who had to reorganize or redesign courses in a manner that would provide successful learning outcomes.²

In an international survey of medical students, the students reported “an overall significant negative impact of the COVID-19 pandemic on their undergraduate training”. However, when the students had an increase in clinical responsibilities, they were less likely to report a negative impact on training.⁵ Because this study included participants from 45 countries, not all countries had the same teaching resources, especially in terms of online, virtual availability.

A survey in pathology education⁶ discovered the pandemic caused a paradigm shift for teaching pathology residents. The study found both faculty and trainees perceived a decrease in the quality and effectiveness of the teaching and learning. This was most likely related to the learning curve necessary in the initial transition to virtual pathology laboratories and to technology limitations. Prior to the pandemic, few programs taught with digital photography, but this teaching modality has become more prevalent and is likely to remain.

A study at the Mayo Clinic⁷ found the addition of a virtual learning component to in-person teaching is practical and “makes life a little easier”. They found online learning may be relaxing for some but stressful for others. They also found programs that required a significant amount of hands-on training, such as phlebotomy and cytology, were more affected. All programs with clinical rotations saw a decrease in clinical rotation time, which was replaced with virtual learning.

The majority of the studies above called for more research into the pandemic’s impact on the education of health profession students, especially with online, virtual, and digital technologies. The purpose for this American Society for Clinical Pathology (ASCP) Board of Certification (BOC) study was to determine the impact of COVID-19 pandemic on the graduates who sat for the BOC certification in their respective professional disciplines from the perspective of PDs.

Methods

The ASCP BOC Research and Development Committee conducted 2 surveys to determine the impact of COVID-19 on healthcare graduates and education programs during the pandemic. One survey was sent to all PDs from National Accrediting Agency for Clinical Laboratory Science (NAACLS), Accrediting Bureau of Health Education Schools (ABHES), and Commission on Accreditation of Allied Health Education Programs (CAAHEP) accredited programs whose graduates are certified by the BOC. A second survey was sent to graduates who sat for the BOC examination from 2020 to the survey launch date in 2022. The surveys were distributed as electronic invitations via Key Survey (an online survey tool) on June 06, 2022. A reminder was sent on July 6, 2022, and the surveys were closed on October 11, 2022. A total of 180 graduates and 201 PDs responded. This article reports on the PDs’ responses. A separate article will report on the graduates’ responses.

Results

Demographics of Respondents

Of the PD respondents, 164 (82%) were from university programs (Medical Laboratory Technician [MLT], Medical Laboratory Scientist [MLS], others), and 35 (18%) were from hospital programs. The PDs represented 42 states and 8 distinct NAACLS/CAAHEP/ABHES accredited programs.

Altogether, MLS and MLT programs directors made up the majority of the respondents (87%), with more MLS PDs responding (MLS PD 49.8%; MLT PD 37.3%). The hospital PDs were from MLS (88.5%) and Phlebotomy (11.5%) programs. Note that MLT programs are considered a university program (ie, community college, technical college, college, etc). University programs responding to the survey in descending order of percentages included MLS (40.8%), MLT (45.7%), Cytology (3.7%), Histotechnician (3.7), Phlebotomy (3%), Technologist in Molecular Biology (1.8%), Histotechnologist (0.6%), and Pathologists’ Assistant (0.6%). Because of the low numbers (13%) of programs other than MLS and MLT responding, the data related to these other programs were collapsed for reporting purposes.

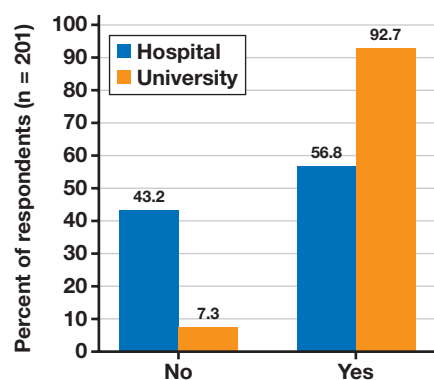
Effect of COVID-19 on Program Structure

Responses on how the programs classes were affected indicated that university programs were more likely to use an online format than hospital programs (92.7% vs 56.8%, respectively) with MLT slightly more likely than MLS programs (97.3% vs 83%, respectively). A smaller percentage (65.4%) of the other programs used an online format. In responses on what formats they used, all groups indicated they used virtual live lectures and recorded lectures, but the university programs were found to use more online student laboratories and simulation laboratory sessions than the hospital programs (FIGURES 1 and 2).

The effects of the pandemic were also measured using factors reflecting faculty effort. University programs were more likely to split up their classes into smaller cohorts to allow for social distancing, which caused additional teaching time for the faculty. Both types of program sites reported spending more time online. Faculty had to adjust their personal schedule to handle online or hybrid classes (FIGURE 3).

The effect of COVID-19 on nonclinical student learning laboratories was greater than that of the didactic portion of the programs, with a greater effect on university programs. Although no hospital programs cancelled their student laboratories, 15.2% of university programs’ laboratories were cancelled. More hospital programs reported no changes in their student (nonclinical) laboratory sessions (37.8%) vs university programs (11.6%). Other methods used to ensure student laboratories were provided included delaying or doubling up on the student laboratories at a later date, moving to an online format or replacing

FIGURE 1. Percentage of programs that moved to online format.



with simulation or other activities (FIGURE 4). It is interesting to note that because California requires clinical hours, programs in the state were able to justify continuing their face-to-face laboratories. Comments in the PD Voices box show how programs responded to the pandemic.

PD Voices—Student Laboratories

“Moved online for final weeks of Spring semester 2020; delayed start for Summer 2020 labs then doubled up when in-person allowed; resumed all in-person labs Fall 2020 with heightened PPE requirements.”

“We used an online format and delayed clinical Mar-May of 2020, and then went to a hybrid format with online lecture and in person lab/clinical from May 2020-Aug 2021. We were fully in person last academic year.”

“In early fall 2020, we divided the class into cohorts to accommodate safe distancing for in-person labs, but went back to fully online about six weeks into the semester. Knowing that was a possibility, we altered the scheduling for some labs to ensure that students got hands-on experience with as many techniques as possible.”

“Replaced with simulation or other activities during Spring and Summer Semesters of 2020”

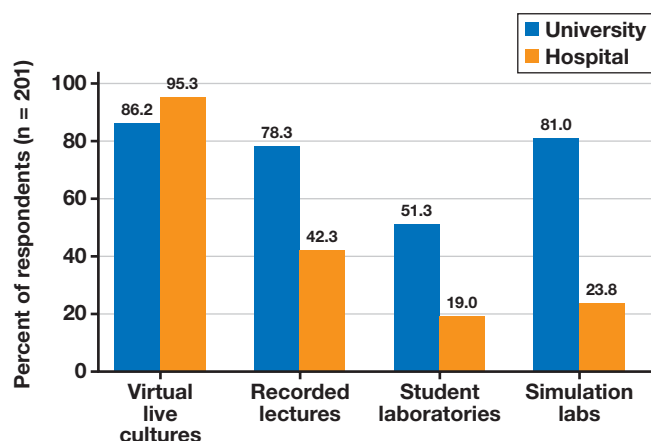
“Second year of pandemic was split into two labs with social distancing and increased precautions”

“We were off campus for 6 weeks. During that time we moved lab online, and also complemented with other activities. Once we were back on campus, we spent some extra time with slide sets.”

“In California all applied education hours (~1700) must be in a CLIA lab- no online or simulation hours may be counted toward training.”

Not only were nonclinical student laboratories affected by the pandemic, but clinical rotations were as well. Again, university programs were more affected than hospital programs. Both types of program sites reported delayed, cancelled, and shortened clinical rotations; but university programs saw a higher percentage of these effects. To provide clinical experiences, students were either placed at a different clinical site or the faculty replaced the experiences with simulations (FIGURE 5). Although all areas were affected, the universities had the most difficulty placing students in blood bank (64.6%) and microbiology (64.6%) rotations with hematology (51.8%) falling closely behind, whereas in hospital programs, chemistry (40.5%), hematology (40.5%), and blood bank (37.8%) rotations were the most affected.

FIGURE 2. Types of online formats utilized.



Effect of COVID-19 on Student Learning

From responses regarding which domains of learning were affected, university programs indicated they observed a larger effect on the psychomotor skill development of their students than hospital programs observed in their students.

However, both university and hospital programs reported an increased effect on the affective domain (ie, the attitudes and values) of their students. When comparing program types, programs other than MLS and MLT saw less of an effect in all domains (FIGURE 6A and B).

Some universities (10.6%) allowed programs to change their grading scale. One option was to offer a pass/fail option on student grades per university requirement. Other options included lowering the passing grade or modified laboratory component of the grade.

When asked whether student grades were affected, twice as many university programs as hospital programs reported a negative impact. A small percentage of university students actually showed a positive effect

FIGURE 3. Pandemic effect on program classes and faculty.

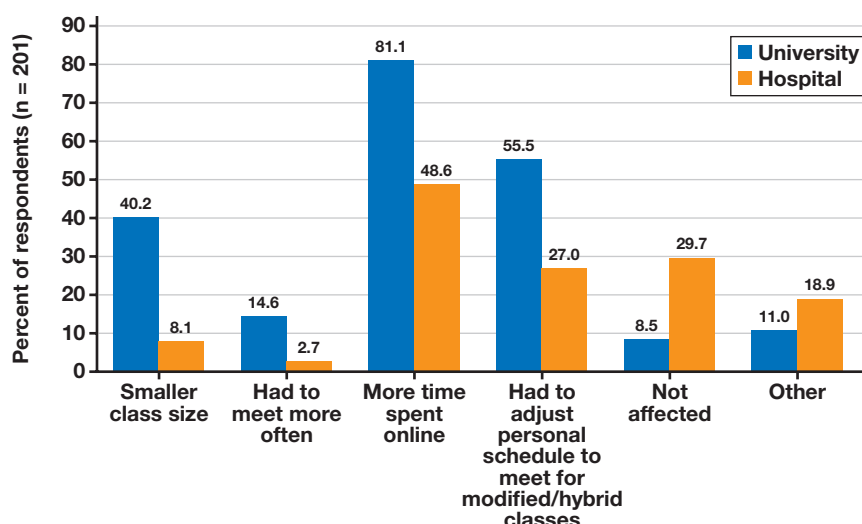
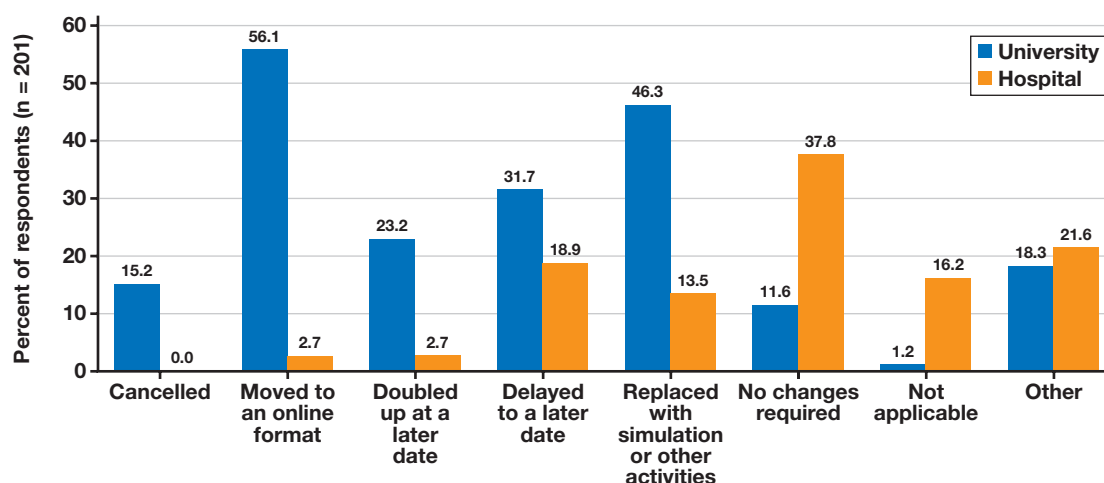
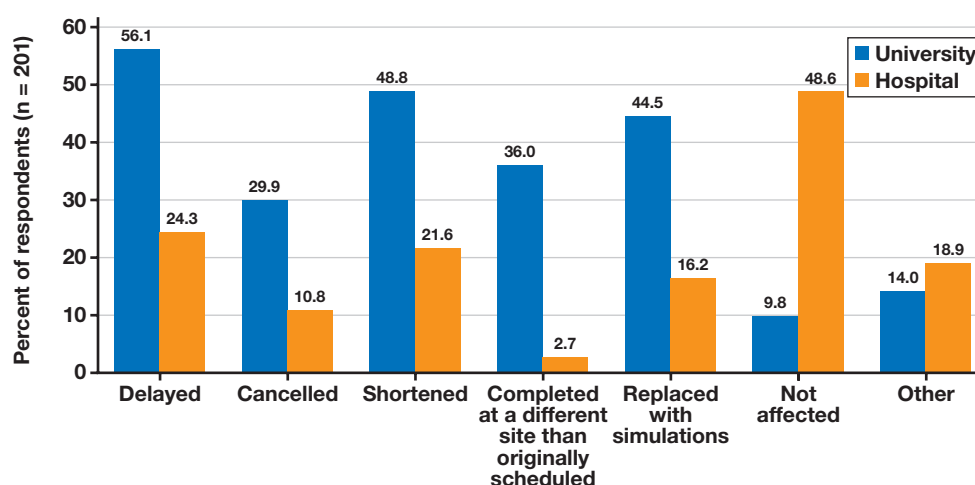


FIGURE 4. Effect of COVID-19 pandemic on student laboratories.**FIGURE 5.** Effect of COVID-19 pandemic on clinical rotations.

on their grades (FIGURE 7). No significant difference between the program types was noted.

PD Voices—Impact on Student Grades

“COVID was especially difficult for borderline students and poor test-takers who would have otherwise buoyed their grades with extra time at the scope - during the first year of the pandemic all rotations were cancelled and during the second there was very limited access to the lab to allow for screening practice. Students in the latter cohort had trouble acclimating to normal scope work and if they were not high performing in the early portion of the year it was difficult to predict how they would handle.”

“I actually think we did a good job handling the move to virtual lectures and labs one day each week. Each group of students (1st yr, 2nd yr, Web-blended, and PHB) were each on campus a different day of the week to avoid overlap. Some labs were successful in the virtual format, such as viewing growth on agar with the entire class at a time. Students’ grades were better, generally due to allowing more “hand-holding”, especially in the lab.”

“Regarding the question about did COVID impact student performance - interestingly some students did better by being at home for a few months and others did not, so it was a very personal type of response. Also - when

we resumed student labs, we limited the # of students so ran every lab twice - this took lots of schedule planning and extra instructor time. We also had to use a larger classroom so the PD spent many hours readjusting the schedule and trying to locate a room to use or use zoom to deliver live instruction”

“Some faculty saw higher grades than normal and had concerns about exam integrity with the online exams - there was no way to be sure students weren’t looking up answers. Our pass rate for the class of 2020 was the lowest in many years.”

Effect of COVID-19 on Students

University programs saw a higher effect of COVID on student retention than hospital programs, which affected student enrollment numbers. Universities reported that 20.1% of students took a leave of absence compared with 2.7% of students in hospital programs. University programs also saw a significantly higher number of students who withdrew from the program than hospital programs (32.3% vs 2.7%). When university programs were compared, MLT programs saw a higher number of students withdraw from the program than MLS programs (42.7% vs 14.0%). University students did have the option of

FIGURE 6. A. Learning domains affected by facility type. B. Learning domains affected by program type.

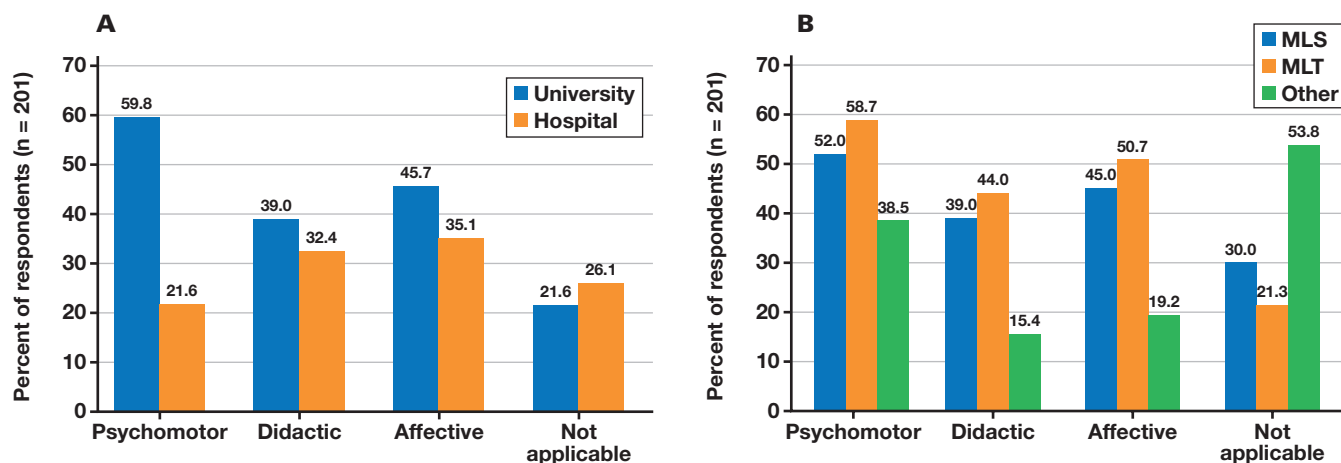
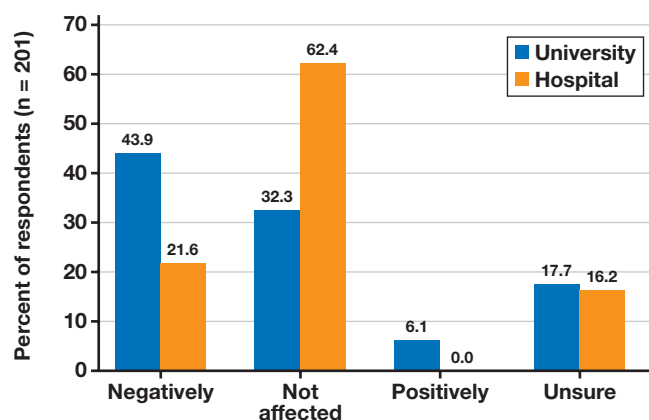


FIGURE 7. How student grades were affected.



taking a reduced course load; 15.2% took advantage of this alternative rather than withdrawing from the program completely (FIGURE 8).

Additionally, although not addressed in the survey questions, several programs indicated an issue with recruitment and admissions.

Given the challenges of a constantly changing educational environment, approximately one-third of university students and one-fourth of hospital students were affected by a delayed program completion date. In addition, students from more than one-half of university programs experienced a delay in taking their certification examinations compared with approximately one-third of hospital programs (56.7% vs 29.7%, respectively). A closer look at the data from university programs revealed that students in MLT programs were twice as likely to be affected by a delay compared with those of MLS programs or other health professions programs. Similarly, a higher percentage of MLT students reported to their PDs they experienced a delay in taking their certification exam than MLS or other programs (61.3% vs 44% vs 53.8%, respectively). Reasons for the delay included a delayed graduation date, trouble finding an exam site, or financial issues (FIGURE 9).

Effect of COVID-19 on BOC Examination Scores

A total of 59.8% of university programs reported that their pass rate was negatively affected whereas 54.1% of hospital programs noticed a

negative effect. A total of 37.8% of university programs and 45.9% of hospital programs reported not being affected by the pandemic.

In terms of scores on the BOC certification exams, 59.8% of university programs and 51.4% of hospital programs reported a negative effect. A total of 39% of university programs and 48.6% of hospital programs reported that scores were not affected. Four (2.4%) university programs actually reported that their board pass rate was positively affected.

COVID-19 Effect on Faculty

Not only did the COVID pandemic affect students, but faculty were also affected. At both university and hospital programs, time to prepare and time to teach significantly extended into their personal time (FIGURE 8). A higher percentage of faculty from the other programs group (15%) than MLS (5%) or MLT (4%) were reassigned. Program directors reported that their faculty had to spend much more time communicating with students, especially about program changes, expectations, and requirements. They also spent a significant amount of time reminding students of assignments and evaluations that were due. Communications with affiliates also increased significantly, as hospitals made changes in the requirements for students to rotate. Students also required increased personal attention, including advising, tutoring, and counseling (FIGURE 10).

PD Voices—Personal Impact

“Overnight, we moved into non-stop course prep. Somedays, things changed by the hour.”

“Converting to delivering all classes by Zoom and providing some ‘dry lab’ experiences increased preparation time. Readjusting the schedule also took lots of extra effort and time to plan it.”

“I have worked harder the past two years tracking students, developing curriculum (mentoring, resilience, adding to professionalism lecture) and revising exams. The students are requiring more attention, more reminders- something I did not experience previously as the students were self-starters and kept themselves on track and met program expectations. Resuming training after the covid break- I know have a weekly recorded update stating what is due, selfcare reminders, expectations in rotations, and revisit program expectations”

FIGURE 8. Reasons student numbers were affected.

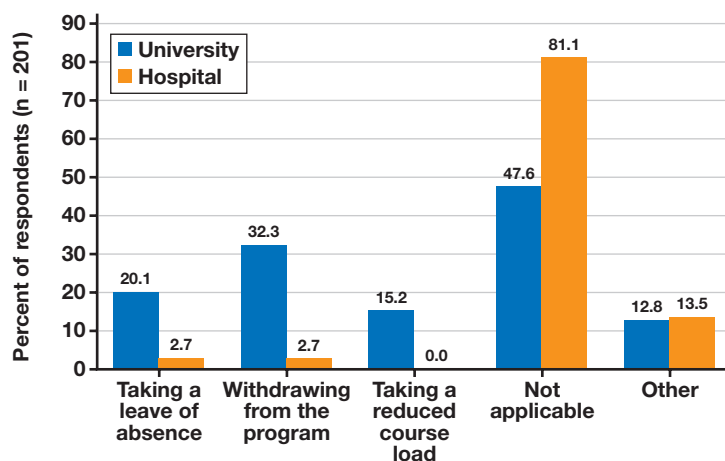
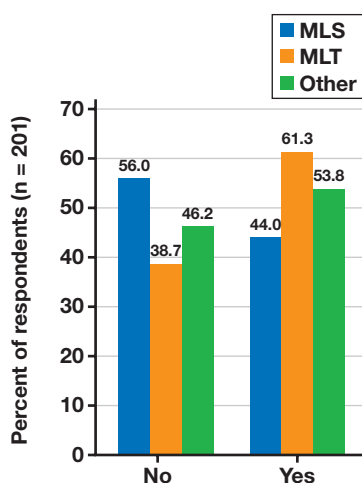


FIGURE 9. Delay in taking certification exam.



"Since we had to have social distancing and smaller labs, all lectures had to be asynchronous due to half the class in lab while the other half were at home. Since we only have one faculty member teaching a course, it was impossible to have live lecture while teaching lab at the same time."

"HUGE amount of prep for faculty regarding virtual labs. Lectures not as difficult."

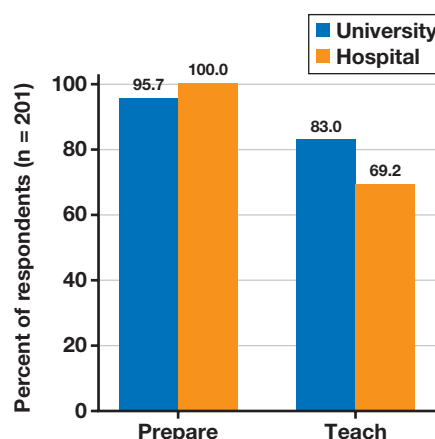
"My theory was already being presented online but because the labs were so changed it caused me to spend more time tutoring weaknesses online with students one-on-one."

"Had to teach instructors how to use Microsoft Teams for lecturing; when we came back on site, had to split into 2 smaller groups for social distancing which meant more time used for student labs"

Despite all of the challenges, 64.6% of university programs and 73% of hospital programs reported that there were no faculty changes. When looking at the breakdown by program type, higher percentages of MLS and MLT faculty retired or resigned vs other programs.

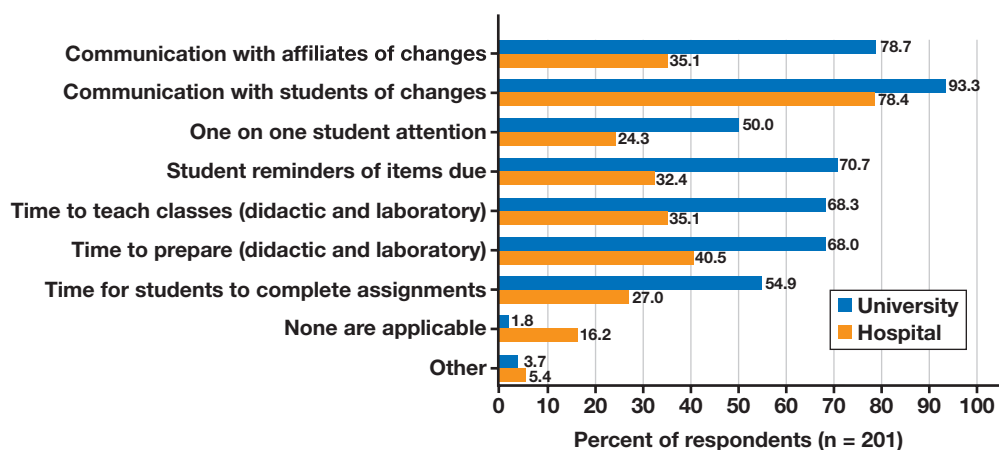
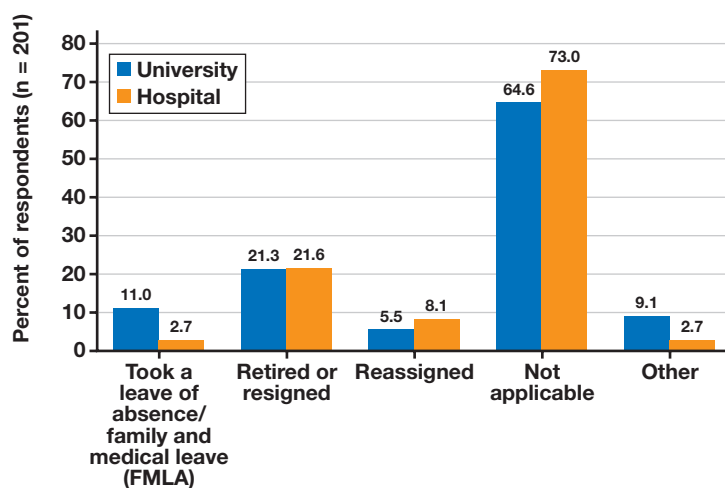
Both university and hospital programs reported that faculty either took a leave of absence or family medical leave, retired/resigned from their position, or were reassigned (FIGURE 11). Comments are included in FIGURE 12.

FIGURE 10. How COVID-19 impacted faculty personal time.



Discussion

The purpose of this study was to characterize the impact of COVID-19 pandemic on US accredited laboratory sciences programs using survey responses from associated PDs. Several themes emerged from the quantitative and qualitative data collected, highlighting commonalities and differences between university and hospital programs. First, the data indicated that the effects from the COVID-19 pandemic were related to the inherent differences between hospital and university programs. University programs had more experience in online program offerings prior to the pandemic. Brown et al⁸ reported a 21.7% increase in online courses and programs offered by universities from 2016 to 2020. However, the same survey data indicated that hospital programs reported 10 online course offerings in 2020 compared to only 1 online course in 2016. This study revealed that the pandemic forced approximately 97% of university programs to reformat classes to virtual learning compared with 58% of hospital programs. Unlike hospitals, learning management systems are commonly used in universities and supported with resources for technology and information technology and pedagogical expertise. For instance, a PD from a hospital program stated that their students were at a disadvantage due to the lack of technology to record live or prerecorded lectures; further, firewalls limited internet access. Thus, their students were unable to review

FIGURE 11. Increased time spent by faculty.**FIGURE 12.** Pandemic effect on faculty retention.

lectures for reinforcement of information. Common to both types of programs, faculty and students were required to learn new technology in a short period of time during the pandemic and develop quality simulations, and internet access/stability was cited as an issue among faculty and students.

Although better equipped to use advanced technology to deliver online classes, university programs faced a greater challenge of finding the time and expertise to develop pedagogical materials to replace the loss of student laboratory sessions. The structure of university programs commonly incorporates student laboratory sessions to train students in basic and intermediate laboratory skills prior to clinical rotations. For this purpose, the majority of university programs (60%) developed simulation laboratory sessions compared with, only 13% of hospital programs. Some programs handled this restriction by delaying or doubling up on student laboratory sessions when allowed.

The pandemic had less of an effect on clinical rotations of hospital programs vs university programs, most likely due to hospital's smaller student cohort size and easier access to and placement of students in the clinical laboratory. Indeed, the data indicated that 49% of hospital programs did not alter clinical rotations. Less than 30% of hospitals' clinical rotations were delayed or cancelled compared with university programs

(56% delayed and 30% cancelled). However, both types of settings found the need to shorten rotations (university, 49%; hospital, 22%).

Overall, the lack of hands-on experience from reduced exposure to student laboratory sessions and clinical rotations produced more problems related to psychomotor and affective domain skills of the students, especially in students from university programs. Indeed, the university PDs observed 3 times more of an effect on psychomotor skills (60% vs 22%) due to program changes than students from hospital programs. Comparing MLS to MLT and other disciplines, the largest impact was observed among MLTs. The lack of interaction between faculty and students that occurs in face-to-face instruction also generated a deficiency in affective domain skills of students in both settings (46% of university programs and 35% of hospital programs). Subsequently, an increase in student problems related to communication, attendance, dependability, and other soft skills were observed in clinical rotations.

Related to the BOC examinations, the pandemic created not only delays in taking the examinations but also lower pass rates for some programs. In this study, the majority of hospital and university PDs reported a negative effect of the pandemic on ASCP BOC scores and pass rates. Based on the ASCP BOC annual statistics, a noticeable decrease in the average pass rates for first-time examinees was observed in both

2021 and 2022 compared with 2019 and 2020 statistics. For MLS, the NAACLS first-time pass rates in 2019, 2020, 2021, and 2022 were 85%,⁹ 83%,¹⁰ 79%,¹¹ and 78%,¹² respectively. For MLT, the NAACLS/ABHES first time pass rates for the same years were 83%, 84%, 78%, and 78%, respectively. In terms of average test scores, it is worth noting that although a decline was observed over 2019 to 2022, the difference in effect was minimal between the years. More information on test scores and pass rates for MLS, MLT, and other programs can be found on the ASCP BOC website.⁹⁻¹²

Based on the comments from the PDs received from the survey, many of the problems derived from processing certification applications, delays in responding to the applicants, and transcript review by ASCP BOC. In addition, comments indicated that students needing more time to prepare for the examinations and locating an available testing site contributed to the delay in scheduling the examination. Students reported to the PDs that the changes in the program structure, especially related to reduced clinical rotations, left them feeling more anxious and less confident in their knowledge. This response coupled with relaxed certification requirements of clinical laboratories employees were suggested reasons for a high number of graduates of the programs who did not elect to take the certification examinations. Although the first-time pass rate was lower, PDs reported that most of these students were successful on the second attempt at passing the examination, evidence that students required more preparation for the examination.

Currently, many health profession programs housed in universities are faced with budget cuts due to a decrease in student enrollment and retention as a result of the pandemic. Program directors reported that 20% of university students chose to take a leave of absence from the program and a significant number withdrew, especially from MLT programs, during the pandemic. Factors such as the vaccine mandate, financial restraints due to the inability to work, and lack of time devoted to academics due to being forced to work overtime were reported in this study. Decreased enrollment and attrition were also attributed to a delay in completing prerequisites or lack of preparation from prerequisite courses.

Unknown are other possible effects from the pandemic on enrollment and attrition, including the lack of disability accommodations in the educational programs, domestic abuse, and lack of household supplies and food. The inability to recruit in-person during the pandemic also had a major impact on enrollment numbers, especially for a health profession program that is less visible than other programs. Historically, hospital programs enroll smaller cohorts from larger applicant pools and are more likely to be at full capacity.

Future Studies

Future longitudinal studies will reveal the long-term effects from the COVID-19 pandemic, including health profession programs' recovery

rates with regards to enrollment, retention, attainment of clinical sites, and student preparedness for the program and the ASCP BOC examinations. In addition, assessment of graduates' skills and affective domain performance in the clinical laboratory workforce should be conducted. Future studies could also reveal the value of innovative teaching strategies that were developed during the postpandemic era.

REFERENCES

1. Kumar A, Sarkar M, Davis E, et al. Impact of the COVID-19 pandemic on teaching and learning in health professional education: a mixed methods study protocol. *BMC Med Educ.* 2021;21(1):439. <https://doi.org/10.1186/s12909-021-02871-w>
2. McGill M, Turrietta C, Lal A. Teaching health science students during COVID-19: cross-hemisphere reflections. *J Univ Teach Learn Pract.* 2021;18(5). <https://doi.org/10.5376/1.18.5.3>
3. Bozkurt A, Karakaya K, Turk M, Karakaya O, Castellanos-Reyes D. The impact of COVID-19 on education: a meta-narrative review. *Tech Trends.* 2022;66(5):883-896. <https://doi.org/10.1007/s11528-022-00759-0>
4. Papananou M, Routsis E, Tsamakis K, et al. Medical education challenges and innovations during COVID-19 pandemic. *Postgrad Med J.* 2022;98(1159):321-327. <https://doi.org/10.1136/postgradmedj-2021-140032>
5. Collaborative TMS. The perceived impact of the Covid-19 pandemic on medical student education and training –an international survey. *BMC Med Educ.* 2021;21(566). <https://doi.org/10.1186/s12909-021-02983-3>
6. Hassell LA, Peterson J, Pantanowitz L. Pushed across the digital divide: COVID-19 accelerated pathology training onto a new digital learning curve. *Acad Pathol.* 2021;8:2374289521994240. <https://doi.org/10.1177/2374289521994240>
7. Patel R, Hoppman NL, Gosse CM, et al. Laboratory medicine and pathology education during the COVID-19 pandemic-lessons learned. *Acad Pathol.* 2021;8:23742895211020487. <https://doi.org/10.1177/23742895211020487>
8. Brown K, Duzan D, Fong K, et al. ASCP Board of Certification Survey of Medical Laboratory Science Education 2020: programs. *Lab Med.* 2022;53(6):e159-e163. <https://doi.org/10.1093/labmed/lmac044>
9. 2019 Examination Statistics for ASCP. *Credential American Society for Clinical Pathology – Board of Certification*, January 2020. 2019: https://www.ascp.org/content/docs/default-source/boc-pdfs/boc_statistical_reports/exam-stats-2019.pdf?sfvrsn=6
10. 2020 Examination Statistics for ASCP Credential. *American Society for Clinical Pathology – Board of Certification*, January 2021. 2020: https://www.ascp.org/content/docs/default-source/boc-pdfs/boc_statistical_reports/exam-stats-2020.pdf?sfvrsn=4
11. 2021 Examination Statistics for ASCP Credential. *American Society for Clinical Pathology – Board of Certification*, January 2022. . 2021: https://www.ascp.org/content/docs/default-source/boc-pdfs/boc_statistical_reports/exam-stats-2021.pdf?sfvrsn=4
12. 2022 Examination Statistics for ASCP Credential. *American Society for Clinical Pathology – Board of Certification*, February 2023. 2022: https://www.ascp.org/content/docs/default-source/boc-pdfs/boc_statistical_reports/exam-stats-2022.pdf?sfvrsn=4

On labmedicine.com

This month, the website features several case studies. In “Is very high platelet count always associated with essential thrombocythemia? An unusual presentation in a child,” Aktekin et al describe a pediatric patient with a very high platelet count who had 2 mutations common in chronic myeloid leukemia. Khanna et al describe 2 patients with chronic lymphocytic leukemia/small lymphocytic lymphoma whose cases transformed to plasmablastic lymphoma, an exceedingly rare occurrence, in “Plasmablastic transformation of chronic lymphocytic leukemia: a review of literature and report on 2 cases.” On the transfusion medicine front, Nivedita et al present the case of a patient with a suspected anti-G antibody in “The exclusion of

anti-D alloantibody in a suspected anti-G antibody in a pregnant 28-year-old Odiya Indian woman.”

Check out these articles and more on labmedicine.com.

Lablogatory

Recent contributions to the blog for medical laboratory professionals include microbiology, hematology, and cytology case studies as well as posts on forensic pathology and laboratory safety. To see why over half a million readers visit Lablogatory each year, visit labmedicineblog.com.

ThinPrep® Processors

Meeting the Demands of Your Lab



THINPREP® GENESIS™
PROCESSOR



THINPREP® 5000
PROCESSOR



THINPREP® 5000
AUTOLOADER

ThinPrep® processors are versatile and scalable solutions for laboratories of all volumes.

The portfolio offers reliable, best-in-class systems that help cytology labs automate their processes – decreasing the need for hands-on labor and increasing laboratory efficiencies.

Explore the
portfolio

